Analysis and Modelling of Pedestrian Movement Dynamics at Large-scale Events

Duives, Dorine

DOI
10.4233/uuid:08831f69-9b8e-44cf-8afe-f4a3e7bc9a9c

Publication date
2016

Document Version
Final published version

Citation (APA)
Duives, D. (2016). *Analysis and Modelling of Pedestrian Movement Dynamics at Large-scale Events*. [Dissertation (TU Delft), Delft University of Technology]. TRAIL Research School. https://doi.org/10.4233/uuid:08831f69-9b8e-44cf-8afe-f4a3e7bc9a9c

Analysis and Modelling of Pedestrian Movement Dynamics at Large-scale Events

Dorine Cornelia Duives

Delft University of Technology, 2016

This thesis is a result from the research program ‘Traffic and Travel Behavior in case of Exceptional Events’ which is sponsored by the Dutch Foundation of Scientific Research MaGW-NWO

Cover illustration: Dorine Duives

Analysis and Modelling of Pedestrian Movement Dynamics at Large-scale Events

Proefschrift
ter verkrijging van de graad van doctor
aan de Technische Universiteit Delft,
op gezag van de Rector Magnificus prof. ir. K.C.A.M. Luyben;
voorzitter van het College voor Promoties,
in het openbaar te verdedigen op maandag 10 oktober 2016 om 15:00 uur
door

Dorine Cornelia DUIVES
Master of Science in Civil Engineering, Transportation System Analysis and Planning,
Northwestern University and
Master of Science in Civil Engineering, Transport & Planning,
Delft University of Technology
geboren te 's-Hertogenbosch, Nederland

This dissertation has been approved by the
promotor: Prof. dr. ir. S.P. Hoogendoorn
copromotor: Dr. ir. W. Daamen

Composition of the doctoral committee:

Rector Magnificus	Chairperson
Prof. dr. ir. S.P. Hoogendoorn	Promotor
Dr. ir. W. Daamen	Copromotor

Independent members:

Prof. dr. C.K. Hemelrijk	University of Groningen
Prof. dr. H.S.M. Mahmassani	Northwestern University
Prof. dr. A. Seyfried	Forschungszentrum Jülich
Prof. dr. M. Sarvi	The University of Melbourne
Prof. ir. F. Wegman	Faculty of Civil Engineering and Geosciences, TU Delft
Prof. dr. ir. B. van Arem (reservelid)	Faculty of Civil Engineering and Geosciences, TU Delft

TRAIL Thesis Series no. T2016/16, the Netherlands Research School TRAIL

TRAIL
P.O. Box 5017
2600 GA Delft
The Netherlands
E-mail: info@rsTRAIL.nl

ISBN: 978-90-5584-208-7

Printed in the Netherlands

‘Keep dreaming big and go for it! The worst thing that can happen
is that you will actually achieve your dreams.’
- D.C. Duives

Acknowledgements / Dankwoord

Waar ik initieel dacht, dat een PhD een redelijk eenzame aangelegenheid zou worden, heb ik het tegendeel ondervonden. Daarom wil ik hier een aantal personen bedanken, die ieder op hun eigen manier een bijdrage hebben geleverd aan het volbrengen van deze taak.

Allereerst zijn dat mijn begeleiders, Serge Hoogendoorn en Winnie Daamen. Jullie hebben mij in de afgelopen acht jaar de mogelijkheid gegeven om te ontdekken of wetenschappelijk onderzoek iets voor mij is. Ik wil jullie bedanken voor het introduceren van de 'speeltuin' en het aanreiken van de financiering en de technieken om dit onderzoek te volbrengen. De support en concrete feedback waardeer ik zeer. Bovendien, doordat jullie mij vele malen 'gecontroleerd' in het diepe hebben gegooid en mij de ruimte hebben gegeven om mijn eigen weg te vinden, zijn de afgelopen jaren vooral een inspirerende rollercoaster-ride geweest.

Deze jaren waren echter minder gezellig geweest zonder mijn collega's. Een aantal daarvan wil ik speciaal noemen. Edwin, mijn steun en toeverlaat tijdens de empirische onderzoeken, maar vooral ook daarbuiten. De persoon die me heeft laten zien dat je geen empirisch onderzoek kan doen zonder koffie, cola, bananen, gezond verstand en een flinke dosis humor. Daarnaast wil ik ook mijn kamergenootjes bedanken voor het gezelschap. Mahtab en Ramon, ik mis onze goede gesprekken nu al. Mignon, een gezelliger en liever kamergenootje had ik me de afgelopen vier jaar niet kunnen wensen.

Moreover, I would like to thank Hani Mahmassani, Majid Sarvi, Armin Seyfried, Charlotte Hemelrijk en Fred Wegman for taking part in my doctoral committee and the valuable feedback on my work over the years. Hani, also thanks for introducing the topic of modelling pedestrian movement dynamics to me. Without the first inspiring discussions about crowd modelling, crowd management and the Hadj, this thesis would probably not have been written. Besides that, I would like to thank Majid and his team for their hospitality during my stay in Melbourne. Without it, I would never have found out that ants, pill bugs and mice could be inspiring.

Empirisch onderzoek naar de bewegingen van voetgangers op grootschalige evenementen is niet mogelijk zonder de medewerking van vele verschillende partijen. Daarom wil ik ook de organisaties achter de marathon van Rotterdam, het bevrijdingsfestival Wageningen, de Vierdaagsemarsen van Nijmegen en de marathon van Amsterdam danken. Verder hebben veel mensen van buiten de universiteit mij keer op keer uit de 'ivoren toren' getrokken en hebben laten zien wat het managen van voetgangersmenigten daadwerkelijk allemaal met zich meebrengt. Ik sta er iedere keer weer versteld van dat deze mensen met de weinig middelen die ze hebben, in combinatie met een enorme bezieling, passie en toewijding ontzettend gave, maar vooral ook veilige, evenementen organiseren. Tevens, de vele gesprekken met Jeroen van den Heuvel, Berend Temme, Daniel Schippers, Robrecht Bavink, Ardo van Kampen, Syan Schaap en het crowdmanagement team van de politie regio Amsterdam zijn zeer waardevol voor mij geweest om inzicht te krijgen in de manier waarop voetgangersonderzoek hen bij hun werk in de praktijk kan ondersteunen.

Als laatste wil ik graag mijn familie bedanken. Mam, Pap, dank voor de onvoorwaardelijke steun door de jaren heen en dank dat jullie me hebben laten zien dat je stoutste dromen kunnen uitkomen, als je er maar voor gaat. En Wouter, Martijn en Mushu, zonder jullie drie zouden de afgelopen jaren een stuk minder boeiend zijn geweest! Jullie hebben van mijn huis een thuis gemaakt.

Dorine Duives, September 2016

Contents

List of Figures

List of Tables

Notation

The main symbols and shorthands that are used in this thesis are presented as follows:

Symbols

a_0 / a_1	Strength parameters of the reaction to interactions of Nomad, see (7.5)	131
$\vec{a}$	Total acceleration of agent of Nomad, see (7.1)	131
$\vec{a}_c$	Acceleration of agent in Nomad - controlled part , see (7.2)	131
A_C	Spatial area of cell C, see (3.3)	58
$\vec{a}_o$	Acceleration of agent in Nomad - interaction with obstacles, see (7.2)	131
$\vec{a}_p$	Acceleration of agent in Nomad - uncontrolled part, see (7.1)	131
$\vec{a}_r$	Acceleration of agent in Nomad - interaction other pedestrian, see (7.4)	131
$\vec{a}_s$	Acceleration of agent in Nomad - path straying, see (7.3)	131
d_A	Interaction distance between the two pedestrians, see (7.5)	131
C_i	Relative weight of characteristic in calibration procedure, see (7.8)	147
$C(\vec{x})$	Capacity of the infrastructure at cross-section, see figure 2.3	29
$\vec{e}_n$	Unit vector along the line of interaction of Nomad, see (7.5)	131
GOF	Goodness of fit of a certain realisation of the model	147, 175
$h_{p,max}$	Maximum interaction distance, see (3.7)	58
$h_{p,q}(t)$	Minimum distance headway, see (3.6)	58
$I_p(t)$	Strength of interaction, see (3.10)	61
LA	Dimensions of the long axis of the ellipse, see section 5.3.2	99
M_{real}	Value of the metric according to the empirical realization, see (7.6)	147
M_{sim}	Value of the metric according to the simulation realization, see (7.6)	147
N_n	Nr. characteristics, see (7.7)	147
N_m	Nr. of sequences, see (7.7)	147
N_{pop}	Number of data points for population pop, see table 4.2	69
N_x	Nr. of cells along x-axis, see (7.7)	147
N_y	Nr. of cells along y-axis, see (7.7)	147
p	Pedestrian under consideration (subscript)	29
q	Pedestrian in the vicinity of pedestrian p (subscript)	29
$q(x,t)$	Flow at cross-section, see figure 2.3	29
r_0 / r_1	Weight parameter of Nomad, see (7.5)	131
SA	Dimensions of the short axis of the ellipse, see section 5.3.2	99

t	Time coordinate, see (3.1)	59
δt	Time step size, see (3.1)	59
$T_{p,q}(t)$	Duration of the interaction between two pedestrians, see (3.10)	61
$SE_{i,n,m}$	Sum of squares of the residuals, see (8.12)	175
SE_{macro}	Squared error of the macroscopic metrics, see (7.6)	147
$SE_{micro/meso}$	Squared error of the microscopic and mesoscopic metrics, see (7.7)	147
$\vec{u}$	Absolute walking speed of class d MDW model, see (8.3)	160
$U(\rho_d)$	Speed-density relation class d MDW model, see (8.2)	160
$\vec{v}_d$	Average walking speed for class d MDW model, see (8.2)	160
$\vec{v}_p(t)$	Walking velocity of pedestrian, see (3.1)	57
$V_p(t)$	Vision field, see (3.7)	58
$V_{p,max}(t)$	Maximum angle of the vision field, see 2.8	33
$V_{p,q}$	Angle of sight, see (3.9)	61
$\vec{v}(\vec{x},t)$	Walking velocity at location, see figure 2.3	29
$\vec{v}_0(t)$	Preferred walking velocity of Nomad, see (7.3)	131
W_n	Weight of characteristic n, see (8.10)	185
X	Set of all possible coordinates, see (3.7)	58
X_C	Set of coordinates describing cell C, see (3.2)	58
$\vec{x}_p(t)$	Location of pedestrian, see figure 2.3	29
α	Gradient of the linear regression analyses, see section 5.2	95
$\alpha_{p,q}$	Angle of interaction, see (3.8)	60
β	Intercept of the linear regression analyses, see section 5.2	95
$\beta_{\delta=d}$	Weight route choice component MDW model - density of class d, see (8.5)	161
$\beta_{\delta\neq d}$	Weight route choice component MDW model - density, see (8.5)	161
β_d^{crowd}	Weight route choice component MDW model -density, see (8.5)	161
β_d^{delay}	Weight route choice component MDW model - delay, see (8.6)	161
β_d^{global}	Weight global route choice component MDW model, see (8.4)	161
β_d^{local}	Weight local route choice component MDW model, see(8.7)	161
$\vec{\varepsilon}$	Error term of Nomad walker model, see (7.1)	131
$\vec{\gamma}_d^{crowd}$	Local route choice component MDW model - crowdedness, see (8.5)	161
$\vec{\gamma}_d^{delay}$	Local route choice component MDW model - delay, see (8.6)	161
$\vec{\gamma}_d^{global}$	Global route choice component MDW model, see (8.4)	161
μ_{pop}	Mean of population pop, see table 4.2	69
ρ	Density, see figure 2.3	29
$\rho(C,t)$	Density experienced in cell C, see (3.2)	58
ρ_d	Density of class d MDW model, see (8.1)	160
$\rho_p(t)$	Density of pedestrian, see (3.2)	58
$\rho(\vec{x},t)$	Density experienced at cross-section, see figure 2.3	29
σ_{pop}	Standard deviation of variable for population pop, see table 4.2	69
τ	Relaxation parameter of Nomad, see (7.3)	131

Shorthands and abbreviations

BD-S	Bidirectional straight movement base case
FD	Fundamental diagram
LF-W	Empirical case: Liberation day festival at Wageningen
McSavi	Muli-Camera Stand-Alone Video Installation
MODT-2	Multi Object Detection and Tracking program
M-A	Empirical case: Marathon at Amsterdam
M-R	Empirical case: Marathon at Rotterdam
Q-A	Empirical case: Queensday at Amsterdam
UD-C	Uni-directional corner movement base case
UD-E	Uni-directional entering movement base case
UD-S	Uni-directional straight movement base case
X	Intersecting movement base case
4D-W	Empirical case: 4Daagse at Wijchen
4D-L	Empirical case: 4Daagse at Lent
4D-H	Empirical case: 4Daagse at Hatert

Summary

History shows that it is extremely challenging to predict when and where crowd movements at large-scale events turn into life threatening crowd crushes and stampedes. Recent advancements in the pedestrian simulation research community enable the use of computer models to provide insights into the movement dynamics of pedestrian crowds. However, the dynamics of pedestrians at large-scale events are not yet entirely understood. In other words, the knowledge that is essential to calibrate and assess pedestrian simulation models for this specific type of movement behaviour is lacking.

The aim of the research detailed in this dissertation is to develop theories and models that describe the operational movement dynamics of pedestrians in a crowd during large-scale events. Special attention is paid to theories which detail the effect of the movement base case on the microscopic and macroscopic movement dynamics of the crowd. This main objective can be broken down into four sub-objectives, namely:

1. to develop a theoretical framework for pedestrian movement dynamics,
2. to assess the validity of this theoretical framework,
3. to develop a theoretical framework for the assessment of pedestrian simulation models,
4. to calibrate two distinct pedestrian simulation models and assess their capabilities specifically for the prediction of pedestrian movement dynamics in crowds at large-scale events.

Conceptual model

A literature review of the findings of empirical studies featuring the movement dynamics of pedestrians has been performed. This review illustrates that the research has been adhoc and as a result disjointed. That is, the empirical research has been focused on directly relating the characteristics of the pedestrian, the environment, the infrastructure and the flow situation to one of the flow variables. It has proven difficult to connect the empirical findings regarding the dynamics of pedestrians in order to create a model that describes the operational movement dynamics of pedestrians in crowds at large-scale events.

However, it was found that insights from the pedestrian modelling community can close the gaps in literature. Based on the findings of the review and some key-findings from the pedestrian

modelling community, a conceptual model of related behavioural hypothesis was developed. In this conceptual model each variable is either related to a cause (i.e. the demographic, physiologic, interaction and infrastructure characteristics) or an effect (i.e. the microscopic and macroscopic flow variables). Due to the structured ordering of the variables in the conceptual model, the model allows for the systematic testing of hypothesis related to the motion of pedestrian crowds.

Data acquisition and testing of the model

However, the data sets necessary to corroborate the conceptual model are not available yet. A review of data collection methods indicates that only one research method can meet the requirements on this wish-list, namely a camera-system with a birds-eye view that records the movements of the crowd and stores it for off-line analysis. By means of the newly developed Multi-camera Stand-Alone VideoInstallation (McSavi) and Multiple Object Detection and Tracking software (MODT) pedestrian trajectory data sets has been captured featuring the movement dynamics of pedestrians at large-scale events. Besides the data collection methodology, also the cases for the empirical data collection have been established. Acquiring data sets featuring distinctive movement base cases was one of the key requirements in order to capture to the largest range of crowd movement dynamics. Furthermore, mathematical definitions have proposed for most of the variables used to describe the operational movement dynamics of pedestrians, such as the instantaneous walking velocity, the density, the distance headway, the angle of interaction, the alignment of interactions and the time-to-collision.

The conceptual model was corroborated by means of the trajectory data sets and linear regression analysis. The basic structure of the proposed model is confirmed by the tests. That is, it was established that a cyclic relation between the microscopic walking velocity, the distance headway and the strength of the interaction as perceived by individual pedestrians lies at the heart of the conceptual model. This cyclic relation suggests that the movement decisions of an individual are not necessarily base on the aggregate features of the crowd's movements, but might also be influenced by the characteristics of the local interactions between two individuals.

Assessment framework for pedestrian simulation models

Besides a theory on the movement dynamics of individual pedestrians at large-scale events, also the crowd movement phenomena that are essential in the correct display of this type of walking behaviour were established based on the data acquired as part of this research. A thorough analysis of the empirical data sets highlighted several interesting crowd movement phenomena, namely 1) a shape change of the no-interaction zone with increasing densities, 2) the general lack of interactions between pedestrians that face each other, 3) an increase of the searching behaviour with increasing densities, 4) a decrease of the distance headway instead of a decrease of the time-to-collision, 5) a non-zero walking velocity at high densities. These and other crowd movement phenomena have been detailed in two lists of requirements. One list of the general crowd movement phenomena and one list of specific crowd movement phenomena which relate to specific movement base cases. These lists of requirements illustrate that some crowd movement phenomena hold for all movement base cases, while others only develop during one specific movement base case.

The two lists of crowd movement phenomena are at the base of the assessment framework for pedestrian simulation models that is proposed in this dissertation. The framework, which ascertains whether a pedestrian simulation model can indeed be used for the simulation of pedestrian movement dynamics at large-scale events, incorporates an assessment of the behaviourally correct display of crowd movement phenomena and the models applicability in complex case studies (e.g. route choice, collisions, groups, and computational burden). Using the assessment framework a broad review of pedestrian simulation models is undertaken featuring Cellular Automata, Social Force models, Velocity-based models, Activity choice models, Continuum models, Hybrid models, Behavioural models and Network models. The assessment illustrates that the models can be divided into slow but highly precise microscopic modelling attempts and very fast but behaviourally questionable macroscopic modelling attempts. The Social Force models, Activity choice models and the next generation Continuum models are found to be the contemporary best models. The capabilities of two of these models have been studied in more detail, namely the microscopic pedestrian simulation model Nomad proposed by Hoogendoorn & Bovy (2004)) and the macroscopic pedestrian simulation model proposed by Hoogendoorn et al. (2014).

Calibration and assessment of pedestrian simulation models

Both models have been calibrated specifically of the operational movement dynamics of pedestrians at large-scale events by means of the empirical trajectory data sets acquired during this study. A new calibration procedure was used in the calibration procedure, which can take into account the micro-, meso- and macroscopic characteristics of the walking behaviour . In case of Nomad, the spatial distribution of the density, velocity and presence, and the distribution of the distance headway, the time-to-collision, and the interaction angle have been taken into account. In case of the continuum model only the spatial distribution of the density and velocity were taken into account.

The assessment results illustrate that the best parameter set is very dependent on the movement base case. The calibration results of the microscopic simulation model Nomad and the Macroscopic Dynamic Walker model show that the best parameter set for each of the two models is very dependent on the movement base case used in the calibration process. Even though the differences in the parameter sets were in general small, the consequences of these differences with respect to the demand at which flow breakdown occurs are extensive.

Additionally, both models have difficulties predicting the anticipation behaviour of pedestrians upstream of bottleneck situations and the dispersion of pedestrians in unidirectional corner flows. Besides that, the assessment results show that Nomad has difficulties predicting the movement behaviour of pedestrians correctly in several movement base cases the model was not originally calibrated for and the MDW models predictions are sensitive to the specified fundamental diagram.

Conclusions

The main conclusion of this thesis is that the walking dynamics of pedestrians within a crowd at large-scale events are less straight forward than originally assumed. The conceptual model illustrates that numerous characteristics impact the movement behaviour of pedestrians. Moreover, the empirical study shows that the walking behaviour changes depending on the context of the situation. The characteristics of the individual, the physiological environment, the infrastructure lay-out, the movement base case, and the amount of oversight influence the aggregate walking behaviour of pedestrians at large-scale events. The additional complexity of the walking dynamics implies that the idea of one generic fundamental diagram that accurately predicts the aggregate movement behaviour in all situations under all contexts might not exist.

A second conclusion that can be drawn from the findings is that understanding and modelling all listed crowd movement phenomena and the 'suboptimal' local route choice behaviour of pedestrians under crowded conditions is essential in order to accurately predict the operational movement dynamics of pedestrians in crowds at large-scale events. Yet, the review of contemporary simulation models and the thorough assessment of two simulation models indicate that many pedestrian simulation models cannot reproduce all the operational movement dynamics displayed by pedestrians at large-scale events. This might results in the predicted of operational walking dynamics that are locally more direct and efficient than the dynamics found to occur in practice. This might result in the overestimation of high density regions by pedestrian simulation models.

Implications

This research has also some implications for practice. First of all, this dissertation shows that context does matter. The same infrastructure can suddenly become dangerous when the circumstances and the complexity of the movement dynamics change. Even though this thesis cannot establish the exact quantitative differences in capacity based on the results presented in this thesis, several velocity decreasing factors were determined. The presence of these factors, and several others which were not studied in this thesis, should be taken into account when managing and/or assessing large-scale infrastructures.

Moreover, pedestrian simulation models are more and more used to assess infrastructures. This thesis has established that a large number of pedestrian simulation models exist, many of which are not capable of simulating all the crowd movement phenomena which are necessary to predict the movement dynamics of crowds at large-scale events realistically. Each model has a specific set of situations it can model realistically. And even models that, considering their mathematical properties, have the ability to capture certain behaviour, do not necessarily produce realistic predictions. As a result, the best model for a task depends on the type of infrastructure that is assessed, the type of knowledge the user requires, the accuracy that is required and the comprehensiveness of the set of situations the model was calibrated for.

Samenvatting

De geschiedenis laat zien dat het een grote uitdaging is om te voorspellen waar en wanneer de beweging van een massa op een grootschalig evenement verandert en er mogelijk hierdoor levensgevaarlijke situaties ontstaan. De vooruitgang van de afgelopen jaren in het voetgangers onderzoek maakt het gebruik van computer modellen om het loopgedrag van voetgangers in een menigte te bestuderen mogelijk. Helaas is het nog onduidelijk hoe het loopgedrag van voetgangers op grootschalige evenementen in elkaar steekt. Dat wil zeggen, de kennis, die essentieel is om de computer modellen te calibreren en valideren voor deze speciefieke vorm van loopgedrag, is nog niet beschikbaar.

Het doel van dit onderzoek is het ontwikkelen van theorieën en modellen die het operationeel loopgedrag van voetgangers in een menigte gedurende grootschalige evenementen beschrijven. Hierbij wordt specifiek aandacht besteed aan theorieën die het effect van de stromingssituatie op de microscopische en macroscopische bewegingsdynamiek van de menigte beschrijven. Dit hoofddoel kan worden opgebroken in vier doelstellingen, zijnde:

- het ontwikkelen van een theoretisch framework dat de bewegingsdynamiek van voetgangers in de menigte beschrijft,
- het beoordelen van de validiteit van dit framework aan de hand van empirische data,
- het ontwikkelen van een theoretisch framework om voetgangerssimulatiemodellen te beoordelen,
- het calibreren en beoordelen van twee voetgangerssimulatiemodellen met betrekking tot het loopgedrag van voetgangers gedurende grootschalige evenementen.

Conceptueel model

De empirische onderzoeken met betrekking tot het loopgedrag van voetgangers zijn onderzocht en beschreven in een literatuuroverzicht. Dit overzicht laat zien dat het onderzoek erg specifiek is geweest en onsystematisch is verricht. Dat wil zeggen, het empirisch onderzoek heeft zich geconcentreerd op het direct relateren van de karakteristieken van de voetganger, de omgeving, de infrastructuur en de stromingssituatie aan één van de beschrijvende variabelen. Het bleek moeilijk om op basis van bevindingen uit de empirische onderzoeken direct een model af te leiden dat het loopgedrag van voetgangers in menigtes op grootschalige evenementen beschrijft.

Echter, inzichten gegenereerd aan de hand van voetgangerssimulatiemodellen bleken in staat deze gaten te vullen. Gebaseerd op de bevindingen uit het literatuuroverzicht en de voetgangerssimulatiemodellen is een nieuw conceptueel model ontwikkeld. In dit model beschrijven de variabelen òf een oorzaak (i.e. demografische, fysiologische of infrastructurele karakteristieken) òf een gevolg (i.e. de beschrijvende variabelen). Doordat de oorzaken en gevolgen geordend zijn, is het mogelijk om deze hypotheses over het loopgedrag van voetgangers systematisch te testen. Daarnaast, omdat er in het conceptueel model indirecte effecten van de beschrijvende variabelen op de relatie tussen de volgafstand en de loopsnelheid beschreven staan, onderbouwt het model waarom het moeilijk kan zijn om één unieke relatie te vinden, die onder alle omstandigheden, de relaties tussen de snelheid, dichtheid en intensiteit beschrijft door middel van een fundamenteel diagram.

Data verzameling en toetsing van het model

Tot op heden ontbraken echter de gegevens die nodig zijn om het conceptueel model te testen. Een overzicht van dataverzamelingstechnieken geeft aan dat er maar één onderzoeksmethode voldoet aan de eisenlijst. Door middel van een nieuw ontwikkeld Multi-camera Stand-Alone VideoInstallatie (McSAVI) en de MultipleObjectDetection&Tracking software (MODT) zijn data sets bestaande uit trajectorie van voetgangers op grootschalige evenementen verzameld. Naast de dataverzamelingsmethodiek, zijn ook de cases betreft het empirisch onderzoek vastgesteld. Het beschrijven van zoveel mogelijk verschillende stromingssituaties was hierin de belangrijkste eis. Verder, was er voor een aantal van de variabelen die genoemd worden in het conceptueel model geen wiskundige definitie. Daarom worden er in deze thesis wiskundige definities gegeven voor de instantane loopsnelheid, de dichtheid, de volgafstand, the hoek van interactie, de duur van de interactie en de tijd tot de eerst mogelijke botsing.

Het conceptueel model is getoetst door middel van lineare regressie analyse gebruik makend van de ingewonnen trajectorie data. In het midden van het conceptueel model bevindt zich cyclyische relatie tussen de individuele loopsnelheid, de volgafstand en de sterkte van de interactie. Dit suggesteert dat het loopgedrag van de voetganger mogelijk niet alleen beïnvloed wordt door de geagregeerde bewegingsdynamiek van de menigte maar ook door de karakteristieken van de lokale interactie tussen twee voetgangers.

Beoordelingsraamwerk voor voetgangersmodellen

Naast een theorie die het loopgedrag van voetgangers op grootschalige evenementen beschrijft, heeft deze thesis ook vastgesteld welke bewegingsfenomenen van belang zijn om de bewegingsdynamiek van voetgangers in een menigte correct te beschrijven. Een diepgaande analyse van de data sets bracht verschillende interessante fenomenen aan het licht, zijnde 1) een verandering van de vorm van de niet-betreedbare ruimte om een voetganger, 2) een algemeen gemis van interacties tussen twee voetgangers die op elkaar aflopen, 3) een intensivering van het zoekgedrag naarmate de dichtheid toeneemt, 4) een afname van de afstand tussen voetgangers in plaats van een afname van het tijd tot de volgende persoon en 5) een gelijkblijvende individuele snelheid onder hoge dichtheden. Deze en andere fenomenen zijn beschreven in twee lijsten. Eén lijst met generieke fenomenen en één lijst met fenomenen die alleen onder bepaalde stromingssituaties optreden. Deze lijsten laten zien dat bepaalde fenomenen specifiek zijn voor bepaalde stromingssituaties.

De twee lijsten van bewegingsfenomen vormen de basis van het beoordelingsraamwerk voor voetgangersmodellen die in deze thesis worden voorgedragen. Dit raamwerk, waarmee kan worden nagegaan of een voetgangersmodel in staat is om de bewegingsdynamiek van voetgangers gedurende grootschalige evenementen te voorspellen, combineert de beoordeling van het model met betrekking tot het correct weergeven van de bewegingsfenomenen in een menigte en de toepasbaarheid van het model in ingewikkelde case studies (bijvoorbeeld route keuze, botsingen, groepsgedrag en zwaarte van de berekeningen). Aan de hand van het raamwerk zijn de voetgangerssimulatiemodellen cellular automata, social force models, velocity-based models, continuum models, hybrid models, behavioural models en network models beoordeeld. Deze beoordeling laat zien dat deze modellen langzaam maar zeer precies het loopgedrag simuleren of juist snel simuleren maar gedragstechnisch vragen oproepen. De social-force modellen, activity choice modellen en de nieuwe generatie continuum modellen kwamen hierbij als beste uit de bus. Twee van deze modellen zijn verder bestudeerd, zijnde het microscopisch voetgangerssimulatiemodel Nomad ontwikkeld door Hoogendoorn & Bovy (2004) en het MacroscopischDynamischWalker model (MDW) ontwikkeld door Hoogendoorn et al. (2014).

Calibratie en beoordeling van voetgangerssimulatiemodellen

Beide modellen zijn gecalibreerd met betrekking tot het specifieke voetgangersgedrag dat optreed gedurende grootschalige evenementen. Hiervoor is een ijkprocedure gebruikt waarin de micro-, meso- en macroscopische karakteristieken van het loopgedrag gebruikt worden om de beste parameterschatting te genereren. In het geval van Nomad zijn de ruimtelijke verdeling van de dichtheid, snelheid en aanwezigheid, en de verdeling van de volgafstand, tijd tot botsing en hoek van de interactie meegenomen in de ijkprocedure. Het MDWmodel is gekalibreerd op basis van de ruimtelijke verdeling van de dichtheid en de snelheid.

De resultaten van de beoordeling illustreren dat de beste parameter set erg afhankelijk is van de movement base case gebruikt tijdens het ijkproces. Zelfs al zijn de verschillen tussen de parameter sets klein, de consequenties van deze verschillen met betrekking tot de intensiteit waarbij een onderbreking van de stroming optreedt kunnen zeer groot zijn.

Daarnaast blijkt dat beide modellen moeite hebben met het voorspellen van het anticipatie gedrag van voetgangers bovenstrooms van knelpunten. Verder laten de resultaten zien dat Nomad minder goed instaat is om het loopgedrag te voorspellen in stromingssituaties waarvoor het orgineel niet gecalibreerd is. Vooral het microscopisch loopgedrag en de ruimtelijke spreiding van de voetgangers kan met moeite worden voorspeld en dat het MDW model gevoelig is betreft de exacte specificatie van het fundamenteel diagram.

Conclusies

De hoofdconclusie is dat het loopgedrag van voetgangers gedurende grootschalige evenementen complexer is dan orgineel gedacht werd. Het conceptueel model illustreert dat vele verschillende karacteristieken van invloed zijn op het loopgedrag van voetgangers in menigten op grootschalige evenementen. De empirische studie toonde aan dat het loopgedrag afhankelijk is van de context van de situatie. De eigenschappen van het individu, de fysiologische omgeving, de infrastructuur, de stromingssituatie en de hoeveelheid overzicht dat men heeft over de situatie bepalen het geaggregeerde loopgedrag van de menigte. De toegevoegde complexiteit betreft het loopgedrag impliceert dat een generiek fundamenteel diagram, dat in alle situaties het loopgedrag nauwkeurig beschrijft, mogelijk niet bestaat.

Daarnaast concludeert dit onderzoek dat het begrijpen en modelleren van alle bewegingsfenomenen van de menigte en het 'suboptimale' lokale routekeuzegedrag essentieel zijn om ook onder zeer drukke omstandigheden het loopgedrag van de voetgangers in de menigte op grootschalige evenementen nauwkeurig te kunnen voorspellen. Wanneer deze fenomenen en het routekeuzegedrag niet correct worden omschreven bestaat een gerede kans dat het model een meer efficiente afwikkeling van de voetgangersstroom voorspelt dan daadwerkelijk optreedt. Dit kan resulteren in een overschatting of onderschatting van huidige toestand van de voetgangersinfrastructuur.

Implicaties

Dit onderzoek heeft ook een aantal implicaties betreffende de praktijk. Allereerst laat dit onderzoek zien dat de context van de situatie belangrijk is. De toestand van de menigte kan plotselijk gevaarlijk worden wanneer de omstandigheden of de complexiteit van de stromingssituatie verandert. Ondanks dat dit onderzoek niet kan vaststellen hoe groot de verschillen in capaciteit zijn, worden er in dit onderzoek verschillende factoren vastgesteld die de loopsnelheid van de menigte negatief beïnvloeden. De aanwezigheid van deze factoren en een aantal andere die niet verder onderzocht zijn in deze thesis, zouden moeten worden meegenomen wanneer men een grootschalig evenementen organiseert of toetst.

Verder worden voetgangerssimulatiemodellen steeds vaker gebruikt om infrastructuur te toetsen. Dit onderzoek stelt vast dat een groot aantal voetgangerssimulatiemodellen bestaat. Vele waarvan zijn niet instaat om alle fenomenen die optreden in voetgangersmenigte realistisch te voorspellen. Daarnaast blijkt, dat zelfs modellen waarvan de wiskundige basis ze in staat zou moeten stellen om deze fenomenen te beschrijven, niet noodzakelijk realistische resultaten produceren. Als gevolg hiervan is het beste model voor een bepaalde taak in de meeste gevallen afhankelijk van het type infrastructuur dat hiermee getoetst gaat worden, het soort kennis dat de gebruiker verlangt, de nauwkeurigheid die nodig is en het aantal verschillende situaties waarop een model gekalibreerd is.

Chapter 1

Introduction

History shows that it is extremely challenging to predict when and where crowd movements turn into life threatening crowd crushes and stampedes. Recent advancements in the pedestrian simulation research community enable the use of computer models to provide insights into the movement dynamics of pedestrian crowds during large-scale events. Pedestrian simulation models are more and more used to describe and predict these dynamics.

The dynamics of pedestrian crowd movements are, however, not yet entirely understood. In other words, the knowledge that is essential to simulate pedestrian walking dynamics and calibrate pedestrian models is currently lacking. In this thesis we establish which dynamics are essential in order to realistically predict crowd movement dynamics and propose an assessment methodology for simulation models that predict the walking dynamics of pedestrians in crowds at large-scale events.

The outline of this introductory chapter is as follows. First, the context of this research is described in section 1.1. In section 1.2 the research objective is mentioned. Section 1.3 delineates the scope, section 1.4 the type of crowd this study focusses on and section 1.5 introduces the research approach. Accordingly, section 1.6 details the contributions of this thesis to science and practice. This chapter concludes with an outline of the remainder of this thesis (section 1.7).

1.1 Need for realistic crowd simulation models

All over the world large-scale pedestrian events are organised frequently, where thousands of pedestrians gather in one place for the sake of a joint experience. During most of these religious, sport or music events, the predominant mode of transport across the event grounds is walking.

The tragedies during the Hadj in Mecca (1998, 2015), the Loveparade in Duisburg (2010), and the New Year's celebration in Shanghai (2014) demonstrate that all over the world pedestrians run the risk of getting severely injured or loose their lives while being part of a crowd during a large-scale event. Records show that in some cases the forces transmitted between pedestrians are high enough to push pedestrians off the sides of buildings (Mecca, 1998) and to bend metal guardrails (Fruin, 1993). When caught within a crowd crush, pedestrians sustain bruises and might even be asphyxiated due to the incredibly high forces transmitted through the crowd (Lee & Hughes, 2006). Furthermore, pedestrians run the risk of getting trampled because of the unstable nature of the movement dynamics (Helbing & Mukerji (2012), Wang et al. (2014)).

Due to the complex nature of pedestrian dynamics, it remains extremely challenging for crowd managers to predict when and where docile crowd movements turn into life threatening crowd crushes and stampedes. Numerous demographic, physiologic and environmental factors are known to influence the movement dynamics of crowds. Besides that, seemingly similar situations might develop completely different due to the nature of human behaviour. For example, while a commuter on the way back home might decide to wait in line to climb the stairs, the same commuter in a rush to get to work might try to push through the waiting crowd.

Recent advancements in the pedestrian simulation research community enable the use of simulation models to provide insights into the walking dynamics of pedestrians. Increases in computer power have opened up the possibility to simulate the walking dynamics of pedestrians in a crowd during large-scale events. While two decades ago the simple Cellular Automata (CA) models of Blue & Adler (1998), which could simulate a hundred agents, were cutting-edge, sophisticated multi-agent systems can nowadays simulate thousands of agents with distinctive characteristics in real-time (Jaklin et al., 2013). By means of these new simulation models, mechanisms that drive crowd movement dynamics can be tested. Furthermore, once calibrated and validated, these pedestrian simulation models could be used to predict and assess the walking dynamics of pedestrians in a crowd during large-scale events.

Even though the capabilities of pedestrian simulation models are nowadays seemingly limitless, it is not known whether these models can simulate the walking dynamics of pedestrians in a crowd during large-scale events in a valid and reliable manner. First and foremost, because it is unclear whether the structure of these models allows for the simulation of all crowd movement phenomena. In addition, pedestrian simulation models have only been scarcely calibrated and validated up to this moment (Isenhour & Löhner, 2014). That is, most contemporary pedestrian simulation models have been calibrated and validated for very specific movement situations, i.e. uni-directional and bi-directional movements of a limited number of individuals. Extrapolating the simulation models beyond the situations for which these models were validated might introduce extensive errors in the resulting movement dynamics.

In order to develop, calibrate and validate a simulation model that can predict the walking dynamics of pedestrians in crowds at large-scale events, one needs to 1) understand the walking dynamics one should capture, 2) understand which crowd movement phenomena are essential in the correct display of these dynamics, 3) obtain empirical data sets which feature these dynamics, and 4) have methods to translate the data sets to empirical findings. While the achievement of the third is mainly dependent on the amount of time and resources one is willing to spend on the acquisition of the data sets, the achievement of the first, second and fourth requirements are subject to the current level of knowledge with respect to the walking dynamics, crowd movement phenomena and the variables which describe these dynamics and crowd movement phenomena.

Since the walking dynamics of pedestrians within a crowd at large-scale events have so far been investigated rudimentary[1], it remains difficult to determine which crowd movement phenomena and state variables are essential to describe and predict the unfolding of large-scale crowd movements. Several researchers, among others Helbing & Molnar (2001) and Campanella et al. (2009a), have described phenomena, such as lane formation, stop-and-go waves, and turbulence, which only occur during large-scale uni-directional crowd movements. Others paid special attention to pedestrians walking around corners (a.o Steffen & Seyfried (2009), Dias et al. (2014b)) and through bottlenecks (Daamen & Hoogendoorn, 2010a).

Even though some crowd phenomena have been identified, the answers to the questions “why do these phenomena only develop during crowd movements?” and “what are the driving mechanisms behind these phenomena?” have yet to be found. The main challenges are 1) our lack of understanding of the crowd movement phenomena which shape the movement dynamics of pedestrians at large scale-events and the generic driving mechanisms behind these phenomena, and 2) which simulation models can be used to predict the development of these phenomena.

1.2 Objectives

This brings us to the central theme of this thesis. The objective of this thesis is to develop theories that describe the movement dynamics of pedestrians in crowds at large-scale events and assess pedestrian simulation models with respect to these movement dynamics. In order to do so, the operational walking dynamics of pedestrian in a crowd during large-scale events are studied empirically. Moreover, the crowd movement phenomena that develop during large-scale events are established. Besides that, the developed theories on pedestrian movement dynamics and crowd movement phenomena are directly utilized to assess two pedestrian simulation models.

[1]The research into pedestrian walking dynamics and crowd movement phenomena generally studied simple stable uni-directional situations with a limited uniform demand and a homogeneous population.

New crowd movement theories and models need to be developed one step at a time. Consequently, the main objective of this thesis is broken down into four sub-objectives:

- To develop a theoretical framework that describes the walking dynamics of pedestrians within a crowd at large-scale events.
- To develop a list of pedestrian walking dynamics and crowd movement phenomena that develop during large-scale events.
- To develop a theoretical framework for the assessment of pedestrian simulation models
- To assess pedestrian simulation models with respect to the walking dynamics of pedestrians in a crowd and crowd movement phenomena that develop during large-scale events.

The research approach for each of these sub-objectives is detailed in section 1.7.

1.3 Scope

Professionals from distinct research fields might interpret the main topic of this thesis (i.e. a study of walking dynamics of pedestrians at large-scale events) differently. Therefore, the following paragraphs details the words ‘walking dynamics’, ‘crowd’ and ‘large-scale event’ in light of this thesis. These definitions will be used throughout this thesis.

1.3.1 Pedestrian walking dynamics

In this thesis, the words ’pedestrian walking dynamics‘ are used to describe the physical operational walking dynamics of individual pedestrians within a demarcated space and a demarcated period of time while interacting with other individuals and being part of a crowd during a large-scale event.

When defining pedestrian movement behaviour in this manner, the scope of this thesis excludes several other behaviours. First and foremost, the movement decisions generated at the tactical and strategic level are not studied within this thesis (see Hoogendoorn & Bovy (2004) for more details). That is, tactical (route choice) and strategic decisions (activity choice and scheduling) are assumed to be known or predetermined via other models. Since the decisions at the tactical and strategic level cannot be completely separated from the decisions at the operational level, the results of the higher-level decision processes will be mentioned when they influence the operational walking dynamics of pedestrians.

Furthermore, only the perceptible movement behaviour of pedestrians is taken into account. The mental and intellectual processes within the brains of pedestrians, such as for instance believes, desires, intentions, stress, vision capabilities and limitations on the processing capabilities of pedestrians, are not studied.

Lastly, this thesis does not account for the influence of grouping behaviour. The behaviour of pedestrians in groups adds to the complexity due to its multidisciplinary nature (e.g.

sociological, psychological, physical). In order to restrict the complexity of the theory developed within this thesis, grouping behaviour is placed outside the scope of this research. Given that previous research suggests that the grouping behaviour might be additive to the basic walking dynamics of singular individuals (e.g. Moussaïd et al. (2010)), the impact of this decision is expected to be limited.

1.4 Type of crowd at large-scale events

In literature the word 'crowd' is adopted in almost every situation where more than two individuals are interacting with each other (Challenger et al., 2010). For instance, Hoogendoorn & Bovy (2004) and Duncan (2009) use the word to describe two entirely different settings, namely the movement dynamics of pedestrians at a train station and the movement dynamics of visitors in front of a music stage. Even in sociology, where crowds have been researched for many years (e.g. LeBon (1895), McPhail (1991) and Wijermans (2011)) the definition is quite broad.

Since this chapter uses a specific interpretation of the word crowd, first the kind of crowd which presents itself during large-scale events, and as such the type of movement dynamics that are the subject of this thesis, is described. In this thesis the following working definition is used:

> *A crowd is a large group of individuals ($N \geq 100$ P) within the same space at the same time and whose movements are for a prolonged period of time ($t \geq 60$ s) dependent on predominantly local interactions ($\rho > 0.5\ P/m^2$) with other pedestrians*

The numbers N (number of individuals), ρ (density) and t (time period) are chosen in a way as to exclude movements during which interaction is non-existent or only present for very short periods of time. Moreover, the type of crowd that is considered in this chapter has the following characteristics:

- The pedestrians are walking.
- The pedestrians are in close contact with each other (interaction distance between individuals is less than 3 meter), making multiple split-second operational movement decisions.
- The pedestrians are under no external pressure to move, but they do have a tentative goal in mind towards which they are walking. That is, these pedestrians have a non-zero walking speed.
- The atmosphere at the location where the crowd movement takes place is friendly.
- The demography of the crowd is not limited to predominantly one age-group and one gender, but is heterogeneous.
- The pedestrians might consider themselves as part of a group.
- The pedestrians carry no baggage other than small backpacks or bags.
- The pedestrians are not necessarily familiar with the layout of the infrastructure.

1.4.1 Infrastructure at large-scale events

Within this thesis the infrastructure is limited to the flow structuring elements within the movement area. That is, the infrastructure consists of the immovable elements of a certain space which structure the aggregate pedestrian flows that arise in the space (i.e. included are for example walls, doors and trees). Moreover, the space is assumed to be flat, fixed and stable. This excludes fixed moving elements such as escalators and elevators and elements that allow pedestrians to transfer between levels such as slopes and stairs. Movable objects such as dustbins, carts, buggies, bikes and vehicles are also ruled out.

Furthermore, in order to determine the effect of the flow situation within an infrastructure, this thesis investigates parts of an infrastructure in which only one dominant flow system (movement base case) is present at a certain moment in time. Since these systems are generally limited in size, this thesis focusses on one corridor, one intersection or a part of a square at the time. An exact description of the movement base cases that will be studied in this thesis is provided in chapter 2.

1.5 Approach to develop crowd movement theories and models

There are several approaches to develop a theory which can explain the walking dynamics of pedestrians within a crowd, which are either of a deductive or an inductive nature. A deductive approach allows one to explore several contemporary theories and models, select the best ones and adapt these until they display the desired behaviour. This way of performing research provides a solid basis for the scientist to depart from. An inductive research approach allows one to analyse the behaviour of the system one wants to understand, deduce its characteristic behavioural rules, and develop a simulation model that adheres to these rules.

While the emphasis in the deductive method is on the development or improvement of a model based on predefined assumptions, the inductive method emphasizes the discovery of the underlying behavioural assumptions of the movement behaviour. This inductive research approach entices the researcher to explore previously undiscovered territory. Since one of the objectives of this research is to provide a theory on the operational walking dynamics of pedestrians in a crowd during large-scale events, the discovery of the underlying behavioural assumptions provides part of the contribution this thesis is aiming for. Therefore, in this study an inductive research approach is used.

As a consequence of the chosen research approach, this study into the walking dynamics of pedestrians within a crowd starts to a certain extent from scratch. That is, this study scrutinizes whether the insights, models and/or theories developed by other researchers in earlier times are substantiated by empirical evidence of crowd movement dynamics gathered and analysed in the empirical research performed as part of this thesis earlier empirical work.

1.6 Contributions

The research presented in this thesis is expected to contribute to the community in several manners. The contributions to science and society are briefly discussed below.

1.6.1 Scientific contributions

This thesis includes the following main scientific contributions:

- A crowd movement theory describing the walking dynamics of pedestrians.
- Analysis, assessment and calibration frameworks to study walking dynamics and assess pedestrian simulation models.
- An analysis of the movement behaviour of pedestrians at large-scale events.
- The calibration and assessment of two existing pedestrian simulation models.
- A data collection and processing methodology for pedestrian trajectory data sets.
- Trajectory data sets featuring pedestrians at large-scale events.

These contributions are discussed in more detail below.

Crowd movement theory

Within this thesis a theory describing the movement dynamics of a pedestrian crowd is developed and tested. This theory places the distance headway and walking velocity at the heart of the movement behaviour of pedestrians. Moreover, it relates the characteristics of the individual, its physiological environment and the infrastructure to these two variables. Besides an improved understanding of the relations between variables which influence pedestrian walking behaviour within a crowd, this newly proposed theory also provides a point of departure for further research into the walking dynamics of pedestrians.

Analysis, assessment and calibration frameworks

Many techniques, methods and metrics have been developed over the years to study and assess pedestrian dynamics. Yet, an overview of these techniques, methods and metrics is lacking. An attempt is made to put the previous research into perspective by means of several frameworks that relate to the execution of empirical research, the analysis of the traffic state in a pedestrian infrastructure, and the modelling of pedestrian walking dynamics at large-scale events. The following frameworks are proposed in this thesis:

- A review of techniques to study the walking behaviour of pedestrians.
- A taxonomy of crowd movement base cases.
- A list of generic and specific crowd movement phenomena.
- A formalisation of variables which can be used to describe the traffic state experienced pedestrians during large-scale events.
- An assessment framework for pedestrian simulation models with respect to their capabilities of modelling crowd movement phenomena.
- A calibration framework for pedestrian simulation models which incorporates multiple criteria related to the walking dynamics of pedestrians at large-scale events.

Calibrated and assessed pedestrian simulation models

The crowd movement theory and the list of crowd movement phenomena provide the foundation of a new assessment framework that have been used to calibrate and assess two distinct pedestrian crowd simulation models, namely Nomad and the Macroscopic Dynamic Walker model. The calibrated version of these two models can be used to simulate and assess crowd movements and crowd management strategies at large-scale events.

Additionally, the models' assessment results provide insights into the contemporary capabilities and shortcomings of these two pedestrian simulation models. These assessment results provide the input for new avenues of model development.

Data collection and processing methodology

Several research tools have been developed to improve the data collection of pedestrian movements in a crowd (McSAVI) and to improve the detection and tracking processes (MODT). By means of the stand-alone multi-camera video installation (McSAVI) video material can be captured in places where there are no opportunities to fix surveillance equipment to the existing infrastructure. In MODT computer vision techniques are implemented, which allows for the semi-automatic detection and tracking of pedestrians that are not equipped with tools that aid in the detection process.

Empirical trajectory data sets featuring large-scale events

As part of the research over 45 new trajectory data sets are acquired, which detail the walking dynamics of pedestrians within a crowd for different movement base cases at several large-scale events within the Netherlands. The existent inductive research into the walking dynamics of pedestrian consists mainly of laboratory studies. To the author's knowledge this thesis is one of the first studies that examines and quantifies these dynamics comprehensively at a microscopic and macroscopic level for several distinct movement base cases based on real-life data. Besides the direct use of these data sets in the derivation of a crowd movement theory and the calibration, validation and assessment of new models, these data sets also present numerous opportunities to study the intricacies of pedestrian movement dynamics.

1.6.2 Societal contributions

Besides contributions to the scientific community, the results from this thesis also provide contributions to practice and society. In the first place, from the structure of the conceptual framework, which is presented in chapters 2 and 4, several lessons can be drawn. Given that the crowd movement theory links the characteristics of the individual, the physiological environment and the infrastructure to the microscopic flow variables, it is concluded that these characteristics all influence the walking dynamics of pedestrians in a crowd, and consequently the fundamental diagram and the capacity of a pedestrian infrastructure. In other words, this theory suggests that the fundamental diagram and the capacity of a pedestrian infrastructure change with the type of pedestrians that resides in it, the weather conditions, the underground, the geometry of the infrastructure and the predominant flow directions within the infrastructure.

Therefore, knowing which type of visitors, which conditions and which movement base cases will occur during a large-scale event is essential to ensure correct assessment and effective crowd management of pedestrian infrastructure.

Moreover, the crowd movement theory suggests a complex interplay between the three types of mentioned characteristics. Consequently, it is not straightforward to predict how a combination of characteristics influences the traffic state and capacity of the infrastructure. This shows that working with multiple scenarios and modelling by means of calibrated pedestrian simulation tools is necessary to evaluate the traffic state at large-scale events during which pedestrian mobility plays a dominant role.

As discussed in section 1.1, calibrated pedestrian simulation models have the potential to realistically predict pedestrian walking dynamics during large-scale events. These models can be used for a quantitative assessment of benefits and risks due to crowd movement dynamics at large-scale events. That is, the pedestrian simulation models calibrated and assessed in this thesis, can be used to beforehand predict the traffic state at the event grounds, and as such can be used to quantify the experience and safety of pedestrians at large-scale events. With these models venue lay-outs can be assessed for both general use and exceptional events before and during events take place.

Furthermore, these models can be used in the training of operational crowd management personnel. By showing the consequences of certain actions, more direct insights into crowd movement dynamics and the management thereof can be developed. The two assessed simulation models, which are specifically calibrated for the movement of pedestrian crowds, provide a first step towards objective risk assessment and crowd management.

These models can also aid in the optimization of network management at large-scale events. By means of scenario analysis, the global implications of local adaptations in the design of event grounds and the used management strategies can be visualized and tested. Through an iterative optimization process of both the infrastructure geometry and management strategies, the capacity of local problematic locations and the capacity of the overall event grounds can be optimized.

1.7 Outline

Figure 1.1 provides an overview of the structure of this thesis and the relation between the chapters. This thesis starts with a literature review of the empirical studies which features the walking dynamics of pedestrians in a crowd during large-scale events (chapter 2). The main objective of this review is to find qualitative and quantitative evidence identifying factors which might influence the walking dynamics of pedestrians within crowds.

Based on this comprehensive review of literature, a conceptual model of related behavioural hypotheses is presented in chapter 2. This conceptual model serves as a first indication of the

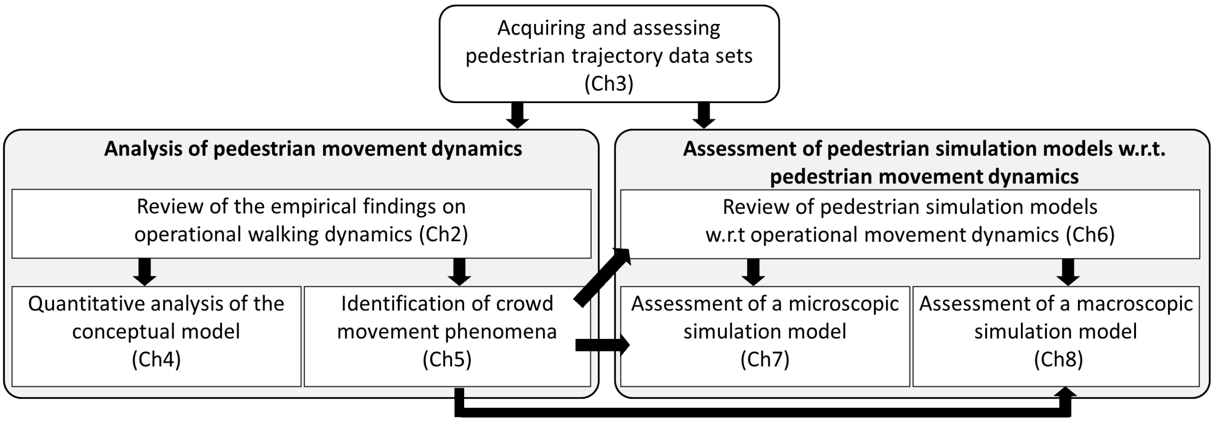

Figure 1.1: Thesis outline

possible ingredients of a new theory which details the walking dynamics of pedestrians within a crowd at large-scale events.

Since some of the factors mentioned in this conceptual model have never been studied empirically, new data sets have been collected in order to test the validity of the conceptual model. Chapter 3 describes the data collection methodology. This chapter elaborates upon the fundamental choices with respect to the techniques of capturing, transcribing and filtering of the trajectory data sets, the case studies and the mathematical description of variables used within this thesis to describe pedestrian walking dynamics.

The validity of the behavioural hypotheses, which are part of the conceptual model deduced in chapter 2, are statistically tested in chapter 4. Accordingly, an analysis of the data sets is presented in chapter 4, which identifies the crowd movement phenomena which develop during large-scale events.

Recent advancements in the pedestrian simulation research community enable the use of simulation models to provide insights into the movement dynamics of pedestrians. However, since many papers do not mention the calibration and validation of the simulation model with respect to the operational movement dynamics of pedestrians during large-scale events nor mention whether crowd movement phenomena can be represented, it is currently unknown whether any of the models can simulate this specific type of movement dynamics in a valid and realistic manner. Therefore, in chapter 6 a literature review on pedestrian simulation models is performed that provides insights in the capabilities of the contemporary pedestrian simulation models.

This review shows that several microscopic and macroscopic pedestrian simulation models are able to predict most crowd movement phenomena. Yet, also for these models it is unknown whether all crowd movement phenomena can be predicted accurately due to the lack of calibration for this specific type of movement. Therefore, the capabilities of a microscopic (Nomad) and a macroscopic model (MDW) are assessed more thoroughly in chapters 7 and 8.

However, before an assessment of any model's capabilities can be made, first the influence of the parameter settings on the model's predictions are studied by means of a sensitivity analysis. Accordingly, the models are first calibrated specifically for pedestrian movements at large-scale events by means of the data sets described in chapter 3. Last of all, the models are assessed using the lists of crowd movement phenomena developed in chapter 5.

The last chapter of this thesis (Chapter 9) puts the work presented in this thesis into a broader perspective. First, the major conclusions of this thesis are presented and discussed. Subsequently the contributions of this thesis are reviewed. This thesis ends with some directions of further study.

Chapter 2

Review of the findings on operational movement dynamics of pedestrians in crowds at large-scale events

Our understanding of crowd movements has rapidly increased over the course of the last decades. The work of among others Henderson (1971), Fruin (1971) and Predtechenskii & Milinskii (1969) has provided methods to quantify the dynamics of pedestrian movements. In recent years, among others Daamen & Hoogendoorn (2003a), Seyfried et al. (2007) and Moussaïd et al. (2009), have improved our understanding of the exact relations between the aggregate movement dynamics of pedestrians and the macroscopic and microscopic flow characteristics mentioned by these earlier studies.

The objective of this chapter is to determine which insights into the movement dynamics of pedestrians in crowds at large-scale events can be derived from empirical studies. This chapter puts forward a comprehensive theory and conceptual model of related behavioural hypotheses which explains how the characteristics of the pedestrians, their physiological environment and the infrastructure influence the operational movement dynamics of the crowd. The behavioural hypotheses incorporated within the conceptual model generate insights into the relations between velocity, density, flow, distance headway, the angle of interaction, the variability of interactions, age, temperature, the number of pedestrians within the infrastructure, and the infrastructure geometry.

This chapter is an adapted and updated version the first part of the following published paper:
Duives, D.C., W. Daamen, and S.P. Hoogendoorn (2015). Proposition and testing of a conceptual model describing the movement of individual pedestrians within a crowd.
Transportation Research Procedia, 9, pp. 36-55.

The remainder of this chapter elaborates on the insights that can be derived from the literature and on the development of a conceptual model. In the following section first the methodology of systematic review of the research literature is briefly elaborated upon. Sections 2.2 to 2.5 detail the results of a comprehensive literature review. Section 2.2 reviews the literature with respect to the influence of demographic characteristics of the pedestrian on the movement dynamics of the crowd. Section 2.3, accordingly, reviews the literature that quantifies the influence of the physiological environment. The influence of the interaction between individuals is reviewed in section 2.4. Section 2.5 reports the quantitative evidence with respect to the influence of movement base cases and infrastructure geometry. Subsequently, the conceptual model is proposed and discussed in section 2.6. Section 2.7 concludes this chapter and puts the conceptual model into context.

In this chapter a conceptual model is derived that describes the movement dynamics of pedestrians in crowds at large-scale events. Since new variables and relations are introduced in the conceptual model, it is necessary to test this model. Therefore, in chapter 4 the model is corroborated based on empirical data sets that are described in chapter 5.

2.1 Systematic review methodology

A large body of literature with respect to pedestrian movement dynamics is available, which considers the engineering as well as the biological, sociological and psychological side of pedestrian movement dynamics. Since the aim of this research is to create insights into the operational movement dynamics of pedestrians within a crowd during large-scale events, this thesis only reviews studies that indicate influences with respect to the actual physical walking movements of pedestrians and variables that describe the situation at large-scale events. As such, most of the psychological and sociological research is outside the scope of this study. Additionally, strategic and tactical route choice behaviour are not discussed.

Furthermore, in the last decade numerous simulation models have been proposed in order to increase the understanding of pedestrian movement dynamics at large-scale events, see chapter 6 for a more elaborate description of these studies. Since most of these studies have refrained from rigorously calibrating and validating their models, the results of most simulation studies can be questioned (Duives, 2012). For that reason, only studies that mention empirical findings with respect to factors that are influential to the movement dynamics of pedestrians in crowds at large-scale events are reviewed in this chapter. In our review, we will consider four categories of factors that influence the movement dynamics of pedestrians in a crowd: a) the personal characteristics, b) the physiological environment, c) the characteristics of the one-to-one interaction and d) the movement base cases that develop within the infrastructure when many pedestrians interact. For each category the relation between the factors and variables that describe the traffic state (such as velocity, density, flow, distance headway, time-to-collisions) are determined.

2.2 Influence of pedestrians' personal characteristics

Each pedestrian is a distinct individual. As such, it is expected that the operational movement behaviour of each pedestrian is slightly different depending on the characteristics of the individual. Four personal characteristics of the pedestrian are discussed, namely age, gender, country of residence and physique.

Several studies within and outside the field of traffic engineering have focused on the relation between *age* of a pedestrian and the walking velocity adopted by the pedestrian (among others Navin & Wheeler (1969), Henderson (1971), Knoblauch et al. (1996), Crosbie et al. (1997), Bohannon (1997), Dunbar et al. (2004), Avineri et al. (2012)). Since the quantitative relationships found by these studies depend severely on the employed age-groups, the results vary between studies. Yet, all studies agree that the average walking velocity of pedestrians decreases non-linearly when pedestrians grow older, for pedestrians over 18 years old and over.

Besides age, the influence of *gender* on the movement dynamics of the pedestrian has been studied. Several European studies from the 80ies and 90ies mention, as a by-product of their study, that there is a significant difference between the walking velocity of men and women (Boles (1981), Tanariboon et al. (1986), Knoblauch et al. (1996), Crosbie et al. (1997), Bohannon (1997), Avineri et al. (2012), Chandra & Bharti (2013), Duives et al. (2014b)). On average, women walk slower than men.

A correlation between the walking velocity and the *country of residence*[2] (also dubbed *culture* in this thesis) of the pedestrians has also been described in the research literature (Tanariboon et al. (1986), Koushki (1988), Tanariboon & Guyano (1991), Chattaraja et al. (2009), Tian et al. (2011), Chandra & Bharti (2013)). In most studies on average walking speed of pedestrians was lower in African and Asian countries than in most Western countries. Chattaraja et al. (2009) is an exception on this rule, given that they found a similar free-flow speed. The results of Lam et al. (1995), Chattaraja et al. (2009) and Tian et al. (2011), furthermore, suggest that cultural differences have a more widespread effect on pedestrian movement behaviour than only the influence on the average walking velocity. Chattaraja et al. (2009), for instance, illustrate that the jam density in the experiments with Indian test persons was higher than in the experiments with German test persons.

The physical dimensions of the pedestrian are expected to be of importance, because the circumference indirectly influences the distance headway and density experienced by pedestrians. Besides that, the physical fitness of a pedestrian is expected to be of influence on the walking velocity. Yet, in the literature no proof is found that the *physical dimensions* or the *physical fitness* of pedestrians play a role in the operational movement behaviour of pedestrians. It is unclear whether these relations do not exist or have not yet been studied. Therefore, no conclusions can be drawn with respect to the relation of this variable and the macroscopic flow variables.

[2]Most studies have been performed based on video data in which only the presence of pedestrians within a certain country is accounted for. Therefore, this characteristic is dubbed country of residence

Table 2.1: Relations between characteristics of the pedestrian and the flow variables, as found in empirical research.

Variable	Characteristics	Relation
Velocity	Age	$>$ 18 years: average walking velocity decreases with age.
Velocity	Gender	On average, males have a higher walking velocity then females.
Velocity	Culture	Pedestrians in Africa and Asia walk slower than pedestrians in most Western countries.
Velocity	Physical dimensions	Undetermined.
Velocity	Physical fitness	Undetermined.

Combining the trends described above, table 2.1 can be constructed. As one can see, only relations between the walking velocity and some of the personal characteristics of the pedestrian have been mentioned in the literature. It is difficult to indicate whether this is due to the lack of studies into the other relations or due to the lack of actual significant results of these studies.

2.3 Influence of the physiological environment

During large-scale pedestrian events the movement dynamics of pedestrians is not only governed by the characteristics of the pedestrian. Most large-scale events take place outdoors. In such situations the physiological environment of the pedestrians also influences their behaviour. The weather conditions and the stability of the substratum are assume to be the most dominant factors of the physiological environment. Therefore, the influence of these physiological characteristics is discussed separately underneath.

Precipitation and sun shine are known to influence the decision to walk (Aultman-Hall et al. (2009)). Yet, studies which investigate the effect of precipitation and/or sunshine on the movement dynamics of pedestrians are rare. Knoblauch et al. (1996) shows that the average walking velocity increases slightly for respectively dry – 1.47 m/s, drizzle – 1.52 m/s, rain – 1.60 m/s and snow – 1.60 m/s. From this study, it might be concluded that a more uncomfortable[3] outdoor environment (snow and rain) results in a higher mean walking velocity.

Several other studies elaborate on the relation between *temperature* and pedestrian movement dynamics (Hoel (1968) as mentioned in Walmsley & Lewis (1989), Rotton et al. (1990)). The findings of these studies disagree with each other. Where Hoel (1968) finds a negative relation, Rotton et al. (1990) find a positive relation between temperature and walking velocity. Yet, based on the differences in the characteristics of the research set-up, it might be concluded that pedestrians react differently depending on the duration of the period a pedestrian experiences a certain temperature.

Also *wind conditions* are mentioned as a factor of influence by some studies. Hunt et al. (1976)[4] summarized previous findings with respect to the response of individuals to wind. This

[3]Uncomfortable does not refer to the condition of the substratum (e.g. slipperiness, stability).

[4]This research studied subjective verbal assessments of pedestrians, not their movement dynamics.

Table 2.2: Relations between the characteristics of the physiological environment and the flow variables, as found in empirical research.

Variable	Characteristics	Relation
Velocity	Physiological environment	Velocities increases if environment becomes less friendly
Velocity	Temperature	Might depend on time period a pedestrian is exposed to temperature
Velocity	Wind (stable)	Negative ($v_{wind} > 13m/s$)
Velocity	Wind (gusty)	Negative ($v_{wind} > 9m/s$)
Energy expenditure	Unevenness of the substratum	Negative
Energy expenditure	Stiffness of the substratum	Negative
Energy expenditure	Gradient of the substratum	Negative ($gradient < -0.1$) or positive ($gradient > -0.1$)
Energy expenditure	Softness of the substratum	Negative
Walking velocity	Type of substratum	Depending on the type of substratum

study concludes that in steady uniform wind conditions pedestrians experienced difficulties walking at wind speeds above 13 m/s. The study also shows that in non-uniform and gusty winds pedestrians experience difficulties walking at average wind speeds higher than 9 m/s. Furthermore, Jordan et al. (2008) conclude that the *orientation with respect to the wind direction* and the *body weight* of a person severely affected the stability of pedestrian movements, and as such their average walking velocity.

Last of all, the *substratum* is one of the common environmental factors that changes during large-scale events. Studies into the influence of this variable find that *energy expenditure* increases with the unevenness of the terrain (Volonoshina et al. (2013)), a decrease of the stiffness of the terrain (Weidmann (1993), Kerdok et al. (2002)), an increase or decrease of the slope with respect to a gradient of -0.1 (Minetti et al. (2002)), and the softness of the terrain (Leicht & Crowther (2008)). Besides that, Leicht & Crowther (2008)) also found that the free walking velocity decreased for pedestrians walking over respectively grass (1.56 m/s), wet beach sand (1.54 m/s) or dry beach sand (1.38 m/s) in comparison to a similar walk over a concrete substratum (1.56 m/s).

The influences mentioned in the research literature with respect to the physiological environment are summarized in table 2.2. The table illustrates that the empirical studies mentioned in this section have been focused specifically on the influence of the physiological characteristics on the walking velocity and the energy expenditure. Besides that, the findings suggest that the movement dynamics of pedestrians are indeed influenced by the weather conditions and substratum characteristics. Therefore, when researching the operational dynamics of pedestrians at large-scale events, it is imperative to record and standardise the physiological characteristics as much as possible.

2.4 Influence of interaction between pedestrians

Pedestrians do not always walk through spaces in which no other pedestrians are present. Interactions with other pedestrians occur. These interactions, which are assumed to represent our reaction on the presence of others, influence the overall walking behaviour of a pedestrian crowd. This section presents the empirical findings on the influence of the characteristics of the interaction on the movement behaviour of pedestrians.

Interaction can take place via spoken signals, physical body-to-body contact or the interpretation of non-verbal signals (i.e. the interpretation of physical signals that communicate a pedestrian's intentions at a distance). Given the scope of this research, this review only discusses the empirical research with respect to this last category.

Several researchers examined the microscopic interaction behaviour of pedestrians (among others Goffman (1972), Wolf (1973), Hill (1982), Alghadi et al. (2002), Moussaïd et al. (2009), Versluis (2010), Daamen et al. (2014)). Most of these only mention the qualitative results with respect to the influence of the characteristics of the interaction on the movement dynamics of pedestrians.

To the author's knowledge, only four studies have examined the microscopic interaction behaviour of pedestrians quantitatively. In case of intersecting movements, Versluis (2010) finds that the *side on which pedestrians pass* each other is dependent on the direction of the approach. Moussaïd et al. (2009) mention that in head-on encounters a binary decision takes place, in which pedestrians have a bias to one side. Next to that, Versluis (2010) illustrates that the more face-to-face the interaction between the two pedestrians becomes, the more pedestrians prefer to pass each other on the culturally biased side. This study also shows that pedestrians who are in a *hurry* are more likely to pass in front (Daamen et al., 2014). The results of Alghadi et al. (2002) suggest that interactions where pedestrians face each other are more efficient. In case of uni-directional movements, Dachner & Warren (2014) conclude that the angular acceleration of a pedestrian is a result of an attempt to minimize the heading difference.

Versluis (2010) moreover mentions that in lateral direction pedestrians simply adjust their direction of motion (and not their walking velocity) to avoid collisions. This study also found that both an increase in *goal-orientation* and *group size* increases the probability of passing in front of another pedestrian in crossing situations.

Additionally, Versluis (2010) analysed the influence of the *angle of interaction* on the collision avoidance behaviour. Versluis (2010) found that pedestrians retain a larger *lateral evasion distance* in bidirectional situations and a larger *longitudinal evasion distance* in intersecting situations. Furthermore, for men a larger evasion distance was found than for women. Besides that, hurried pedestrians were found to retain a larger lateral evasion distance than normally walking pedestrians. Similarly, individuals retained larger evasion distances with respect to small groups than to other individuals.

Table 2.3: Relations between the characteristics of the interaction of two pedestrians and flow variables, as found in empirical research.

Variable	Characteristics	Relation
Side of passing	Direction of approach	Dependent on the direction of the approach.
Side of passing	Head-on encounter	A binary decision, with bias to the right side.
Side of passing	Angle of interaction	The larger the angle, the more pedestrians prefer passing each other on the culturally biased side.
Side of passing	Goal orientation	More hurry, the more likely to pass in front
Evasion distance	Flow situation	Depending on the interaction situation, a larger lateral or longitudinal evasion distance is retained.
Evasion distance	Gender	Men retain a larger evasion distance than women.
Evasion distance	Group size	Individuals retain a larger evasion distance with respect to groups.
Heading difference	Angular acceleration	Angular acceleration increases if the heading differences increases.
Efficiency of walking	Direction of approach	The more pedestrians are approaching in opposite directions, the more efficient.

Table 2.3 summarizes the findings of the empirical research mentioned in this section. The table shows that the empirical research on the influence of one-to-one interactions between pedestrians has mainly been focused on the qualitative characteristics of the passing behaviour of pedestrians. Some first results on the influence of the evasion distances is mentioned.

2.5 Influence of the movement base case

Crowd movements arise from the aggregate motion of numerous interacting pedestrians, all of which make their own decisions, have their own goals and follow their own path. Even though the underlying walking behaviour seems random, within an infrastructure several configurations of flows can be distinguished. In the following section first the idea of a movement base case is explained. Afterwards this section reviews the empirical findings with respect to the influence of the movement base cases within an infrastructure on the movement dynamics of pedestrians.

2.5.1 Derivation of movement base cases

This section identifies a comprehensive list of distinct movement base cases that might occur when pedestrian flows mingle. The movement base cases have been chosen such that only one predominant action is performed by the pedestrians at any given time. Moreover, the cases together cover the range of pedestrian crowd movement dynamics occurring often during large-scale events.

Figure 2.1 presents the taxonomy describing the crowd movement base cases. Figure 2.2 subsequently shows the eight resulting crowd movement base cases. Yet, the research literature with respect to the influence of movement base cases does not distinguish all eight movement base cases. Instead, the studies on this topic can roughly be divided into five more aggregate cases, namely: a uni-directional straight flow, a uni-directional flow through a corner, a

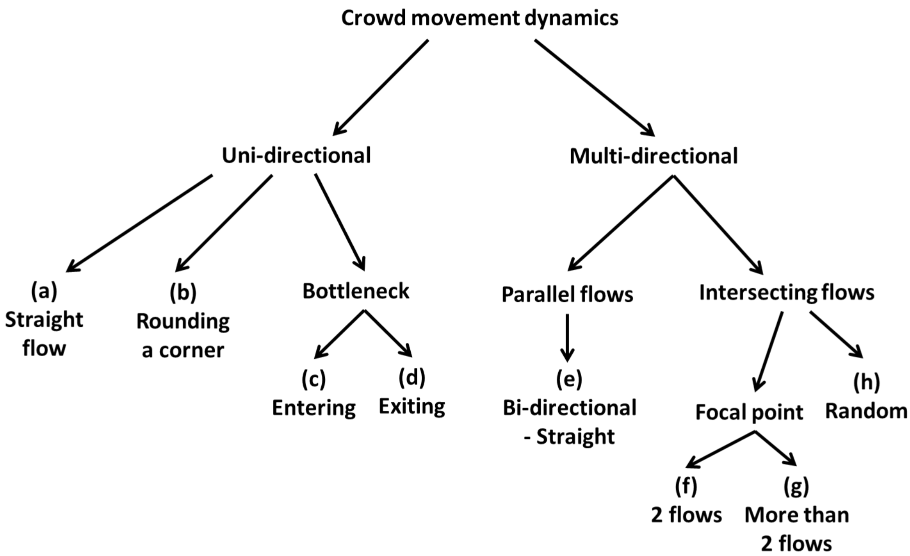

Figure 2.1: Taxonomy crowd movement base cases.

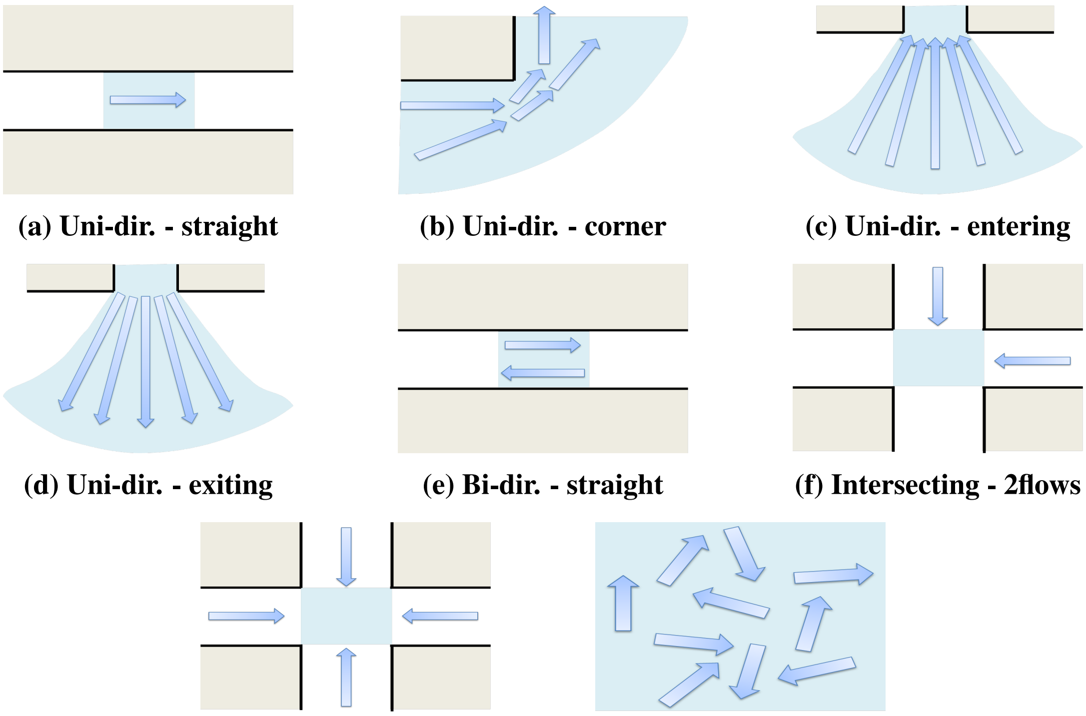

(a) Uni-dir. - straight (b) Uni-dir. - corner (c) Uni-dir. - entering

(d) Uni-dir. - exiting (e) Bi-dir. - straight (f) Intersecting - 2flows

(g) Intersecting - 4flows (h) Intersecting - random

Figure 2.2: Visualization of crowd movement base cases.

uni-directional flow through a bottleneck, a bi-directional flow, and an intersecting flow (generally a focussed intersection of two flows under a 90° angle).

Figure 2.1 shows that two categories of the contemporary research literature have been further specified. The research by Daamen & Hoogendoorn (2010b) and Duives et al. (2014a) provides an indication that at an aggregate level behavioural differences exist between movement base cases c and d. In this thesis it is assumed that the operational movement behaviour of pedestrians during these two movement situations can differ. Therefore, the category "uni-directional bottleneck movement base case" has been split into two separate categories, namely a uni-directional entering flow and a uni-directional entering flow.

Next to that, the category 'intersecting flow' can be further disentangled based on the number of flows present at the intersection and the space available to complete the intersecting movements. The interaction of several flows within a large open space (i.e. market square) might cause a random intersecting situation (Fig. 2.2h), where each pedestrian interacts consecutively with individual pedestrians shortly after each other. However, when only limited space is available for pedestrians to complete the intersecting movements, they are forced to interact with multiple pedestrians at the same time. Besides that, in the case of only two flows pedestrians always interact under a similar angle of interaction (Fig. 2.2f&g), while in the case of multiple flows the angle of interaction changes per interaction over time and over space (Fig. 2.2h). Consequently, depending on the amount of flows, the predictability of the movement base case changes.

Since the research endeavours carry many similarities within a category, but differ severely between categories, underneath the findings of the existing research is discussed per category. As mentioned before, only five of the eight movement base cases have been mentioned in literature (i.e. a, b, c+d, e and f). Therefore, only these five categories will be discussed in the following subsections. Furthermore, in order to establish (dis)similarities between research results, it is essential to know which research methodology was followed. Therefore, only the papers that mention the methodology of the empirical research and quantitative results of such endeavours are mentioned in the following section.

2.5.2 Uni-directional straight flow

A great number of studies have investigated the pedestrian movement behaviour of pedestrians walking in the same direction. In such situations, generally no flows in other directions and no flow-hampering infrastructure (bottlenecks) are present. Many researchers indicate to have performed research into this movement base case, but quite a lot of them did not mention whether they actually studied a bi-directional (two opposite interacting flows) or uni-directional straight movement base case. This section reviews all studies that do not explicitly mention the presence of a counter flow.

Most studies featuring a uni-directional straight movement base case mention quantitative results concerning one of the macroscopic flow variables (among others Milinskii (1951), O'Flaherty & Parkinson (1972), Tanariboon et al. (1986), Mori & Tsukaguchi (1987), Koushki (1988), Tanariboon & Guyano (1991), Lam et al. (1995), Sarkar & Janardhan (1997), Daamen & Hoogendoorn (2003b), Seyfried et al. (2007), Helbing et al. (2007b), Kholshevnikov et al. (2008), Zhang et al. (2010), Rahman et al. (2012), Zhang et al. (2013), Chattaraja et al. (2013)). Free flow speeds ranging between 1.19 m/s (Lam et al. (1995)) and 1.58 m/s (Daamen & Hoogendoorn (2003b)) are mentioned. Many studies do, however, not indicate the density levels experienced by the pedestrians during the experiments. The studies that do, mention density values between 0 and 7 P/m^2. Two exceptional results are presented by Milinskii (1951) (according to Kholshevnikov et al. (2008)) and Helbing et al. (2007b), since these studies both recorded local densities higher than 9 P/m^2 at a stable velocity of approximately 0.3 m/s.

Several researchers studied the relation between the macroscopic flow variables. These studies all agree that the velocity of a pedestrian is negatively correlated with the density experienced by a pedestrian. There have been attempts to unify these findings by means of a fundamental diagram which relates velocity, density and flow rate (e.g. O'Flaherty & Parkinson (1972), Tanariboon et al. (1986), Mori & Tsukaguchi (1987), Koushki (1988), Tanariboon & Guyano (1991), Sarkar & Janardhan (1997), Daamen & Hoogendoorn (2003b), Seyfried et al. (2007), Helbing et al. (2007b), Kholshevnikov et al. (2008), Zhang et al. (2010), Rahman et al. (2012), Zhang et al. (2013)). However, these attempts have not resulted in a uniform diagram. The shape of the curve, the capacity, the free-flow velocity and the jam-density are not agreed upon.

In recent years also the relation between the individual walking velocity and the distance headway has captured the attention of researchers. Seyfried et al. (2007), Chattaraja et al. (2013) and Lv et al. (2013) mention a positive non-linear relation between these two variables. Song et al. (2013) and Appert-Rolland et al. (2014b), however, establish that this relation is linear and can be divided in parts that are separated by sharp transitions, namely a free flow regime, a weakly constrained regime and a strongly constrained regime.

Besides relations between the macroscopic and microscopic flow variables, several self-organisation phenomena have been mentioned in literature. Self-organisation is defined as the spontaneous establishment of qualitatively new behaviour through the non-linear interaction of many objects or subjects (Helbing & Johansson, 2010) without the intervention of external influences (Camazine et al., 2010). For a uni-directional straight flow movement base case Helbing et al. (2007a) found Stop&Go waves at the Jamarat bridge. These are temporarily interrupted longitudinally waves that appear at higher densities in a uni-directional straight movement base case. In even more dense regimes, turbulent flows were found (e.g. Jiayue et al. (2014)). That is, a pedestrian has no control over its own movements any more and is moved by the surrounding crowd. Local force-based interactions between pedestrian bodies occur during turbulent situations.

2.5.3 Walking around a corner

Several studies consider the movement of pedestrians around corners with different angles (Steffen & Seyfried (2009), Zhang et al. (2011b), Gorrini et al. (2013), Dias et al. (2014b,a) and Corbetta et al. (2014)). The studies by Steffen & Seyfried (2009) and Corbetta et al. (2014) only qualitatively describe the movement of the pedestrians. Both studies find that pedestrians cut the inside corner a little bit, but that they regain their former distance with respect to the wall. Furthermore, these studies mention that the inner part of the corridor is generally not used. Most other studies showed similar effects. Moreover, Corbetta et al. (2014) illustrate that the *distance to the inside of the corner* depends on the presence of a counterflow. That is, pedestrians walk more towards the right during a bi-directional flow situation.

One of the first to quantitatively describe this movement base case is Zhang et al. (2011b), who study the quantitative differences in movement dynamics *upstream and downstream* of the corner by means of a fundamental diagram. The resulting relations between velocity and density deduced for the movement behaviour before and after the bend are found to be negative and alike. Within the bend, no fundamental diagram has been deduced.

Three studies mention the negative influence of the *turning angle* of the corridor on the movement dynamics (i.e. Gorrini et al. (2013), Dias et al. (2014a,b)). Gorrini et al. (2013) mention a similar decrease of the flow rate in a controlled experiment with students. A significant decline of the walking velocity and flow rate were found between paths with angles of $45-60$, $0-60$, $0-90$ and $45-90$ degrees. Dias et al. (2014a) and Dias et al. (2014b) find that the decrease of the walking velocity occurs at the moment that pedestrians turn the corner. Moreover, the latter two studies find an almost linear increase of the instantaneous walking direction.

2.5.4 Entering and exiting flows

A third group of studies has focussed on the movement of pedestrians through a bottleneck. Most of these studies (Yanagisawa et al. (2009), Cepolina & Tyler (2005), Kretz et al. (2006b), Zhang et al. (2008), Daamen & Hoogendoorn (2010b), Liao et al. (2014)), find a decline of the maximum flow rate, also named capacity, with a decreasing *bottleneck width*.

The capacity found by these studies differs severely. These differences are, among other things, ascribed to physical characteristics of the population (e.g. Daamen & Hoogendoorn (2010b)) and the geometry of the infrastructure (e.g. Zhang et al. (2008), Liddle et al. (2009)). One research group mentions a step-wise decline (Hoogendoorn, 2004), while most others found a linear decline of the maximum flow rate for bottlenecks with a door width of more than $0.8m$ (Kretz et al. (2006b), Seyfried et al. (2009), Liddle et al. (2009), Song et al. (2011), Liao et al. (2014)).

Liddle et al. (2009) and Zhang & Seyfried (2014b) show that the *bottleneck length* has no influence on the maximum flow rate. Only really short bottlenecks were found to perform different, due to the turning movements pedestrians make at the bottleneck location. These body turning movements around the edge of the bottleneck allow more pedestrians to enter and exit the bottleneck simultaneously. This movement has only been registered for experimental set-ups with very short bottlenecks, such as for instance door openings (a.o. Daamen & Hoogendoorn (2010b)).

To the author's knowledge no study directly related the walking velocity to the *geometry of the bottleneck*. Berg (2009), however, shows that the walking velocity increases after the moment of passing the bottleneck. Besides that, one study mentions the results with respect to the influence of the bottleneck geometry on the density. Liddle et al. (2009) show that the density becomes highest directly upstream of bottlenecks of a limited width.

Three studies relate the macroscopic flow variables by means of a fundamental diagram (Daamen & Hoogendoorn (2003a), Seyfried et al. (2009), Song et al. (2011)). The resulting graphs are different in shape, free flow velocity and jam density. As such, it is difficult to draw conclusions based on these results.

Daamen & Hoogendoorn (2003b) moreover, show that depending on the *measurement location*, the fundamental diagram changes shape. This finding suggests that there might be differences between the movement behaviour of pedestrians upstream, in and downstream of a bottleneck. The study by Duives et al. (2014a) further substantiates this so-called 'anticipation effect'.

Three other self-organisation phenomena have been described at an operational level upstream, in and downstream of bottlenecks, namely herding (Helbing et al., 2005), the zipper-effect (Hoogendoorn & Daamen, 2005) and the faster-is-slower effect (Helbing & Johansson, 2010). The first effect describes the case where individuals follow each other instead of taking the global optimal route. The zipper-effect describes the situation in which individuals allow others within the territorial space diagonally in front of them, as long as the direct space in front of their feet is still empty, which implies that pedestrians do not follow the pedestrian closest by, but the pedestrian directly in front of them. It allows for narrower lanes in a bottleneck than the expected width of a pedestrian's territorial zone. The third effect (faster-is-slower) describes the situation where higher densities cause collisions that (temporarily) stops a group of pedestrians by arc formation from moving forwards and consequently limit the flow rate.

2.5.5 Bi-directional straight flows

Many researchers have quantitatively studied the movement behaviour of pedestrians in a bi-directional flow. Generally, the studies recorded densities of $0P/m^2 < \rho < 4P/m^2$ and walking velocities of $0\ m/s < v < 1.75\ m/s$. Exceptional in this group of studies is the study of Alghadi et al. (2002), which record densities between 2.7 P/m^2 and 5.86 P/m^2.

Most of the research into bi-directional movement base cases has been focussed on the capacity of the corridor (Navin & Wheeler (1969) according to Weidmann (1993) and Zhang et al. (2012), Fruin (1971), Lam et al. (2002), Helbing et al. (2005), Kretz et al. (2006a), Zhang et al. (2012)). The results of these studies do not agree on the influence of bi-directional movement base cases on the reduction of the flow rate. Navin & Wheeler (1969) and Liu et al. (2014) mention a slight reduction of flow dependent on directional imbalances, while Lam et al. (2002) reveal that flow rates are equal. Helbing et al. (2005) indicate that counter flows are significantly more efficient than unidirectional flows. This while the results of Kretz et al. (2006a) show a decrease of the flow rate in case of a bi-directional straight movement base case. This last study, furthermore, illustrated that pedestrians react to the existence of a bi-directional flow by accepting higher densities and using the available space more efficiently. Since these studies used different experimental set-ups, it is difficult to establish whether these studies are contradictory, or whether they investigated different issues. The efficiency gain might possibly be due to the self-organisation phenomenon 'lane formation' (e.g. Hoogendoorn & Daamen (2004)). During this process a number of lanes of varying width form dynamically in a corridor, where a lane is stream of pedestrians who walk in each other's footsteps and follow a similar route through the infrastructure.

Besides the influence of a bi-directional movement base case on the flow rate, several studies also researched the influence of this movement base case on the walking velocity. Saberi et al. (2015), illustrate that the velocity distribution of highly mixed and stable segregated crowds (i.e. lane-formation) does not largely differ. Alghadi et al. (2002) mention that the velocity of a directional group is dependent on the concentration levels in each of the opposing pedestrian streams present at a cross-section. In addition, Daamen & Hoogendoorn (2007) discover a reduction of the velocity due to the interaction with the opposing flow. A recent study by Guo et al. (2012), furthermore, indicates that the walking velocity is also negatively correlated with the densities of the pedestrians downstream from them moving along in the same direction (i.e. look-ahead behaviour).

The only two studies to explore the effects of bi-directional behaviour on the shape of the fundamental diagram are Zhang et al. (2012) and Zhang et al. (2014). These studies indicate that head-on conflicts in situations with multiple lanes have a similar negative influence on the movement behaviour as the conflicts at the borders of stable separated flow lanes for densities $\rho \leq 3.5\ P/m^2$. Additionally, they find no significant difference between the fundamental diagrams of uni-directional and bi-directional movement for densities $\rho\ \leq 1.0\ P/m^2$ (free flow). However, for densities $\rho \geq 1.0\ P/m^2$, the recorded velocities in a uni-directional flow are larger than that of bi-directional flow. Consequently, the fundamental diagrams, and as such the capacity, of these two movement base cases appear to be different.

2.5.6 Intersecting flows

The last strand of empirical research into movement base cases relates to intersecting flows. In the research literature five studies were discovered which study the movement behaviour of pedestrians in a situation where two flows are intersecting[5]. Of the five studies only three mention quantitative results.

[5]Pedestrians are intersecting when their velocity vectors are under an angle between 10° and 170° and the movements of pedestrians is influenced by the presence of pedestrians of the other direction.

An elaborate study by Wong et al. (2010) deduces a negative relation between the *intersection angles* ranging from 45° to 180° and the walking velocity of pedestrians. The reduction of the walking velocity is hypothesized to be due to an increase of the interaction effects between the conflicting streams, which in turn is due to an increase of the intersection angle. This is in line with the findings of Asano et al. (2007) (according to Asano et al., 2010), who conclude that the intersection angle of the two flows negatively influences the walking velocity of pedestrians.

Moreover, during a crossing situation with a 90° angle, pedestrians tend to avoid collision by waiting (temporal avoidance) rather than changing direction sideways (spatial avoidance). This dissimilarity with the findings of Versluis (2010) might be due to the lack of benefits that can be gained when speeding up in crowded situations. The study of Wong et al. (2010), furthermore, shows that the walking velocity is asymmetrically affected in case of an unequal flow distribution. That is, the major stream retains a higher walking velocity relative to the minor stream. This difference becomes larger when the imbalance between the flows increases.

Three studies have determined a fundamental diagram for intersecting flows, namely Wong et al. (2010), Plaue et al. (2011) and Zhang & Seyfried (2014a). However, except for the negative relation between walking velocity and density, not a lot of similarities exist between the three diagrams. The free flow velocity, the jam density and the shape of the curve all differ. This might be due to the cultural difference between the demographics of the populations used in the two studies (Western European vs. Asian). Zhang & Seyfried (2014a) shows that the diagrams for uni-directional and intersecting movements that their research group found in recent years do not differ a lot.

2.5.7 Combined trends

The preceding review of the literature on the influence of the movement base case on the movement behaviour of pedestrians shows that only very specific relations have been studied, see table 2.4 for a summary of the relations described in the literature. The self-organisation phenomena mentioned in literature have not been mentioned in this table, since cause and effect have not yet been described.

The table indicates that especially relations with respect to either the flow or the walking velocity have been studied. While the research into bottleneck behaviour and movement through a corridor under an angle has been focussed on relations with respect to the specific flow, the research into uni-directional and bi-directional flows has been specifically focussed on relations with respect to the walking velocity of individuals. Yet, depending on the movement base case distinct explanatory variables have been used. Consequently, it is difficult to establish whether the behavioural trends found for one movement base case also occur during other movement base cases. As a result, the extent to which one can extrapolate the empirical results mentioned in this section is currently unknown.

Table 2.4: Relations between the characteristics of the movement base case and the flow variables, as found in empirical research, where (X) indicates the movement base case: UD-S = uni-directional-straight, UD-C = corner, BD-S = bi-directional, BN = uni-directional bottleneck, X = intersecting.

Variable	Characteristics	Relation
Velocity (UD-S, UD-C, BN)	Density	Negative
Velocity (UD-S)	Distance headway	Positive, non-linear, 3 zones.
Velocity (BN)	Distance to bottleneck	Negative
Velocity (BN)	Density	No relation in case of anticipation
Velocity (UD-C)	Position in corner	Negative upto 45°, Positive afterwards
Velocity (BD-S)	Density of opposing flow	Negative
Velocity (BD-S)	Density of same flow ahead	Negative
Velocity (X)	Flow distribution	Asymmetrical effected - high flow results in high velocity
Velocity (X)	Angle of intersection	Negative ($45°angle - 180°$)
Velocity (UD-S)	Spatial headway	Negative (piecewise linear)
Walking direction (UD-C)	Position in corner	Positive
Density (UD-S, UD-C, BN)	Flow	Inclining less than linearly
Specific flow(BN)	Bottleneck width	Linear and continuous function for $b > 0.8$ m for corridors without doors
Specific flow (BN)	Bottleneck length	No influence
Specific flow (BN)	Density upstream of bottleneck	Negative
Specific flux (UD-S)	Angle of corner	Negative if angle $> 60°$
Specific flux (BD-S)	Imbalance of flow ratios	negative
Specific flux (BD-S)	BD-S movement base case	Negative, yet limited proof
Fundamental diagram (BN)	Location in bottleneck	Depends on layout
Fundamental diagram (UD-C)	Location in bend	Independent of layout
Fundamental diagram(UD-S, BD-S)	Flow situation	1.0 m^{-1} (free flow) no difference between FDs

2.6 Development of a conceptual model on the operational movement dynamics of pedestrians

In the previous sections empirical results concerning the influence of the characteristics of the person, the physiological environment, the interactions and the movement base case on the microscopic and macroscopic flow variables were reviewed. Yet, based on only the relations that are described in the literature it is difficult to establish a model that explains the operational movement dynamics of pedestrians at large-scale events, due to the adhoc nature of the research. Gaps between the empirical findings exist. Besides that, the most well-known models, i.e. Helbing & Molnar (1995), Paris & Donikian (2007), Moussaïd et al. (2011), Campanella et al. (2009b), suggest that several other factors such as risk assessment, visibility and several behavioural thresholds (e.g. shy away distance, personal space, cultural bias, etc.) might influence the operational movement dynamics of pedestrians. Yet, of their influence no empirical proof has not yet been delivered.

When combining the empirical relations described in literature with the factors that are suggested by the modelling work, it is possible to fill the gaps in the literature and develop a model that adheres to the largest part of the empirical findings that implements some of the suggestions from the modelling community. In this section exactly this is done. The fundamental flow variables are used as a point of departure. Subsequently, blocks of related behavioural hypotheses are added.

Based on the findings from pedestrian modelling community and logical reasoning several blocks of interrelated hypotheses can be added to this point of departure; being two blocks related to the velocity and distance headway, one block related to the impact of infrastructure and one block related to the impact of interactions. These four additional blocks are included because the empirical literature or modelling work contains hints that factors, related to these four blocks, influence the movement dynamics of crowds.

A more in-depth explanation of the choices for these building blocks and their configuration can be found in the following sections. The complete model is represented in section 2.6.6. Afterwards the validity of the conceptual model is briefly discussed in section 2.6.7.

2.6.1 The point of departure of the conceptual model

A theoretical framework is used as a point of departure for the conceptual framework because it provides a solid foundation for further development. The theoretical framework, $q = \rho * \vec{v}$, is often used in pedestrian and vehicular traffic and describes the relation between velocity $\vec{v}(\vec{x},t)$, density $\rho(\vec{x},t)$ and flow $q(\vec{x},t)$ at an aggregated level.

In this theoretical framework, two of the three macroscopic flow variables (i.e. velocity and density) can be related directly to the two microscopic flow variables velocity $\vec{v}_p$ and distance headway $h_{p,q}$ (see figure 2.3). As a consequence, this steppingstone allows for a clear-cut transition boundary between the macroscopic and microscopic variables.

As one can see, the author assumes that instead of a direct relation between the velocity of an individual pedestrian and space mean density, this relation is found in the empirical research literature as a result of the combination of two underlying relations between respectively, the indirect relation between the individual velocity and the distance headway, and the direct relation between the distance headway and the space mean density. Moreover, the position $\vec{x}_p(t)$ is placed in-between the velocity and distance headway, as a change in velocity will directly influence the future position of a pedestrian. These two assumptions are in line with the current practice in the simulation community, which show that pedestrians adapt their individual walking velocity $\vec{v}_p(t)$ based on the minimum time/distance headway $h_{p,q}(t)$ (Johansson (2009a), Paris & Donikian (2007)).

2.6.2 An upper limit on the velocity of pedestrians

In pedestrian research literature the word ‘velocity’ is used to describe the pace with which pedestrians walk. Generally a distinction between the ‘velocity’ and the ‘free flow velocity’ is made. While the first indicates the pace of a pedestrian given the circumstances that a

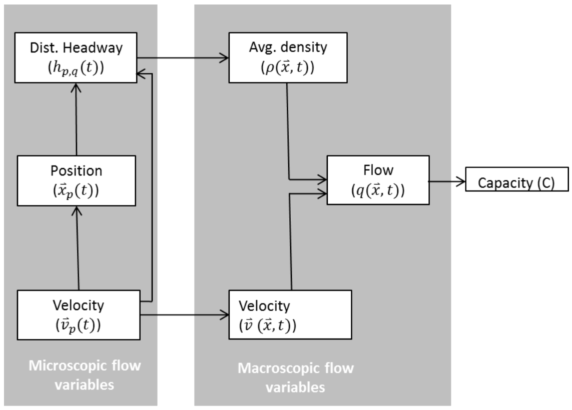

Figure 2.3: Relations between microscopic and macroscopic flow variables that provide the point of departure for the new conceptual model of related behavioural hypotheses.

pedestrian experiences, the latter indicates the pace at which pedestrians move along when their movements are not hindered by objects, infrastructure and other pedestrians. Also in the conceptual model, this distinction is adopted.

In most microscopic pedestrian simulation models the movability of the population within a model is partly managed by means of a velocity threshold, which is often named the free flow velocity. The simulation models incorporate an upper limit on the velocity to prevent agents from adopting physically impossible speeds, because the free flow velocity of a pedestrian is not regulated naturally in simulation models. This while in real-life the physical capabilities of the pedestrian pose a limit on the free flow velocity.

The review of empirical findings mentions several demographic and physiological factors that influence the walking velocity of pedestrians. Logically, many of these factors (e.g. age, gender, temperature) limit the physical capabilities of pedestrians. This lets the author to assume that several demographic and physiological factors do not directly influence the adopted velocity nor the density, but instead influence the free flow velocity of a pedestrian.

Findings in the simulation modelling field and the empirical evidence both suggest that an upper limit on the velocity is an essential variable to depict pedestrian movement dynamics correctly. Therefore, the block of relations explained in the previous paragraphs is added to the theoretical framework as limit on the adopted walking velocity. Figure 2.4 presents a visualization of the proposed configuration of the related behavioural hypotheses mentioned in this subsection.

2.6.3 Intervening factors in distance headway-velocity relation

The author assumes that there are also factors which serve as thresholds on the distance headway. The lower limit on the distance headway is naturally determined by the body circumference of pedestrians. That is, if pedestrians are in physical contact with each other, the distance between their centres is minimal.

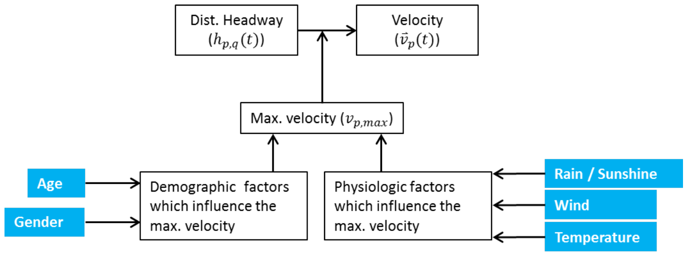

Figure 2.4: The block of related behavioural hypotheses which provide a boundary on the walking velocity.

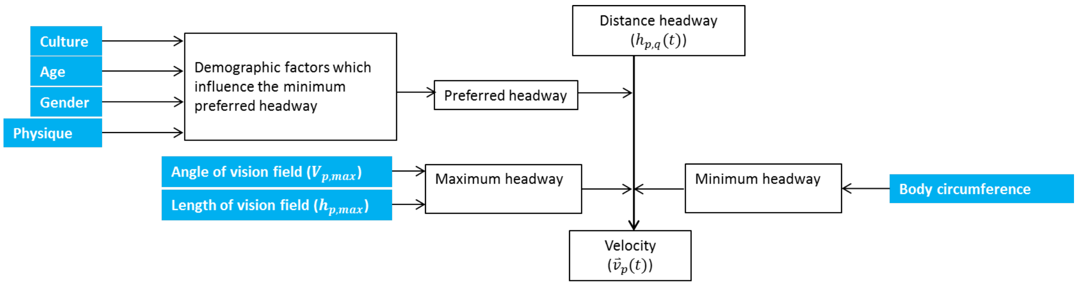

Figure 2.5: The block of related behavioural hypotheses which provide a boundary on the minimum distance headway

Besides a lower limit induced by physical properties, many microscopic simulation models also employ a threshold which governs the maximum strength of the influence of the interaction distance on the current velocity with respect to surrounding obstacles and other pedestrians. This social lower bound is dubbed minimum preferred distance headway in this thesis. The author hypothesizes that also culture influences the distance headway that pedestrians minimally prefer.

Logically speaking there should also be a maximum distance headway at which pedestrians are not influenced by other pedestrians any more. In most simulation models this threshold is often enforced through the region of interaction or the radius of the vision field. The maximum sight length and angle of a pedestrian's vision field with respect to the current movement direction might be possible explanatory factors.

Consequently, three bounds on the distance headway are incorporated in the conceptual model, namely the length of the vision field, the angle of the vision field and the demographic factors. The first two are combined, since they both provide a lower bound on the distance headway. These three bounds are assumed to affect the link between the distance headway and the velocity, since these characteristics will alter the range at which the relation between the distance headway and the velocity is valid but are not expected to change the shape of the relation. The block of interrelated behavioural hypotheses which describes these adaptations is presented in figure 2.5.

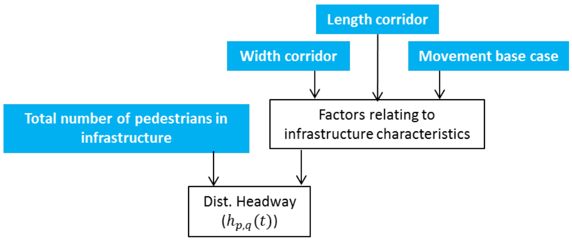

Figure 2.6: The block of related behavioural hypotheses describing the influence of the infrastructure.

2.6.4 Influence of infrastructure characteristics on headway

The literature mentions several relations between the characteristics of the infrastructure and the flow rate within the infrastructure. These findings lead the author to assume that the movements of individuals are directly and indirectly governed by the geometry of the infrastructure (among others length (e.g. Liddle et al. (2009)), width (e.g. Kretz et al. (2006b), Zhang et al. (2008)), angle of corridor (e.g. Dias et al. (2012b)) in which pedestrians reside and the total demand of the infrastructure (i.e. number of pedestrians within the infrastructure). In order to assure that all behavioural hypotheses are included in the conceptual model, the influence of the characteristics of the infrastructure is one of the blocks added to the theoretical framework.

The author suggest that microscopic interactions between pedestrians cause this relation between the characteristics of the infrastructure and the macroscopic flow variable density. When the geometry of the infrastructure changes, also the space available for pedestrian movements changes and as such induces shorter distance headways. This happens when the length or width of the infrastructure changes or when the movement base case within the infrastructure induces a more limited use of the available space (for instance bends in corridors, where pedestrians tend to cut the corner (Dias et al. (2012a), Steffen & Seyfried (2009)). The limitations of the infrastructure induce shorter distance headways between individuals.

The configuration of this block of related behavioural hypotheses is visualized in figure 2.6. As one can see, only a few characteristics of the infrastructure are mentioned. It is assumed that other characteristics, such as level differences or the presence of obstacles, will also influence the distance headway. However, since no papers were found in the research literature which detail their influence, it is difficult to understand how these characteristics will impact the operational movement dynamics. Therefore, for now they have been left out of the model.

2.6.5 Influence of interaction on walking velocity of individual

The literature review mentions that the angle at which flows intersect is negatively correlated with flow rate. This relation cannot be described by means of the theoretical framework that served as point of departure, nor by any of the three proposed building blocks. Therefore, a last building block is added to the conceptual model. Within the theoretical framework the flow rate is the result of a realisation of the velocity and the density. Therefore, instead of a relation

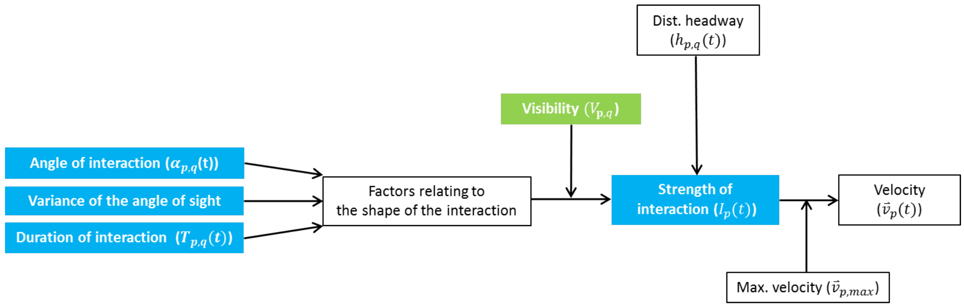

Figure 2.7: Relation between characteristics of the infrastructure and the walking velocity of a pedestrian.

between the type of interaction and the flow rate, a relation between the type of interaction between pedestrians and the walking velocity adopted by an individual is proposed.

The contemporary Social Force (Helbing & Molnar, 1995), Collision Avoidance (Paris & Donikian (2007), Moussaïd et al. (2011)) and Velocity-based (Chraibi et al., 2011) modelling approaches suggest that the interactions between a pedestrian and its neighbours can be quantified and added together. As a result of the formulation, nearby pedestrians are generally more strongly reacted to than pedestrians that are located further away. This concept of quantifiable and additive interactions is also adopted in the conceptual model and dubbed the 'strength of interaction'. In this variable all properties of the interaction are combined and weighted. The author assumes that the interactions between pedestrians are additive, but that the extent to which interactions are accounted for in the pedestrian's choice behaviour depends on the centrality of the interaction with respect to the current movements of the individual

The studies by among others Helbing & Molnar (1995), Paris & Donikian (2007), Moussaïd et al. (2011) and Chraibi et al. (2011) illustrate that a pedestrian might adopt a walking velocity based on the type and intensity of the surrounding interactions. Consequently, the interaction variables are logically placed in between the distance headway (input of the decision process) and the velocity (output of the decision process). Several properties of an interaction can accordingly logically be derived, such as the distance between two individuals (distance headway), the angle under which pedestrians perceive each other, the angle under which they approach each other and the duration of an interaction.

The mentioned modelling works generally assume that pedestrians only react on neighbours that they can see. Therefore, also the visibility of neighbours is included in the conceptual model. This variable is assumed to be a binary variable placed in between the factors that influence the strength of interaction and the strength of interaction. This because it is hypothesized that if a pedestrian is not visible, it will not be accounted for in the total strength of interaction. When combining the considerations above, the configuration depicted in figure 2.7 arises.

2.6.6 Conceptual model

The complete conceptual model of related behavioural hypotheses, which has been developed in the previous sections, is presented in figure 2.8. There has been attempted to depict the results of the sections 2.2-2.5 in the conceptual model. However, due to the complex interplay of the behavioural hypotheses, the new conceptual model does not allow for a one-to-one mapping of all empirical findings. Therefore, in the visualization of the conceptual model the signs of some relations have been omitted. These findings have, however, been used to determine the logic behind the conceptual model. Each of the variables in the new configuration of the conceptual model is either related to a cause (i.e. the demographic, physiological, and infrastructure characteristics) or an effect (i.e. the microscopic and macroscopic flow variables).

At the heart of the conceptual model a cyclic relation arises between the microscopic walking velocity, the distance headway and the strength of the interaction. Based on the empirical findings, the direction of this cyclic relation cannot be determined (e.g. chicken vs. egg). However, based on the logical inference that pedestrians have the opportunity to improve their current position through an adaptation of their velocity, but have no opportunity to single-handedly alter either their distance headway or their interactions with other pedestrians, it is hypothesized that the distance headway and the interaction are the cause and the adaptation of the velocity is the effect. As such, the current direction of the depicted cyclic relation is assumed to be counter clockwise.

The new conceptual model is made up of a multitude of variables, many of which have never been put into context before. The model structure allows for the clear separation between variables used to describe the aggregate motion of the crowd (macroscopic flow variables), the variables used to compute the actual movement dynamics of individual pedestrians (microscopic flow variables), the flow composition (demographic characteristics of the population) and the variables used to describe the situation in which pedestrians move (physiological environment and infrastructure characteristics). Due to the structured ordering of variables in the conceptual model, the model allows for the systematic testing of hypotheses related to the operational movement dynamics of pedestrian within a crowd.

2.6.7 Validity of the model

The behavioural hypotheses found in the research literature leave room for interpretation. Two important questions can be raised with respect to the current version of the conceptual model. First of all, is the proposed conceptual model the only possible interpretation of the empirical findings mentioned in the research literature? Secondly, is the proposed conceptual model comprehensive? That is, are all characteristics that influence the movements of pedestrians at large-scale events included in the current version of the model? Both questions will be briefly discussed underneath.

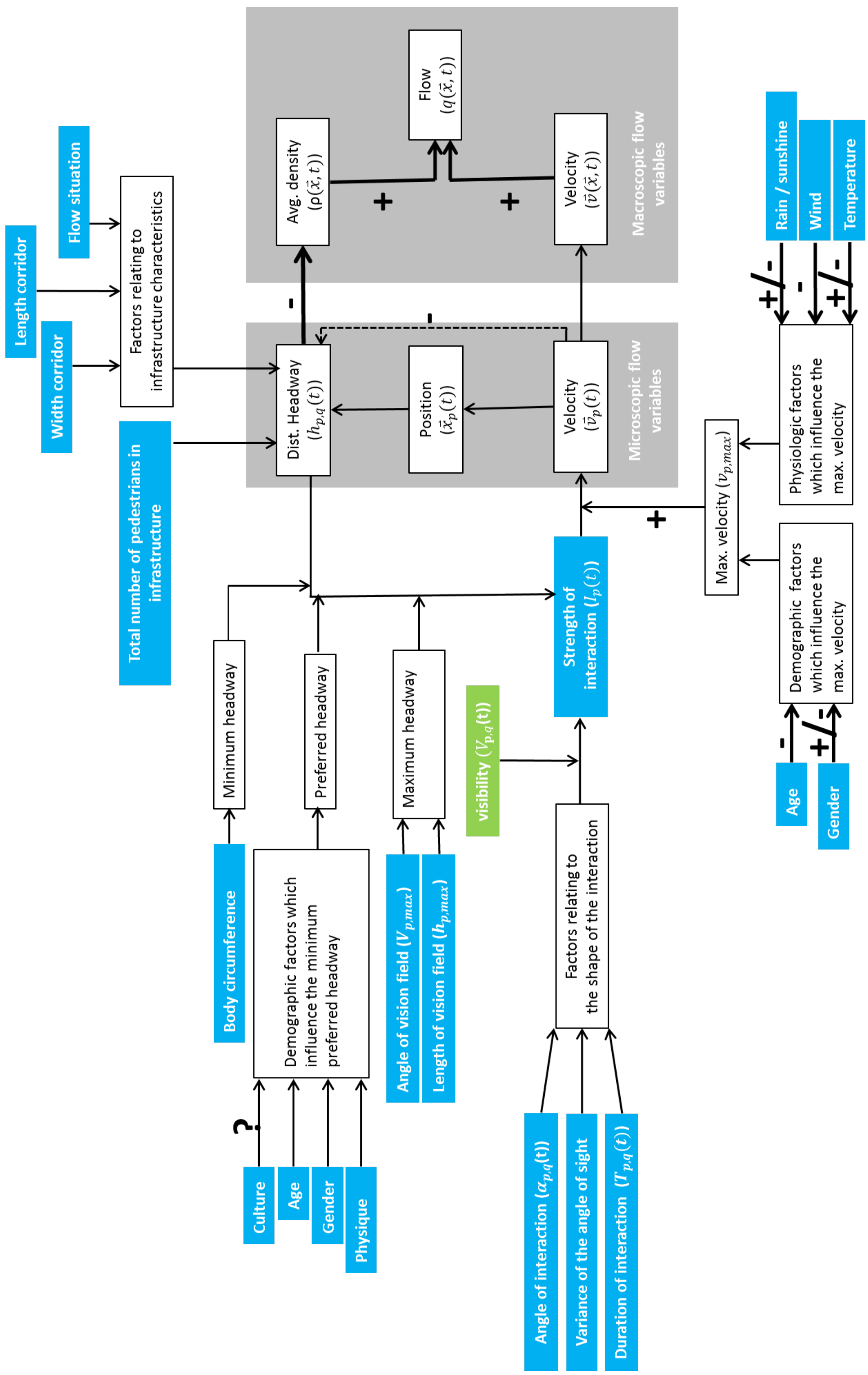

Figure 2.8: Full conceptual model of related behavioural hypotheses describing the operational movement dynamics of pedestrians.

The first issue relates to the uniqueness of this interpretation of the empirical findings. Most papers mention quantitative results, but far less papers describe the conditions under which the results were gathered and the methods that are used to develop the results. Moreover, even though research into the operational movement dynamics of pedestrians is progressing swiftly, many research gaps still exist. Consequently, assumptions regarding the empirical findings and the research gaps have been made. The conceptual model has been developed in a manner that allows all the relations, which were discovered in previous empirical studies, to remain valid. The work from the pedestrian simulation community is used to fill the gaps between the empirical findings. The author acknowledges that the proposed model is only one way of interpreting and connecting the empirical findings. Other interpretations and shifts in the indicated relations are possible. However, the majority of the relations depicted in the current configuration are not expected to change direction, since causes and effects are easily distinguishable.

The second issue relates to the comprehensiveness of the current version of the conceptual model. Since the literature detailing empirical research into pedestrian movement dynamics has been used as a basis for the conceptual model, the author has not included some influential factors that are not yet part of the scientific empirical discourse or that of which the connection to other factors is undetermined. Especially the introduction of new variables might have a far-reaching effect on the movement dynamics described by the proposed conceptual model, since these new variables might introduce new correlations between existing branches of the conceptual model. Self-organization is one of the concepts which might, in the future, link several branches of the proposed framework. Yet, since the underlying mechanisms of self-organisation are not yet understood, it is difficult to determine the exact relations that need to be added to the conceptual model. As a result, the author does not suggest that the conceptual model is comprehensive. Nevertheless, it is expected that the most important sources of influence on the movement dynamics of pedestrians within a crowd have been covered. Future research is needed in order to determine a comprehensive version of the conceptual model.

2.7 Conclusion and a look ahead

In this chapter a systematic review has been performed of factors that influence the walking behaviour of pedestrians in crowds at large-scale events. This review has focussed on four distinct categories of factors, namely the characteristics of the individual, the physiological environment, the interaction and the movement base case. The review has shown that the research has been adhoc and as a result disjointed. It has proven difficult to connect the empirical findings in order to create a model that describes the operational movement dynamics of pedestrians in crowds at large-scale events.

However, it was found that insights from the pedestrian modelling community could close the gaps. As a result, in this chapter a conceptual model of related behavioural hypotheses has been developed which describes the movements of individual pedestrians within a crowd. In this model the characteristics of the individual pedestrian, the pedestrian's physiological environment and the movement base case have been related to the macroscopic flow variables velocity, density and flow. Several new variables have been introduced to describe the interactions between individuals within a crowd.

The microscopic variables distance headway and walking velocity now form the core of the conceptual model. The location of these two microscopic flow variables at the heart of the framework implies that the movement decisions of an individual are not necessarily based on only the aggregate features of the crowd movement, but might also be influenced by the characteristics of the local interactions between two individuals.

In the conceptual model most of the explanatory factors do not directly relate to the macroscopic flow variables. Instead, most of these factors are known (or hypothesized) to influence intermediate parameters, that in turn are used by pedestrians in their operational decision-making process. Due to the indirect effects of the explanatory factors on the relation between distance headway and walking velocity, the proposed model explains why it is difficult to determine one single relation, which is applicable under all circumstances, between the macroscopic flow variables (often related via the fundamental diagram). Consequently, the structure of the conceptual model implies that one generic fundamental diagram might not exist.

Furthermore, the conceptual model shows that, while studying the relation between two variables, one needs to account for some of the other characteristics as well. For instance, one cannot study relations between the flow rate and the infrastructure geometry without accounting for the arising movement base case and the demographic composition of the crowd.

This chapter has shown that the contemporary research efforts have not provided enough insights into the movements of pedestrian crowds at large-scale events to determine the structure of the conceptual model beyond doubt. In order to test the main elements of proposed the conceptual model more elaborate empirical research into these movements is necessary. This thesis will perform the first steps in the testing of the conceptual model by means of a set of empirical experiments at large-scale events.

However, currently no data sets are available that can be used to test the conceptual model. Therefore, data regarding the operational movement dynamics of pedestrians at large-scale events will need to be gathered. Chapter 3 will detail the data collection and processing methodology as part of this PhD research. Afterwards, chapter 5 will discuss the main characteristics of the acquired data sets. These data sets are accordingly used in chapter 4 to quantitatively test the proposed conceptual framework.

Chapter 3

Acquiring and assessing pedestrian trajectory data sets

The review of the research literature with respect to empirical studies into pedestrian walking dynamics has resulted in the proposition of a conceptual model of related behavioural hypotheses in chapter 2. The proposed model contains characteristics of pedestrian movement dynamics in crowds at large-scale events which have not been researched before. In order to study these characteristics of these movement dynamics (e.g. the interactions between pedestrians within a crowd), data sets are needed that capture these walking dynamics. To the author's knowledge no data sets exist that can be used to study the metrics in the conceptual model with respect to the operational movement dynamics of pedestrians at large-scale events. That is, several data sets exist, but these do not sufficiently to cover all the variables and relations identified in the conceptual model and feature the movement dynamics at large-scale events. Consequently, new data need to be gathered in order to test the validity of the conceptual model. This chapter determines the type of data sets that are necessary and elaborates on the methodology used to capture, transform and analyse data sets that feature the walking dynamics of pedestrians in a crowd during large-scale events.

The chapter begins with a discussion of the requirements of the data collection methodology used in this research. The first three sections explain the choices made in the design of the empirical research methodology. In these sections requirements posed by the subject of the study (section 3.1) and the data (section 3.2) are respectively elaborated upon. Accordingly, the contemporary data collection methods are reviewed in light of these requirements in section 3.3. Afterwards the data collection and processing methodology to be applied in this thesis is presented in section 3.4. Subsequently, section 3.5 elaborates on the choice with respect to the cases used to capture the required data sets. Last of all, the analysis methodology is discussed in section 3.6. This chapter closes with a summary and look ahead in section 3.7.

3.1 Requirements posed by the research subject

In the conceptual model of related behavioural hypotheses proposed in chapter 2 microscopic and macroscopic characteristics have been incorporated. Microscopic movement information can be aggregated in order to describe also the macroscopic characteristics of a movement. However, deriving microscopic information from macroscopic characteristics is difficult if not impossible. Therefore, a research method is needed which generates information about the walking dynamics of the pedestrians at a *microscopic* level.

Furthermore, some microscopic characteristics in the conceptual model account for the presence of all other pedestrians nearby. In order to compute for instance the distance headway, time-to-collision and density, this information is essential. Therefore, the research method needs to be capable of capturing the coordinates of *all* other nearby pedestrians at any given moment in time.

Additionally, some characteristics account for the time-aspect of the interactions between pedestrians (e.g. duration of interaction, computation of the density by means of the XT-method). In order to determine these characteristics of the pedestrians' movements it is necessary to record the walking dynamics of individual pedestrians continuously through time. This is often named *trajectory data*.

Pedestrian trajectory data can be gathered using either empirical research or simulation studies. To the author's knowledge only one study is available that specifically studies crowd movement dynamics at large-scale events (i.e. Duives (2012)). The results of this study imply that the movement behaviour of pedestrians at large-scale events differs from the behaviour of similar pedestrians under other circumstances, for example rush hour at a train station or walking experiments in a laboratory environment. Therefore, in order to study pedestrian walking dynamics in crowds during large-scale events empirical trajectory data sets at large-scale events need to be captured.

Yet, pedestrians are known to behave senseless when they know they are being studied (i.e. wave at the camera, dance funny, etc.). In order to ensure that the captured movements are indeed a proxy for the natural operational walking dynamics of pedestrians at large-scale events, the research method needs to be *non-invasive*. That is, the research equipment should not capture the eye of the pedestrians, nor hamper the movements of the pedestrians. Moreover, the pedestrians should not be aware that their movements are being studied. This poses limits on the size, location and emission of noise of the equipment.

From the preceding paragraphs it can be concluded that the research method needs to be capable of capturing trajectory data of all pedestrians present within a certain area and during a certain time period at large-scale events by means of equipment which does not hamper the flow, nor capture the eye of the pedestrians.

3.2 Information requirements

The previous section reviewed the requirements posed by the research subject. However, the suitability of a data collection methodology also depends on the type of information one requires. Therefore, in this section first the variety, the detection rate, the reliability, and the update-time of the information are discussed.

Variety of information

The information generated about a flow of pedestrians differs depending on the measurement technique. The measurement location, the specificity of the information, the production process, the availability of the information and the possibility of identification together define the type of information. In this section these topics will be discussed.

A first distinction can be made based on the locations where the information is gathered. There are a lot of techniques that only generate information about a specific location or a small area (*area-bound techniques*). For instance, video systems can only record what happens within the current vision field. Other measurement techniques can be used to gather information about the crowd movements in larger regions (*not area-bound techniques*). Given that this research is focussed on small parts of the total infrastructure of a large-scale event a location-bound technique that captures information about the movements of pedestrians within an area of approximately 15 x 15 m[6] would suffice.

A second distinction between techniques can be made based on the specificity of the gathered information. There are techniques which are capable of retrieving the location of the pedestrian (*location specific*). That is, the exact X- and Y-coordinates of the pedestrian are known for certain moments in time. Other measurement techniques can only identify that a certain pedestrian has been present within the range of a sensor (*not location specific*). This research needs trajectory data, as such, the captured information needs to be location-specific.

One more distinction can be made based on the availability of the information. The information can either be of a *discrete* or a *continuous* nature. In the first case information about the presence and/or location of pedestrians is only available for certain locations or for particular moments in time. In the latter case, information about the presence and/or location of pedestrians is continuous in time and space. Due to the research nature of this study, a continuous or nearly continuous determination of the location of each pedestrian (approximately 10 data points per pedestrian per second) is necessary to understand and analyse why pedestrians adopt certain behaviour.

Another distinction can be made with respect to the manner in which the information is produced. A pedestrian can voluntarily provide information about its current location and/or status of well-being (*information push*). This type of information can be intentionally pushed towards an organisation, or unintentional provided as part of the meta-data associated with a message or photo pushed towards the social media. Yet, pedestrians can also be actively asked

[6]These dimensions are related to the approximate width of the corridors at most large-scale events.

to provide information about their location (and sometimes status of well-being) at a certain location (*information pull*). In the latter case the location of the pedestrian is actively determined at certain moments in time and/or at certain locations within the infrastructure. Since one needs information about the location of the pedestrians at quite a high frequency, a system that pulls information is more suitable for the job at hand.

Last of all, some systems are capable of identifying the pedestrian. Based on this personal (yet hashed) id, the time at which a pedestrian passed certain sensors within the infrastructure can be linked (*connecting data points*). By means of these time tags, that relate to one individual, more information about the movement dynamics of the individual (speeds, flows, routes, etc.) can be determined. In order to research pedestrian movement behaviour a string of connected data points per pedestrian is a prerequisite.

Sample detection rate

Besides the variety of the information, the amount of information provided is important. The amount is generally dependent on the cover ratio of the measurement technique. A video system in combination with a detection and tracking software, for instance, generates information about all individuals within its vision field. As such, these systems have a cover ratio of almost 100%[7]. On the other hand, the cover ratio of measurement techniques based on WIFI-signals is dependent on the amount of phones transmitting a 3G/4G signal within reach of the antenna. The previous section established that a detection rate of (nearly) 100% is required.

Reliability of information

Next to the variety and amount of information, there are differences in *trustworthiness* of the generated information with respect to the used measurement system. Systems which are error-prone (for instance counting based on filtered video or infra-red signals) provide less reliable information than systems that are known to contain no or very limited errors (for instance RFID-chips). In this case trustworthiness describes the possible presence of mistakes in the generated counts and positional information of the pedestrians. The nature of this study requires highly trustworthy data. That is, data in which the movement dynamics of a pedestrian can be established at each point in time for the entire duration of its presence within the study area.

Retrieving the information

From a practical perspective one does want to generate the necessary information about the pedestrians as efficiently as possible. As such, an *automated* measurement system is preferred over a *manual* measurement systems. Automation generally also limits the potential error in the processing. Besides that, one can also distinguish between the moment at which the information becomes available to the user. There are systems that can provide the information at the moment that the pedestrian movements are happening (*online*). From others the information can only be retreived afterwards (*offline*). Given that the research method is not used for management purposes, an offline research method does not pose problems.

[7]The cover ratio is also dependent on the angle of the camera, the occlusion and the correct detection of all pedestrians within the vision field. A 100% detection rate can never be guaranteed

3.3 Review of data collection methods

The preceding section showed that this study requires an off-line, automated, area-bound research method that produces highly trustworthy continuous information with respect to the location of 100% of the pedestrians in the area. Furthermore, the method needs to be able to pull information and effectively retrieve and combine the data points into trajectory data sets.

In the last two decades technology has progressed quickly. How information about the dynamics of moving crowds is retrieved, the speed with which this information can be accessed at another location and how this information is analysed has changed. While manual counts (a.o. Milinskii (1951)) and stop-motion videos (a.o. Hankin & Wright (1958)) were the only viable research methods to study pedestrian movement behaviour in 1990, nowadays there is a wide range of methods available to map the walking dynamics of pedestrians within a crowd.

The development of measurement systems is ongoing. Therefore, discussing these systems at a product level is found to be inappropriate. Instead, this section reviews the general characteristics of each research method and compares these with the requirements identified in the previous section. The references provided in this section serve as examples of cases where the mentioned techniques have been used to analyse pedestrian movements. Even though several other research methodologies, for instance questionnaires, virtual-reality experiments, exist which can be used to study pedestrian movements and choice behaviour, this section only reviews the research methods which can potentially provide information about the position of pedestrians at large-scale events.

Each research method has a specific set of characteristics, which carries consequences for the applicability of the method in this research. Subsections 3.3.1-3.3.4 provide a short introduction of the methods. The sections discuss human and automatic counting systems(3.3.1), video systems(3.3.2), antenna systems (3.3.3) and social media queries (3.3.4). Afterwards, a conclusion is drawn about the possibilities of each method for the analysis of the operative movement dynamics of pedestrians in a crowd during large-scale events. Based on a list of characteristics, the research methods are categorized in subsection 3.3.5. For a description of the adopted data collection methodology one is referred to section 3.4.

3.3.1 Counting systems

In the last few decades several systems have been introduced that can be used to determine the amount of pedestrians within a region or at a cross-section. The simplest method to count pedestrians consists of persons with a tally counter (*human counters*). A slightly different system can be used to determine the crowdedness at large squares, namely the so-called *'crowd watchers'*. These trained individuals approximate the amount of pedestrians at the square using photos taken with a birds-eye view[8].

[8]These methods are mainly used in practice, therefore no references can be provided from literature that detail the mentioned procedures.

Besides manual counting systems, several automated counting systems have been introduced over the years (Yang et al., 2010). One example of this type of system is the RFID-chip, which records the passage of pedestrians at certain cross-sections within the infrastructure (among others Quan et al. (2011) and Treiber (2015)). This system is often used during events where pedestrians or athletes follow a specific route. Besides that, also counting cameras (e.g. Masoud & Papanikolopoulos, 2001), infra-red cameras, depth-sensors (e.g. Seer et al., 2014) and laser-sensors (e.g. Gidel et al., 2010) can be used to count pedestrians. In these systems individual pedestrians are identified based on contrasts in video images or depth information. As such, these cameras count all pedestrians within the vision field of the camera or sensor, where the output consists of the number of pedestrians that cross a certain cross-section. Some of these systems are also capable of determining the direction of movement of pedestrians across a cross-section.

The information generated by counting systems is generally area-bound, not location specific and discrete in nature. Only RFID systems provide interpolatable information, which is especially useful if the sample of RFID readings is sufficiently large. Additionally, all of the above mentioned systems are capable of counting pedestrians with a reasonable accuracy depending on environment, density, light and weather conditions. However, most counting systems cannot identify the identity of pedestrian, and as such not track pedestrians through space. Moreover, none of the mentioned systems is fail-proof and the exact error is difficult to establish. A human counter can miss a pedestrian while a counting camera or laser sensor might count one where there are two pedestrians walking arm-in-arm.

3.3.2 Camera systems

Besides measurement techniques that are specifically developed to count pedestrians, there also are techniques where counting is just one of the by-products of its other functions. Smartly aimed cameras can be used to provide counts as well as density measurements. Furthermore, the walking velocities and flow rate can sometimes be estimated qualitatively based on video images. A quantitative estimation of these characteristics is only possible if the camera is calibrated, has a stable position, directed orthogonally and the zoom function is left untouched during the measurement period.

Next to camera systems which are already present in public space because of safety purposes, additional systems can be added at the moment that exceptional crowd movements are expected. Statcams, i.e. cameras attached to a balloon that floats at a height of 50-100 m, or helicopters are often used by crowd management organizations to get a sense of the crowd movements across large event terrains. Since these cameras reside high in the sky, the resolution of the images is generally too low to count pedestrians or estimate densities (Duives, 2012).

Besides overview cameras, also cameras at lower heights can be added in order to assess the crowd movements within a specific part of the infrastructure (among others Daamen & Hoogendoorn (2003b), Duives et al. (2012b), Zhang et al. (2011a), Zhang et al. (2013)). In order to perform research into pedestrian movement dynamics, this type of camera is generally aimed orthogonally, and therefore only covers a small area. With this type of camera the researcher can potentially identify individual pedestrians. Therefore, privacy issues might arise. Moreover, by means of off-line video analysis, it is possible to also determine walking velocities, densities and trajectories of all pedestrians within the range of the camera. Due to the computational effort involved, these data sets generally become available a few days after the recording of the videos took place.

The information generated by camera systems is location-bound, location specific and continuous. By means of camera systems one can online qualitatively assess crowd movement dynamics. Only by means of off-line computer vision techniques it is currently possible to derive quantitative information about the pedestrian movement dynamics within the infrastructure.

3.3.3 Antenna systems

In 2014 almost 98 % of all individuals within the Netherlands already had a mobile phone and 92% of the world population (Keij (2014)). Due to rapid development of smart phone technology (i.e. the increases of battery life and the presence of loading docks at festival terrains), it is safe to assume that by now also at event terrains almost everyone carries a mobile phone. As a result, it becomes more and more promising to use mobile phone signals to harvest information on pedestrian movements at event terrains.

Pedestrians can be tracked by means of any of these communication signals (Aly & Youssef (2013), Dahlgren & Mahmood (2014), Malinovskiy et al. (2012), Danalet et al. (2013)). Yet, the range of the sensors differs severely. Generally speaking, Bluetooth and Wi-Fi sensors only capture pedestrians at short ranges, the mobile internet signal is a little stronger, and the GSM signal can be detected over very long distances.

Besides that, all systems that work via antenna signals use the identification number of the mobile devices to track the device. As such, the techniques mentioned above all use privacy sensitive information. Special precautions need to be taken before this type of systems can be used to study the walking dynamics of pedestrians.

Up to now, only the GSM signal has been used for triangulation purposes (i.e. positioning, heat maps and routing), while Bluetooth and Wi-Fi are often used to establish route choice behaviour (Danalet et al., 2013). Yet, even GSM event data knows many uncertainties with respect to the detection location and coverage (Keij, 2014). As such, generally the provided information is area-bound, not location-specific and continuous in time and discrete in space. Antenna systems can not be used in this study, because location-specific information and a nearly 100% detection rate are required.

3.3.4 Social media

The last group of research systems that can used to determine characteristics of crowds are the social media such as Twitter, Instagram and applications provided by the organizer (e.g. Kraft et al. (2013) and Bocconi et al. (2015)). Often these systems are used to communicate by and with the pedestrians about ongoing events (e.g. show what the program is, warn for crowding, communicate changes in the schedule). Given that most information is pushed by the pedestrians, privacy is generally not considered to be an issue.

Several of these systems can also be used to qualitatively (Twitter) and quantitatively assess the movements of the crowd (Bocconi et al., 2015). Yet, the information provided by both systems is generally incomplete and of a qualitative nature. First of all, because only a sub-sample of the population will use social media to communicate with each others. Secondly, because the message contains words and photos taken from a perspective inside the crowd which renders incomplete information about the traffic state. That is, a pedestrian that is part of the crowd cannot oversee the entire crowd movement situation and it can only provide information about its own experiences and feelings.

3.3.5 Comparison of data collection methods

In table 3.1 the above mentioned research systems have been scored based the on the characteristics of the information mentioned above. That is, for each data collection method the table expresses the type of information, the type of retrieval process of the trajectory data, and whether privacy related issues are expected to arise when handling the obtained information. Moreover, the table identifies the type of experiment that is necessary to acquire the information and the type of information that is produced by the method.

If one compares the results from this table with the ”wish-list” presented in section 3.2, it becomes apparent that only one system can provide microscopic trajectory of a specific area with a detection rate that approximates 100%. This is a camera-system with a birds-eye view that records the walking dynamics of pedestrians within a crowd at large-scale events and stores it for off-line analysis. Given that high detection rates and high precision are required, the off-line analysis of these video recordings is necessary. This does, however, not pose problems as the results are used in a research project which has no stringent deadline. Given that similar data collection techniques have already been used to analyse the operational driving behaviour of vehicular traffic (e.g. Hoogendoorn et al. (2003), Yilmaz et al. (2006)), it should be feasible to develop a data collection method based on video sequences specifically to study of the operational walking dynamics of pedestrians at large-scale events.

Table 3.1: Review of measurement techniques for the analysis of pedestrian walking dynamics

	Experiment				Type of information						Information requirements									
	Field	Laboratory	VR environment	Survey	Counting	Movement	Route	Activity	Timing	Sentiment	Area-bound	Information push	Continuous(c) / Discrete (d)	Connecting datapoints possible	Detection ratio (fair - full)	Online management	Offline analysis	Manual	Automated	Privacy sensitive information
Requirements	**x**					**x**					**x/-**	**pull**	**c**	**yes**	**good**		**x**		**x**	**no**
Human counters	x	x			x						x	pull	d	no	fair	(x)	x	x		no
Crowd watchers	x	x			x					x	x	pull	c	no	fair	x	x	x		no
RFID	x	x			x		x	x	x		x	pull	d	yes	full	x	(x)	x	x	sometimes
Counting cameras	x	x			x						x	pull	c	no	good		x		x	sometimes
Camera systems in public space	x	x			x	x			x	x	x	pull	c	no	good	x	x	x	x	sometimes
Stat-cam (hot air balloon)	x	x			x						x	pull	c	no	fair	x	x		x	no/sometimes
Research installation with cameras	x	x			x	x					x	pull	c	yes	good		x	x	x	no
Bluetooth	x	x			x		x	x	x		x	pull	c	yes	poor/fair	x	x		x	yes
Wi-Fi	x	x			x		x	x	x		x	pull	c	yes	poor/fair	x	x		x	yes
GSM	x	x			x	x	x	x	x		–	pull	c	yes	full	x	x		x	yes
GPS	x	x			x	x	x	x	x		–	push	c	yes	poor/fair	x	x		x	yes
Twitter/Instagram	x						x	x		x	(x)	push	d	yes	poor	x	x		x	yes
Facebook	x						x	x		x	(x)	push	d	yes	poor	x	x		x	yes
Chat	x						x	x		x	(x)	push	d	yes	poor	x	x		x	yes

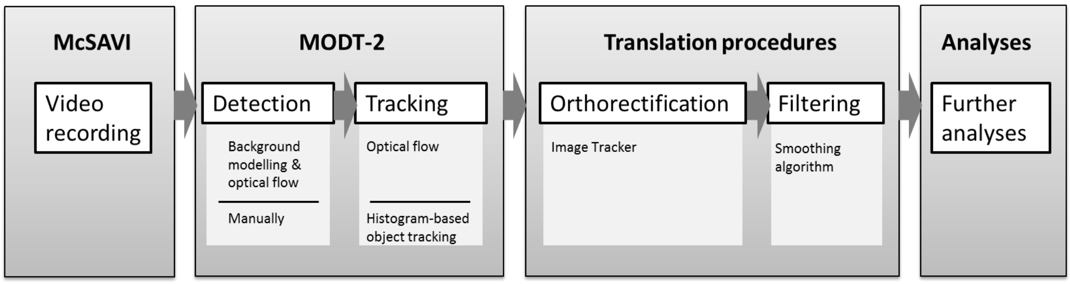

Figure 3.1: Flowchart of the adopted data collection and processing methodology.

3.4 Data collection and processing methodology

The outline of the data collection and processing methodology is visualized in figure 3.1. The methodology combines a Multi-camera Stand Alone Video Installation (McSAVI) and the software package MODT-2. First, the McSAVI captures stable video recordings from an orthogonal high vantage point. Afterwards, MODT-2 is used to detect and track pedestrian movements within a crowd. After this process, the resulting trajectory data sets can be analyzed more in-depth by more specialized tools, i.e. Biogeme and Matlab.

In the following section the data collection and processing methodology are described in more depth. Afterwards also the filtering procedures and the precision of the trajectory data sets are briefly touched upon. First, the McSAVI is introduced. Accordingly, the detection and tracking procedures are briefly described. Subsequently, the trajectory transformations which are necessary to convert from raw image coordinates to real-world trajectory are briefly reviewed. Subsequently, the trajectory smoothing procedure and precision of the resulting trajectory data sets are discussed.

3.4.1 Camera system - McSAVI

The McSAVI is shown in figure 3.2. The installation is designed to record videos during large-scale pedestrian events within or near moving crowds. Consequently, the installation is self-sustaining for approximately 10 hours, waterproof, securely locked and to a large extent hooligan-proof.

Due to the high vantage point ($8-10\ m$) of the cameras, occlusion of pedestrians within high density crowd movement video sequences is limited. Densities up to 5 P/m^2 should pose no problems. Remote steering allows the user to move the cameras in the most advantageous position for any situation. To track pedestrians, the optimal angle of the cameras would be entirely orthogonal. However, recordings with a camera angle up to 40 degrees can still be used to research the general patterns and interactions within a crowd qualitatively and quantitatively.

The capturing speed of the cameras is between 5 and 15 frames per second. The capturing speed is dependent on the light conditions, image size and the stability of the mast which supports the camera. The frame rate decreases if the mast becomes more unstable as a result of internal

Figure 3.2: Multi-camera Stand Alone Video Installation (McSAVI)

stabilization software. Even though the capturing speed of the McSAVI is quite low compared to ordinary cameras, each pedestrian is still detected at least every 15 cm due to the low walking speeds of pedestrians in a crowd.

3.4.2 Orthorectification - ImageTracker

In order to correctly track pedestrians in video images one needs to account for the fact that the camera records a 2D image of a 3D scene. Consequently, the raw video frames, which are images directly cut from the video sequence, are distorted. One can orthorectify these frames to cancel out these distortions. During the orthorectification process the frames are rotated, stretched out and compressed, which causes the boundaries between pedestrians and the background to blur slightly. Since both the detection and tracking procedures make use of these abrupt boundaries, pedestrians are more difficult to recognize in the orthorectified video frames. The detection and tracking results improve when pedestrians are detected and tracked in the raw video frames instead of the orthorectified frames. Therefore, there has been chosen to first detect and track the pedestrians, and afterwards orthorectify the trajectory data sets. The parameters and algorithm of the software program ImageTracker (Knoppers et al., 2012) are used to convert the pedestrian pixel coordinates into world coordinates. This software program corrects for lens distortion, searches for the transformations necessary to match sequential images and applies this transformation to stabilize each following image with respect to a reference image. Since the McSavi produces stable image sequences one transformation can be applied to all trajectory data sets captured during one case. If an image sequence distorts dynamically due to wind effects, orthorectification of the entire sequence would be necessary.

3.4.3 Tracking and detecting of pedestrians - MODT-2

In Duives (2012) the basis of the MODT-software is explained. In the adapted version (MODT-2), the trajectories can be recovered automatically from the video sequence or semi-automatically using a combination of manual detection and automated tracking depending on the density of the crowd in the recorded images.

In the case of low densities, a combination of background modelling (Yin et al., 1996) and optical flow (Sun et al. (2008, 2010)) is applied. The combination of both methods identifies moving objects with respect to a stable background. In high density situations, the user has to take over the detection process, since for the detection of pedestrians still no better algorithm exists than the human eye (Dollar et al., 2012). Tracking is in both cases automated by means of a velocity predictive Kalman filter and histogram-based object tracking algorithm (Yilmaz et al., 2006). In order to account for small differences in the histogram due to shifting light conditions, an adaptation procedure is implemented which allows the histogram to change slightly over time.

In both manual and automated tracking procedures issues related to the continuous tracking of pedestrians might occur. The object tracking method uses the histogram of pixel values of a certain pixel region (set by the user dependent on the cameras vantage point) to identify the tracked object. Even though a stringent evaluation function is used, due to noise, shifting light conditions and pedestrian behaviour, the possibility exists that the tracking algorithm loses the identified individual. Moreover, video sequences containing high density crowd movements might contain occlusion[9]. MODT-2 searches for the pedestrian on its predicted location when lost for less than 5 frames (approximately 0.5 s). Therefore, most occlusion instances do not pose a problem as pedestrians re-appear nearby their last seen location. Only when pedestrians are occluded for longer time periods, their trajectories are split into two separate ones. Even though both issues ensure that a semi-automatic detection procedure is necessary for high density situations, still detection rates up to 100 % can be achieved with MODT-2.

3.4.4 Filtering of the trajectory data

After capturing the videos, orthorectification, detection and tracking, the produced trajectories may still be incorrect (e.g. the trajectory can still float slightly within one person). Swaying of stationary pedestrians increases this instability. In order to get rid of the most problematic instabilities within the trajectories, a smoothing filter has been applied. A locally weighted linear regression is used to smooth the trajectory data. The regression weight of this function is quadratic polynomial and chosen in a way that the algorithm is resistant to sudden outliers.

This smoothing procedure is potentially capable of also removing the naturally present randomness of human movement within the trajectories (both swaying and sudden increases/decreases

[9] A pedestrian cannot be seen from the vantage point of the camera and cannot be found by the tracking algorithm

in velocity). However, since the span of the algorithm is small (max. 10% of the data of a single trajectory), only the large outliers are filtered out of the data sets and the typical pedestrian walking behaviour, such as swaying, will be kept intact. As such, it is expected that most decision points are not filtered from the trajectory data sets.

3.4.5 Precision of the trajectory data sets and its implications

In high density video sequences only the head and shoulders of a pedestrian are visible. Given that the conversion algorithm assumes that it translates a flat image at a certain height, this algorithm also assumes that the height of all pedestrians in the video recording is equal. This assumption might introduce a source of error in the converted trajectories. For image series recorded from a high and orthogonal vantage point, the difference between the actual position of the head of a pedestrian and the detected position in the image frame (width and width) is less than 15 pixels. Depending on where in the image this error occurs, the actual error in the trajectory data sets is small ($\varepsilon < 0.05m$ if located in the centre of the images) or substantial ($\varepsilon < 0.3m$ at the boundaries of the images). The detection of children within a crowd of adults deteriorates this issue.

Besides the representation error, also errors in the location of detection of a pedestrian occur. A choice was made to detect all pedestrians at their neck. In that case the width of the detection area is small but clearly recognizable, see figure 3.3. As a result, the tracking becomes more stable because the edges and histogram are more distinctive. Therefore, only minor errors in the detection occur ($\varepsilon < 5 pixels$), i.e. the trajectory can still slightly float with respect to the original point of detection. Depending on the camera angle the representation error results in an error in the orthorectified trajectories between 0.05 and $0.15m$.

The two sources of error mentioned above impact the validity of the trajectory data sets. That is, the captured, detected, tracked, orthorectified and filtered trajectories might still not entirely correctly identify the exact location of pedestrians. This results in a slight misrepresentation of the actual movement behaviour of the pedestrians' captured within the data sets. It is difficult to estimate the size of this error, since no ground truth trajectory data set is available.

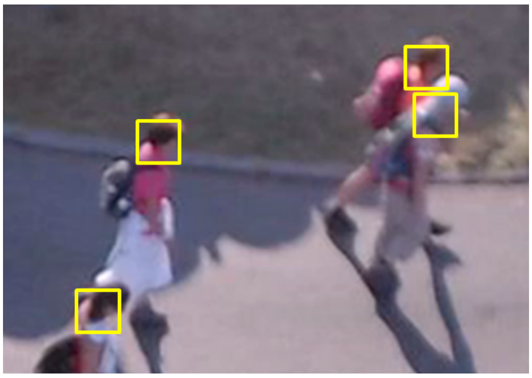

Figure 3.3: Visualisation of the point of detection

This measurement error also impacts the results of the analysis of these trajectory data sets. Given that the computation of the walking velocity is dependent on the difference between detection points of the same individual, these two sources of error do not pose a lot of problems. However, the distance headway and density depend on the distance between pedestrians. As such, the two sources of error might introduce noise in the representation of these two flow variables. In order to limit the noise in the representation of the density and distance headway, there has been chosen to ignore video recordings in which large height differences between individuals are present (e.g. parents and children).

3.5 Cases to assess pedestrian movement dynamics

Data sets are necessary to test and further develop the conceptual model. While sections 3.1 - 3.4 have established how to correctly capture trajectory data sets, this section determines during which large-scale events trajectory data sets are to be captured given the characteristics of the necessary information and the requirements posed by the data collection and processing methodology.

During large-scale events the corridors and squares are generally relatively wide. As a result, also in corridors several types of movement base case arise. Here, a certain motion base case is assumed to arise when the predominant flows in the infrastructure are following the patterns described in section 2.5.1. Based on the research literature, it is expected that the movement dynamics between movement base cases might differ. In order to test the conceptual model as comprehensively as possible, it is essential to incorporate these distinct movement dynamics. Therefore, an attempt has been made to find as many distinct motion base cases as possible. Given that eight distinct movement base cases have been identified, a relatively large amount of data sets is to be acquired.

Besides the type of motion base case, several other characteristics of the situation are of importance to get usable data sets, such as the type of population, the goal-orientation within the infrastructure, the type of weather, and the presence of dynamic obstacles.

The general purpose of most pedestrians at large-scale event terrains is to get entertainment. While doing so, pedestrians walk around or stand still watching attractions. This thesis focusses on the walking behaviour of pedestrians. Therefore, especially areas at event terrains are sought for where all pedestrians are leisurely walking.

Moreover, the literature review showed that the physiological environment also has an impact on the walking behaviour of pedestrians. There has been chosen to limit the impact of the weather as much as possible. In this thesis only cases are accounted for if it was not raining, the wind strength was limited and the temperature was between 15 and 35° Celsius. Under these conditions, pedestrians are assumed not to be impeded in their walking movements by the physiological environment.

Table 3.2: Cases to analyse pedestrian movement dynamics at large-scale events empirically

Case study	Abbreviation	Goal-orientation	Location	Date	Time	Motion base case
Marathon Rotterdam	M-R	Sports event walking not main objective	Coolsingel - Rotterdam	14-04-2013	11:00-17:00	UD-entering
Queensday Amsterdam	Q-A	Music event	Museumbrug Amsterdam	30-04-2013	10:00-17:00	BD - straight
Liberation day festival Wageningen	LF-W	Music event	Markt - Wageningen	05-05-2013	12:00-19:00	Intersecting - random
4Daagse - day 1: Lent	4D-L	Sports event walking main objective	Oude groenelaan Lent	16-07-2013	11:00-16:30	UD-corner
4Daagse - day 2: Wijchen	4D-W	Sports event walking main objective	Markt Wijchen	17-07-2013	10:00-14:00	UD-straight
4Daagse - day 3: Hatert	4D-H	Sports event walking main objective	Hatert	18-07-2013	5:00-10:00	UD-corner
Marathon Amsterdam	M-A	Sports event walking not main objective	Stadionbrug Amsterdam	20-10-2013	11:00-17:00	Intersecting - random

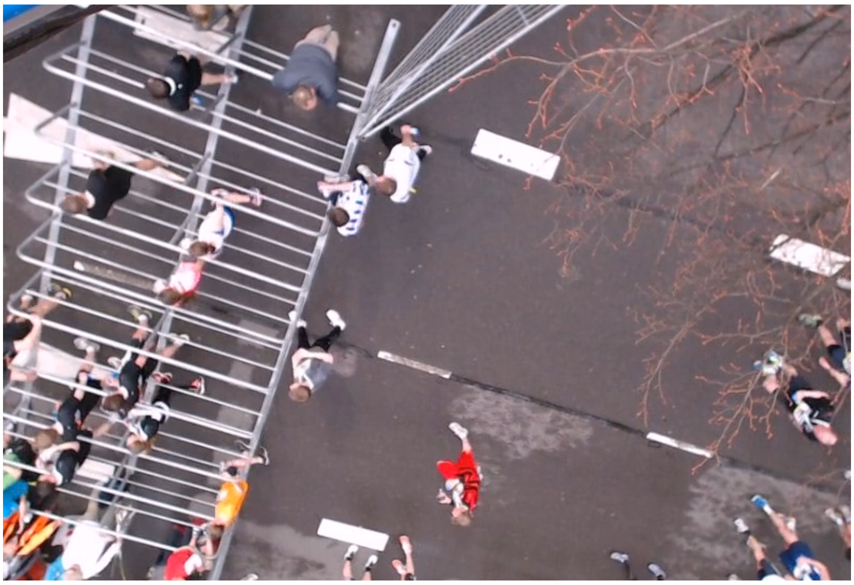

Figure 3.4: View from the camera - case: Rotterdam Marathon.

3.5.1 Marathon Rotterdam

The Marathon of Rotterdam is one of the largest annual marathons in the Netherlands. This sports event drew approximately 925,000 spectators and 20,000 runners into the city centre of Rotterdam on Sunday April 14th 2013. During the event, all runners (10k, 20km, 42km) passed the finish on the Coolsingel. After the finish they entered the finish/treatment/refreshment area. After a medical check and some refreshments, the runners exited the closed terrain again via the gate on the Pompenburg on their way towards the changing rooms. The exit consisted of 8 parallel gates which were $0.7m$ wide, and were separated by fences that were $3m$ long $1.2m$ high. Since the area behind the exit was the first instance where spectators could meet the runners, a waiting area originated downstream the exit gates. In this case the movements of the runners within the confinement area while moving towards the exit are studied.

During large-scale events pedestrians are also encountering dynamic large objects, such as bicycles, vehicles, carts, buggies. The influence of these objects is not taken into account in this thesis. Therefore, video sequences in which this type of objects made their presence are ignored in the analysis process.

As mentioned before, the height difference between individuals is positively correlated with the noise in several flow variables. In order to limit the amount of noise in the data sets, events with individuals of almost the same size are sought. As such, the search has been limited to events where predominantly adults are present.

Table 3.2 mentions the events that are selected. As one can see, it has practically not proven to be possible to capture all different motion base cases described in section 2.5.1 and to capture all data sets at one type of event. However, it is assumed that enough distinct motion base cases are covered by the data sets to corroborate the conceptual model. Besides that, these cases all

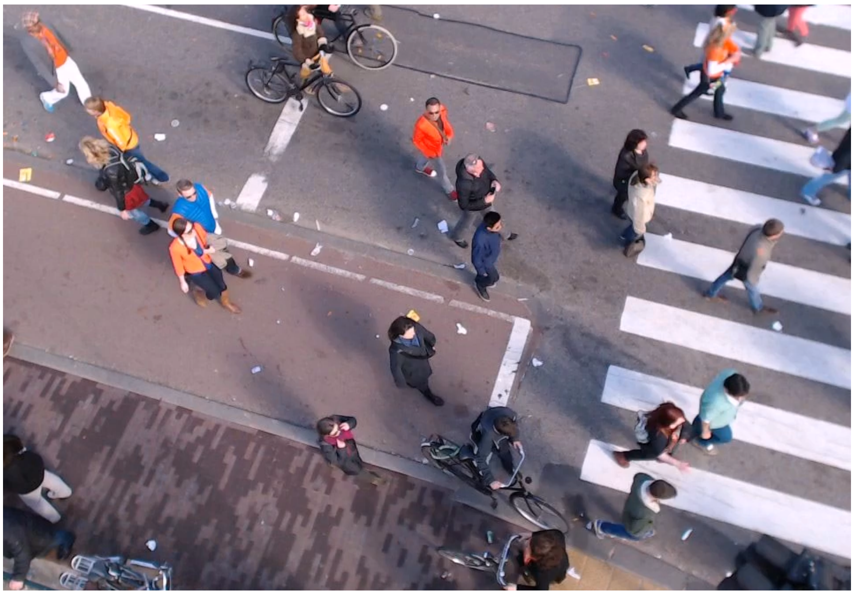

Figure 3.5: View from the camera - case: Amsterdam Queensday

adhere to the requirements posed with respect to the type of population, the presence of dynamic obstacles and the goal-orientation of pedestrians. The cases are briefly introduced below.

3.5.2 Queensday Amsterdam

During Queensday on the 27th of April 2013, 700,000 visitors assembled in the city centre of Amsterdam to take part in the festivities. On the bridge a bi-directional flow of pedestrians to and from the Museumplein developed, see figure 3.5 for a visualisation of the location. The entire intersection just right of this image was closed for vehicular traffic.

Many pedestrians walk around in groups during Queensday. These groups were either families or groups of friends[10]. Both inhabitants of the Netherlands and tourists walked across the intersection. The split between genders was approximately 50-50. As one can see in figure 3.5, several pedestrians pushed prams or bikes across the bridge amidst the crowd. Also some carts, mopeds and vehicles were present on the bridge during the day, though very infrequent. The video sequences in which the prams, bikes, carts, vehicles, etc. influenced the movements of pedestrians are disregarded in this study.

3.5.3 Liberation day festival Wageningen

On Liberation Day (May 5th, 2013) several large-scale music events are organized in the Netherlands. The Liberation day Festival of Wageningen draws more than 60 thousand visitors each year. The trajectory data sets describe the movements of pedestrians alongside the Southern part of the market square in Wageningen, see figure 3.6. Most pedestrians walk through the study area. Some pedestrians stop, only to resume walking after some time.

[10]The social bond is deduced based on visual inspection only at the case study area by the researchers.

Figure 3.6: View from the camera - case: Liberation day festival in Wageningen

Flows from all four directions to all four directions were found, where the largest demand came from the bottom. Visual inspection of the videos showed that pedestrians depict both goal-oriented and not goal-oriented behaviour (i.e. strolling, sightseeing). The demand from the four sides has been approximately similar during the day, namely 13% from the left, 19% from the right, 37% from the bottom and 30% from the top. The most dominant flows were left-right and right-left. The distribution over the destinations depends on the sequence. There has been attempted to select the video sequences in a way that these represent the movement situation during the entire day of events, i.e. distinct density situations and flow situations have been included.

Only trajectory data sets in which no visitors were hampered by static obstacles or vehicles have been included. The individuals who are standing still in the area have been taken into account, because the moving pedestrians interact with these stationary individuals.

3.5.4 4Daagse Nijmegen

The International Four Days Marches are held in Nijmegen, The Netherlands, every year. During the 97th version of the Marches 42,493 pedestrians started on Tuesday July 16th 2014, and walked a march of 30km (youth, elderly, impaired), 40km (adults) or 50km (mainly military and security personnel) every day for four days. After four days 39,396 pedestrians finished along the Wedren in Nijmegen. Drop-outs occur regularly during the march due to blisters, muscle aches etc. Yet, most participants that were recorded appear to move unhampered.

During the four days the uni-directional movements of the participants were recorded at several locations. In this thesis three cases will be used. In all three cases (captured at distinct days and locations) data sets have been chosen in which the participants of the march are not hampered by infrastructure, the general public, other vehicles or physical illness.

The first case during the 4Daagse studied the walking dynamics of pedestrian at the Market square in Wijchen on July 17th, 2014. A uni-directional straight flow situation arose, see figure

Figure 3.7: View from the camera - case: 4Daagse - Wijchen

Figure 3.8: View from the camera - case: Lent.

Figure 3.9: View from the camera - case: 4Daagse - Hatert

3.7 for a visualisation of the situation. The participants walked through a straight corridor of approximately 10 meters wide in between two sets of low fences, which kept the spectators at a distance. The participants could physically interact with the spectators on the other side of the fence, although this rarely happened. 50 meters downstream from the study area a slight narrowing of the corridor occurred. As a result, queueing occurred at the study area due to the clogging of the downstream bottleneck.

The second case was located at a bend of approximately 90 degrees at the intersection of the Oude Groenelaan and the Waaldijk in Lent. At this location the participants transferred from an urban road onto a dike with steep slopes at both sides. Figure 3.8 provides an impression of the case study location.

As a result of the steep slopes of the dike, most of the participants walked on a black-top surface. During their movements around the bend, two possible distractions presented itself. First of all, there were spectators encouraging the participants of the march. However, at this specific location most spectators were sitting or standing on the slopes of the dike, well out of reach of the participants. Secondly, a small market stall that was placed at the outside of the bend. Even though customers were rare, some interaction between the participants and the market stall took place.

The third day of the 4Daagse the route of the marches passed Hatert, a neighbourhood on the outskirts of the city Nijmegen. The study area consisted of the T-intersection of two urban blacktop roads (Malderburchstraat and Hatertseweg), see figure 3.9. The angle between the two roads is approximately 100 degrees. The radius of the bend is fairly large. As such, only the first part of the bend is analysed. This might influence the representativeness of the case. A grassy field was located on the inside of the bend. Yet, most participants remained on the paved roads. Given that the marches start at 6.00 a.m., the first participants reached the case study area by 6.30 a.m. Pedestrians were seemingly not hampered by muscle aches or tiredness. Consequently, no disturbances occurred.

3.5.5 Marathon Amsterdam

The Amsterdam Marathon was held in the city of Amsterdam on October 20th, 2013. During the course of 2 days, 42,600 runners completed a run of 10km, half marathon or a marathon. The case study area was located at the intersection of the Na-Druk-Geluk-Brug and the IJsbaanpad in Amsterdam. This area is accessible for the general public and the athletes walking to and from the event. The area was positioned in between the sports hall, where the runners changed their gear, and the start-/finish line. Even though both roads are designed to handle vehicular traffic, during the day of the marathon this part of the IJsbaanpad was regulated by traffic controllers which only sparingly allowed cars to pass. At this intersection a roundabout resides. As a result of the roundabout, pedestrians could enter the case study area from three sides, namely at the left, the top-right and bottom-right of the case study area (see figure 3.10).

Figure 3.10: View from the camera - case: Amsterdam Marathon

3.6 Describing operational movement dynamics

The conceptual model, which was presented in chapter 2, mentions several variables of the pedestrians' walking behaviour, some of which were not yet defined in the literature. Besides that, Duives et al. (2012b) illustrates that over the years several distinct definitions have been presented for some of the variables that are used to describe the walking behaviour of pedestrians. This section establishes the definition for all variables that are mentioned in the conceptual model to describe the operational movement dynamics of pedestrians.

First, the mathematical definition of the flow variables velocity, density, distance headway and time-to-collision are provided. Accordingly, new definitions are provided for the angle of interaction, angle of sight, and the strength of interaction. Last of all, the capturing of the demographic characteristics are discussed in more detail.

In the following paragraphs for each of the metrics a mathematical description is given, which are used in this study to test the validity of the conceptual model in chapter 4 and to describe the walking dynamics of pedestrians in chapter 5. Besides giving a definition of the variables, also the implications of the choices made in the process of establishing these definitions are reviewed.

Walking velocity

During this study pedestrian p's instantaneous walking velocity $\vec{v}_p(t)$ is computed as follows:

$$\vec{v}_p(t) = \frac{\vec{x}_p(t+dt) - \vec{x}_p(t)}{dt} \tag{3.1}$$

where $\vec{x}_p(t+dt)$ is the location of pedestrian p at time t and dt is the time step between consecutive realisations of the location of pedestrian p after the filtering procedure described in section 3.4 has been applied. In the data sets dt is approximately 0.1 s, slightly dependent on the frame rate of the camera. Since the trajectories have already been filtered as part of the data collection procedure, no additional smoothing is applied. Due to the tracking procedure (tracking heads) and the used definition of walking velocity, the movements of the upper body are taken into account in the velocity computation.

Density

In Duives et al. (2015) it was found that the Voronoi-method proposed by Steffen & Seyfried (2010) and the X-T method adapted from Edie (1963) can describe the density of a pedestrian flow best. Since the results of the adapted X-T method are less strongly influenced by the chosen boundary conditions, the density is computed by means of the X-T method adapted from Edie (1963), which is mathematically defined as follows:

$$\text{if } x_p(t) \in X_C \quad \Rightarrow \quad \rho_p(t) = \rho(C,t) \tag{3.2}$$

$$\rho(C,t) = \frac{\sum_q (t_{q,end} - t_{q,begin})}{A_C * T} \tag{3.3}$$

where:

$$t_{q,begin} = \min(t - \frac{1}{2} t_{limit}, t_{q,entering\ cell}) \tag{3.4}$$

$$t_{q,end} = \max(t + \frac{1}{2} t_{limit}, t_{q,leaving\ cell}) \tag{3.5}$$

Where t_{limit} represents the temporal boundaries of the time-space box, $t_{q,begin}$ the moment that pedestrian q enters the time-space box C defined by the set of coordinates X_c, $t_{q,end}$ the moment that pedestrian q exits time-space box C, T the time period for which the time-space box is defined and A_c the spatial area of the time-space box. For any pedestrian p the local density is determined for the time-space box where the pedestrian resides at the centre. In this thesis for the local and global density a time-space box with a spatial width and length of 2 m and a temporal length of 1 s has been adopted.

Distance headway

Following the work by Goffman (1972), it is assumed that the movement behaviour of pedestrians is anisotropic. That is, pedestrians react more strongly to the presence of pedestrians they can see, than to pedestrians they cannot see. Consequently, a vision field is included in the computation of the distance headway. The minimum distance headway belonging to pedestrian p with respect to all other pedestrians q which are present within the vision field $V_p(t)$ of pedestrian p is defined as follows in this paper:

$$h_{p,q}(t) = \min \mid \vec{x}_q(t) - \vec{x}_p(t) \mid \qquad \forall\, \vec{x}_q(t) \in V_p(t),\ q \neq p \tag{3.6}$$

where

$$V_p(t) = \{\vec{x} \in X : \frac{\vec{v}_p(t)}{|\vec{v}_p(t)|} \cdot \frac{\vec{x} - \vec{x}_p(t)}{|\vec{x} - \vec{x}_p(t)|} \geq 0.5 \cap (\vec{x} - \vec{x}_p(t)) \leq h_{max}\} \tag{3.7}$$

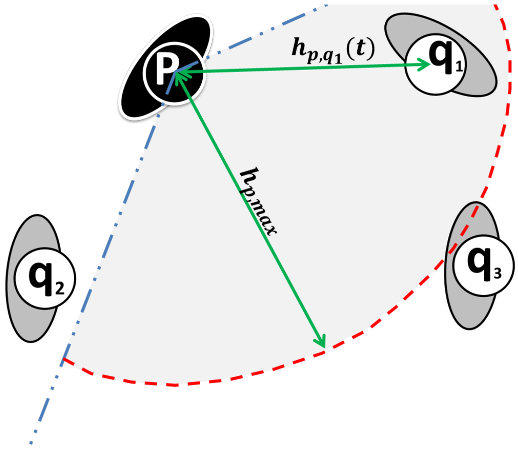

Figure 3.11: Visualization vision field and distance headway, where the grey region indicates the vision field of pedestrian *p*.

Where $\vec{v}_p(t)$ is the walking velocity, $\vec{x}_q(t)$ the location of pedestrian q, $h_{p,max}$ is the maximum interaction distance (see figure 3.11), and $V_p(t)$ the vision field of 120° of pedestrian p at time t. The dot-product of two normalized vectors under an angle of 60° is 0.5[11]. In this interpretation, only pedestrians in front of pedestrian p within 60° of its current angle of movement are taken into account in the computation of the minimum headway. The maximum distance headway $h_{p,max}$ is set to be 3 m.

This is another definition of the distance headway than was proposed in Hoogendoorn & Daamen (2005). Pedestrians in the movement base cases are not always following each other along one line. As such, the nearest pedestrian q is not always directly in front of pedestrian p[12]. A vision field is included in order to restrict the field in which the walking dynamics of other pedestrians are taken into account. The centre point of the vision field of a pedestrian is assumed to always be aligned with the current walking direction of that pedestrian. The dimensions of the vision field have been chosen a little bit less stringent than the shape of this field found by Kitazawa & Fujiyama (2010) in order to also account for most pedestrians directly in front of pedestrian p.

The distance headway does not take into account the walking direction of pedestrian q. As such, this metric provides information about the spatial distribution of all pedestrians a certain pedestrian can see, not the risk that is caused by the walking speed and directionality of pedestrians.

[11] The dot-product of two vectors represents the relative alignment of the vectors. The result is 1 if the vectors align perfectly, 0 if the vectors are orthogonal and -1 if the vectors point in completely opposite directions.

[12] This definition does not account for two types of walking behaviour which have been hinted at in literature, namely the zipper-effect (Hoogendoorn & Daamen, 2005) and pressure from the back, since the development of these phenomena is not understood yet.

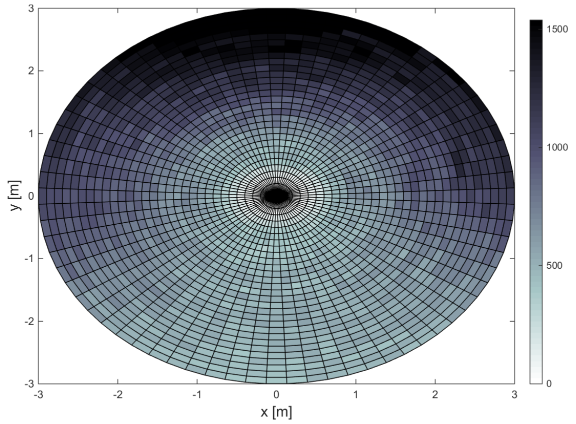

Figure 3.12: Visualization of the spatial distribution of interactions

Spatial distribution of interactions

A distance headway is related to a direction of movement. As such, the distance headway itself does not provide information with respect to the distribution of pedestrians over space relative to the position of pedestrian p. In order to understand the distance pedestrians retain with respect to other pedestrians depends on the angle of interaction the spatial distribution of the interactions is determined (see figure 3.12 for a visualization). This graph displays the frequency of spatial distribution of interactions between any two pedestrians. The position of any pedestrian q is logged with respect to the position and movement direction of pedestrian p for all realisations of the location of pedestrian p within the study area.

Time-to-collision

While the distance headway provides information about the available space to take the next step, the time-to-collision illustrates the risk of actually colliding with another pedestrian. The concept of time-to-collision has been used by among others Fiorini & Shiller (1998a), Pettre et al. (2009) and Berg et al. (2011) to derive collision-free routes for objects in dynamic environments. This measure represents the earliest moment in time that pedestrian p would collide with any other pedestrian if both maintain their current walking direction and speed. To compute the exact moment of collision, as described by Fiorini & Shiller (1998a), is rather expensive. Therefore, in this research a heuristic approach is used. It is assumed that a collision occurs if two pedestrians touch, which happens if their circumferences intersect (see figure 3.13 for a visualization). The circumference is assumed to be a circle with a radius of 0.20 m in order to limit the computational complexity.

Alignment of interactions

The angle of interaction between two pedestrians is defined as the dot-product of the normalized velocity vectors (i.e. walking direction) of two interacting individuals, see figure 3.14 for a visual representation of the alignment of interaction. This metric can be interpreted as the relative alignment of the current movement directions of pedestrians p and q. The alignment of interaction is determined with respect to all pedestrians q that are in the vision field of pedestrian p at time t.

$$\alpha_{p,q} = 1 + \frac{\vec{v_p}}{|\vec{v_p}|} \cdot \frac{\vec{v_q}}{|\vec{v_q}|} \qquad \forall \vec{x}_q(t) \in V_p \tag{3.8}$$

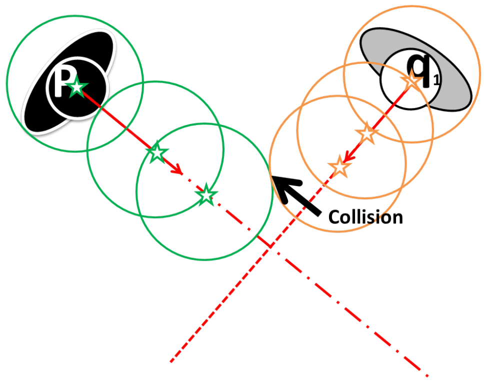

Figure 3.13: Visualization computation of the time-to-collision

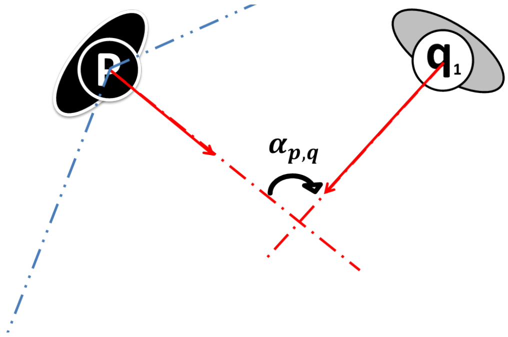

Figure 3.14: Visualization alignment of interaction.

Alignment of vision location and walking direction

In order to establish whether the alignment between the current location of pedestrian q and the current movement direction of pedestrian p influence the walking velocity of pedestrian p, also the alignment of the sight location has been quantified. This metric identifies only the location and not the movement direction of pedestrian q. As such, no correlation with the alignment of interaction is expected. Figure 3.15 provides a visualization of the angle under consideration, while eq. 3.9 provides the mathematical description.

$$V_{p,q}(t) = 1 + \frac{\vec{v}_p}{|\vec{v}_p|} \cdot \frac{\vec{x}_q(t) - \vec{x}_p(t)}{|\vec{x}_q(t) - \vec{x}_p(t)|} \tag{3.9}$$

Total strength of interaction

In the proposed conceptual model all metrics relating to the interaction between pedestrians p and all other pedestrians q come together in a variable named the Strength of Interaction. In the remainder of this thesis this variable is computed as follows:

$$I_p(t) = \sum_p \left[\frac{1}{h_{p,q}} * (\alpha_{p,q}) * \frac{V_{p,q}(t)}{V_{p,max}} * T_{p,q}(t) \right] \tag{3.10}$$

In this formulation the strength of an interaction between two pedestrians increases when

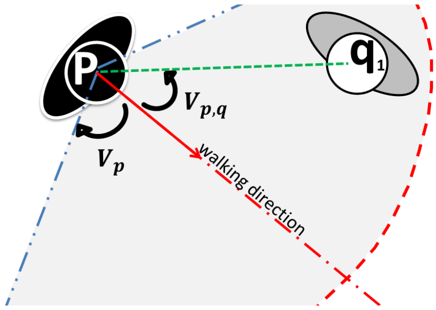

Figure 3.15: Visualisation of the angle of sight.

the distance headway between pedestrians p and q decreases ($1/h_{p,q}$), the angle between the walking direction of p and q increases ($\alpha_{p,q}$), the location of pedestrian q becomes more dominant within the vision field of pedestrian p ($V_{p,q}$), and the duration of the interaction increases ($T_{p,q}(t)$).

The variables that are considered in the computation of the total strength of interaction can be combined in several ways. In this study these metrics are combined in such a manner that the movements of pedestrians who are more prominent within another pedestrian vision field (i.e. being nearby, coming towards you or are within a pedestrian vision for a long time) are reacted to more strongly.

Demographic characteristics of the crowd

Previous research found that the main demographic (age and gender) characteristics influence the walking dynamics of the pedestrians. The videos are recorded orthogonally, as such, so it was not possible to determine the exact age of every person in all sequences. Instead a division into age groups is made based on visible characteristics of the pedestrians by means of manual identification. The used age groups are child, adolescent, adult, and elderly. Also gender could sometimes not be determined due to the lack of distinguishable physical features. The results with respect to age and gender depicted in this thesis are related only to individuals and groups for which both characteristics could be determined.

3.7 Summary and a look ahead

This chapter has determined a data collection methodology that can be used to study the operational walking dynamics of pedestrians in a crowd at large-scale events. This chapter established that this specific research subject (i.e. pedestrians at large-scale event terrains) requires a data collection methodology which is capable of capturing trajectory data sets at large-scale events by means of equipment which does not hamper the flow, nor captures the eye of the pedestrians.

Subsequently, the required type of information was determined. To produce the type of information required for the analyses in this thesis one could suffice with an off-line, area-bound research method that produces very precise continuous information with respect to the position of all pedestrians within a certain area. Additionally, this automated data collection method needs to be able to actively retrieve the position data (”pull”) of all pedestrians.

A review of data collection methods indicated that only one research method can meet the requirements on this ”wish-list”, namely a camera-system with a birds-eye view that records the movements of the crowd and stores it for off-line analysis. This methodology consists of a Multi-camera Stand-Alone VideoInstallation (McSAVI) to record the pedestrian movements, a detection and tracking software program (MODT-2) and a trajectory filtering procedure.

Besides the data collection methodology, also the cases for the empirical data collection have been established. Acquiring the movement base cases was one of the key requirements. The taxonomy of these base cases was introduced in chapter 2. Besides that, several other requirements were mentioned with respect to the type of population (mainly adults), the type of weather (dry and temperature 15-35$°C$), presence of dynamic obstacles (no interfering dynamic obstacles) and the goal-orientation of pedestrians (predominantly walking). Based on these requirements, seven study locations have been selected.

Finally, this chapter has mentioned several variables that can be used to assess the movement behaviour of pedestrians within a crowd. A mathematical definition of the flow variables velocity, density, distance headway, the time-to-collision, the alignment of interaction and the strength of interaction has been provided. Besides a definition also the implications of the choices made in the process of establishing these definitions have been reviewed.

The trajectory data sets, captured by means of the data collection and analysis methodology detailed in this chapter, are used in chapter 4 to test the conceptual model presented in chapter 2. In chapter 5 the general qualitative and quantitative trends related to the operational walking dynamics of pedestrians are established. Furthermore, the data sets are used to calibrate and validate a microscopic and macroscopic model in chapters 7 and 8.

Chapter 4

Testing the conceptual model

A conceptual model of related behavioural hypotheses has been proposed in chapter 2. The model relates distinct characteristics of the pedestrian, its physiological environment, and the flow situation. The literature mentioned in chapter 2 has not provided enough insights into the movements of pedestrian walking dynamics at large-scale events to corroborate the conceptual model.

The data sets described in chapter 3 can be used to generate insights with respect to the walking dynamics of pedestrians in crowds at large-scale events and as such provide the opportunity to test the proposed conceptual model. In order to perform these tests, first hypotheses with respect to the relation between the variables of the conceptual model are put forward. Accordingly, statistical tests are performed to test the significance of the hypotheses. Based on the results a final version of the conceptual model is presented.

The first section (4.1) describes the derivation of the hypotheses based on the conceptual model described in chapter 2 and the results of the statistical tests. Based on these results a finalized version of the framework is presented in section 4.2. Afterwards, section 4.3 briefly discusses the validity of the conceptual model. This chapter finishes with conclusions regarding the movement behaviour of pedestrians within a crowd during large-scale events in section 4.4.

This chapter is an adapted and updated version the first part of the following published paper:
Duives, D.C., W. Daamen, and S.P. Hoogendoorn (2015). Proposition and testing of a conceptual model describing the movement of individual pedestrians within a crowd.
Transportation Research Procedia, 9, pp. 36-55.

4.1 Introduction and testing of the hypothesis

In this section the testing of the conceptual model is performed based on the trajectory data sets gathered at large-scale events. To the best of the author's knowledge, this is the first time that empirical trajectory data is used to test a conceptual model of related behavioural hypotheses which describes the movement dynamics of pedestrians in a crowd. Comprehensively testing the entire conceptual model is a daunting task that is considered too elaborate for this thesis. Even though testing by means of multi variate models or factor analysis, thus considering the influence of several variables at once, would be preferential, this study starts by testing the basic configuration of the model by means of a straightforward regression analysis of individual pairs of variables. The author assumes that if the relations between the variables are tested and found to be significant, the main structure of the proposed configuration of the conceptual model is valid.

4.1.1 Testing procedure

From the conceptual model, many behavioural hypotheses can be deduced. The most dominant ones are tested in this chapter. Two distinct procedures have been used to test the hypotheses. Therefore, the testing procedure is split in two parts, namely the hypotheses that are tested by means of linear regression and the hypotheses that are tested by means of a Welch's t-test. The behavioural hypotheses for which tests are performed are mentioned in table 4.1 and table 4.2. Every row represents one behavioural hypothesis consisting of the relation between variable 1 and variable 2.

Several relations tested in this study have also been derived in previous studies (e.g. velocity-density , velocity-distance headway, velocity-flow, distance headway-density). The reader is referred to chapter 2 for a discussion of these results. These hypothesis tests are repeated in order to establish the consistency of the findings of this thesis with the findings described in literature. Since the results of these specific hypothesis tests, which are mentioned in table 4.1, are similar to the empirical findings described in literature, it is assumed that the current data sets are sufficient to test the configuration of the conceptual model.

A subset of the empirical data sets described in section 3.5 has been used to test the hypotheses in order to limit the computational effort involved. Data sets from the 4Daagse in Lent, Hatert and Wijchen, the marathon in Rotterdam, Queensday in Amsterdam and the Liberation day festival in Wageningen have been used to corroborate the configuration of the conceptual model. After filtering, 1188 trajectories consisting of over 90 thousand data points (approximately $8 - 10$ fps) have been considered in this set of tests, featuring several distinct movement base cases.

Similar to most studies into animal movements (Dray et al., 2010), during the quantification of pedestrian movement behaviour highly spatially and temporally autocorrelated data is used. This results in a violation of the assumptions of the least squares assumption. As a result of the autocorrelation of data points, it is expected that the sampling variance of the regression coefficient β is underestimated and as such the t-statistic is overestimated (Ossen & Hoogendoorn, 2005). Even though several researchers, among others Dray et al. (2010), have proposed sophisticated methods to deal with autocorrelation, this thesis is not accounting for this effect since the impact of these methods on the results in case of pedestrian movement research is undetermined.

4.1.2 Testing by means of linear regression

Linear regression is used to test the hypotheses. The author does, however, not suggest that all these relations are indeed of a linear nature. Linear regression has been used to determine the presence and sign of the relation between the variables. In general, the shape of the data cloud did not suggest reasons to deviate from this type of test. For all hypotheses the relation detailed by equations 4.1 and 4.2 is estimated.

$$Y_i = \alpha + \beta \cdot x_i \tag{4.1}$$

$$H_0 : \beta = 0, H_1 : \beta \neq 0 \tag{4.2}$$

In table 4.1 the column 'Aggregation' mentions the aggregation level at which the data sets are compared. The comparison can be based on individual data points per time step (Individual), data points per pedestrian averaged per trajectory (Trajectory), data points per time step averaged for the population (Time step), or data points averaged over both time and population per data set (Data set). The following columns represent the variables of the regression analysis. The last three columns represent the sign of the found relation, the t-statistic of the hypothesis test of the gradient and the significance level of the test.

The results show that all tested hypotheses turn out to be significant. Moreover, the signs of the tested hypotheses agree with the findings in the empirical literature. Furthermore, the signs of multiple linked hypotheses in the conceptual model that together describe one empirical findings agree. For instance, while the minimum distance headway and the walking velocity are positively correlated, the relations hypothesized to be in-between in the conceptual model (i.e. the minimum distance headway and total interaction, and the total interaction and walking velocity) are both negatively correlated.

There are three remarkable results among the findings. First, the behavioural hypotheses relating to the quantification of the interaction between individual pairs of pedestrians are significant. Collision Avoidance models (e.g. Paris & Donikian (2007) and Moussaïd et al. (2011)) assume that the local interactions between pedestrians determine the movements of every pedestrian. Therefore, the significance of the findings in this chapter indicate that this type of pedestrian simulation models might describe the operational walking dynamics of pedestrians within a crowd correctly. Secondly, even though the quantification of the strength of

Table 4.1: Hypotheses derived from the conceptual model which are tested using the data sets mentioned in the methodology by means of linear regression analysis, where $**$ is significant at the 95% level. Number of data points considered in the regression depends on level of aggregation (Individual - $n = 90912$, Trajectory $n = 1188$).[a]

Variable 1	Variable 2	Aggregation	α	std(α)	β	std(β)	Sign	t-stat	Sign.
Velocity	Density	Individual	-0.154	0.002	1.349	0.004	-	-75.71	**
Velocity	Distance headway	Individual	0.338	0.004	0.644	0.006	+	85.10	**
Velocity	Flow	Individual	-0.154	0.002	1.349	0.004	-	-75.70	**
Density	Flow	Individual	0.948	0.01	0.588	0.012	+	94.83	**
Distance headway	Density	Individual	-0.21	0.002	1.690	0.005	-	-86.06	**
Distance headway	Number of people in infrastructure	Time step	-0.002	0.0005	1.36	0.017	-	-2.97	**
Max. velocity	Temperature	Data set	0.048	0.021	0.420	0.45	+	2.20	**
Max. velocity	Velocity	Trajectory	1.06	0.020	0.267	0.020	+	52.4	**
Velocity	Angle of interaction	Individual	-0.277	0.003	0.712	0.005	+	92.25	**
Velocity	Angle of sight	Individual	0.293	0.004	0.804	0.005	+	62.89	**
Velocity	Cumulative duration of interactions	Individual	0.112	0.017	0.914	0.031	+	6.296	**
Velocity	Variance of interaction duration	Trajectory	0.537	0.085	1.136	0.102	+	6.30	**
Velocity	Variance of interaction angle	Trajectory	-0.454	0.046	1.230	0.023	-	-9.89	**
Velocity	Total interaction	Individual	-0.012	0.000	1.14	0.003	-	-25.66	**

[a] These hypotheses tests do not account for the autocorrelation in the data sets. Therefore, high significance levels are found.

Table 4.2: Hypotheses derived from the conceptual model tested using the data sets mentioned in the methodology. The comparison is based on the mean of the sub-populations. The mentioned abbreviations represent uni-directional straight movements (UD-S), uni-directional movements around a corner (UD-C), bi-directional movements under a 180 angle (BD-S) and randomly intersecting movements (X).

Relation	Pop 1	Pop 2	μ_{pop1}	σ_{pop1}	N_{pop1}	μ_{pop2}	σ_{pop2}	N_{pop2}	t-stat	Sign.
Gender - min. distance headway	Female	Male	1.05	0.46	2307	1.39	0.62	8256	-24.39	**
Gender - max. velocity	Female	Male	1.45	0.51	50	1.84	0.56	163	-4.33	**
Gender - velocity	Female	Male	1.23	0.40	2492	1.51	0.39	9006	-31.17	**
Infrastructure - min. distance headway	UD-S	UD-C	0.92	0.17	4440	1.56	0.37	16769	-112.2	**
Infrastructure - min. distance headway	UD-S	BD-S	0.92	0.17	4440	0.76	0.3	6265	32.19	**
Infrastructure - min. distance headway	UD-S	X	0.92	0.17	4440	0.88	0.6	24030	4.76	**
Infrastructure - min. distance headway	UD-C	BD-S	1.56	0.37	16769	0.76	0.3	6265	153.23	**
Infrastructure - min. distance headway	UD-C	X	1.56	0.37	16769	0.88	0.6	24030	131.25	**
Infrastructure - min. distance headway	BD-S	X	0.76	0.3	6265	0.88	0.6	24030	-14.91	**

interaction was reasonably adhoc, also the relations that considered this variable were found to be significant. This implies that this variable might indeed be of importance in the quantification of the operational walking dynamics of pedestrians. Thirdly, the average walking velocity was found to be positively correlated with the temperature of the environment. It is unclear whether this anomaly in the results might be due to other correlated factors within the same data sets, such as for instance the movement base case or event characteristics.

4.1.3 Testing by means of a Welch's t-test

For all relations expressed in table 4.2, the sample means have been compared in order to determine whether the samples indeed belong to distinct sub-populations. For gender two sub-populations (male and female) and five sub-populations are established for the movement base cases (Uni-directional - Straight (UD-S), Uni-directional - Corner (UD-C), Uni-directional - Entering (UD-E), Bi-directional - Straight (BD-S) and Intersecting (X)) that were found at the studied events. Hypothesis test 4.3 is used to test all behavioural hypotheses mentioned in table 4.2. A Welch's t-test is used to test the mean of two populations. This test has been chosen because it can not be assumed beforehand that the population variances are equal and the number of observations per population differs.

$$H0: \ \mu_{pop1} = \mu_{pop2}, \quad H1: \ \mu_{pop1} \neq \mu_{pop2} \tag{4.3}$$

In table 4.2, every row represents one behavioural hypothesis. The following two columns express the means of the sub-populations which are compared. The mean value, the standard deviation and the number of data points belonging to the respective sub-populations are subsequently mentioned. The last two columns express the t-statistic of the hypothesis test and the corresponding significance level.

The table shows that gender is indeed of influence on the movement of pedestrians. The results, moreover, show that also the movement base case within the infrastructure significantly affects the distance headway adopted by pedestrians. However, also in this case correlations with other factors are expected, such as the goal-orientation and the distance headway distribution, that would further limit the significance of the findings described above.

4.2 Presentation and discussion of the conceptual model

Based on the hypothesis tests several behavioural hypotheses depicted in the conceptual framework can be confirmed (visualized in figure 4.1 with bold lines). Others could not be tested using the current data sets (relations drawn with thin lines). Figure 4.1 illustrates that the basic structure of the conceptual model is confirmed by the hypothesis tests.

In the corroborated conceptual model most of the explanatory factors do not directly relate to the macroscopic flow variables. Instead, most characteristics are known (or hypothesized)

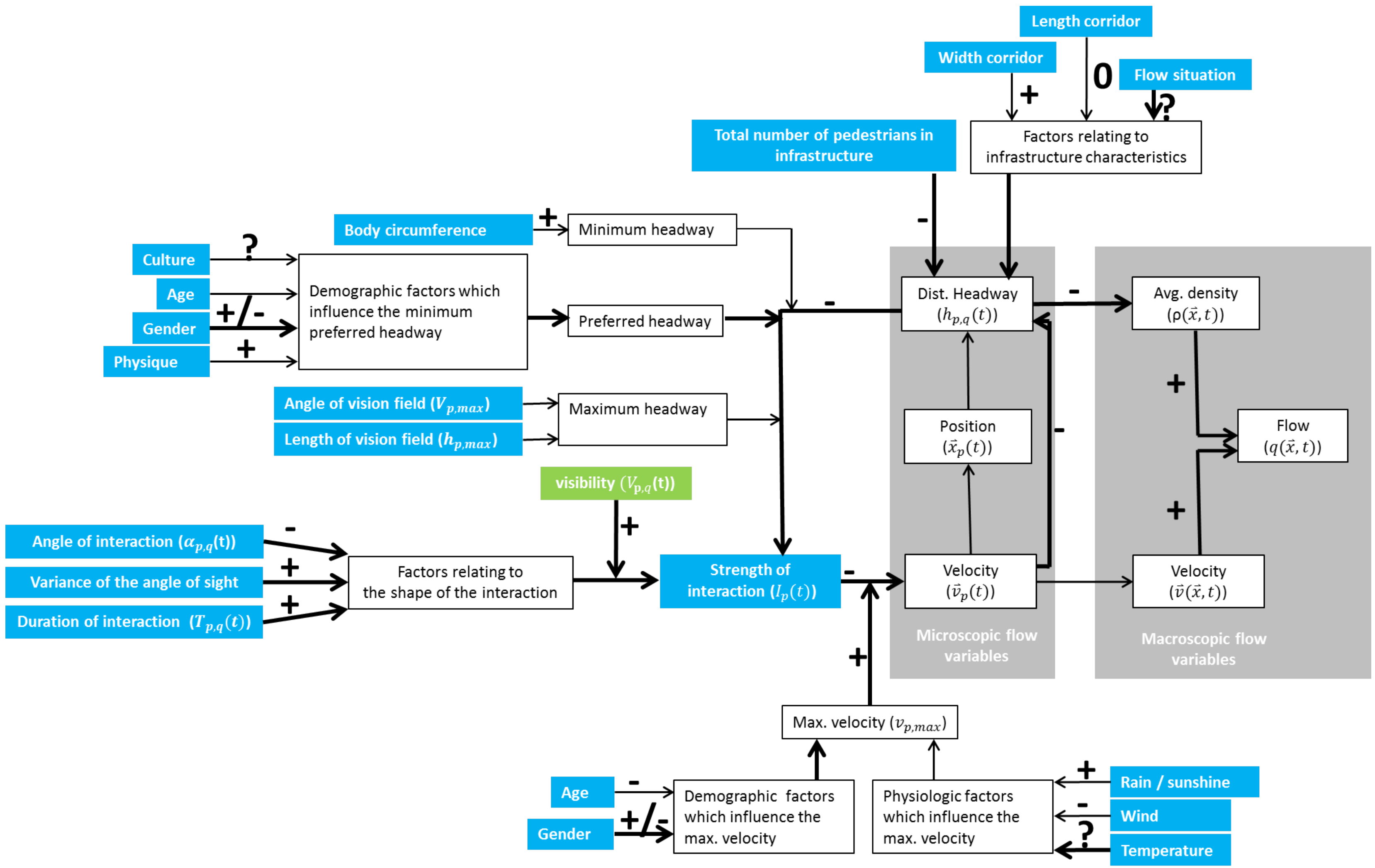

Figure 4.1: The corroborated conceptual model of behavioural related hypotheses including the results of the statistical tests. In the framework + and - respectively represent a positive, negative relation between the variables, while +/- and ? represents relations of which the sign is dependent on the exact realization of the variable or could not be established for all realizations of the variable.

to influence other characteristic that in turn are used by pedestrians in their operational movement decision-making process. Due to the indirect effects of the explanatory factors on the macroscopic flow variables, the proposed model explains why it is difficult to determine one relation, which is applicable under all circumstances, between the macroscopic flow variables velocity, density and flow (often related in the fundamental diagram).

Furthermore, the conceptual model shows that, while studying one relation between two variables, some other characteristics need to be accounted for as well. For instance, one cannot study relations between flow rate and the infrastructure geometry without accounting for several other factors, for instance the movement base case and the demographic composition of the crowd.

4.3 Validity of the conceptual model

The conceptual model has been tested using several data sets and two different tests. The validity of the model depends on the accurateness of the data sets and correct tests for the task at hand. Underneath, the issues related to the data sets and tests is discussed.

Generally 'ceteris paribus' is assumed when testing models. That is, the relation between two variables is tested given that all other influencing factors are equal. In this research, however, empirical data sets are used that are captured at several distinct events, which results in differences in population, goal-orientation, the physical and the physiological environment that might influence the results of the tests. As mentioned before, an attempt is made to limit the extend of these differences. Therefore, no changes in the presence and sign of relationships are expected. However, additional tests should be performed with data that adhered to 'ceteris paribus' in order to establish the conceptual model without doubt.

The conceptual model is tested by means of linear regression and a Welch's test. Both test, which can be considered straightforward, are adopted in order to test the configuration of the conceptual model. These tests cannot be used to test indirect effects and correlations, nor be used to establish the quantitative relation between variables. The author agrees that more sophisticated testing procedures, such as factor analysis and multivariate analysis, are needed in order to establish the presented conceptual model beyond doubt. This is, however, seen as one step to far within this dissertation.

4.4 Conclusions and a look ahead

In this chapter a conceptual model of related behavioural hypotheses describing the walking dynamics of individual pedestrians within a crowd has been tested using linear regression analysis and a Welch t-tests. In this model the characteristics of the individual pedestrian, the pedestrian's physiological environment and the movement base case have been related to the macroscopic flow variables velocity, density and flow. Several new variables have been introduced which quantify the interactions between individuals within a crowd. The basic structure of the proposed conceptual behavioural model confirmed by the performed tests.

The testing results show that this conceptual behavioural model can be used to link characteristics of the crowd, the physiological environment and the infrastructure to the macroscopic flow variables describing pedestrian movements. When all intermittent relations are understood completely, a pedestrian infrastructure can be assessed based on only these high-level properties substantiated by the insights when to use and when not to use such aggregated rules of thumb.

In the following chapters the basic structure of the conceptual framework is kept in the back of our minds, while studying, calibrating and assessing pedestrian simulation models. First of all, the combined results of this and the following chapter are used to determine whether contemporary crowd simulation models can theoretically represent the movement dynamics of pedestrians within crowds. In subsequent chapters, the results also provide a foundation for the calibration and assessment of a microscopic and a macroscopic model in chapters 6 to 8.

Chapter 5

Identification of crowd movement phenomena

A understanding of crowd movement phenomena is essential to realistically model and predict crowd dynamics. Chapter 2 listed behavioural characteristics that are relevant to predict crowd movement phenomena. These characteristics were derived from the existing literature on pedestrian movement dynamics. However, due to the numerous research gaps in this field of study it is questionable whether all crowd movement phenomena have already been mentioned in the research literature.

The cases identified in chapter 3 describe a broad range of movement base cases. In each of these situations distinct crowd movement phenomena arise. To be able to simulate the range of movement base cases described in the previous chapter, all these phenomena need to be captured by a simulation model. The aim of this chapter is to identify which crowd movement phenomena should be taken into account when modelling the movement dynamics of pedestrians in a crowd at large-scale events.

The data analysis method described in section 3.6 is used to explore the characteristics of the movement dynamics captured in the data sets captured as part of this thesis. Besides phenomena related to the operational movement dynamics, this study also focusses on the evidence related to self-organisation (e.g. lane and stripe formation). This identification process regarding the crowd movement phenomena will consist of two steps, namely a preliminary broad analysis and a more thorough review of some remarkable characteristics discovered during the first step related to the fundamental diagram and the microscopic characteristics distance headway, spatial distribution of pedestrians and time-to-collision.

Section 5.1 presents a preliminary qualitative analysis of the data sets captured during this research. Accordingly, several characteristics, identified in section 5.1 are studied more thoroughly in sections 5.2 and 5.3. Based on the results of sections 5.2 and 5.3, and the literature review presented in chapter 2, a list of generic and a list of specific crowd movement phenomena are presented in section 5.4.

5.1 Exploration of the empirical empirical data sets

Crowd movement phenomena can be related to the three levels of the decision making process that were first introduced by Hoogendoorn & Bovy (2004) (i.e. strategic, tactical and operational). Even though the main focus of this thesis is on the operational movement dynamics of pedestrians, the authors need to assure that no phenomena are missed that are caused by decisions taken at higher levels of the decision making process. Therefore, only in the following chapter the decision making and movement dynamics related to all three levels are assessed comprehensively.

Table 5.1 displays the choices related to the respective decision levels and the metrics that can be used to analyse these decisions. Given that the objective of this chapter is to generate a comprehensive list of the movement dynamics and crowd movement phenomena contained in the empirical data sets, the net of analyses is cast wide. As such, both microscopic and macroscopic characteristics of the movement base cases are considered. Therefore, besides the metrics that were identified in the conceptual model in chapter 2, some additional metrics are used in the analyses presented below. Moreover, several metrics mentioned in table 5.1, for instance trajectories, can be used to provide information about more than one decision.

In the following section the macroscopic characteristics of the cases are examined by means of spatial distributions of the velocity and density, and trajectories. Additionally, the microscopic characteristics of the cases are studied by means of the distance headway and the characteristics of the interaction (e.g. angle and spatial distribution). All variables are computed as defined in section 3.6. Contingent upon whether or not the discovered phenomena have been described in literature before, a more thorough quantitative analysis of the phenomena is performed in sections 5.2 and 5.3.

This section proceeds with the discussion of the cases performed during the Marathon of Rotterdam, Queensday in Amsterdam, the Liberation day festival in Wageningen, the 4Daagse

Table 5.1: Variables used during the preliminary analysis of the empirical data sets.

Level of analysis	Decisions	Analysis metrics
Strategic	Activity choice Activity location choice	Activities in the study area Origin choice Destination choice
	Global route choice	Route/Trajectory
Tactical	Self-organisation	Spatial distribution of density Spatial distribution of velocity
	(Local) route choice	Trajectories
Operational	Activity performance	Description of movement behaviour
	Interaction behaviour Walking dynamics Collision avoidance	Distance headway Spatial distribution of interaction Time-to-collision Alignment of interaction
	Biomechanimal dynamics	Swaying rithm step length

in Nijmegen and the Marathon of Amsterdam. These cases will be discussed in order of increasing complexity of the movement base cases. That is, the section starts out with a discussion of the uni-directional straight movement base case captured at Wijchen during the 4Daagse and ends with the intersecting movement base case captured at the Amsterdam Marathon. For each case the movement dynamics of pedestrians during a low and high density situation are compared by means of 9 sequences. Each of the sequences lasts approximately 30 seconds. The results of the preliminary analyses are summarized in table 5.9.

5.1.1 Uni-directional Straight - 4Daagse - Wijchen (4D-W)

As can be expected, the trajectory plots for both low (figure 5.1.a) and high (figure 5.1.b) density situations display almost straight trajectories. In case of the high density situation, however, the trajectories of the participants change direction more often (i.e. the swaying of the pedestrians movement becomes more visible in the trajectories).

The experienced densities in Wijchen are high. Yet, also in case of queueing densities did not reach more than $\rho = 6\ P/m^2$. As one can see, the density is not equally distributed over space in high density situations. A high density region is found that might be a result of the upstream merging point, since more pedestrians joined from the bottom-right than from the top-right. Within the study area no attraction nor repulsion factors are present. As such, it is assumed that the high density region is an artefact of this specific case and not a generic property of the a uni-directional movement base case in which the inflow is randomly distributed over space.

Figures 5.1.d shows that the velocity is spread fairly evenly over the case study area. Table 5.2, furthermore, shows that the standard deviation of the velocity is higher for low density situations than for high density situations. In the latter situation pedestrians can only follow and not overtake. As such, pedestrians cannot retain their own walking velocity in high density situations, but are forced to adjust to the crowd's velocity.

Table 5.2: Quantitative summary of two different data sets of the 4Daagse at Wijchen

Conditions:	Light		Heavy	
Number of pedestrians in sequence	128		242	
Macroscopic variables				
	μ	σ	μ	σ
Velocity $[m/s]$	1.31	0.21	0.27	0.15
Density $[P/m^2]$	0.60	0.28	3.37	1.29
Microscopic variables				
	μ	σ	μ	σ
Nr. of interactions [-]	7.07	2.90	58.68	18.02
Alignment of interaction [dotproduct]	1.96	0.16	1.73	0.47
Headway distribution $[m]$	1.21	0.47	0.50	0.17
Time to collision distribution $[s]$	2.61	1.38	1.73	1.31

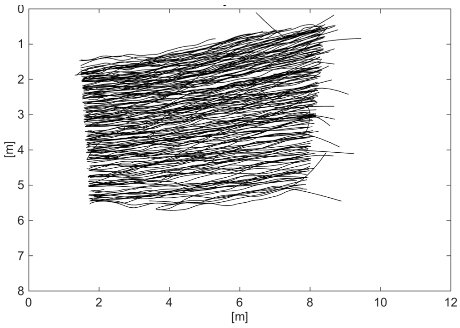

(a) 100 trajectories captured during a quiet period

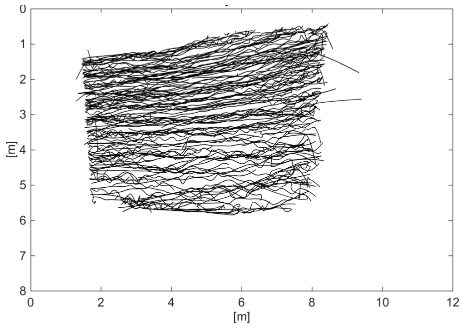

(b) 100 trajectories captured during a busy period

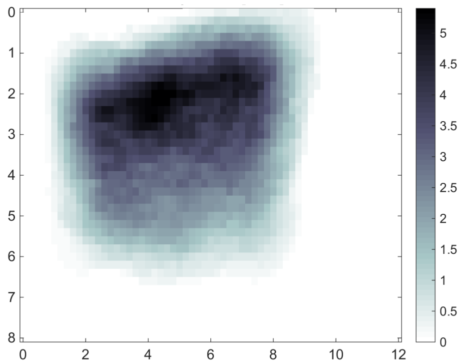

(c) Average density at t=15 s during a high density situation, the colour depicts the density $[P/m^2]$

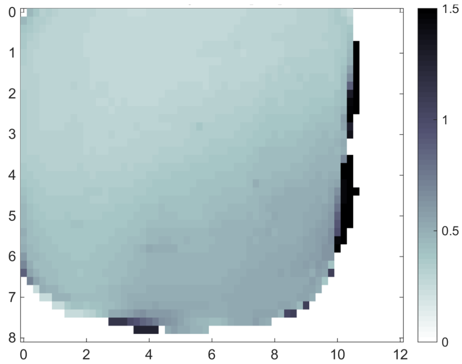

(d) Average velocity at t=15 s during a high density situation, the colour depicts the velocity $[m/s]$

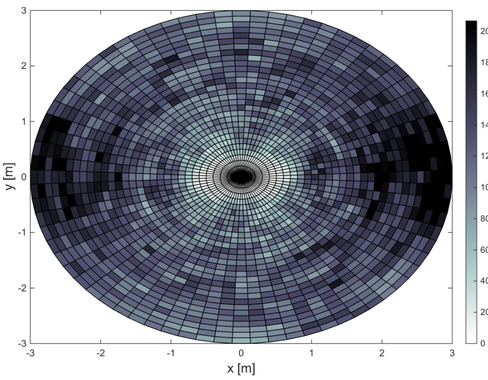

(e) Distribution of the measured interactions over space, the colour represents the frequency of occurance - *low density*

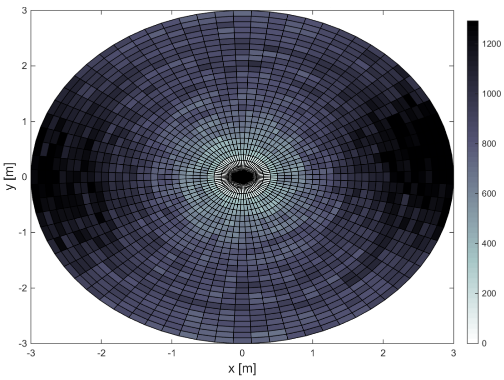

(f) Distribution of the measured interactions over space, the colour represents the frequency of occurance - *high density*

Figure 5.1: Visualizations of the case study 4Daagse at Wijchen

When studying the interactions between the pedestrians more thoroughly by means of the statistics provided in table 5.2, it becomes visible that also in this case most pedestrians interact mainly with pedestrians who walk in the same direction. The headway is found to decrease in high density conditions. In the latter case, the average minimum headway has decreased to 0.48 m, which is a little less than the average step length of a pedestrian (Seitz et al., 2014). At the same time, the average time-to-collision only decreases slightly from 2.61 s to 1.73 s. The short following times are hypothesized to be due to the high predictability of the movements of the other pedestrians in this specific situation.

5.1.2 Uni-directional Entering - Marathon of Rotterdam (RM)

The movement behaviour of the participants of the Rotterdam Marathon is visualized in figure 5.2 and quantitatively described in table 5.3. While the trajectories in low density situations are fairly smooth, the trajectories in the high density situation are very irregular. Moreover, in low density situations pedestrians often exit through the nearest gate, while this choice is less straight forward during dense conditions. That is, pedestrians in the latter situation sometimes choose a gate which is further away from the location where they entered the study area. This might be due to the nuisance of waiting in line for the nearest gate.

Table 5.3 mentions that the velocity during the low density situation is generally high. During high density situations the velocity drops considerably. Furthermore, even though the statistics mention a large standard deviation from the average walking velocity of the participants, the velocity is generally uniformly distributed across the infrastructure (see figure 5.2). However, in crowded situations the speed remains low at the lower left gates, while it increases at the other gates, see figure 5.2c. Additionally, figure 5.2c suggests that the density decreases in the direction of the centre of the gates in both longitudinal and lateral direction. This is probably due to inequality in the demand between the centre and outer sets of gates, which is due to the funnel shape of the infrastructure. The impact of these points on the walking velocity can,

Table 5.3: Quantitative summary of two different data sets of the Rotterdam Marathon

Conditions:	Light		Heavy	
Number of pedestrians in sequence	65		235	
Macroscopic variables				
	μ	σ	μ	σ
Velocity [m/s]	1.12	0.35	0.17	0.17
Density [P/m^2]	0.29	0.16	2.00	0.72
Microscopic variables				
	μ	σ	μ	σ
Nr. of interactions [-]	4.09	2.72	51.60	18.92
Alignment of interaction [dotproduct]	1.84	0.38	1.09	0.68
Headway distribution [m]	1.73	0.59	0.66	0.23
Time to collision distribution [s]	2.70	1.19	1.26	1.31

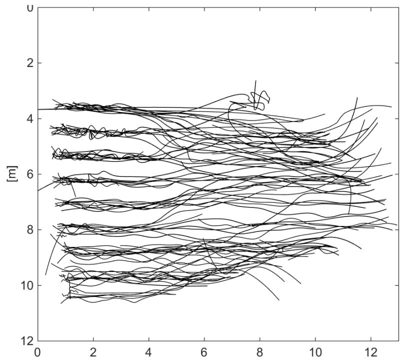

(a) Trajectories captured during a quiet period

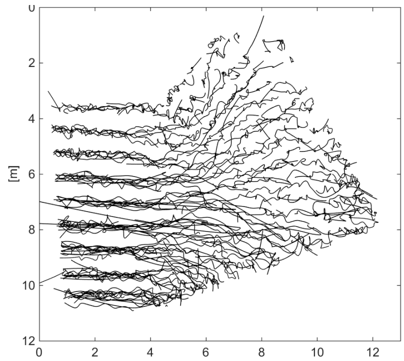

(b) Trajectories captured during a busy period

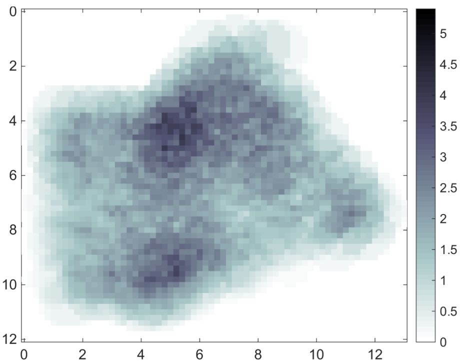

(c) Average density at t=15 s, the colour depicts the density [P/m^2]

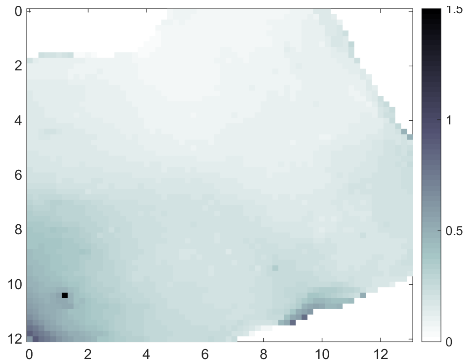

(d) Average velocity at t=5 s, the colour depicts the velocity [m/s]

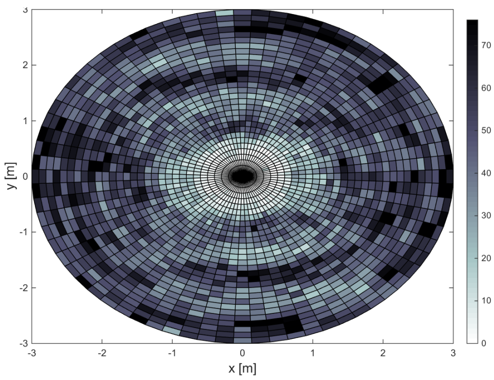

(e) Distribution of the measured interactions over space - low density, the colour represents the frequency of occurance

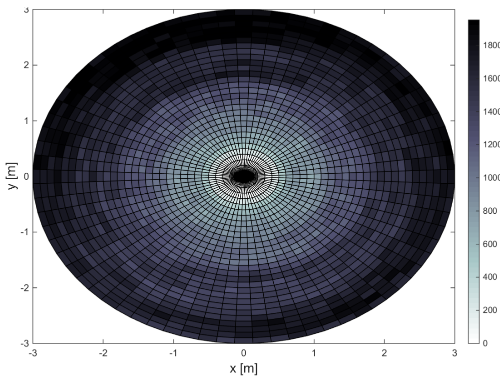

(f) Distribution of the measured interactions over space - high density, the colour represents the frequency of occurance

Figure 5.2: Visualizations of the case study Rotterdam Marathon

Table 5.4: Quantitative summary of two different data sets of the 4Daagse at Lent

Conditions:	Light		Heavy	
Number of pedestrians in sequence	72		327	
Macroscopic variables				
	μ	σ	μ	σ
Velocity $[m/s]$	1.12	0.63	0.83	0.35
Density $[P/m^2]$	0.23	0.15	0.93	0.43
Microscopic variables				
	μ	σ	μ	σ
Nr. of interactions [-]	4.63	7.95	23.47	21.19
Alignment of interaction [dotproduct]	1.53	0.57	1.795	0.47
Headway distribution $[m]$	1.72	0.69	0.98	0.40
Time to collision distribution $[s]$	1.81	1.33	2.75	1.26

however, not be distinguished in figure 5.2d.

In table 5.3 some microscopic characteristics of the data sets are mentioned. This table illustrates that the number of pedestrians a pedestrian interacts with at the same time increases with the density. Moreover, given that the alignment of interaction distribution displays a wide spread, it is assumed that pedestrians walk as individuals and not as clusters that stay together. For the finish terrain of an individual sports event this is as expected.

Table 5.3, moreover, illustrates that most pedestrians interact in a predominantly longitudinal direction with other pedestrians (Alignment of interaction $\alpha_{p,q} >> 1$). Moreover, the minimum distance headway is short, namely $0.66 - 1.73$ m on average. At high densities the average distance headway and the time-to-collision decrease. Since the participants adopt a low walking velocity at high densities, an increase of the minimum time-to-collision is a logical result.

Another distinction between the interaction behaviour of pedestrians at low and high densities is visible in figures 5.2e and f. In both figures zones are visible in which no or a limited amount of interactions occur. Yet, the shape of these two zones differs. Depending on the average density, the shape of the zone changes from an ellipse to a circle. This changes of the in-between distance and position might be caused by the increased number of pedestrian in the infrastructure.

5.1.3 Uni-directional Corner - 4Daagse - Lent (4D-L)

The trajectory plots show that depending on the density distinct manners of rounding the bend exist. In case of low densities (figure 5.3.a) pedestrians tend to cut the corner. That is, pedestrians which walk on the outside upstream of the bend veer towards the inside at the centre of the bend and downstream veer outwards again. Consequently, just upstream of the centre of the bend the trajectories compress. In case of relatively high densities (figure 5.3.b),

[13]The angle of the corner in figure 5.3 is different from figure 3.8, since the y-axis is flipped vertically in the analysis.

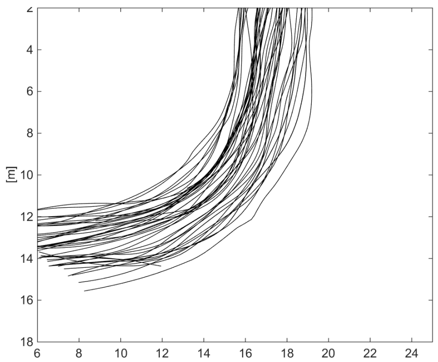

(a) Trajectories captured during a quiet period [13]

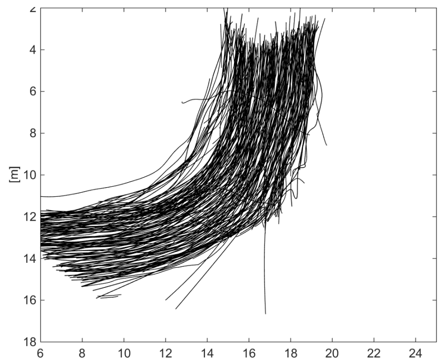

(b) Trajectories captured during a busy period [13]

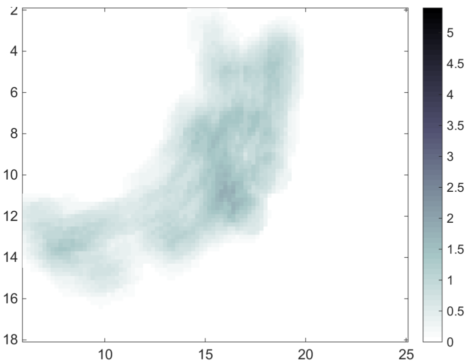

(c) Average density at t=25s, the colour depicts the density $[P/m^2]$

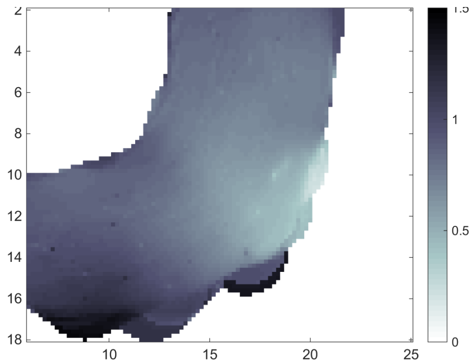

(d) Average velocity at t=25s, the colour depicts the velocity $[m/s]$

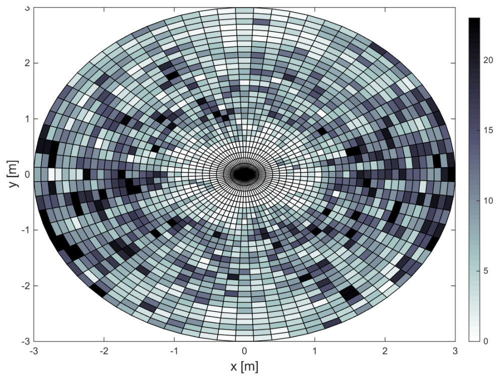

(e) Distribution of the measured interactions over space - low density, the colour represents the frequency of occurance

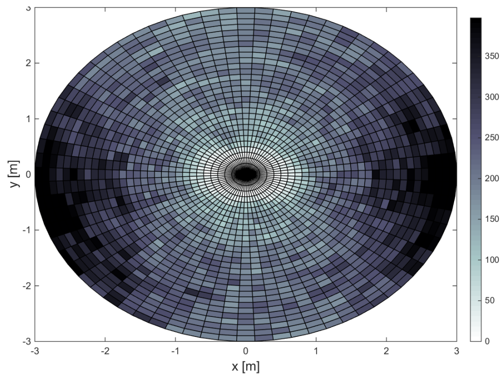

(f) Distribution of the measured interactions over space - high density, the colour represents the frequency of occurance

Figure 5.3: Visualizations of the case study 4Daagse at Lent

this compression is not visible. Yet, the statistics display that even though a compression in the trajectories is found, the density experienced by the crowd does only increase slightly (see table 5.4).

The velocity graph, however, shows that upstream of the bend the average instantaneous absolute speed of pedestrians temporarily diminishes (figure 5.3.b). Downstream of the corner the absolute speed increases again. Furthermore, counter intuitively, especially at the outside of the bend the absolute speed is diminished. Based on the literature, among others (Zhang et al., 2011a), one would expect the opposite to occur, namely a decrease of the absolute speed on the inside of the corner. The low velocity at the outside of the corner can be caused by the interaction with the stall which was located there. The lack of a decrease on the upstream inside of the corner is hypothesized to be due to the lack of obstacles in the vision field in this specific case. Moreover, the lack of a constricting wall or structure at the inside corner might result in lower densities, and as such higher walking velocities, than in the middle of the crowd.

At a microscopic level, pedestrians have only limited interaction with other pedestrians due to the uni-directional nature of the situation (see table 5.4). The number of interactions is also much lower than in the previous case. This difference might be caused by the individualistic nature of the first and the group nature of the second case. The table moreover shows that the alignment of interactions is nearly 2, which only occurs if pedestrians are moving in the same direction while following almost parallel paths. Consequently, even though the minimum distance headway between pedestrians is limited at high densities and pedestrians are present at all angles with respect to the individual, the minimum time-to-collision of the pedestrians is fairly large and actually increases for higher densities.

5.1.4 Uni-directional Corner - 4Daagse - Hatert (4D-H)

Table 5.5 illustrates that only medium high density are measured in Hatert, where in most sequences captured at Hatert the average density is considerably lower than in the cases of Wijchen and the Rotterdam Marathon. As a result, in both the high and low density situation the trajectories shown in figure 5.4a and b are fairly smooth and parallel. This might be due to the low number of frames per seconds of the Hatert sequences, which smooths the trajectories. Besides that, from the trajectories it can be inferred that pedestrians do not overtake each other, nor shift places often.

Furthermore, figure 5.4b shows that the pedestrians use a greater part of the cross-section upstream of the corner (bottom) than downstream of the corner (right). Given that the infrastructure along the corner is at least 4 meters wide, this movement behaviour is not due to external influences but the result of the most optimal (i.e. shortest distance) route through the corner.

[14]The angle of the corner in figure 5.4 is different from figure 3.9, since the y-axis is flipped vertically in the analysis.

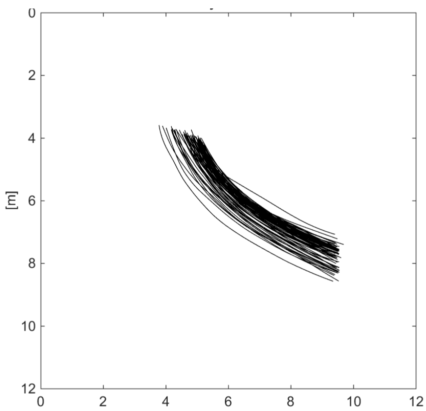

(a) Trajectories at a quiet period [14]

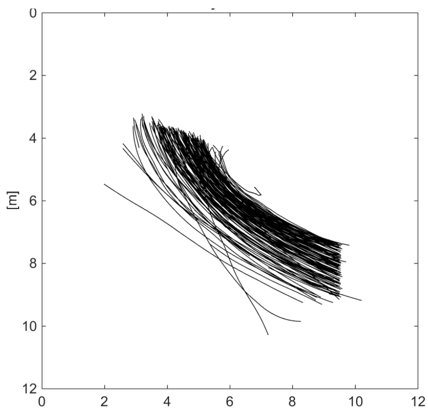

(b) Trajectories at a busy period [14]

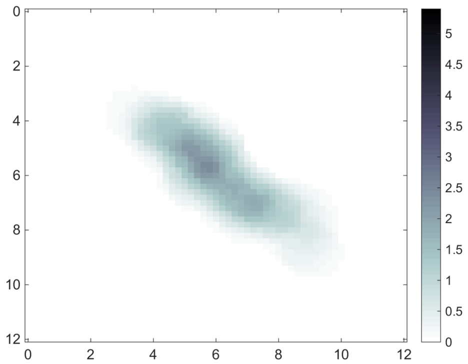

(c) Average density at t=20 *s*, the colour depicts the density

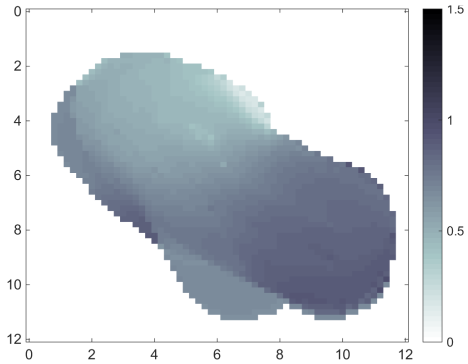

(d) Average velocity at t=20 *s*, the colour depicts the density

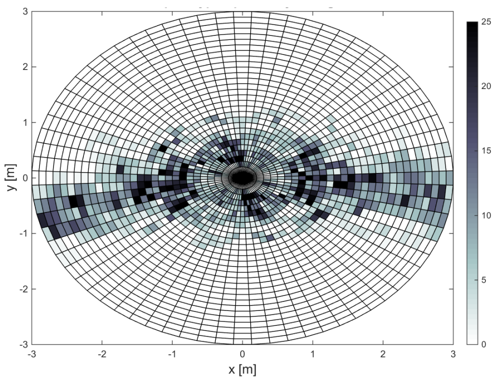

(e) Distribution of the measured interactions over space, the colour represents the frequency of occurance -*low density*

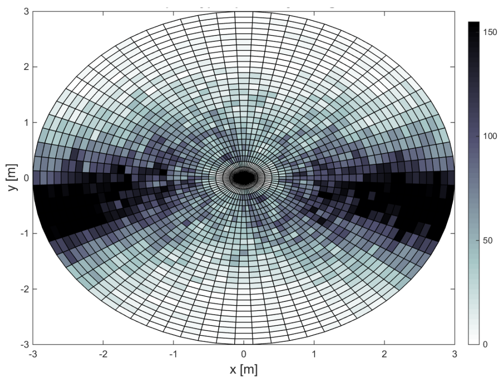

(f) Distribution of the measured interactions over space, the colour represents the frequency of occurance

Figure 5.4: Visualizations of the case study 4Daagse at Hatert

Compared to the other cases, the average walking velocity at the intersection is high. This might be due to the moment of day the movement dynamics were captured in this case, namely relatively early along the route of that day. Besides that, figure 5.4.c and d indicate that upstream of the corner, the average density is higher and the velocity is lower than downstream of the corner. Moreover, the velocity seems to increase and afterwards decrease again. Why this happens, is not entirely understood. Yet both the density and velocity are distributed reasonably uniformly over space. Contrary to the expectation but similar to the previous uni-directional corner case, no lower velocities nor higher densities are found on the upstream inner side of the corner.

An analysis of the interaction behaviour between pedestrians shows that most pedestrians interact with a select stable cluster of other pedestrians, that walk parallel into the same direction (see figures 5.4e and f). Front-to-back interactions[15] are far more common than interactions under an 90° angle. The average alignment of interaction at Hatert is even higher than in the Wijchen case. Given that the average walking velocity never decreases to the extent where a path deviation might produce a temporal shorter path, the lack of a decrease of the average alignment of interaction is probably due to the lack of overtaking and swaying in the Hatert case.

Moreover, according to the results in table 5.5, both the distance headway between pedestrians and the average time-to-collision is limited. In addition, figure 5.4.f illustrates that the no-interaction zone remains approximately ellipsoid during the high density situation.

5.1.5 Bi-directional Straight - Queensday Amsterdam (QA)

A general overview of the characteristic movement behaviour captured at this study area is presented in figure 5.5 and table 5.6. The trajectory graphs show that during low density

[15]Front-to-back is a description of an interaction during which the interaction angle between two pedestrians is nearly 2 (dotproduct). As a result, the pedestrian is staring at the back of the person it is interacting with.

Table 5.5: Quantitative summary of two different data sets of the 4Daagse at Hatert

Conditions:	Light		Heavy	
Number of pedestrians in sequence	72		278	
Macroscopic variables				
	μ	σ	μ	σ
Velocity $[m/s]$	1.83	0.37	1.62	0.49
Density $[P/m^2]$	0.35	0.23	1.89	0.90
Microscopic variables				
	μ	σ	μ	σ
Nr. of interactions [-]	1.74	1.76	20.14	15.42
Alignment of interaction [dotproduct]	1.99	0.01	1.86	0.46
Headway distribution $[m]$	0.88	0.54	0.67	0.33
Time to collision distribution $[s]$	1.09	0.99	1.44	1.20

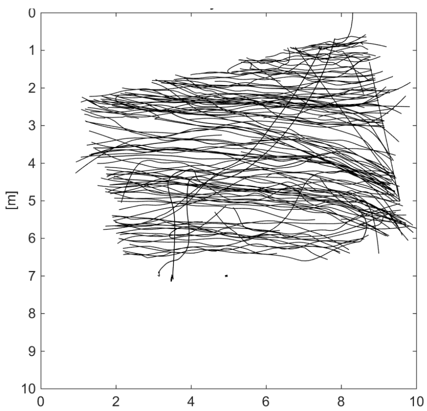

(a) Trajectories at a quiet period

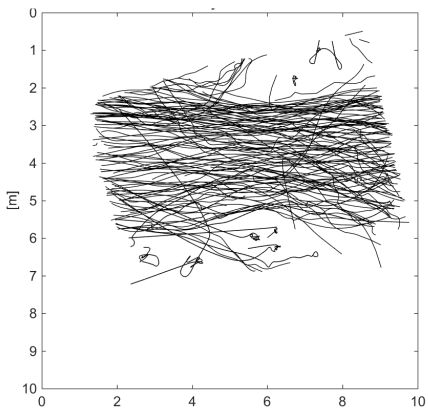

(b) Trajectories at a busy period

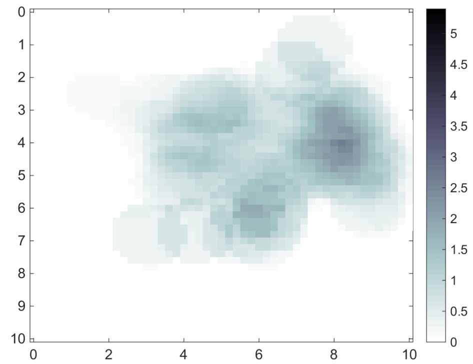

(c) Average density at t=10 *s*, the colour depicts the density

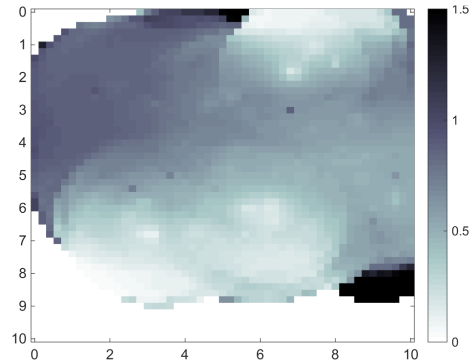

(d) Average velocity at t=10 *s*, the colour depicts the density

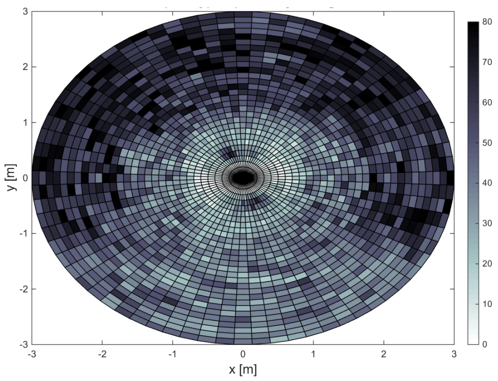

(e) Distribution of the measured interactions over space, the colour represents the frequency of occurance -*low density*

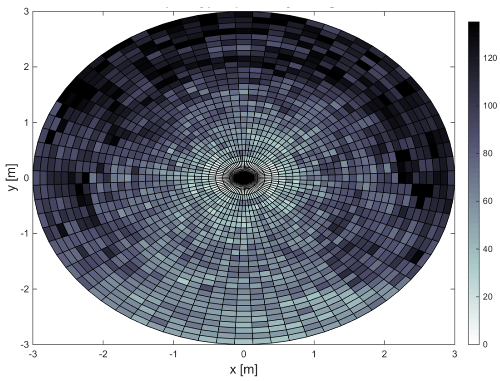

(f) Distribution of the measured interactions over space, the colour represents the frequency of occurance

Figure 5.5: Visualizations of the case study Amsterdam Queensday

situations the movements of pedestrians are more randomly intersecting, while at high-densities predominantly bi-directional straight movements are found. Besides that, the trajectories are fairly stable in both situations (i.e. the swaying is limited), which is probably due to the lack of high densities in both situations. The trajectory plots also show that during high density situations two dominant lanes arise: one from left-to-right (bottom) and one from right-to-left (top).

At this study location the velocities ranged from 0 to 1.3 m/s and the density ranged from 0 to 3 P/m^2. Compared to the pedestrian movements at the Rotterdam Marathon, the velocity and density realizations are very diverse, spatially as well as temporally. This might be due to the impact of the movements of groups or the difference in trip purpose between this and the Rotterdam case. Moreover, in figures 5.5c and d depict high density and low velocity regions. These regions are located nearby pedestrians that stopped or slowed down to watch attractions on the water on both sides of the bridge.

The microscopic analysis illustrates that some pedestrians come to a stand still, and walk away again after a while, thus interacting with almost all moving pedestrians[16]. In low density situations pedestrians on average have a higher number of interactions than in high density situations. These interactions are, unexpectedly, mainly between pedestrians who walk in the same direction as their own direction of movement. That is, most interactions are front-to-back even though a bi-directional movement base case is developing. This might be due to the idea that following pedestrians which move in the same direction results in less effort than trying to find a new/unique path through the crowd.

[16]Even though the focus is on moving pedestrians, the random movements of individuals who are standing still cannot be ignored, since they influence the remaining pedestrians' movements.

Table 5.6: Quantitative summary of two different data sets of Queensday.

Conditions:	Light		Heavy	
Number of pedestrians in sequence	92		128	
Macroscopic variables				
	μ	σ	μ	σ
Velocity [m/s]	0.60	0.61	0.50	0.35
Density [P/m^2]	0.47	0.40	0.90	0.50
Microscopic variables				
	μ	σ	μ	σ
Nr. of interactions [-]	6.11	5.89	23.12	12.31
Alignment of interaction [dotproduct]	1.19	0.79	1.20	0.85
Headway distribution [m]	1.24	0.73	1.01	0.53
Time to collision distribution [s]	1.92	1.45	1.90	1.29

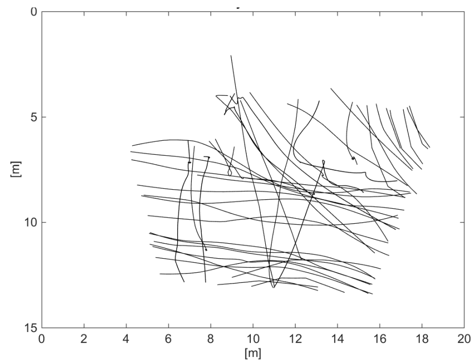

(a) Trajectories at a quiet period

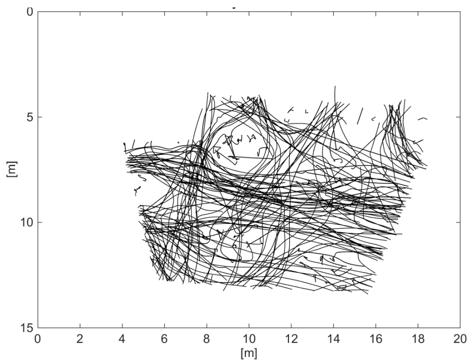

(b) Trajectories at a busy period

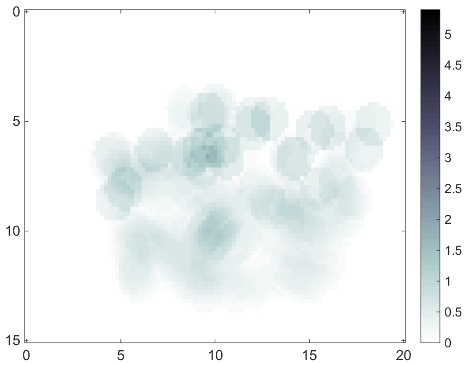

(c) Average density at t=15 *s*, the colour depicts the density

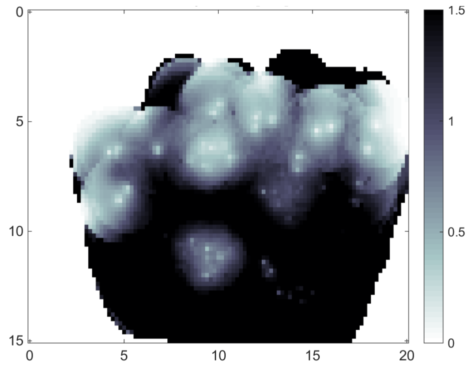

(d) Average velocity at t=15 *s*, the colour depicts the density

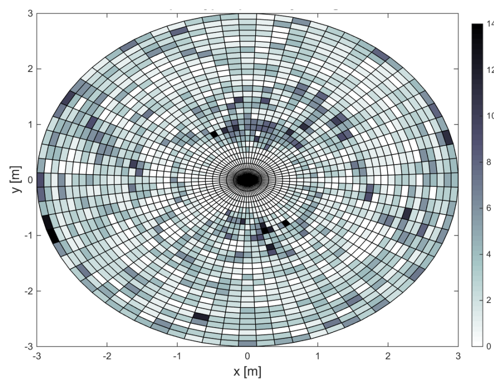

(e) Distribution of the measured interactions over space, the colour represents the frequency of occurance *-low density*

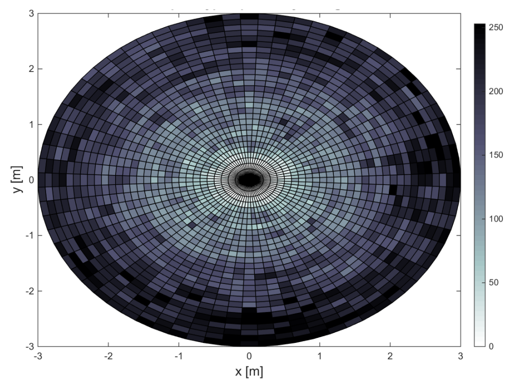

(f) Distribution of the measured interactions over space, the colour represents the frequency of occurance

Figure 5.6: Visualizations of the case study Liberation Day Festival in Wageningen

The shape of the distribution of interactions over space (see figure 5.5e and f) shows a similar trend as the previously discussed data sets. The shape of distribution of interactions over space resembles an elliptical zone in which limited interactions take place. In more crowded conditions, the probability of other pedestrian being near the current location of a pedestrian increases and the shape of the no-interaction zone becomes slightly more cyclic. In contrast to some of the previous cases, the interactions are equally spread over all sides of the circle. That is, on average the pedestrians interact with an similar number of pedestrians in front of them, behind them, on their right and on their left.

5.1.6 Intersecting - Liberation day Festival - Wageningen (LW)

The sample of trajectories depicted in figures 5.6a and b indicate a similar trend as the previous data sets, namely that the trajectories show more swaying movements during high density movement situations. Moreover, the paths between origin (entrance of the camera view) and destination (departure of the camera view) are less straight-forward. This is hypothesized to be due to an increase of the way-finding behaviour of pedestrians at the study area due to a lack of general oversight of the situation. Furthermore, dominant routes between origin and destination arise during high density situations. This is probably due to the fact that pedestrians start following other pedestrians through the crowd.

Compared to the pedestrian movements at the Rotterdam Marathon, the average density and velocity are much lower. Additionally, the spatial change in the average walking velocity is abrupt (figure 5.6d). The density and velocity in low and high density situations is non-uniformly distributed over time and space, which is illustrated by the high standard deviation of the velocity and density. Next to that, the average density increases in high density situations, while the average velocity retains a similar value (see table 5.7). From this we can conclude, that even though the density increases, there is still enough space left in the study area to walk.

Table 5.7: Quantitative summary of two different data sets of the Liberation day festival in Wageningen

Conditions:	Light		Heavy	
Number of pedestrians in sequence	44		200	
Macroscopic variables				
	μ	σ	μ	σ
Velocity $[m/s]$	0.94	0.69	0.92	1.12
Density $[P/m^2]$	0.27	0.20	0.73	0.40
Microscopic variables				
	μ	σ	μ	σ
Nr. of interactions [-]	2.25	2.61	21.91	18.48
Alignment of interaction [dotproduct]	1.31	0.76	1.21	0.71
Headway distribution $[m]$	0.44	0.45	0.02	0.50
Time to collision distribution $[s]$	1.41	1.42	1.45	2.67

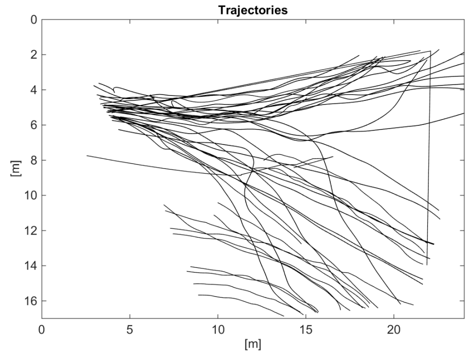

(a) Trajectories at a quiet period

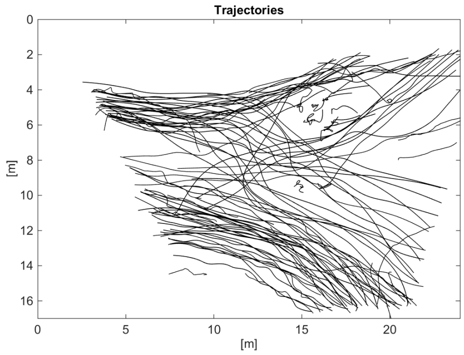

(b) Trajectories at a busy period

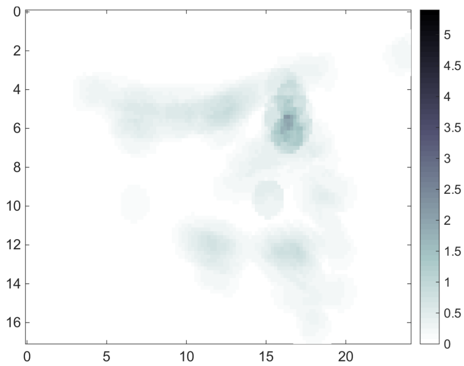

(c) Average density at $t = 20\ s$, the colour depicts the density

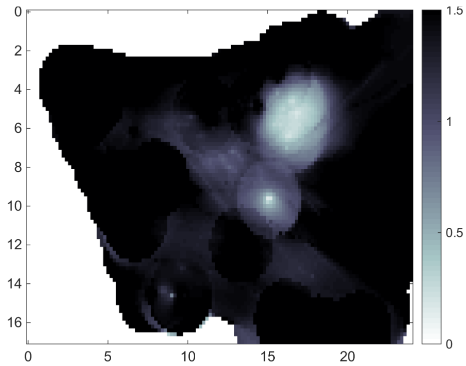

(d) Average velocity at $t = 20\ s$, the colour depicts the density

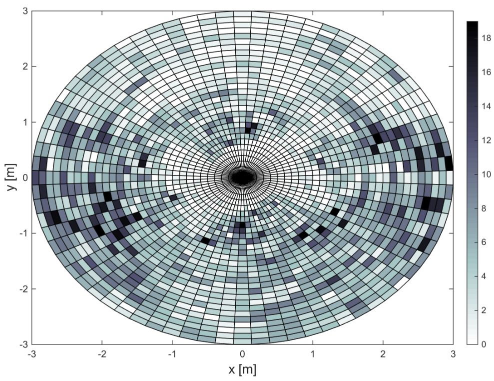

(e) Distribution of the measured interactions over space, the colour represents the frequency of occurance *-low density*

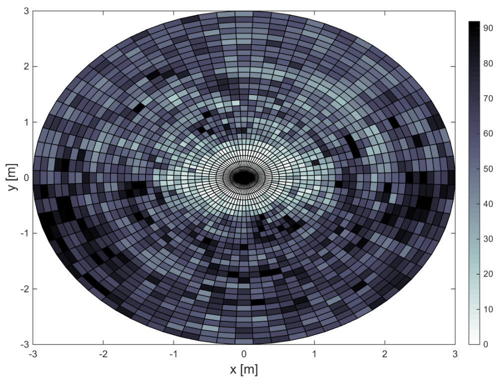

(f) Distribution of the measured interactions over space, the colour represents the frequency of occurance

Figure 5.7: Visualizations of the case study Amsterdam Marathon

An analysis of the microscopic movement behaviour reveals that most pedestrians have a limited number of interactions, all of which are brief encounters. The spread in the connection graph implies that these interactions occur between pedestrians that entered the study area from different sides. The statistics depicted in table 5.7 further corroborate this implication since a wide spread in the alignment of interaction is found within the study area.

The table furthermore shows that the minimum distance headway and time-to-collision are both fairly small considering the previous two cases. It is hypothesized that these differences with respect to the previous two methods are necessary to cope with the increasing number of non-parallel interactions (i.e. interactions with an interaction angle of more than 30°).

Also in these data sets an elliptical non-interaction zone is found (see figure 5.6f). In this case, the elliptical shape is only visible in the high density situation. This is probably due to the limited average density encountered in the low density data set.

5.1.7 Intersecting - Marathon Amsterdam (AM)

The density remained fairly low throughout the entire day, because the study area was relatively large and no peaks in the flow rate existed. Consequently, most individuals had enough space to adopt their preferred velocity. Yet, the velocity distribution of one of the sequences illustrates that the average walking velocity is far higher and the variation in velocities far larger than expected based on the literature for free-flow conditions (see table 5.8). The high average speed might be due to goal-oriented walking behaviour or the relative freshness of the athletes at the study area. The variation of velocities is probably due to the presence of a mixture which includes demographic groups who can be expected to walk slower than average (e.g. parents with children) as well as groups which are expected to walk faster than average (e.g. healthy runners).

Table 5.8: Quantitative summary of two different data sets of the Amsterdam Marathon

Conditions:	Light		Heavy	
Number of pedestrians in sequence	45		89	
Macroscopic variables				
	μ	σ	μ	σ
Velocity $[m/s]$	1.68	0.48	0.95	0.58
Density $[P/m^2]$	0.16	0.11	0.57	0.33
Microscopic variables				
	μ	σ	μ	σ
Nr. of interactions [-]	3.68	3.38	21.09	9.32
Alignment of interaction [dotproduct]	1.47	0.83	1.06	0.85
Headway distribution $[m]$	1.85	0.62	1.24	0.57
Time to collision distribution $[s]$	2.03	1.44	1.59	1.15

An analysis of the interactions between the pedestrians reveals that the minimum distance headway and time-to-collisions are large in comparison to the results of the other cases. The statistics, summarized in table 5.8, suggest that there is a large variation in the alignment of interaction between pedestrians. From this one can conclude that head-on interactions are rare. Even in a random intersecting flow situation, pedestrians interact predominantly with pedestrians that walk approximately into the same direction.

Yet, at the same time both the distance headway and the time-to-collision are found to be fairly large. This might be explained by the large variation in the angle of interaction. That is, pedestrians who interact at a large range of angles, need a larger distance headway to cope with the differences between the interactions.

5.1.8 Conclusions of the preliminary analysis

In this section the movement dynamics has been analysed of pedestrians captured during the Marathon of Rotterdam, the 4Daagse in Nijmegen, Queensday in Amsterdam, the Liberation day festival in Wageningen and the Marathon of Amsterdam. Several macroscopic and microscopic characteristics of the movement behaviour have been identified. In table 5.9 the results of the analyses are summarized. The table illustrates that several characteristics were found in all cases, namely:

- The probability of a longer route being chosen increases depending on the density
- A *negative* relation between the walking velocity and the density exists
- A *negative* relation between the distance headway and the density exists
- The number of interactions with a small dot product at high densities increases when the density increases
- The shape (i.e. ellipse vs. circle) of the no-interaction zone changes when the density increases

To determine the exact interplay between the variables mentioned above, a more thorough quantitative analysis each of these five points required. Given the macroscopic nature of the second characteristic and the microscopic nature of the last three characteristics, these groups of characteristics will be quantitatively analysed in distinct sections. Besides that, the first characteristic mentioned above falls outside the scope of this research as defined in chapter 1, and will therefore not be analysed further.

5.2 The influence of macroscopic flow characteristics

The influence of the density on the walking speed is investigated by means of an essential concept in traffic flow theory, named the fundamental diagram. This diagram relates two of the three macroscopic variables speed (v), density (ρ) and flow (q) to each other. Since Greenshields

Table 5.9: Summary of the preliminary analysis, where Y = characteristic present in the data sets of case, N = characteristic not present in data sets of this case, – = undetermined.

Variable	Effect	4D-W	M-R	4D-L	4D-W	Q-0A	LF-W	M-A
Route choice	Minimum path at low densities	Y	Y	Y	Y	–	Y	Y
	Increase of detour at higher densities	N	Y	Y	–	N	Y	Y
	Lane formation occurs	N	N	N	N	Y	–	N
Velocity - density relation	Density increase, velocity decrease	Y	Y	Y	Y	Y	Y	Y
	Anticipation - High density, low non-zero velocity	Y	Y	–	–	N	N	N
Velocity	Uniform spatial distribution at densities $<2P/m^2$	Y	Y	N	N	N	N	Y
	Uniform spatial distribution at densities $>2P/m^2$	Y	N	N	N	N	N	N
	Stable low velocity regions at specific locations	N	Y	Y	Y	N	N	N
Density	Uniform spatial distribution at densities $<2P/m^2$	Y	Y	N	N	N	N	Y
	Uniform spatial distribution at densities $>2P/m^2$	N	–	N	N	N	N	N
	Stable high density regions at specific locations	N	N	N	Y	N	N	N
Headway	Decrease of headway at high densities	Y	Y	Y	Y	Y	Y	Y
Time to collision	Decrease of time to collision at high densities	Y	Y	N	N	Y	N	Y
Interaction	Mainly front2back interactions at high densities	Y	Y	Y	Y	N	N	N
	Mainly interaction angles between $0-90$ degrees	N	N	N	N	N	Y	Y
	More interactions with small dot product at high densities	Y	Y	Y	Y	Y	Y	Y
	Interaction duration increases with density	Y	Y	Y	Y	N	Y	Y
	Number of interactions increases with density	Y	Y	Y	Y	Y	Y	Y
	Clusters are present in the data sets	Y	N	Y	Y	Y	N	N
Interaction zone	Cyclic no-interaction zone at low densities	Y	Y	Y	Y	Y	Y	Y
	Ellipsoid no-interaction zone at high densities	Y	Y	Y	Y	Y	Y	Y
Swaying	Trajectories become irregular at higher densities	Y	Y	–	–	–	–	–

(1934) first introduced the relation between these three variables, many theories have been derived, predominantly for vehicular traffic, which make use of this concept.

Also for pedestrian traffic fundamental diagrams have been specified in several studies (e.g. Weidmann (1993), Seyfried et al. (2007), Daamen & Hoogendoorn (2010a), Zhang et al. (2011b), Duives et al. (2014a)). The literature study presented in chapter 2 mentions that the exact shape of the diagram is still under discussion for pedestrian traffic. Yet, a general consensus exists with respect to the existence of several branches in the fundamental diagram, namely free-flow, flow degradation and congestion. Figure 5.8 displays the general shape of the two most used versions of the fundamental diagram for pedestrian traffic.

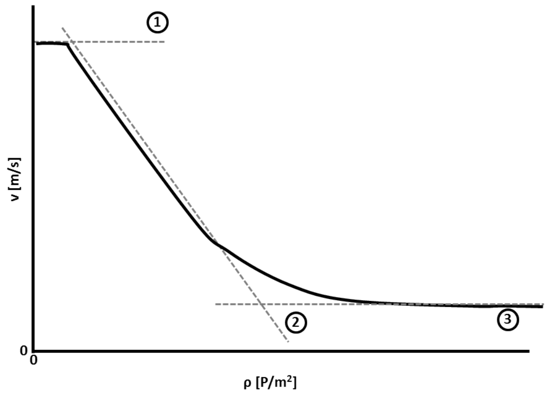

(a) Speed - Density

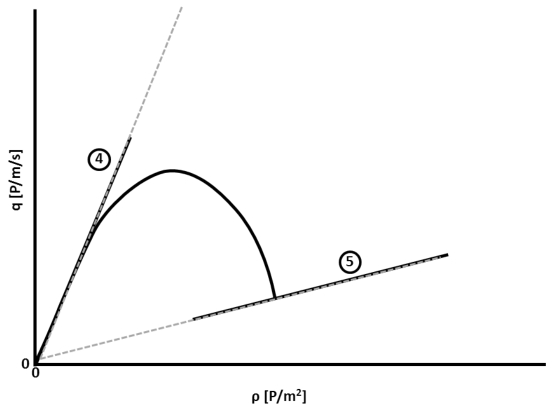

(b) Flow - Density

Figure 5.8: Approximation of the fundamental diagram, where the numbers indicate the linear relations that are approximated in this study.

The main characteristics in these two diagrams can be captured by a piecewise linear approximation. Figure 5.8 displays five dotted black lines, which capture the free-flow regime (lines 1 & 4), the flow degradation regime (line 2) and the congestion regime (lines 3 & 5).

To estimate each of the lines, a specific slice of the data points belonging to one of the cases introduced in section 3.5 is used, namely:

- line 1 is estimated based on the data points near the y-axis with a density of approximately $0 \leq \rho \leq 1$
- line 2 is estimated based on the data points which together describe the negative slope at densities of approximately $1 \leq \rho \leq 4$
- line 3 is estimated based on the dark cloud of data points parallel to the x-axis.
- line 4 is estimated based on the dark cloud of data points with the steepest angle.
- line 5 is estimated based on the dark cloud of data points with the smallest angle.

Moreover, the slope of line 1 and line 2 and the intercepts of lines 4 and 5 have not been estimated, since it can be assumed that these are 0. Besides that, lines 1, 3 and 5 might not always be determined based on the available data sets, given that free flow (1) or flow breakdown (3 and 5) has to occur for these branches to become visible[17].

[17]Different slices are used to determine the linear relations. It is possible that a relation is found in one graph.

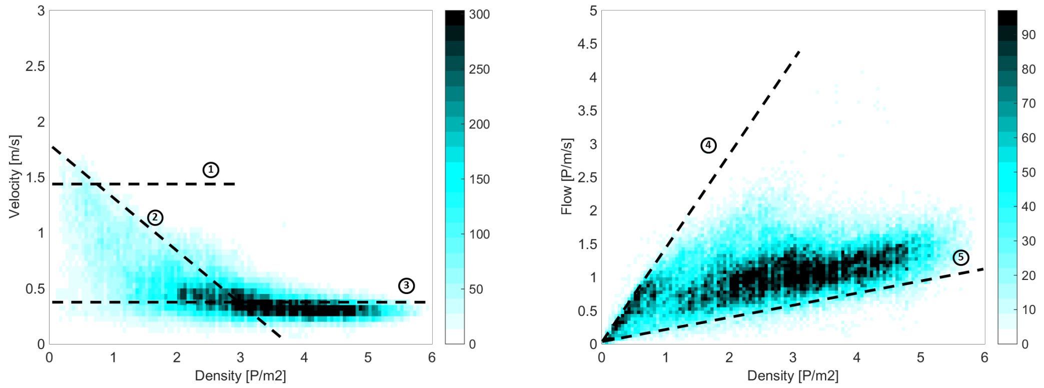

(a) Velocity - Density **(b) Flow rate - Density**

Figure 5.9: Quantitative analysis of the density-velocity and density-flow diagrams of 4Daagse - Wijchen, where the colour indicates the number of data points contained within a certain cell of the graph

Table 5.10: Estimation of characteristic linear relations in the density-velocity and density-flow diagrams for pedestrian movements for distinct cases, where a represents the slope and b the intercept of the linear function $y = a \cdot x + b$.

Serie	Flow situation	1	2		3	4	5
		β	α	β	β	α	α
4Daagse - Wijchen	Uni-dir	1.38	-0.49	1.71	0.35	1.14	0.17
Marathon - Rotterdam	Entering	1.23	-1.02	1.47	0.20	0.89	0.07
4Daagse - Hatert	Corner	2.11	-0.72	2.28	-	2.17	0.52
4Daagse - Lent	Corner	1.40	-0.63	1.58	-	0.92	-
Queensday Amsterdam	Bi-dir	1.15	-0.53	1.21	-	0.79	0.06
Liberation day - Wageningen	Random	1.49	-1.11	1.68	-	1.28	0.05
Marathon - Amsterdam	Random	1.48	-0.84	1.68	-	1.24	0.08

In the data sets captured as part of this study five lines can be identified. See figure 5.9 for an example of the regression analysis for the case study of Wijchen. A similar analysis has been performed for all cases mentioned in section 5.1. In table 5.10 the intercept and slope of each line, which are estimated by means of ordinary least squares, are provided.

From the table three things can be deduced. First of all, the signs of the slopes of all lines are similar. That is, the slope of line 2 is always negative and the slope of lines 4 and 5 is always positive. Consequently, one can conclude that a negative relation between velocity and density, often mentioned in the research literature, is also corroborated by these data sets.

Secondly, in the cases where congestion was observed, the slope of the congestion branch in de flow-density diagram (line 5) is often larger than zero. That is, even during severe congestion a non-zero flow rate is found. Based on the diagrams it is only possible to conclude that even during heavy density situations pedestrians attempt to move. Whether the movements of the pedestrians are directed towards their goal (goal-oriented) or random is difficult to determine in these cases since the instantaneous speed is depicted in the fundamental diagram.

Last of all, the exact intercept and slope of each the lines differs quite a lot. Especially the intercept of lines 1 and 2 vary greatly between the movement situations. As such, it is concluded the empirical data sets of the seven cases cannot be unified by means of a single fundamental diagram.

The origin of these differences is difficult to assess based on the fundamental diagrams alone, given the aggregate nature of this analysis. Even though we attempted to minimize the differences in the pedestrians' demographics, physiologic characteristics, the flow situation and the measurement noise, the remaining differences and measurement noise could still influence the results presented in table 5.10. For example, the relative freshness of the pedestrians at the 4Daagse on the distinct days might still have had an influence on the captured free-flow speed. In order to assess whether the variance in the results only arises at the aggregate level, also an analysis of the microscopic movement behaviour is necessary, which is provided in the following section.

5.3 The influence of the microscopic flow characteristics on the operational movement dynamics

Also several microscopic characteristics were found in the preliminary analysis of the data sets with respect to the headway and the length and width of the no-interaction zone. In the following section an attempt is made to understand under which circumstances these characteristics occur and whether they are generic or case specific. To do so, first the distribution of the distance headway is analysed for each case. Subsequently, spatial distribution of the interactions is discussed. This section finishes with an in-depth analysis of the time-to-collision distribution.

5.3.1 Analysis of the distance headway distributions

In order to understand why pedestrians adopt a certain velocity it is not only essential to know the average amount of space available per pedestrian at an aggregate level, but also how that amount of space is allocated around each pedestrian. That is, how much of that area is actually usable, e.g. located in front and on the sides of a pedestrians' body. While the density can be used to quantify the average amount of space, the minimum distance headway quantifies the usable space.

In this subsection the distance headway with respect to the nearest pedestrian in the vision field is studied, see section 3.6 for a mathematical description of the method used to compute this measure. Because the available space decreases when the density increases, in this study only the distance headway distributions of pedestrians who encounter the same density are compared, see figure 5.10 for an example.

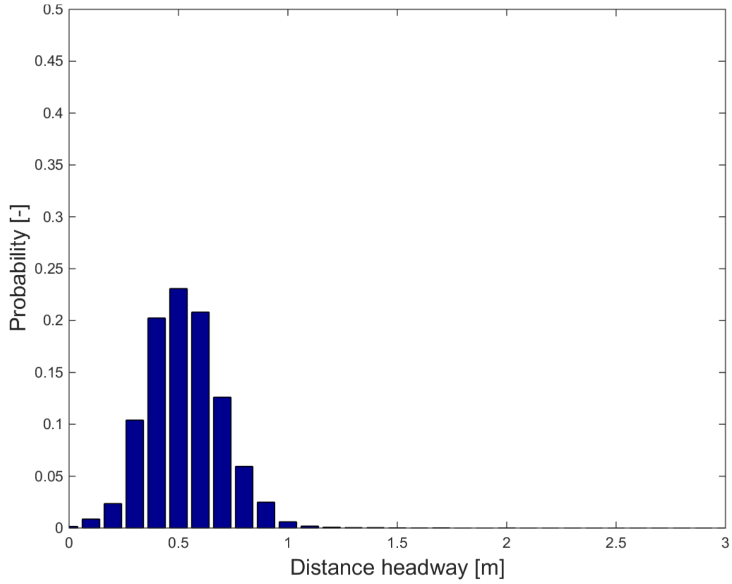

Figure 5.10: The distance headway distribution for the case of Wijchen for a density range of $2 \leq \rho \leq 3$

Table 5.11 outlines the results, which indicates that pedestrians generally retain large distance headways when encountering low density situations. In higher density regimes, the average distance headway retained by pedestrians decreases. At high densities the average distance headway is found to be less than the free step-length of pedestrians (Murray et al., 1964).

Surprisingly, the data also shows that the standard deviation of the results is fairly high for low densities and decreases when the density increases. Large differences in the retained distance headways are found in the crowd at low densities. That is, besides pedestrians with a very small distance headway also pedestrians with a very large distance headway are present that retain a similar velocity. Even though there are several neighbours within close proximity, the pedestrians within the vision field are not equally distributed over space in low density situations. This would suggest an uneven spread of pedestrians across the area at low densities and a more uniform spatial distribution of pedestrians at higher densities. The preliminary analysis of the empirical data sets showed a similar trend.

Table 5.11: Quantitative analysis of the distance headway distributions in metres, where I_{pq} $[-]$ **represents the alignment of interactions and** ρ $[P/m^2]$ **the density experienced by pedestrians.**

Serie	Situation	I_{pq}	$0 < \rho \leq 1$		$1 < \rho \leq 2$		$2 < \rho \leq 3$		$3 < \rho \leq 4$	
		μ	μ	σ	μ	σ	μ	σ	μ	σ
4D-H	UD-C	1.93	0.57	0.38	0.45	0.20	0.42	0.17	0.39	0.14
4D-L	UD-C	1.84	0.99	0.43	0.73	0.26	0.56	0.18	-	-
4D-W	UD-S	1.73	0.78	0.39	0.64	0.24	0.52	0.17	0.45	0.13
Q-A	BD-S	1.31	0.87	0.54	0.72	0.42	0.59	0.27	-	-
M-R	UD-E	1.23	1.00	0.46	0.68	0.21	0.58	0.15	0.49	0.13
LF-W	X	1.12	1.04	0.51	0.76	0.34	0.64	0.13	-	-
M-A	X	1.08	1.09	0.58	0.71	0.35	-	-	-	-

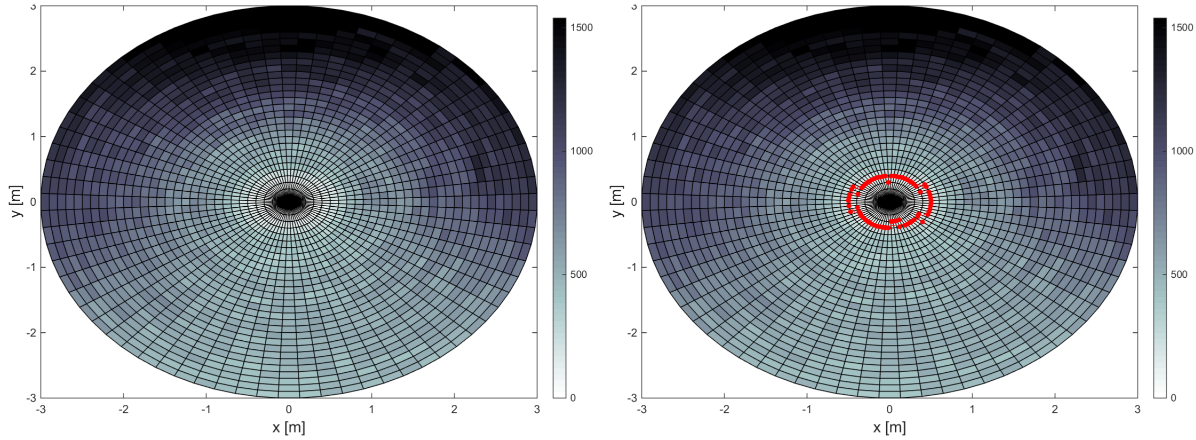

(a) Interaction landscape **(b) Interaction landscape with fitted ellipse**

Figure 5.11: Analysis of the interaction landscape for the case of the 4Daagse in Wijchen for $1 \leq \rho < 2$. The interaction landscape is the result of all interactions within a given case for a pedestrian that experiences a density within a given density range. The colour represents the number of data points with reside in a certain grid cell.

Table 5.11 also shows another trend. If the cases are ranked with respect to the average alignment of interaction, the results suggest that on average pedestrians retain a larger distance headway during the situations in which more interactions under an angle take place. This would suggest that the increase of the distance headway is a coping strategy to handle with these more complex interaction situations.

5.3.2 Analysis of the spatial distribution of the interactions

Next to the distance also the location where a neighbour resides influences the movement opportunities of a pedestrian. That is, a neighbour who stands directly in front of a pedestrian is more likely to hamper a pedestrian's movements than a neighbour who stands at the boundary of their vision field (e.g. 60 degrees with respect to the pedestrian's current movement direction).

The spatial characteristics of the interactions between pedestrians are determined by means of a normalized frequency diagram of the interactions between any two pedestrians. In the graph the frequency of occurrence of the location of all neighbours within a radius of 3 *m* is visualized. In contrast to the graphs in the preliminary analysis, this set of graphs only merges the interaction data of pedestrians which experience a specific density. As a result, this analysis provides a two-dimensional image of the interaction landscape surrounding a pedestrian at a given density. See figure 5.11 for an example of the representation of this landscape for the case of Lent.

The exact shape of this zone is quantified for all cases and several density categories. An ellipse has been fitted which describes the space in which pedestrians encounter only a limited amount of interactions (i.e. less than 50 interactions per cell). This threshold has been chosen independent of the total amount of interactions. In table 5.12 the length of the axes of the ellipse have been specified for all density cases that had enough data to fit the ellipse.

Table 5.12: Quantitative analysis of the spatial distribution of interactions, where LA = long axis, SA = short axis, and $-$ displays that ellipse could be estimated but the amount of data is limited. The lengths are measured in meters.

Serie	Situation	$0 < \rho < 1$			$1 < \rho < 2$			$2 < \rho < 3$		
		LA	SA	$\frac{LA}{SA}$	LA	SA	$\frac{LA}{SA}$	LA	SA	$\frac{LA}{SA}$
4D-W	UD-S	0.60	0.48	1.25	0.49	0.37	1.32	0.40	0.29	1.38
M-R	UD-E	0.62	0.59	1.05	0.5	0.5	1.00	0.4	0.4	1.00
4D-H	UD-C	0.79	0.36	2.2	0.59	0.31	1.96	0.54	0.31	1.74
4D-L	UD-C	0.73	0.52	1.40	0.71	0.55	1.29	-	-	
Q-A	BD-S	0.82	0.34	2.4	0.76	0.48	1.58	-	-	
LF-W	X	0.62	0.49	1.27	0.71	0.63	1.13	-	-	
M-A	X	0.91	0.61	1.49	-	-		-	-	

The results illustrate large differences in the length of the long and short axis per movement situation. This is partly due to noise in the computation and the fact that a fixed number of interactions has been determined as threshold. Yet, in general, one can conclude that the no-interaction zone has the shape of an ellipse ($\frac{LA}{SA} > 1$) for lower densities ($\rho \geq 2P/m^2$) and turns into a circle for higher densities. In the case of Wijchen, this phenomenon does not occur because the length of the short axis decreases more than the length of the long axis. While the other cases, the short axis remains fairly stable with respect to the density and the long axis decreases in length at higher densities. The decrease of the long axis is hypothesized to be due to the effort of pedestrians to retain the space next to their body for as long as possible. Yet, under high densities this becomes more problematic. As a result the average length of the long axis of the ellipse decreases. The space in front of their feet is retained under all situations

5.3.3 Analysis of the time-to-collision

Yet, a small distance headway does not automatically lead to collisions. Only in cases where the distance headway between two pedestrians is small and decreases quickly over time (i.e. the closing speed is high), collisions occur. The risk of a collision can be quantified by means of the time-to-collision. This measure computes for every pedestrian the minimum time which can pass before a collision is imminent, given that both interacting pedestrians retain their current speed and direction of movement.

The distribution of the minimum time-to-collision is estimated for every case study. Figure 5.12 visualizes an example of the minimum time-to-collision distributions for the case study of the 4Daagse - Wijchen. In general, the shape of the time-to-collision distribution is exponential. Since the time-to-collision is also dependent on the available space, distinct distributions are estimated per density category.
Table 5.13 summarizes the results of the procedure. The average time-to-collision times ranges from 2.74 s during free-flow conditions in Hatert, to 0.90 s during congested conditions in Amsterdam during Queensday. By means of a Kolmogorov-Smirnov test, it is established that the distributions estimated for the distinct density categories within one movement situation are generally significantly different at a 5% significance level. Yet, the differences in the means of

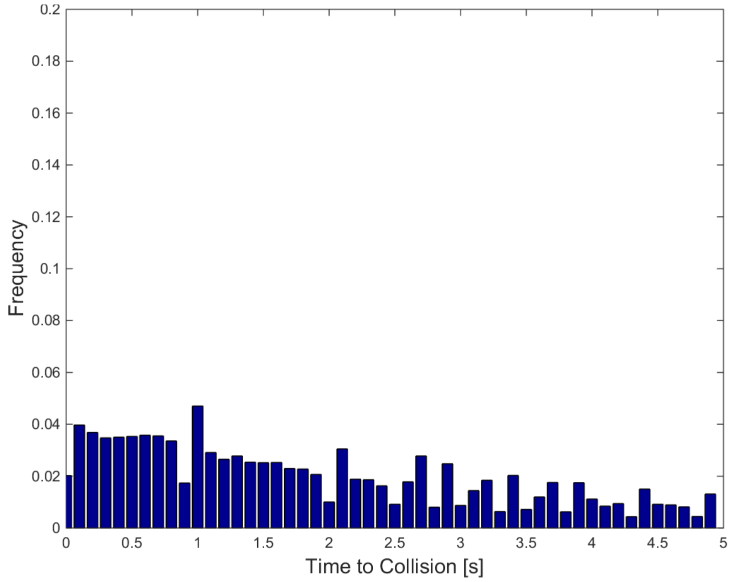

Figure 5.12: Analysis of the time-to-collision distribution for the case of Wijchen for $2 \leq \rho \leq 3$

Table 5.13: Analysis of the time-to-collison distributions

Serie	Situation	$0 \leq \rho < 1$		$1 \leq \rho < 2$		$2 \leq \rho < 3$		$3 \leq \rho < 4$	
		μ [s]	σ [s]	μ [s]	σ [s]	μ [s]	σ [s]	μ [s]	σ [s]
4D-W	UD-S	2.03	1.42	1.96	1.36	1.83	1.32	1.67	1.29
M-R	UD-E	2.31	1.31	2.30	1.29	2.21	1.28	2.03	1.28
4D-L	UD-C	2.74	1.24	2.64	1.30	2.04	1.22	-	-
4D-H	UD-C	1.71	1.23	1.71	1.35	1.57	1.27	1.67	1.31
Q-A	BD-S	1.99	1.29	1.52	1.22	1.14	0.90	-	-
LF-W	X	1.93	1.22	1.87	1.26	1.36	1.29	-	-
M-A	X	1.60	1.23	1.47	1.17	-	-	-	-

the distinct distribution are considered small. Besides that, it is assumed that the temporal and spatial autocorrelation within the trajectory data sets has increased the significance of the results. As such, even though these results are statistically significant, it is questionable whether these results remain significant when the autocorrelation within the data sets is taken into account.

In the previous paragraphs distinct differences in the distance headway distributions were presented. These differences in distance do not necessarily lead to a similar change in time-to-collision. This implies that pedestrians adopt their speed in dense situations to retain a similar time-to-collision. That is, a limitation of the distance headway between pedestrians entices pedestrians to reduce their walking speed in order to limit the additional risk on a collision. This finding is similar to the trends found in the diagrams presented in section 5.2. The table, moreover, shows that the time-to-collision is highly correlated with the direction of movement and as such the overall flow situations. This implies that the gradient of the speed reduction is dependent on the flow situation. As a result, the analyses of the microscopic characteristics might explain why one fundamental diagram, irrespective of the movement base case, is possibly not obtainable.

5.4 Lists of crowd movement phenomena

In this chapter the data sets captured during the empirical research have been qualitatively and quantitatively analysed. Several characteristics were discovered with respect to the operational movement dynamics of pedestrians in a crowd during a large-scale event. In the literature review, presented in chapter 2, also several other characteristics were mentioned. These characteristics can be combined into two lists, namely a list of the general crowd movement phenomena and a list of crowd movement phenomena which relate to specific movement base cases. No quantitative values are provided, since the results show that the exact quantitative relations might differ depending on many characteristics.

The first list is presented in table 5.14. Many of the phenomena mentioned in this table have also been established by earlier studies. This study has shown that these phenomena do not only hold in a few specific uni-directional cases, but also hold for more intricate movement base cases.

To the author's knowledge, the list of general crowd movement phenomena includes only one phenomenon that has not yet been mentioned in literature, namely the changing of the characteristics of the operational route choice as a function of the density. During almost all movement base cases the pedestrians were found to follow a direct path between origin and destination during low densities. However, during high density situations ($\rho > 2\ P/m^2$) their routes deviated from this optimal path. The alternative paths changed direction often, which indicates that under these conditions pedestrians have more difficulties navigating through the crowd. The searching behaviour might be due to the lack of oversight in high density situations. If this is the case, the assumption that pedestrians have global knowledge of the traffic state in the network does not hold any more at high densities. Given that global knowledge is one of the major assumptions which underpins almost all contemporary modelling attempts of pedestrian movement dynamics (substantiated in chapter 6), it becomes questionable whether these contemporary models can realistically model pedestrian movement behaviour during high density situations in large crowds during events.

Supplementary to the list of generic crowd movement phenomena, also the phenomena which are specific to specific movement base cases are summarized in a list, see table 5.15. This list consists of the characteristics which develop during specific movement base cases, but which are not explained by the list of general characteristics. The third column of this table mentions the characteristics which were expected based on the literature but were not found. Given that the lack of a trend also provides insights into the movement behaviour of pedestrians, these have also been included.

This second table illustrates two interesting things. First of all, a general lack of interactions during which two pedestrians face each other is missing at a microscopic level in all of the examined cases (i.e. interactions with an angle between 0 to 90 degrees). This might indicate that pedestrians at large-scale events move along in clusters that travels along a similar path for the time being. Since a social connection between the pedestrians that were part of a cluster could not be identified in all cases, it is assumed that this behaviour is due to the self-organisation of the crowd rather than the effect of group structures in the crowd. As a result, many of the anticipated interaction movements that one sees in the laboratory experiments (for example Daamen (2004)) might not occur, since only the leaders of such a group are interacting with the leaders of other groups.

Secondly, the study shows that the density and velocity are not always directly negatively correlated. During several instances upstream of a bottleneck the velocity is uniformly distributed over space, while the density might not be distributed uniformly. This is only possible if the pedestrians do not adjust their velocity directly the density they are experiencing and/or expecting downstream. Earlier works by Daamen & Hoogendoorn (2010b) and Duives et al. (2014a) also found evidence of this effect. Anticipation on adverse traffic conditions downstream might be at the root of this phenomenon.

5.5 A look ahead

In this chapter two comprehensive lists of crowd movement phenomena have been deduced which together describe the characteristics of the movement dynamics of pedestrians during large-scale events. These lists can be used to compose new behavioural theories with respect to the movement dynamics of pedestrians in crowds at large-scale events.

These lists also provide a basis for researchers to assess pedestrian simulation models with respect to the movement dynamics of pedestrians in crowds at large-scale events. A realistic model should be able to simulate most crowd movement phenomena. These lists can be used to select and adopt the best (i.e. most realistic) simulation models.

In the following chapters, the two lists of phenomena that are identified in this chapter, are first used to assess the capabilities of contemporary pedestrian simulation models in chapter 6. Accordingly, in chapters 7 and 8 these two lists are used in the calibration and assessment of a microscopic and a macroscopic pedestrian simulation model.

Table 5.14: List of generic crowd movement phenomena.

Variable	Characteristics
FD - V-ρ	• If density increases, velocity decreases. • Three regimes: a free-flow, a transition and a congestion zone. • At high densities pedestrians will retain a velocity.
FD - q-ρ	• If density increases, the flow rate increases upto capacity. • The transition zone is unstable and knows directional differences. • At high densities, flow might diminish but will not stop entirely.
Headway	• If density increases, the distance headway decreases. • If the avg. interaction angle decreases, the distance headway increases.
Interaction zone	• If the density increases, the length of the lateral axis of the no-interaction zone decreases. • The length of the longitudinal axis of the no-interaction zone is independent of the density.
Route choice	• Searching behaviour is of pedestrian increases during high density situations. • The swaying behaviour of pedestrians becomes more dominant during high density situations.

Table 5.15: List of crowd movement phenomena that are specific for one movement base case.

Flow situation	Characteristics found	Char. expected not found
Uni-dir - straight	• Density uniformly spread spatially • Velocity uniformly spread spatially • Trajectories become more unstable • Predominantly front2back interactions • Lane formation occurs under high densities	• Stop&Go waves • Turbulence
Uni-dir - Corner	• Density increased upstream of corner • Density increase at inner upstream side • Velocity decreased upstream of corner • Predominantly front2back interactions	• Lane formation (Dias et al., 2014b)
Uni-dir - Entering	• Density increases towards bottleneck both longitudinal and lateral • Density focuspoint upstream of bottleneck • Velocity is not decreasing towards the bottleneck • Many short interactions • Predominantly front2back interactions • Wayfinding increased at high densities	• The zipper-effect • Herding • The faster-is-slower effect
Bi-dir	• Density uniformly spread over cross-section • Velocity uniformly spread over cross-section • Trajectories more unstable at high densities • Interactions predominantly front2back • Wayfinding decreased at high densities • Lane formation	• No face-to-face interactions • Increase in wayfinding
Intersecting - Random	• Density uniformly spread over cross-section • Velocity non-uniformly spread over cross-section • Trajectories more unstable at high densities • Interaction angle mainly between 0 and 90 degrees • Wayfinding increased at high densities • Lane formation between dominant origins and destinations	• No peak in face-to-face interactions

Chapter 6

Review of pedestrian simulation models

Many pedestrian simulation models have been developed to predict the walking dynamics of pedestrians in a crowd at large-scale events. However, most models have been developed and calibrated specifically for low density situations of a specific nature (e.g. movement in a shopping centre, movement along a corridor, movement through bottlenecks). It is questionable whether models developed for these specific situations are capable of accurately simulating the walking dynamics of pedestrians within a crowd at large-scale events.

Several scientists have reviewed the available pedestrian simulation models before. Papadimitriou et al. (2009) and Schadschneider et al. (2009), for instance, assessed the existing models on pedestrian walking behaviour, thereby providing a comprehensive review of pedestrian movement models. Helbing & Johansson (2010) assess complex collective behavioural patterns visible within pedestrian crowds and mentioned models that were capable of modelling those phenomena. Bellomo & Piccoli (2012) focus on the mathematical properties of both traffic and pedestrian models. These four works did, however, not study the applicability of the simulation models in the case of crowd movement behaviour during large scale events.

We hypothesize that good pedestrian simulation models can simulate a the whole range of crowd movement phenomena that might develop in the application area. None of the above mentioned reviews links the reviewed simulation models directly to the phenomena occurring during dense crowd movement situations. Moreover, a limited number of simple movement base cases are taken into account. Consequently, the assessment of pedestrian simulation models with respect to crowd motion at large-scale events is currently lacking an important behavioural dimension, namely that of comprehensiveness.

This chapter is an adapted and updated version of the following published paper:
Duives, D.C., W. Daamen, S.P. Hoogendoorn (2013). State-of-the-art crowd motion simulation models. *Transportation Research - Part C: Emerging technologies*, 37, pp. 193-209.

This chapter assesses the capabilities of contemporary pedestrian movement models with respect to pedestrian movement dynamics and crowd movement phenomena that develop at large-scale events. It provides a broad, but not exhaustive, overview of the current literature on pedestrian simulation models of the last decades. The objective of this chapter is to highlight the differences between the modelling approaches with respect to the movement dynamics of pedestrians at large-scale events and to indicate whether gaps in the field of crowd modelling research exist. Next to the operational walking dynamics also other characteristics (e.g. computational effort) are important since they partly determine the applicability of a pedestrian simulation model. Therefore, the scope of the framework developed in this chapter is broader than the scope adopted in the rest of this thesis.

The outline of this chapter is as follows. Afterwards, section 6.1 elaborates upon the research methodology. The crowd movement phenomena used in this review, consisting of eight movement base cases and six self-organisation movements, are elaborated upon in section 6.2. The subsequent section (6.3) mentions some additional characteristics of simulation models which will be used to assess the applicability of the models in case of large-scale events. Section 6.4 afterwards introduces the models that are taken into account in this review, among others Cellular Automata, Social Force models, Collision Avoidance, Continuum and Hybrid models. The last section (6.5) compares the models with respect to the characteristics described in sections 6.2 and 6.3. This chapter ends with a discussion of the comparison results and concluding remarks in section 6.6.

6.1 Systematic review methodology

In this chapter, the simulation models are compared with respect to their potential of modelling crowd movement. The potential of each model is assessed using different types of indicators. First of all, each model is rated with respect to the flow situations that can be simulated by the model, see section 6.2 for the exact situations which are taken into account. Secondly, the models are appraised with respect to the valid prediction of self-organising phenomena. Section 6.2 mentions the self-organisation phenomena tested for in this review. Next to these two types of indicators, the models are assessed with respect to a number of characteristics that represent the general applicability and usage of the models (for instance computational complexity and the ability to handle new infrastructure lay-outs). These characteristics are explained in section 6.3.

The information about the simulation models mentioned in this comparison is taken from the papers describing the respective models. The author assumes that the description of the simulation models presented in papers agrees with the model implementations. This chapter discusses the advantages and disadvantages of pedestrian simulation model classes. The basis of comparison within this study is not in the difference between the mentioned models (which would be similar to comparing apples with oranges), but the difference between each model and the characteristics of the crowd's movement dynamics that an ideal simulation model should be able to capture.

The focus of this study is first and foremost on the capabilities and possible extensions of the current models with respect to the simulation of crowd movement phenomena at large-scale events and less on the precision with which each of the models captures the behaviour. In most cases calibration and validation will improve the applicability of a simulation model. However, the author assumes that the basic characteristics of the mathematical structure of simulation models have a much larger impact on the applicability of the models than their proper calibration with respect to the representation of the crowd movement phenomena. As such, this chapter assesses whether models can potentially represent the characteristics, not whether and to which extent they actually do in literature.

The author realizes that most pedestrian simulation models are built with a specific goal in mind and not designed to capture the whole range of pedestrian crowd motion. Even if these models have been developed to simulate one specific situation, they might also be used to simulate more general crowd movement situations. That is, its usage is not limited to the specific application the model was originally developed for.

6.2 Behavioural assessment framework for pedestrian simulation models

In order to represent crowd behaviour a model should be able to simulate the crowd, the movement dynamics and the phenomena that might occur during the movement of crowds at large-scale events. The characteristics of the crowd, the movement dynamics and the movement phenomena are used in the assessment of the contemporary pedestrian simulation models.

The crowd the model is trying to simulate is briefly described in section 6.2.1. An explanation of the manner in which movement base cases are incorporated to represent the movement dynamics is provided in section 6.2.2. Subsequently, section 6.2.3 elaborates upon the choice of the crowd movement phenomena as assessment criterion.

6.2.1 The modelled crowd

In section 1.4 a definition is provided for the type of crowd that is studied in this thesis. This definition does not directly define the characteristics that a model would need to incorporate in order to simulate the operational movement dynamics of pedestrians in such a crowd. Therefore, this definition is translated into engineering terms, which provides a more direct meaning with respect to the characteristics a pedestrian simulation model should possess in order to correctly model the operational movement behaviour of pedestrians in crowds during large-scale events.

The first three items of the list provided in section 1.4 describe pedestrians that perform predominantly operational movements, are walking (entertainment or standing still is not their main goal), know their 'tentative' destination (which might change over time) and do not necessarily need to be at a certain place at a certain time (no time-related-penalties). Besides that the atmosphere is friendly. Consequently, movement dynamics related to evacuation strategies and stress do not have to be taken into account. That is, the models are only assessed with respect to operational walking dynamics under 'normal' conditions.

Moreover, the demography of the crowd is assumed to be heterogeneous. As such, a good pedestrian simulation model for crowds should be able to handle several distinct types of pedestrians with different free flow speeds (velocities pedestrians adopt when not hindered by other objects and/or individuals) and different shapes of their personal space.

Additionally, the pedestrians in the crowd are assumed to be part of a group. A pedestrian simulation model which can predict this type of movements can predict how the interpersonal connections between pedestrians change their operational movement dynamics.

Last of all, the list mentions that pedestrians do not have to be familiar with the infrastructure. Consequently, pedestrians are expected display both searching and optimal route choice behaviour. As a result, a pedestrian simulation model should be able to predict both searching and optimal route choice behaviour.

6.2.2 Movement base cases

Section 2.5.1 has identified eight distinct movement base cases that the models should be able to model. These movement base cases have been chosen in a way that only one predominant movement base case is present within each situation (e.g. rounding a corner, exiting, crossing an intersection). The set of movement base cases cover the whole range of pedestrian movement behaviour. For more information about the derivation of the movement base cases the reader is referred to section 2.5.1.

Each simulation model is rated according to the following rating system:

X	Not possible to model this movement base case using this model
✓	Possible to model this movement base case using this model
!	Possible to model this movement base case using this model, however the resulting behaviour is not similar to pedestrian behaviour in reality
?	Unknown whether the model can simulate this movement base case

The exclamation mark in this rating system has been included to identify models that are partly able to simulate this base case, but where the resulting behaviour is not corresponding to reality. For instance, simulation models that model egress behaviour, without taking into account interpersonal forces that create fanning motions downstream of the bottleneck do cover the egress behaviour but do not always predict a realistic outcome.

6.2.3 Self-organisation phenomena

Besides distinct types of motion, also distinct types of crowd movement phenomena can be separated. In literature six types of crowd self-organisation phenomena have been mentioned, namely lane-formation, stop&go waves, turbulence, herding, the zipper-effect and the faster-is-slower effect.

The self-organisation phenomena that develop during large crowd movements are generally only described qualitatively. Moreover, only lane-formation is regularly presented by papers as proof of self-organisation in pedestrian simulation models. To the author's knowledge Moussaïd et al. (2012) and Duives et al. (2013) are two of the first attempts to describe lane-formation quantitatively. Yet, also these studies did not succeed to define clear rules regarding the moment in time when the movement dynamics in the crowd are to be defined as self-organised. As a result, there are no tests yet to determine whether self-organisation can develop in a pedestrian simulation model

Consequently, assumptions have to be made about the capabilities of the pedestrian simulation models to predict the other forms of self-organisation. This chapter assumes that stop&go waves can be predicted by models in which individuals need adaptation time to decrease or increase their velocity and acceleration. As a consequence of the presence of adaptation time in a model, the reaction time of pedestrians to new traffic situations increases and thereby the current traffic state is under- or overestimated. This overreaction on the traffic state causes the walking velocity to decrease or increase more than appropriate under the circumstances, which in turn leads to waves. Similarly, it is assumed that models predict turbulent movements if they can simulate interpersonal local force-based interactions, which are not necessarily physical in nature. The author moreover assumes that herding can occur in models that account for the influence of the destination and the walking direction of other pedestrians on the choices of pedestrian under investigation. The zipper-effect is assumed to appear when provisions have been made for a decrease in personal space at the bottleneck, either via a decrease in the repulsive forces interpreted by each individual or a decrease in the personal space of each individual at an angle in front of the individual. Additionally, it is expected that the faster-is-slower effect can be predicted by models which incorporate friction and body contact.

The presence of self-organisation phenomena within the models will be rated according to the following scheme. Since this behaviour is either present or not, only three different symbols will be used.

X	Not possible to model this self-organising movement using this model
✓	Possible to model this self-organising movement using this model
?	Unknown whether this self-organising movement is present within the model

6.3 Application assessment framework for pedestrian simulation models

The reviews by Papadimitriou et al. (2009), Schadschneider et al. (2009), Helbing & Johansson (2010) and Bellomo & Piccoli (2012) show that not all models can be used in all situations. A behaviourally correct model is one thing, but if it cannot be used in practice due to operational constraints this limits its applicability. Therefore, besides an assessment of the behavioural aspects, also an assessment of the applicability of the simulation models is performed. The assessment of the applicability of pedestrian simulation models will assess more than just the characteristics needed to only predict the operational movement dynamics of pedestrians in crowds during large-scale events, since some higher level processes will also introduce limits on lower level decision making processes.

To evaluate the applicability of the simulation models a few other characteristics of the models are rated. The chosen characteristics cover some of the most seen operational constraints of a simulation model. Among others, the provisions of the pedestrian simulation models for strategic processes, global route choice algorithm, adaptive route choice algorithms, collision avoidance, pressure, group structures, multiple user classes are assessed in this chapter. Furthermore the computational burden of the initialisation and large crowds is determined. Last of all, the possibility of introducing new events and/or new infrastructure is ascertained. Underneath these characteristics are briefly elaborated on before the rating scheme is introduced.

Strategic processes

Pedestrian's operational movement dynamics are known to be influenced by decisions taken at a more strategic level. These strategic decisions might be the result of for instance physiological processes or other (psychological/sociological/physical) considerations. This category is included in order to assess which simulation models are indeed capable of simulating pedestrian's strategic decisions.

Global route choice

When pedestrians walk they are assumed to have a tentative destination or activity area in mind (Hoogendoorn & Bovy (2004), Borgers & Timmermans (1986)). Depending on the situation the route towards their intermediate or final destination may change en-route. Besides that, not every person has a strict final destination: their destination might switch over time; therefore their global route might also change over time. An example of the latter is a pedestrian who finds out that the queue for drinks is too long and decides to go to the toilet first. The local route that pedestrians follow towards their 'final destination' is as such influenced by their global route choice.

Local route choice

Locally, congestion might cause the adopted global route to become less suitable (i.e. a route with a longer distance might have a shorter travel time). In reality pedestrians would divert if possible in such case, a model becomes more realistic when implementing adaptive route choice behaviour. Therefore, the availability of an adaptive (local) route choice model based on the current situation within the simulation models is rated in the comparison. A model is assumed to implement adaptive route choice when a local objective is present that causes local re-routing, for instance in case of congestion or high densities.

Collision avoidance

From literature it is known that people start adjusting their paths several meters before reaching a conflict to reduce the interaction and to avoid collisions with other pedestrians (Goffman (1972)). To make insightful whether this characteristic is built into the simulation models, collision avoidance is one of the characteristics rated in this review. In this chapter the local definition of collision avoidance is assessed. That is, whether a simulation model has intrinsic or built-in rules to consciously avoid collision with other (moving) agents.

Pressure

The Hillsborough stadium disaster showed that the pressure built-up in crowds during large events can cause life-threatening situations (Challenger et al. (2010)). When assessing safety in crowd events not only the density, but also the pressure in the crowd should therefore be considered. Helbing et al. (2007b) for instance found that the sudden release of pressure can lead to sudden stress releases and earthquake-like mass displacements of many pedestrians, which may cause hazardous situations. The possible result of the pressure built-up, i.e. crushing, is not taken into account.

Groups within a crowd

Since the influence of groups on crowd dynamics is a quite recently discovered type of behaviour, most models do not comment on the possibility of modelling this feature. Therefore, it is assumed that all microscopic models that can set attraction properties of individual agents are capable of simulating group behaviour. For both meso- and macroscopic models it is assumed that microscopic group behaviour cannot be implemented. However, depending on the model, one might be able to adapt the flow function with respect to the group distribution in a crowd, recreating the flow reduction effect of group movements within a crowd. The application of group movements in hybrid structures is dependent on the manner in which the models have been coupled. Hybrid models are rated based on the resulting movement descriptions described by the paper.

Multiple pedestrian classes

In a crowd the behaviour of each pedestrian is different. Since the presence of dissimilarities between pedestrians is severely influencing the movement characteristics of the crowd (e.g. Weidmann (1993)), this possibility of pedestrians with distinct characteristics should be available in crowd models. This can be done by either implementing multiple pedestrian classes or by making the macroscopic functions of velocity, density and flow dependent on the characteristics of the event population. Differences between pedestrian classes can lead to differences in collision avoidance behaviour and overtaking. Consequently, a pedestrian simulation model is only assumed to be capable of predicting multiple user classes if these differences are accommodated as well.

Computational burden of initialisation

Every model has a different way of representing the infrastructure, the (moving) obstacles and the pedestrian's movement decisions. The computational burden of a model can be divided into the computational burden of initialisation and the computational burden of simulating large crowds within an infrastructure. The computational burden of initialisation rates each model is based only on the basic complexity that is necessary to initialise the model, that is, the basic complexity of the infrastructure, the size of the infrastructure and the origin-destination table.

Computational burden of large crowd simulation

Besides the computational burden of the initialisation, also the increment of the computational burden for simulations involving large amount of pedestrians ($N > 1000$ P) during the same time period is assessed. The complexity of the calculations is estimated using the description of the simulation models within the mentioned papers.

New infrastructure

Most models are calibrated and/or validated based on only a limited amount of data. Depending on how and what parts of a simulation model are calibrated, models are more or less capable of simulating situations they have not originally been calibrated for. Besides that, the capability of simulating previously not encountered events and infrastructure depends on the theoretical foundation of the model. Due to their structure, some models are not capable of modelling more than one class of events. This last characteristic rates the models' capabilities of simulating new environments (a new location lay-out and/or different event). It is implicitly assumed that the results after adaptation and/or calibration of the models all give an accurate prediction of reality (as much as the models allow for it).

Rating schemes

The first seven and the last characteristic are rated according to the following scheme.

X	Not possible to simulate this characteristic by means of the model
$\sim$	The characteristic is implemented rudimentary
✓	Possible to simulate this characteristic by means of the model
?	Unknown whether it is possible to simulate this characteristic by means of the model

The computational burden of certain aspects of the model cannot be rated according to this scheme. Therefore, a second scheme is introduced for this assessment. Based on the description of the pedestrian simulation models it is possible to make a distinction between four levels:

++	Very low computational burden
+	Low computational burden
-	High computational burden
- -	Very high computational burden

Especially the older models do not mention the computational burden/computational speed of the initialisation and according computations. Besides that, the author specifically does not want to compare the current implementation of a model, but its mathematical structure because the computational burden can differ severely depending on the exact implementation. Furthermore, a comparison of computation speeds is practically impossible. Therefore, the computational burden is estimated based on an approximation of the complexity of the models' mathematical structure as presented in the respective papers. The author assumes that the implementation of the models is optimised and that the implemented algorithms do not hamper the efficient running of the simulation models.

6.4 Introduction of stereotypical pedestrian simulation models

Many simulation models have been presented in the last years comprising pedestrian motion. Several areas, such as evacuation movements, pedestrian movements in transit stations and local interaction behaviour, were studied. This chapter focuses on the stereotypical models that are distinct in their methodology of modelling pedestrian movements. The reviewed pedestrian simulation models have been selected on the basis that they have a specific set of characteristics, different from most other models in the review. Since multiple almost similar models have been proposed, only one stereotypical simulation model for a whole group of models might be mentioned, while other simulation models with a similar set of characteristics exist. It is assumed that the reviewed model scores similar to the other models that were left out of the review. The reviewed models provide an overview of the broad spectrum of crowd simulation models available within the field of pedestrian motion research and analysis.

In the following section Cellular Automata, Social Force models, Activity Choice models, Collision Avoidance models, Behavioural models, Network models, Continuum models and Hybrid models are discussed. Each of the reviewed models represents a unique combination of features. Cellular Automata are microscopic models with grid-based motion decisions. Social Force models are also microscopic models, but with a continuous representation of space. Activity-choice-models differ from Social Force models in the sense that they incorporate a strategic decision making process. A completely different view on pedestrian motion is presented by the Collision Avoidance models. These models assume that pedestrians actively seek a free path through the crowd by avoiding 'moving' objects that are within their vision field. The Behavioural models have been developed to take the strategic/social/psychological decision behaviour of pedestrians into account. In contrast with the previous five types of models, Network models represent pedestrian facilities as a network of walkway sections either in a microscopic or a macroscopic manner. Continuum models represent movement only in a macroscopic way. However, in this type of models the total crowd motion is represented by a set of differential equations, generally based on fluid mechanics. The last type of models (Hybrid models) attempts to combine the advantages of both microscopic and macroscopic models. Within each set of models a base model and several characteristically distinct adaptations of the model will be selected. For each mentioned type of simulation model the features are mentioned in the following sections, all of which are accordingly included in the model comparison.

6.4.1 Cellular Automata

One of the well-known models in this comparison is the Cellular Automaton (CA) model. This is a discrete model based on spatially and temporal discrete movements of pedestrians through a grid of cells, each in one of a finite number of states. One of the first to research pedestrian movements using a Cellular Automaton was Blue&Adler (i.e. Blue & Adler (1998) and Blue & Adler (1999)). The model has a discrete spatial representation as well as a discrete time representation to represent both the simulated environment and the moving entities. The decision of the direction of movement is based on the status of neighbouring cells. The pedestrians' decision on a target cell depends on the current interpretation about their surroundings (e.g. their desired direction, destination, infrastructure, other pedestrians and other objects). The pedestrian movements in the system are updated after solving all conflicts in the system. In the model originally proposed by Blue & Adler (1998) all movements are updated in parallel. Differences in velocity are achieved by the decision not to move during an iteration.

Several adaptations have been proposed to improve the predictions of CA models, such as implementation of alternative grid shapes (for instance, hexagonal - Leng et al. (2014), triangular - Chen et al. (2014), Voronoi - Hiyoshi et al. (2014) and rectangular 3D - Wei et al. (2015)), additional floor fields (e.g. Schadschneider (2002)), new updating procedures (e.g. Arita et al. (2014)), and velocity adaptation schemes (e.g. Song et al. (2005), Sarmady (2010), Köster et al. (2011)). In addition, several researchers have increased the sophistication of choice behaviour of the agents. Intelligence has been improved by the inclusion of vision fields (i.e. Bandini et al. (2011a,b)), sophisticated interaction rules (e.g. Bandini et al. (2014)), repulsion and attraction forces (i.e. Köster et al. (2011), Suma et al. (2012), Bandini et al. (2014)), back-pressure (e.g. Qi (2015)) and specialistic behaviour (e.g. waiting - Davidich et al. (2013), special routines - Alghadi & Mahmassani (1991)).

Given that many Cellular Automata have been proposed, it is inconceivable to assess all models. Therefore, only the models which propose new features that change the movement behaviour of the agents significantly are reviewed. That is, in the review next to the base model of Blue & Adler (1998) the following models are discussed: Alghadi & Mahmassani (1991), Schadschneider (2002), Song et al. (2005), Bandini et al. (2011a), Köster et al. (2011), Arita et al. (2014), Chen et al. (2014), Bandini et al. (2014) and Qi (2015).

6.4.2 Social Force models

The fluid crowd modelling method of Henderson (1974) has been the starting point of the Social Force model (Helbing & Molnar (1995), Helbing et al. (2000), Helbing (2001) and Helbing et al., 2005). The latter model is a microscopic continuous model with deterministic force-based interactions. The concept is based on the assumption that changes in the movement of pedestrians are guided by force fields. The notion of this model can be summarized as the superposition of attractive and repulsive effects determining the behaviour of individuals. The exact effects might differ between pedestrian instances and models. All Social Force models are used to study the movements of pedestrians at a microscopic level. Since the effects or forces do not have to be physical in appearance, also other effects such as evacuation exits, sound effects, light effects, stress levels and differences in density can be modelled by means of a Social Force model.

The model assumes that pedestrians mostly face standard conditions. Therefore, these models apply optimised behavioural strategies that they have learned over time such as cooperation and object avoidance. The optimisation is part of the model formulation. The actual movements of pedestrians are thus partly based on the macroscopic behaviour of the crowd and less on the personal characteristics of the pedestrian (e.g. congestion patience and free flow velocities). The system optimises the amount of entropy/energy/interaction.

Later adaptations to the original Social Force model include implementations of a vision field (Xi et al. (2010)), collision offset/bias, group formation (Xi et al. (2010) and Moussaïd et al. (2010)) and specialistic movements (e.g. waiting behaviour - Johansson et al. (2015) and corner rounding - Dias et al. (2014b)) . Besides adaptations of the original model by means of additional additive linear forces, some researchers have also implemented additional non-linear forces, such as Chraibi et al. (2011). Additionally, some research groups have proposed models in which the velocity instead of the acceleration of agents is influenced by the sum of the forces (e.g. Dietrich et al. (2014)).

6.4.3 Activity-choice-model

Another type of model was presented by Hoogendoorn & Bovy (2004), called Nomad. The researchers have tried to define the foundation of the simulated behaviour based on behavioural rules. This modelling approach also includes route choice in continuous time and space. It combines the local operational strength of an adapted Social Force model with the previously unknown possibility of pedestrian activity choice modelling. Nomad is activity based, meaning that actions of pedestrians in the simulation model are dependent on the activities pedestrians want to perform while being present within the facility (Campanella et al. (2009b) and Campanella et al. (2014)).

The operational and strategic route choice behaviour are based on the prevailing traffic conditions, allowing pedestrians to update their strategic planning and movements throughout the simulation. Also in Nomad the superposition of attracting and repulsive effects determines the behaviour of individuals. Operational walking decisions are influenced by decisions made at the tactical level, concerning destination and route choice. The routes in Nomad are not considered explicitly; instead, the route is determined by a minimum expected cost function. However, different from other models, Nomad does not only take into account the distance to a destination in the expected cost function. The pedestrians for instance incur a penalty when not arriving at their destination in time. The incorporated route choice behaviour complements the local operational movement dynamics, which makes the modelling of decisions at a strategic level possible.

6.4.4 Collision Avoidance models

A fourth type of models has been proposed by the gaming industry (i.e. Paris & Donikian (2007),Moussaïd et al. (2010),Karamouzas & Overmars (2010)). These Collision Avoidance models that predominantly simulate collision avoidance among virtual characters are closely related to the velocity-obstacle approach introduced by Fiorini & Shiller (1998b). Collision Avoidance models are based on two behavioural heuristics:

1. A pedestrian chooses the direction that allows the most direct path to a destination point, taking into account the presence of obstacles.
2. A pedestrian maintains a distance from the first obstacle or pedestrian in the chosen walking direction that ensures a minimum time to collision.

Thus, rather than being repelled by neighbouring pedestrians and objects, individuals are assumed to actively seek a free path through the crowd. This path is computed in three steps, namely exploration of the reachable space of the individual, a search for the possible collisions of other neighbouring individuals and the deduction of the optimal path for the near future.

In the last years two adaptations of Paris's Collision Avoidance model have been presented. In Moussaïd et al. (2011) intentional and unintentional movements resulting from interaction forces caused by collision with other bodies are taken into account. Karamouzas & Overmars (2010) have attempted to reduce the computational burden by taking into account how imminent potential collisions are, thereby allowing for a reduction of the set of movement options under consideration.

6.4.5 Continuum models

Several instances of Continuum models have been presented, which are essentially motion synthesis models for large crowds without agent-based dynamics. Hughes was the first to describe crowd movements by a continuous potential field approach, which is closely related to fluid dynamics (Hughes, 2002). Several studies have used hydrodynamic principles as the foundation for their simulation models (a.o. Treuille et al. (2006), Xiong et al. (2010), Jiang et al. (2015)). In recent years, also macroscopic Continuum models based on other principles have been proposed. Interactions of individuals among animal societies were used as inspiration of the Self-Organised Hydrodynamics model (Degond & Hua, 2013). Additionally, Cristiani et al. (2011) proposed a measure-based macroscopic model, Colombo et al. (2011) a model based on the Lighthill-Whitham-Richards (LWR) model and Hänseler et al. (2014) a model based on the cell-transmission model. The microscopic principles of velocity-obstacle based models and the Social Force model provided the basis for respectively the macroscopic models proposed by Appert-Rolland et al. (2014a) and Hoogendoorn et al. (2014).

6.4.6 Hybrid models

A sixth type of models, developed in the gaming industry, combines the advantages of both microscopic and macroscopic simulation models. The goal of most Hybrid models is to simulate microscopic interactions while achieving a large reduction of computation time with respect to most microscopic pedestrian simulation models. The way in which communication between the models is structured influences the computational burden of the combined models severely. The communication between the two sub-models used within a Hybrid model depends on the modelling instance.

Xiong et al. (2009) presented a multi-resolution approach which incorporates both a complete macroscopic model and a microscopic model and runs them inter-changeably for the same spatial location depending on the stability of the predicted crowd movement. Communication between the models takes place on the spatial division (boundary) between the models. Both models are running simultaneously and are thus communicating frequently. A little later, Xiong et al. (2010) proposed a simulation environment which is partitioned in terms of the present crowd characteristic. The same microscopic and macroscopic models as in Xiong et al. (2009) are used, but in the Xiong et al. (2010) model each spatial partition is modelled either in a macroscopic or a microscopic way. No spatial overlap between models is necessary during the execution of the simulation: the models work simultaneously on the corresponding partitioned parts of the total area. On the borders of the partitions information is passed between the models by means of aggregation and disaggregation of data. This model has currently only been proposed for a very simple corridor situation, but it can easily be extended for large-area applications. Besides that, the stability issues that might arise at the boundaries are not a addressed in the mentioned papers.

A completely different way of connecting a macroscopic and a microscopic pedestrian simulation model is proposed by Banerjee et al. (2008), who distribute the intelligence of the macroscopic model in the terrain, which is accordingly read by a simplistic agent model during the actual simulation. Both models are run consecutively. Because movement directions are calculated and captured by a floor field only once at initialisation of the simulation, only one-directional movements of pedestrians can be simulated by this model. That is, the dynamic interactions of pedestrians that arise and dynamically change during multi-directional traffic cannot be captured by the floorfield.

6.4.7 Behavioural models

Most previously described models are developed to predict pedestrian movement based on their revealed movements. Another type of models has been developed that also covers the 'soft' effects that pedestrians take into account while moving. One of these models uses a discrete choice model to integrate the response to the immediate environment, non-physical impulses and the presence of other pedestrians. Robin et al. (2009) developed a model that simulates the short range behaviour of a pedestrian as a response to her immediate environment and the presence of other pedestrians.

This model simulates both constrained and unconstrained pedestrian movements. Robin et al. (2009) assume that pedestrians optimise their utility while moving, which consists in this case of the shortest path towards their desired destination, the tendency to keep the current direction and minimising both acceleration and deceleration with respect to free speed. The global route choice is considered exogenous. In this model only the basic characteristic movement parameters are taken into account. However, this model allows for more impulses to be considered during the simulation of movement that are in nature less tangible (e.g. lighting, social safety, shadows).

Wijermans (2011) also proposed a Behavioural model that displays movement decisions in more depth. This multi-level theoretical model reflects the dynamic interplay between individuals and their environment. The model's three levels simulate behavioural patterns, behaviour generation and behaviour affecting. It adds a description of behaviour at an intra-individual level. The movement of pedestrians is therefore not only based on an activity list, but also on the influence of the social context. Since the model proposed by Wijermans (2011) does simulate predominantly strategic decisions, this model has to be linked to a second simulation model that describes the operational movement dynamics to be able to simulate the operational movement dynamics of pedestrians at large-scale events. This model has been included in the review since the implementation of several behavioural layers makes this a unique stereotypical model that provides insights into the movement behaviour of crowds, even though not at an operational level.

6.4.8 Network models

Several scientists used mathematical approaches to solve crowd movement problems. Lovas (1994) for instance modelled building evacuations (EVACSIM) as a queuing network process. The pedestrian facility is modelled as a network of walkway sections, where the nodes represent rooms and the links represent doors. Each pedestrian is treated as a separate flow object, interacting with the other pedestrians on the link. Based on the pedestrian's goal the pedestrian selects a destination and determines the route towards its destination.

Daamen (2002) proposed a model that used the network representation in quite the opposite manner. In SimPed a pedestrian facility is modelled as a network where the links represent parts of the walkway and nodes represent the connections/ intersections (with or without having any physical space). Pedestrians are modelled as unique flow objects, each with their own destination and their own free speed. The link-flow-time of each individual pedestrian is dependent on the overall density present at the link where the individual is residing. Flow through a node is dependent on the supply of incoming links and demand of outgoing links. The model implements a horizontal queue, and is able to model spillbacks. Because propagation speed of pedestrians is an individual property linked to a global link parameter (density), bi-directional flow can be modelled on each link. However, since the model is using a network structure, the interaction between pedestrians undertaking a completely random crossing movement within a crowd remains difficult to simulate using SimPed.

Another network model has been proposed by Borgers & Timmermans (1986). They also use a network representation. Each node corresponds to a city-center entry point, a departure point or an intersection of shopping streets. Each link denotes a different shopping street. The walkable space is represented by a network graph and any movement occurs along the links between two consecutive nodes. The model is based on time-varying Markov chains and three sub-models that predict transition probability matrices. This model needs experimental data to be estimated and is therefore less useful to simulate movements during unknown events.

In yet another approach by Chalmet et al. (1982) dynamic programming is used to determine the minimal time to evacuate a building. In the static model, which is based on a transshipment model, the nodes represent portions of the building, while the destinations represent building exits. The model assumes that the flow rates in the model are independent of the link usage. The model is capable of using link costs to model preference and/or dislike of certain links. The model described in Chalmet et al. (1982) is quite similar to a vehicular cell transmission model.

6.5 Discussion of the review results

Given that every model mentioned in the previous section has quite distinct characteristics, not the overall model category, but the stereotypical models mentioned in the previous section are compared. In table 6.1 the results of the comparison are displayed. In the following sections the scores of the models with respect to the possibility of modelling the movement base cases, the types of self-organisation phenomena, and all other remaining factors will be elaborated upon.

6.5.1 Movement base cases

The results of the review illustrate that Network models, the older Continuum models and Hybrid models perform poorly on this criterion. This is especially due to the fact that these more macroscopic approaches have either a limited description of the simulation environment or a limited description of the walking dynamics of the individuals within the model.

Bellomo & Piccoli (2012) state that the microscopic scale is conceptually the most appropriate scale for building crowd simulation models, as it allows to focus directly on individuals and one-to-one interactions. Table 6.1 illustrates that this statement holds. The results show that the Social Force models, Activity-choice models and the Cellular Automata are capable of simulating the most comprehensive range of movement base cases. The models which are part of these types of indicators might have difficulties modelling exiting behaviour realistically because the widening of the wedge at the exit, which is based on interpersonal repulsive forces, is not included in most models in the review.

Table 6.1: Results of simulation model comparison with respect to their capabilities of modelling crowd movement dynamics - part 1.

		Motion base cases								Self-organisation						Model applicability									
Model	Category	Unidirectional flow	Bi-directional flow	Four-directional flow	Crossing flows	Turning corners	Entering	Exiting	Random	Lane formation	Stop-and-Go waves	Turbulence	Herding	Zipper-effect	Faster-is-slower	Strategic processes	Global route choice	Addaptive route choice	Collision avoidance	Pressure	Group formation	Multiple Ped-classes	Computational burden	Large crowds (> 1000)	New infrastructure
Wijermans [2011]	Behavioral	✓	✓	✓	✓	✓	✓	!	✓	?	?	X	?	X	X	✓	✓	X	∼	X	✓	✓	-	–	–
AlGhadi&Mahmassani [1991]	Cellular Automat	✓	✓	!	✓	✓	!	!	!	X	?	X	X	X	X	X	✓	X	X	✓	✓	X	0	+	–
Blue&Adler [1998-2001]	Cellular Automat	✓	✓	✓	✓	✓	✓	!	✓	✓	X	X	X	X	X	X	✓	X	∼	X	X	✓	-	–	+
Schadschneider [2002]	Cellular Automat	✓	✓	✓	✓	✓	✓	!	✓	✓	X	X	X	X	X	X	X	X	∼	X	✓	✓	-	-	+
Song et al. [2005]	Cellular Automat	✓	✓	✓	✓	✓	✓	✓	✓	✓	X	X	✓	X	✓	X	✓	X	∼	X	✓	✓	+	++	+
Nishinari et al. [2008]	Cellular Automat	✓	✓	!	!	!	✓	!	✓	?	X	X	?	X	X	X	✓	X	X	X	✓	✓	-	–	+
Sarmady [2010]	Cellular Automat	✓	✓	✓	✓	✓	✓	!	✓	✓	X	X	X	X	X	X	✓	X	∼	X	X	✓	–	–	+
Bandini et al. [2011]	Cellular Automat	✓	✓	X	X	X	X	!	✓	?	X	X	X	X	X	X	✓	X	∼	X	X	✓	-	–	∼
Bandini et al. [2014]	Cellular Automat	✓	✓	✓	✓	✓	✓	!	✓	✓	X	X	X	✓	X	X	✓	X	∼	✓	X	✓	-	–	+
Chen et al. [2014]	Cellular Automat	✓	✓	✓	✓	✓	✓	!	✓	✓	X	X	X	X	X	X	✓	X	∼	X	X	✓	-	–	+
Arita et al. [2014]	Cellular Automat	✓	✓	✓	✓	✓	✓	✓	✓	✓	X	X	X	X	✓	X	✓	X	∼	X	X	✓	-	–	+
Köster et al. [2011]	Cellular Automat	✓	✓	✓	✓	✓	✓	!	✓	✓	X	X	X	X	?	✓	✓	✓	∼	X	X	✓	-	–	+
Qi et al. [2015]	Cellular Automat	✓	✓	✓	✓	✓	✓	!	✓	✓	X	X	✓	X	X	X	X	X	∼	X	✓	✓	-	–	+
Hughes [2000-2003]	Continuum	✓	X	X	X	✓	✓	!	X	X	?	X	X	X	?	X	✓	X	X	✓	X	X	++	++	?
Treuille et al. [2006]	Continuum	✓	✓	X	✓	!	!	!	✓	✓	?	X	X	X	?	X	✓	X	X	✓	X	X	++	++	?
Cristiani et al. [2011]	Continuum	✓	X	X	X	X	✓	✓	X	?	X	X	X	X	X	X	✓	X	X	X	X	X	++	++	?
Degond et al. [2013]	Continuum	✓	✓	✓	✓	✓	!	X	✓	✓	X	X	X	X	X	X	✓	X	∼	X	X	X	++	++	?
Appert-Rolland et al. [2014]	Continuum	✓	✓	✓	✓	✓	✓	✓	✓	?	X	X	X	X	X	X	✓	X	∼	X	X	X	++	++	?
Hänseler et al. [2014]	Continuum	✓	✓	✓	✓	✓	✓	✓	✓	?	X	X	X	X	X	X	✓	X	∼	X	X	X	++	++	?
Hoogendoorn et al. [2014, 2015]	Continuum	✓	✓	✓	✓	✓	✓	✓	✓	✓	X	?	X	X	X	X	✓	✓	∼	X	✓	✓	++	++	?

Table 6.2: Results of the review of pedestrian simulation models with respect to their capabilities of modelling crowd movement dynamics - part 2.

		Motion base cases								Self-organisation						Model applicability									
Model	Category	Unidirectional flow	Bi-directional flow	Four-directional flow	Crossing flows	Turning corners	Entering	Exiting	Random	Lane formation	Stop-and-Go waves	Turbulence	Herding	Zipper-effect	Faster-is-slower	Strategic processes	Global route choice	Addaptive route choice	Collision avoidance	Pressure	Group formation	Multiple ped-classes	Computational burden	Large crowds (> 1000)	New infrastructure
Xiong et al. [2009]	Hybrid	✓	X	X	X	X	✓	!	X	?	X	X	X	X	?	X	✓	X	~	X	X	X	+	+	~
Xiong et al. [2010]	Hybrid	✓	X	X	X	X	✓	!	X	X	X	X	X	X	?	X	✓	X	~	X	X	X	++	++	–
Banjeree et al. [2008]	Hybrid	✓	✓	✓	✓	✓	✓	!	✓	?	X	X	✓	X	?	X	✓	X	X	X	✓	✓	+	++	+
Antonini et al. [2008]	Discrete choice	✓	✓	✓	✓	✓	✓	✓	✓	✓	✓	X	~	?	?	✓	X	✓	~	?	✓	✓	0	-	+
Borgers&Timmermans [1986b]	Network	!	!	!	!	!	!	!	!	X	X	X	X	X	X	✓	✓	X	X	X	✓	✓	++	++	+
Chalmet et al. [1982]	Network	!	X	X	X	!	!	!	X	X	X	X	X	X	X	X	✓	X	X	X	✓	✓	++	+	++
Lovas [1994]	Network	!	X	X	X	!	!	!	X	X	X	X	!	X	X	!	✓	X	X	X	?	?	++	++	+
SimPed [2002]	Network	!	!	!	!	!	!	!	!	X	?	X	X	X	X	X	✓	X	X	X	✓	✓	+	-	+
Hoogendoorn & Bovy [2000]	Activity-choice	✓	✓	✓	✓	✓	✓	✓	✓	✓	✓	?	?	✓	✓	✓	✓	✓	+	✓	✓	✓	-	–	+
Helbing et al. [1995-2005]	Social Force	✓	✓	✓	✓	✓	✓	✓	✓	✓	✓	✓	?	X	✓	?	✓	X	?	✓	✓	✓	-	–	++
Xi et al. [2010]	Social Force	✓	✓	✓	✓	✓	✓	✓	✓	✓	✓	✓	?	X	✓	?	✓	X	?	✓	✓	✓	0	–	++
Chraibi et al. [2011]	Social Force	✓	✓	✓	✓	✓	✓	✓	✓	✓	✓	✓	X	X	✓	X	✓	✓	✓	X	✓	✓	-	–	+
Dietrich et al. [2014]	Social Force	✓	✓	✓	✓	✓	✓	✓	✓	✓	✓	✓	X	X	✓	X	✓	✓	✓	X	✓	✓	-	–	+
Fiorini et al. [1998]	Collision Avoidance	✓	✓	✓	✓	✓	!	!	✓	✓	?	X	X	X	X	X	X	X	✓	X	✓	✓	–	–	+
Paris et al. [2007]	Collision Avoidance	✓	✓	✓	✓	✓	!	!	✓	✓	?	X	X	X	X	X	X	X	✓	X	✓	✓	–	–	?
Moussäid et al. [2010]	Collision Avoidance	✓	✓	✓	✓	✓	!	!	✓	✓	✓	✓	X	X	✓	X	?	X	✓	X	✓	✓	-	–	?
Karamouzas&Overmars [2010]	Collision Avoidance	✓	✓	✓	✓	✓	!	!	✓	✓	X	X	X	X	X	X	?	X	✓	X	✓	✓	0	+	+

6.5.2 Self-organisation

The results show that most models score poorly on most of the six generic forms of self-organisation[18]. For instance, Network models do not score well on self-organising phenomena. Since Network models have a macroscopic nature where links represent walkways in 1D, specific movements occurring within the walkway cannot be represented by a Network model. On the other hand, the microscopic models, which were expected to be able to simulate all movement base cases, performed reasonably well on self-organisation phenomena too. Yet, table 6.1 demonstrates that this is certainly not the case.

Table 6.1 shows that almost all models received a negative score on both turbulence and the faster-is-slower effect. These two forms of self-organisation are hypothesised to be due to local force interactions between pedestrians (Helbing et al. (2000), Helbing & Molnar (2001)). Given that these force-based interactions can only be simulated by six models, the negative ratings for the other models are a logical result.

Besides that, most models score badly with respect to their representation of herding. It is hypothesised by the author that herding is caused by a shifting of the priorities of people between familiar and unfamiliar or adverse conditions. Because most models incorporate objective functions that only account for time, distance and obstacles, they cannot incorporate this shift in priorities.

The zipper-effect is rated most negatively of all phenomena. Only one model, Nomad, is actually capable of modelling this effect. This is due to the fact that Nomad is the only model that is able to specify such specific interactions with the surrounding infrastructure. It is, however, expected that this phenomenon can be implemented in most Social Force models and Cellular Automata by means of local field adaptations at bottleneck locations, as was shown by Bandini et al. (2014).

The prediction of the last of the self-organisation phenomena (stop&go waves) was assumed to be possible when a model incorporated non-instantaneous speed adaptation. Given that this is only possible in models where speed is described in a continuous way, one would expect that only the force based models would score well. However, some of the more specialistic discretised models (e.g. Alghadi & Mahmassani (1991), Antonini et al. (2004) and Arita et al. (2014)) are also capable of calculating movement velocities in a continuous way. Therefore, these models might also be capable of simulating this form of self-organisation.

[18]Table 6.1 shows a few question marks in the self-organisation section. Given that in some of the mentioned papers neither a clear description of these behaviours, nor the assumed related model characteristics were found, these models cannot be scored negatively or positively.

6.5.3 Remaining comparison factors

To evaluate the applicability of the simulation models several other characteristics of the models were rated. The description of these characteristics is found in section 6.3. Below, the incorporation of strategic processes, global route choice, local route choice, collision avoidance, pressure computations, group structures, multiple classes of pedestrians are discussed. Furthermore, the computational burden of initialisation and large crowds is elaborated upon. Additionally the ease of using the pedestrian simulation models for the prediction of crowd movement dynamics in new infrastructure or new events is reviewed.

Strategic processes

Four models certainly incorporate a internal decision process at a tactical or strategic level, which therefore score positively in this category. However, one has to keep in mind that since most other models are actually operational in nature, they can easily be combined with a high-level decision model that incorporates the more strategic decision process. That is, the activity choice and route choice can be implemented by means of a two-step model, in which first the global route choice behaviour and accordingly the operational walking behaviour is computed.

Global route choice

Most models make use of a global route choice algorithm. Even though predominantly operational models are proposed, each model makes assumptions with respect to the destination and route choices of each individual. In general, the objective function of the minimisation/maximisation algorithms tends to differ between models (Duives et al. (2012a)). Four distinct groups of models can be indicated, namely models with an objective function (1) that minimise the shortest paths, (2) that minimise the deviation with respect to the destination, (3) that maximise their utility while walking, or (4) that minimise walking discomfort. The complexity of the choice algorithm tends to increase with the number of conflicting objectives involved in the objective function. It is noticed that more complex global route choice algorithms are generally coupled to the least complex (microscopic) simulation models. Possibly the complexity at a higher level of the decision making process limits the need for a complex description of the operational walking dynamics, or a simple operational model is included in order to decrease the computational burden of these pedestrian simulation models.

Local route choice

Table 6.1 depicts that local recalculation of the objective function based on density is only applied sparingly in the models under review. Depending on the model, the route is either recalculated completely every time (e.g. Kretz (2014)), only recalculated at the locations where queuing behaviour might influence the agents' movements (e.g. Campanella et al. (2014)) or adopted based on changing negative forces or gradients (e.g. Köster et al. (2011), Hoogendoorn et al. (2014)).

Collision avoidance

Only the Vision-Based, Social Force models and high-end Cellular Automata perform well with respect to collision avoidance, because in these three types of models longer range forces can be implemented. All other models in the review work on a strictly local scale, or do not possess the microscopic view that is necessary to incorporate a collision avoidance mechanism.

Pressure

Force-based models are also the only microscopic crowd movement simulation models that can realistically predict crowd pressure. However, since pressure is a force based interaction that can also be estimated from macroscopic data, also some Continuum models could possibly predict pressure. This is dependent on the exact model description of the Continuum model.

Group movements

Group movement is caused by the desire of pedestrians to be near other specific individuals. In section 6.3 it was assumed that models which can simulate long range forces can also simulate group formation. The ratings in table 6.1 show that especially the strictly locally operating microscopic models cannot simulate this type of behaviour. Additionally, because macroscopic models cannot specify the interactions between specific individuals they cannot model group movements per se. However, most of these models allow for the adaptation of the macroscopic flow functions depending on the percentage of group movements within the aggregate crowd movements. Yet, given that group movement will not only influence the macroscopic flow function, but also change the manner in which en-route strategic decisions are made, the macroscopic models were rated negatively.

Multiple user-classes

Similar to the group formation comparison, only one of the reviewed macroscopic models (both Continuum and Network models) is currently able to simulate heterogeneous demographics by identifying each individual pedestrian, namely Hoogendoorn et al. (2014). However, depending on the model structure, also some of the other macroscopic models could possibly simulate the effects of distinct heterogeneous demographics without major model adaptations.

Furthermore, in section 6.3 it was assumed that microscopic models in which individual agents possess personalized characteristics with respect to free flow velocity, interaction distances and collision avoidance can simulate heterogeneous crowds. However, since not all microscopic models have this capability, also several negative ratings are found among them.

Computational burden of initialisation

The results in table 6.1 illustrate why new models are still being proposed frequently by the research community. For example, the microscopic models (Vision-Based models, mainy force-based models and Cellular Automata), which overall have a very positive rating, are all rated quite badly on the expected computational burden necessary to load the model based on the mathematical description provided in the papers. Especially Cellular Automata and force-based models, which often need to define a grid beforehand to compute directional floor fields to guide the pedestrian's operational walking dynamics, need quite some computation time during the initialisation.

Computational burden of large-crowd-events

The difference between macroscopic and microscopic models becomes even larger when also accounting for the computational burden of large-scale events. Especially the macroscopic models and Hybrid models can simulate large crowds easily, because it is not (or only in some parts of the infrastructure) necessary to keep track of the singular agents. The models which use complex agent models, such as the Collision Avoidance and Behavioural models, are expected to have a very high computational burden which is at least proportional to the number of pedestrians present in the simulation.

Unknown infrastructure/events

Yet, when analysing which models are actually capable of simulating an event where both the layout and the event itself are different from the situations for which the model was previously calibrated, the microscopic models that simulate only the operational movements of the agents come out on top. Particularly because these models only use the loaded layout and event information as boundary conditions, but do not use this information to deduce the movement behaviour of pedestrians itself. That is also the reason why for instance the new generation Continuum models and the model of Alghadi & Mahmassani (1991) do not perform well in this category. While the first group of models needs a correct description of aggregate behaviour of the crowds beforehand (which is known to differ due to the characteristics of the population, infrastructure, etc.), the latter needs site-based information in order to instruct their agents.

Overall assessment 'remaining comparison factors'

A more global glance at the comparison table shows another interesting trend. The differences between the models with respect to the applicability become visible. One can however make a distinction between (1) models that score well with respect to the prediction of the decision process, local route choice, collision avoidance and pressure, but bad on the other four factors, and (2) models that score well with respect to the latter four factors and bad with respect to the other categories. It seems that the computational burden of a model is positively correlated with the complexity of a model. Consequently, models that incorporate more sophisticated features of the pedestrian walking behaviour generally have a higher computational burden.

6.6 Conclusions and a look ahead

This chapter has compared a large number of pedestrian simulation models, thereby providing a broad overview of the current literature on crowd motion models of the last decades. An assessment of Cellular Automata, Social Force models, Collision Avoidance models, Activity choice models, Continuum models, Hybrid models, Behavioural models and Network models was made based on their expected performance with respect to the simulation of pedestrian crowd movement during large-scale events. The models were rated on their capabilities with respect to the correct prediction of movement base cases, self-organisation phenomena, as well as other factors related to crowd simulation modelling, such as the pedestrians' decision process, route choice algorithm and computational burden.

The results of the review indicate that several models are capable of reproducing a large set of crowd movement phenomena, being Cellular Automata that implement longer-range interactions, most Social Force models, Activity choice models and the new generation Continuum models. Therefore, these models can be indicated as the contemporary best pedestrian simulation models with respect to the walking dynamics of pedestrians within a crowd during large-scale events.

This chapter argues that any model which is used for the simulation of the pedestrians' walking dynamics in crowds during large-scale events should be able to simulate most of the phenomena indicated in this chapter. Contrary to Bellomo & Piccoli (2012), based on this review no indication can be given of a simulation model that is capable of modelling all crowd movement phenomena and can be applied in all situations. Either the models have a large computational burden, or they do not have the capability to simulate heterogeneous crowds, or they have difficulties with destination and route choices or they cannot cope with situations the models were not specifically calibrated for.

6.6.1 Directions of applicability

The author acknowledges that the factors taken into account in the comparison are not of similar significance. Yet, when modelling the walking dynamics of pedestrians within a crowd, it can be assumed that the correct[19] display of crowd movement base cases and phenomena are of major significance. Provided that most applications of a pedestrian simulation model require realistic results, but do not have the same requirements with respect to the remaining characteristics (ability to model pressure, global route choice, computational effort) it is deemed important that one implements a simulation model which is best suitable for a certain type of application.

The current field of crowd simulation shows three large fields of application. Pedestrian simulation models are currently most used in evacuation time calculations. This type of simulation does not necessarily need fast computations (computations do however need to be finished within a reasonable time span to be viable for commercial use), as long as they are reliable. Evacuation simulations do, however, need correct estimations of destination and route choices AND behavioural changes during the evacuation AND a correct prediction of occurring crowd movements on an aggregate level (speed, density and capacity). In this review a number of models has been reviewed can simulate global route choice and multiple pedestrian user classes. These models, i.e. Social Force models, sophisticated Cellular Automata and the Continuum models, can be used for these applications.

A second field of application of pedestrian simulation models is in pedestrian movement research. The work in this field asks for simulation models that correspond as much as possible to reality. That is, next to a realistic prediction of operational walking dynamics, this type

[19] Correctness of prediction does not necessarily overlap with the specific indication of every pedestrians' movements. That is, macroscopic models can correctly predict the aggregate trends, while not indicating the pedestrian's position at every moment in time. Therefore, macroscopic and microscopic models have the possibility to produce results in accordance to reality.

of model should also be capable of predicting most self-organisation phenomena. A high computational burden is not necessarily an issue. In this review several models where found capable of modelling all movement base cases. None of those was found able to simulate all self-organisation phenomena. However, the models described in the papers by Helbing (1997), Hoogendoorn & Bovy (2004), Chraibi et al. (2013), Xi et al. (2010), Appert-Rolland et al. (2014a), Hänseler et al. (2014) and Hoogendoorn et al. (2014) are capable of simulating most of them. Therefore, Social-Force, Activity-choic and Continuum models are recommended for crowd movement research.

A third application can be found in practice, where the infrastructure layout of major crowd events needs to be assessed before and during the course of events. The design of an event is helped by a reasonably accurate (correct prediction of high density locations and friction points) but also reasonably fast running simulation model. However, the review shows that the models best describing crowd motion are also the models with the greatest computational burden. The pedestrian movement simulation models can roughly be divided into slow but highly precise microscopic modelling attempts and fast macroscopic modelling attempts in which the predicted aggregate walking behaviour needs to be calibrated for every event. The computational burden of especially the Continuum, Network and Collision Avoidance models is limited. Yet, some models present an interesting combination of high validity and a reasonably low computational burden. Depending on the exact simulated crowd event a Network model, a Cellular Automata, a Hybrid model or a Continuum model is recommended.

6.6.2 A look ahead

In the review it is found that two directions of modelling are developing within the field of pedestrian simulations. On the one hand, currently the more computer simulation related applications reside which focus on simulating pedestrian walking dynamics with a reasonable accuracy at high computational speed. On the other hand, we have the pedestrian simulation models that accurately predict reality, but have such high computational burden that they can only be used in an offline-modus.

Both types of models lack to a certain extent either correctness of displayed behaviour and/or computational speed. For crowd simulation models to be used in the crowd management practice, the gap needs to be closed. Bringing forward a model that has both is a first step in the direction of viable online pedestrian prediction models.

Yet, the review also illustrates that this model does not have to be developed from scratch. Several models have been proposed that can simulate all movement base cases and most self-organisation phenomena and can potentially simulate the movements at large-scale events reasonably fast. Yet, none of the mentioned models has ever been properly calibrated and assessed with respect to the prediction of pedestrian movement dynamics during large-scale events.

Therefore, before further developing these models, first these models need to be assessed in more detail with respect to the validity of their predictions. In total seven stereotypical models were found to be the best to use for research purposes, namely Helbing (1997), Hoogendoorn & Bovy (2004), Chraibi et al. (2013), Xi et al. (2010), Appert-Rolland et al. (2014a), Hänseler et al. (2014) and Hoogendoorn et al. (2014). Among those, two are in the authors possession. Therefore, in the following chapters these two models, namely the microscopic model proposed by Hoogendoorn & Bovy (2004) in chapter 7 and the macroscopic model proposed by Hoogendoorn et al. (2014) in chapter 8, are calibrated for the operational walking dynamics of pedestrians in crowds during large-scale events and accordingly assessed regarding the correctness of the models' predictions.

Chapter 7

Assessment of a microscopic pedestrian simulation model

Many papers do not mention the calibration and validation of the simulation model with respect to the operational movement dynamics of pedestrians during large-scale events nor mention whether the crowd movement phenomena described in chapter 5 can be represented. Consequently, it is currently unknown whether any microscopic pedestrian simulation model can simulate the specific crowd movement phenomena that develop during large-scale events in a realistic manner.

Chapter 5 has established which crowd movement phenomena are essential in the realistic prediction the walking dynamics of pedestrians in crowds at large-scale events. The literature review on pedestrian simulation models (chapter 6) shows that Nomad is one of the microscopic pedestrian simulation models which might be able to predict most of these crowd movement phenomena. Yet, also for this model it is unknown whether all crowd movement phenomena can be predicted accurately.

The aim of this chapter is to assess whether Nomad is capable of accurately modelling the crowd movement and self-organisation phenomena. In order to assess the model, first the model is calibrated specifically for pedestrian walking dynamics at large-scale events by means of the data sets described in chapter 3. Accordingly the model is assessed using the lists of crowd movement phenomena developed in chapter 5.

Section 7.1 provides a brief description of the key characteristics of Nomad. Subsequently, in section 7.2 a generic framework for the calibration of pedestrian simulation models is proposed. The calibration steps mentioned in this framework are put into practice in sections 7.3 and 7.4. These sections respectively detail an analysis of the sensitivity of the predictions of Nomad with respect to the parameter settings (section 7.3) and the quantitative calibration of Nomad (section 7.4). Accordingly, section 7.5 assesses the capabilities of Nomad. The conclusions and suggestions for future research are presented in section 7.6.

7.1 Introduction to Nomad

The present section introduces the pedestrian simulation model Nomad, which was first proposed by Hoogendoorn & Bovy (2002, 2004). This model assumes that the movement of pedestrians through space can be modelled by means of an activity based normative theory. That is, pedestrians attempt to maximise the balance between the utility gained while performing their activities and the utility lost when moving between origin and their final destination. Nomad simulates the tactical and strategic decision behaviour of pedestrians as well as the operational walking dynamics. The remainder of this section briefly introduces the pedestrian decision behaviour and the operational movement dynamics of Nomad. For a detailed description of the model the reader is referred to Campanella et al. (2014) and Campanella (2016).

7.1.1 Modelling decision behaviour of pedestrians

The decision behaviour of pedestrians within Nomad comprises of the three distinct levels (Hoogendoorn & Bovy, 2004). At a *strategic* level pedestrians decide on their activities, departure time and their global route choice. The route choice is based on the minimum walking cost principle and is subject to change due to events that occur during the trip itself, such as waiting time and congestion. At a *tactical* level pedestrians adapt their schedule and route to optimise their walking experience. Nomad dynamically reschedules activities and re-routes pedestrians depending on the activity list. At the lowest level (*operational*) decisions are made with respect to the velocity and acceleration pedestrians adopt. The acceleration of pedestrians is optimised given the directionality, speed and location of surrounding objects. At this level pedestrians take short-term decisions necessary to move through space while avoiding obstacles and other pedestrians.

As explained in section 1.4.1, the movement dynamics of pedestrians for specific movement base cases are studied that are generally limited in size. Due to this restriction, the strategic and tactical decision behaviour are assumed to have a limited influence on the realised traffic state. Therefore, only the lowest level of the decision making in Nomad is taken into account in the remainder of this chapter. The simulation of decisions at the strategic and tactical level are considered fixed, and will not be studied.

7.1.2 Modelling the operational movements of pedestrians

In the following paragraphs the walker model (eq. 7.1-7.5) is briefly discussed. For an in-depth discussion of the intricate details of the walker model one is referred to Campanella (2016).

Physics of movement

Within Nomad, the movement of pedestrians is assumed to be due to the interaction between a controlled $\vec{a}_c$ and a non-controlled $\vec{a}_p$ reaction to the impulses pedestrians receive from their environment (see equation 7.1) that together form the acceleration of the pedestrian. The walker model also incorporates a noise term $\vec{\varepsilon}(t)$ which simulates the natural fluctuations of pedestrian movements. As a result of the noise term, the walker model is stochastic.

$$\vec{a}(t) = \vec{a}_c(t) + \vec{a}_p(t) + \vec{\varepsilon}(t) \tag{7.1}$$

$$\vec{a}_c(t) = \vec{a}_s(t) + \vec{a}_O(t) + \vec{a}_r(t) \tag{7.2}$$

$$\vec{a}_s(t) = \frac{\vec{v}_0(t) - \vec{v}(t)}{\tau} \tag{7.3}$$

$$\vec{a}_r = \vec{a}_{rn} + \vec{a}_{rl} \tag{7.4}$$

$$\vec{a}_{rn}(t) = -a_0 \cdot \vec{e}_n \cdot e^{\frac{-d_A}{r_0}} \tag{7.5}$$

The reaction $\vec{a}_p$ is the result of the physical interaction with other pedestrians and objects. Because other pedestrians exert this force on pedestrian p, this force is not controlled by the pedestrian itself. The corresponding physical acceleration force in the walker model is based on a particle-based collision model. The controlled reaction $\vec{a}_c$ is the result of the decision behaviour of the pedestrians, in which $\vec{a}_s(t)$ represents the path straying component, $\vec{a}_O(t)$ represents the obstacle interaction component and $\vec{a}_r(t)$ represents the pedestrian interaction component. Equation 7.2 provides the mathematical formulation of this term.

The parameters of Nomad do not influence the movement dynamics of the simulated crowd to a similar extent, since not all forces are always present. Forces with respect to obstacles and pedestrians are only significant if the pedestrian resides within range of obstacles or pedestrians. During large-scale events pedestrians mainly encounter other pedestrians due to the wide open spaces in which they move. Consequently, when studying the operational walking dynamics of pedestrians in crowds at large-scale events, the parameters of the Nomad model that influence the walking behaviour as a result of the interaction of a pedestrian with other neighbouring pedestrians are dominant. Therefore, in the remainder of this chapter attention is paid to the correct calibration of the parameters that shape this interaction, namely τ, a_0 and r_0. For details on the object interaction component one is referred to the literature.

Path straying component - $\vec{a}_s$

The strategic and tactical levels of the decision making process result in a desired velocity that is aligned along the optimal route towards the destination of the pedestrian. Nomad assumes that deviations from the optimal speed and/or direction incur increasing costs. Therefore, pedestrians always attempt to return to their optimal velocity, see equation 7.3, where $\vec{v}_0(t)$ represents the desired velocity of a pedestrian at time t, $\vec{v}(t)$ the current velocity of a pedestrian and τ the relaxation term. In this formulation τ expresses the urgency of the desire of pedestrians to keep moving towards their goal along their intended global path. A large τ allows pedestrians to deviate from their desired path and to smoothly return to their preferred path after a deviation, while a small τ forces pedestrians to walk closely along the optimal path. As a result, τ can be interpreted as the reaction time of pedestrians.

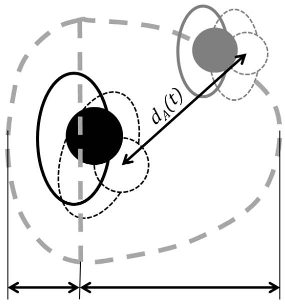

Figure 7.1: Vision field of Nomad's walker model (Campanella et al., 2009b), where the dashed pedestrians represent the anticipated future positions of the pedestrians.

Interaction with other pedestrians - $\vec{a}_r$

The Nomad walker model uses game theory to model the collision avoidance behaviour by means of a non-cooperative strategy (Hoogendoorn & Bovy, 2002). Nomad assumes that pedestrians anticipate the movement of others and themselves in order to minimise their own costs of walking.

The model furthermore assumes that pedestrians have a limited area in which they interact with other pedestrians and obstacles (see figure 7.1 for visualization of the elliptic interaction area as described in Campanella et al. (2009b)). The costs related to the interaction between two pedestrians are assumed to be inverse to the distance between the pedestrians. As a consequence, pedestrians who are near each other experience larger avoidance forces than pedestrians that are further away from each other (see equation 7.5). In the equation a_0 represents the interaction strength parameter, r_0 the interaction distance parameter, $d_A(t)$ the anticipated distance between pedestrians in the next time step and $\vec{e}_n(t)$ the unit vector pointing in the direction of the other pedestrian.

Besides the 'normal' interaction component $\vec{a}_{rn}(t)$, an additional lateral interaction component $\vec{a}_{rl}(t)$ is taken into account. This second component averts non-realistic movement behaviour in cases where pedestrians approach each other from opposite directions and follow a collision course. Due to the lateral 'bias', pedestrians will avoid each other instead of slowing down to a complete stop, thus potentially creating deadlocks. The two interaction components are assumed to be additive.

7.2 Framework for the calibration of pedestrian simulation models

Even though calibration and validation are considered important parts of the development process of simulation models, several studies mention that researchers currently apply inconsistent calibration and validation procedures or partially test the pedestrian simulation models due to the lack of international standards for calibration and validation of pedestrian flows and pedestrian simulation tools for general use (among others Isenhour & Löhner (2014)).

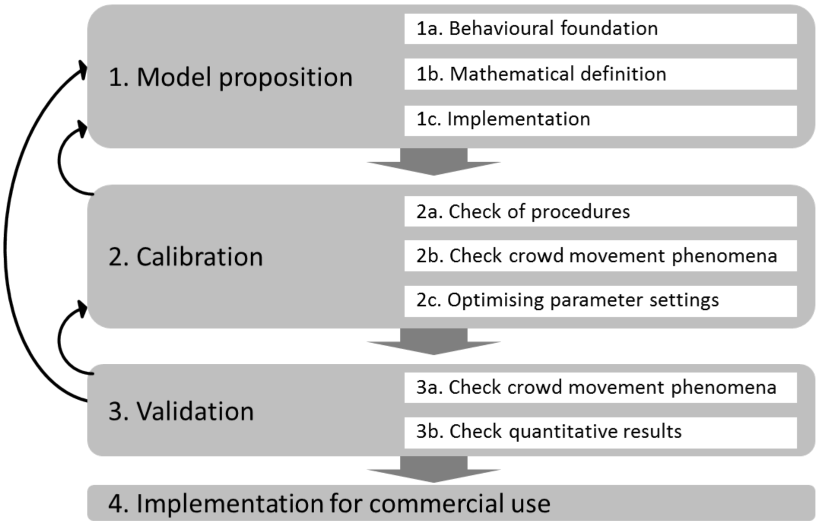

Figure 7.2: Generic framework for the proposition, calibration and validation of pedestrian simulation models - the entire process which a pedestrian simulation model has to go through from initial idea to a software package for commercial use.

Campanella et al. (2009b) indicate that most reports on the calibration of pedestrian simulation models focus on a few aggregate aspects of the flow and generally only account for only one movement base case. Campanella et al. (2009b), moreover, indicate that there is not much evidence that pedestrian simulation models have been calibrated to correctly predict self-organisation phenomena. Besides that, the influence of the behavioural parameters of pedestrian simulation models on the predicted movement dynamics is scarcely analysed (Rudloff et al. (2011)).

Yet, recently several studies have attempted to assess the sensitivity of pedestrian simulation models with respect to the model's parameters (e.g. Johansson et al. (2015)), to determine which calibration technique to use (e.g. Rudloff et al. (2011) and Wolinski et al. (2014)), to calibrate these models (e.g. Strege & Ferreira (2014)), or to validate these models (e.g. Seer et al. (2014)). However, each of these studies mentions only one step of the calibration and validation process.

In figure 7.2 the author has attempted to put the steps of the calibration process mentioned in literature into perspective. This has resulted in a four-step process in which a model is proposed (1), calibrated (2), validated (3) and implemented for commercial use (4). The main steps of this process can be sub-divided and put in chronological order. For example, if a new model is proposed generally the behavioural foundation of model (1a - e.g. Moussaïd et al. (2011)), the mathematical definition of the model (1b - e.g. Hoogendoorn & Bovy (2004), Helbing & Molnar (1995)) and the technicalities of implementation (1c - e.g. Xiong et al. (2010)) are described. During the calibration step the correctness of the procedures is checked by means of simple case studies (2a - e.g. Hoogendoorn et al. (2014)), the phenomena that the model should be able to capture are studied by means of more sophisticated case studies (2b - e.g. Duives et al. (2016a)) and an optimal parameter set is computed by means of a optimisation procedure

(2c - Campanella et al. (2009b)). Accordingly, using other data sets, the validity of the predictions is qualitatively (3a) and quantitatively (3b) assessed during the validation step. While the first (1a-1c) and last step (4) predominantly focus on comprehensively describing the model and its future use, during the intermediate steps (2a-3b) an effort is made to test the capabilities of the pedestrian simulation model.

Only one step within the entire process is directed towards finding the optimal parameter set of the simulation model. The first sub-steps (1a-2a) of the four-step process have already been performed for Nomad (Hoogendoorn & Bovy (2004), Campanella et al. (2009b) and Campanella (2016)). Therefore, in the following section the following four steps of the framework are performed for Nomad. First, a sensitivity analysis (step 2b) is performed in section 7.3 during which the influence of the parameter sets on the predicted movement dynamics is determined. Accordingly a quantitative calibration (step 2c) and assessment (steps 3a and 3b) of Nomad is performed in section 7.4.

7.3 Sensitivity analysis of Nomad

Given that the Nomad walker model has been calibrated on reasonably 'small' laboratory data sets, it is currently undetermined what the impact of the parameters of the walker model is on the predicted operational walking dynamics of pedestrians in crowds during large-scale events. Especially differences in the interaction behaviour between pedestrians are expected. The sensitivity of Nomad's prediction results with respect to the model's parameters is determined in order to determine the range of parameter values that results in realistic movement dynamics, and as such is to be used in the quantitative calibration of Nomad.

The following section first mentions the analysis methodology (section 7.3.1). Afterwards, the sensitivity of Nomad with respect to the relaxation time τ and the interaction strength parameters a_0 and r_0 are discussed in sections 7.3.2-7.3.4. The joint effect of the three parameters is reviewed in section 7.3.5. Afterwards, the conclusions of the sensitivity analysis are mentioned in section 7.3.6.

7.3.1 Analysis methodology

The literature review of empirical research efforts (chapter 2) and the analysis of the empirical data (chapter 5) showed that the occurrence of crowd movement phenomena is dependent on the movement base case. As a consequence, it is impossible to determine the sensitivity of the parameters by means of one simple case study (e.g. a straight corridor with a uni-directional flow). Therefore, a combination of movement base cases is used to assess the sensitivity Nomad. Of the eight movement base cases five have been studied in the first part of this thesis, namely uni-directional straight, uni-directional bottleneck, uni-directional corner, bi-directional and intersecting movement base cases. The phenomena deduced for the uni-directional straight movement base case, are also found in the other four movement base cases. Therefore, there has been chosen to adopt the latter four movement base cases in the sensitivity analysis, namely:

- a uni-directional bottleneck flow
- a uni-directional flow around a corner
- a bi-directional flows in a straight corridor
- an intersecting flows under an angle of 90 degrees

As mentioned before, the Nomad model has been calibrated for basic flow situations. Consequently, it is assumed that a re-calibration of the most influential parameters will provide the largest gain with respect to the realistic prediction of the walking dynamics of pedestrians at large-scale events. In the previous section it was established that the interaction behaviour of pedestrians is dominant during large-scale crowd movements, and as such parameters a_0, r_0, and τ are most influential in the modelling of this type of movement dynamics. Hence, in the present section the sensitivity of Nomad with respect to these three parameters of the walker model is assessed with respect to the qualitative crowd movement phenomena mentioned in the literature and described in chapter 5.

Special attention is paid to the development of self-organisation phenomena, diffusion of the flow after a bottleneck and the development of high density regions similar to the ones described in the list of crowd movement phenomena in chapter 5. As already mentioned in **??**, to the author's knowledge no quantitative rules exist to identify self-organisation in pedestrian flows within the field of pedestrian simulation modelling. Upto now Moussaïd et al. (2012) and Duives et al. (2013) have attempted to determine the point at which self-organisation arises by means of group allocation and the polarisation coefficient respectively. However, both studies find no clear-cut transition between non-organised and organised flow situations.

Consequently, it is difficult to determine when self-organisation has developed within Nomad using a quantitative metric. Yet, qualitatively self-organisation is well defined as can be seen in chapter 2. These descriptions are used in this research to identify a rudimentary metric to identify self-organisation. It is generally found that when the crowd organised stable movement patterns arise that can be identified using the density fields of the respective clusters within the crowd. This results in the following qualitative rules regarding the identification of self-organisation in the simulation results. In a bi-directional movement base case the existence of the lines in the density field is used as identification of lane formation. That is, the density profile which considers only the pedestrians walking from left to right will depict gaps at the places where pedestrians walking from right to left are located. In case of stripe formation during a intersecting movement base case empty striped are found appear that move along with the flow. The existence of these stripes is used to identify the onset of stripe formation.

In the sensitivity analysis straightforward infrastructure settings are used to mimic the movement base cases, which are visualised in figure A.1. In all four cases a spatially and temporally uniformly distributed demand of 1 $P/m/s$ is used. Besides that, the crowd is assumed to be homogeneous and is described by the default parameter settings of the pedestrians in Nomad as mentioned in Campanella et al. (2009b).

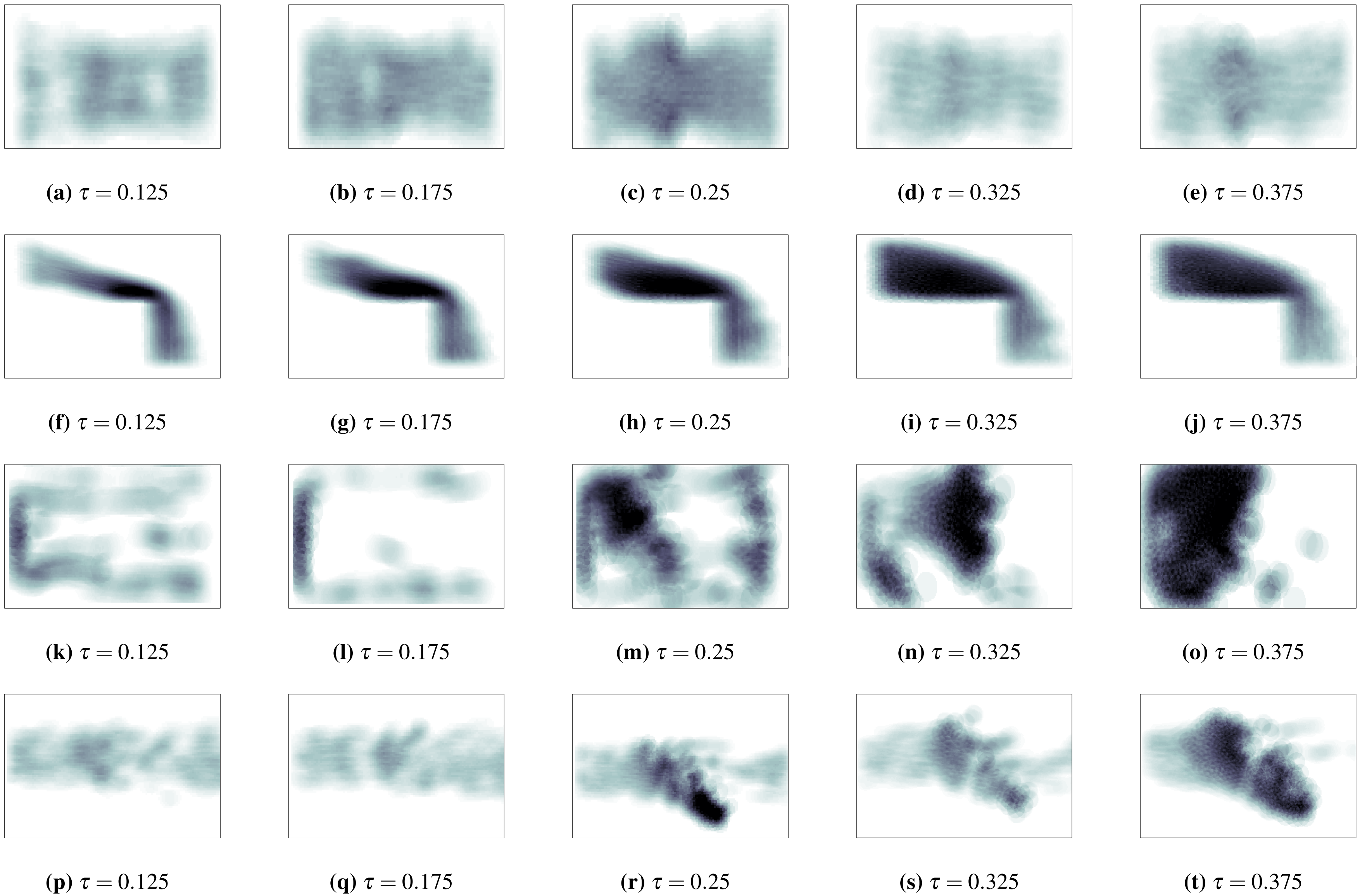

Figure 7.3: Influence of τ on the density distribution [white - $0 \leq \rho \leq 5.4$ - black], where figures a-e display a uni-directional bottleneck, figures f-j a uni-directional corner , figures k-o a bi-directional and figures p-t a intersecting movement base case. In figures k-t the density distribution of the one of the two classes of pedestrians is displayed.

7.3.2 Effect of τ on crowd movement phenomena

The influence of τ, the relaxation time, on the realisation of the density after 90 seconds is depicted in figure 7.3. The simulation of the uni-directional flow through a bottleneck shows that the dispersion of pedestrians upstream and downstream of the bottleneck increases for higher values of τ (see figure 7.3.a-e). Moreover, with an increase of the value of τ, the average density upstream of the bottleneck increases. Both trends are probably due to a decrease of velocity at the bottleneck location caused by the decrease of the acceleration towards the free speed downstream of the bottleneck location.

Also in the uni-directional corner flow situation higher values of τ result in more dispersion of the flow upstream and in the corner. The trajectories become less focussed on the shortest distance path. Due to the widening of the flow at the corner, the velocity at the corner increases with an increase of τ.

The bi-directional straight movement base case illustrates the development of self-organisation, though to a limited extent (see the elongated stripes in figure 7.3.k). Also in the intersecting flow situation self-organisation occurs, though the patterns cannot be visualised in the density profile because of the limited size and duration of the stripes. The results moreover show that congestion forms for relatively high values of τ for medium flow rates (see figure 7.3.m-o, r-t). This is quite unexpected since the average density is nowhere near the jam density. It is, however, expected that the onset of congestion is brought forward due to the diminished capabilities of pedestrians to avoid collisions when τ is relatively high.

Considering the results presented above, it can be concluded that τ influences the traffic state in two ways. First and foremost, the reaction time of pedestrians increases for higher values of τ, which leads to suboptimal walking behaviour. That is, the diminishing influence of the path straying component $\vec{a}_s(t)$ limits the effectiveness of pedestrians' collision avoidance behaviour which causes pedestrians to deviate from the optimal path. Secondly, the increase of the τ causes the walking velocity of pedestrians to increase and decrease more slowly over time. This results in a diminished outflow rate, which in turn decreases the capacity of bottlenecks for higher values of τ.

7.3.3 Effect of a_0 on crowd movement phenomena

The influence of the interaction strength parameter on the resulting traffic state is visualised in figure 7.4. Figure 7.4.a-e illustrates that in the uni-directional bottleneck flow situation an increase of a_0 leads to an increase of the queue length and dispersion upstream of the bottleneck. Figure 7.5 shows that the increase of the interaction forces leads to a decrease of the velocity inside and downstream of the bottleneck for high values of a_0. As a result, the capacity of the bottleneck decreases for high values of a_0.

In case of the movements of pedestrians through a corner, non-linear effects are encountered (see figure 7.4.f-j). The dispersion in and downstream of the corner does not seem to be affected

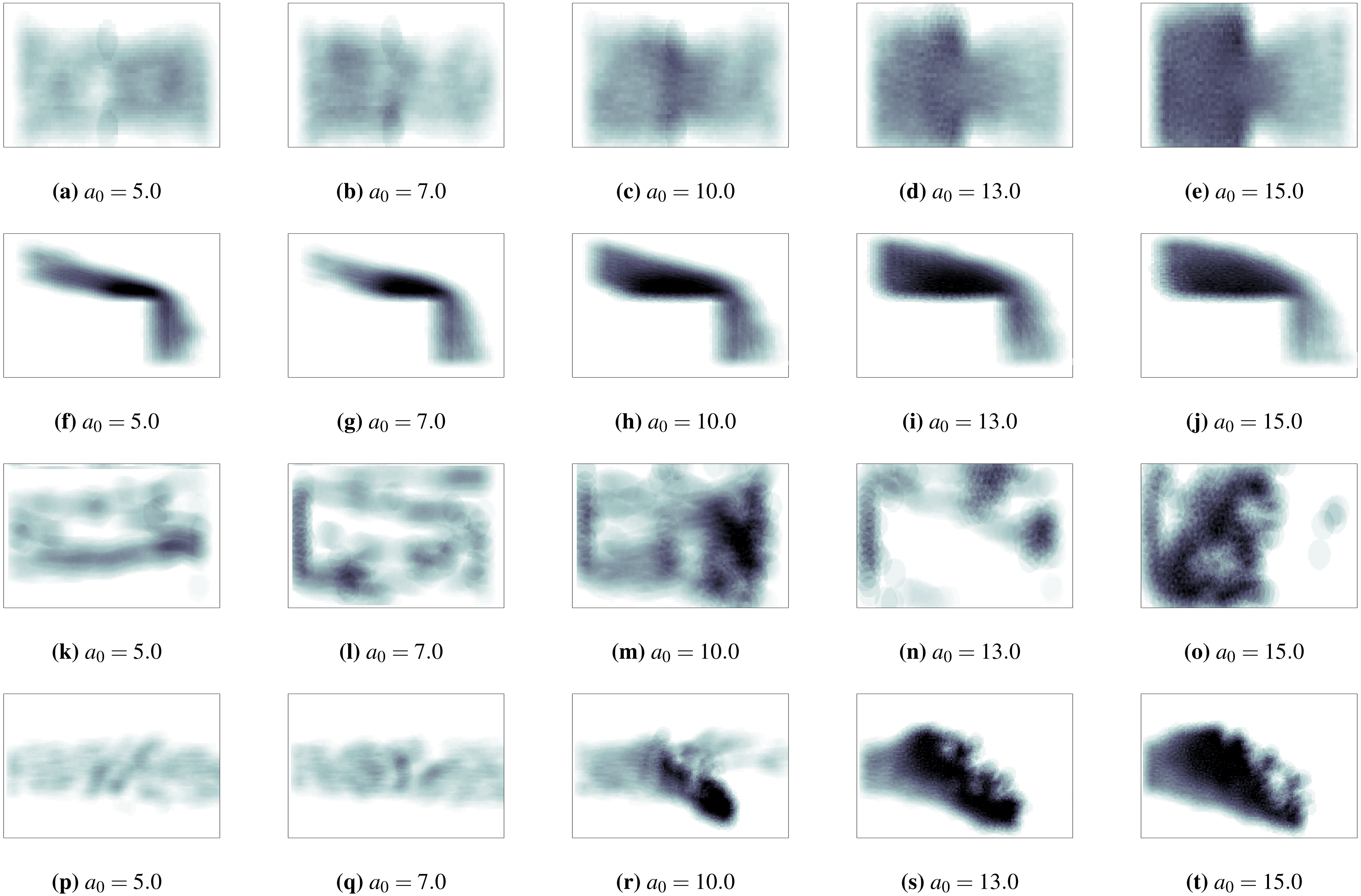

(a) $a_0 = 5.0$ **(b)** $a_0 = 7.0$ **(c)** $a_0 = 10.0$ **(d)** $a_0 = 13.0$ **(e)** $a_0 = 15.0$

(f) $a_0 = 5.0$ **(g)** $a_0 = 7.0$ **(h)** $a_0 = 10.0$ **(i)** $a_0 = 13.0$ **(j)** $a_0 = 15.0$

(k) $a_0 = 5.0$ **(l)** $a_0 = 7.0$ **(m)** $a_0 = 10.0$ **(n)** $a_0 = 13.0$ **(o)** $a_0 = 15.0$

(p) $a_0 = 5.0$ **(q)** $a_0 = 7.0$ **(r)** $a_0 = 10.0$ **(s)** $a_0 = 13.0$ **(t)** $a_0 = 15.0$

Figure 7.4: Influence of a_0 on the density distribution [white - $0 \leq \rho \leq 5.4$ - black], where figures a-e display a uni-directional bottleneck, figures f-j a uni-directional corner , figures k-o a bi-directional and figures p-t a intersecting movement base case. In figures k-t the density distribution of the one of the two classes of pedestrians is displayed.

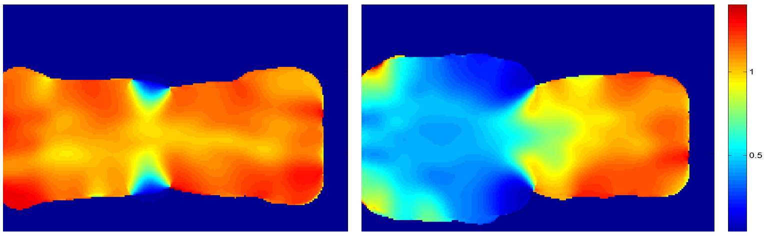

(a) $a_0 = 5.0, -50\%$ **(b)** $a_0 = 15.0, +50\%$

Figure 7.5: Velocity profile at $t = 30$ s of the total crowd movement during a uni-directional flow through a bottleneck for distinct realisations of a_0, where the colour scale represents blue:0 m/s-red:1.3 m/s.

by a_0. Furthermore, the density experienced upstream of the bottleneck increases, for increasing values of a_0. However, for even higher values of a_0 a slight decrease of the density and queue length are found. The balance between the decrease of the density at the corner and the increase of the dispersion upstream of the bottleneck might cause the relatively stable size of the flow through the corner. Yet, since the velocity is decreasing severely due to the increased interaction forces the capacity diminishes for increasing values of a_0.

In the bi-directional and intersecting flow situations lane-formation respectively stripe-formation clearly arises for low values of a_0 (see figure 7.4.k-t). For high values of a_0 lane-formation initially starts, but dies out fairly quickly. Blockage occurs for very high values of a_0 (figure 7.4.n-o and r-t). The blockage most likely occurs because of the increasing interaction force, which does not allow the pedestrians to pass near each other any more. Because more space per pedestrian is required, the capacity of the infrastructure decreases for higher values of a_0. Besides blockage, also gaps in the density profile occur for low values of a_0 (figure 7.4.k-l). That is, the flows into both directions are not directly touching each other. For higher densities and higher values of a_0 these gaps disappear and pedestrians are distributed more equally over space.

From the results presented in this section, it is deduced that a_0 influences the traffic state in two ways. Firstly, a_0 influences the balance between the path straying and the pedestrians interaction components. As a result, high values of a_0 force pedestrians away from the globally optimal path and distribute them more evenly over space. Secondly, a_0 influences the capacity of the infrastructure in two or more-directional flow situations, since an increase of a_0 leads to more problematic collision avoidance behaviour since pedestrians need more space to pass other pedestrians.

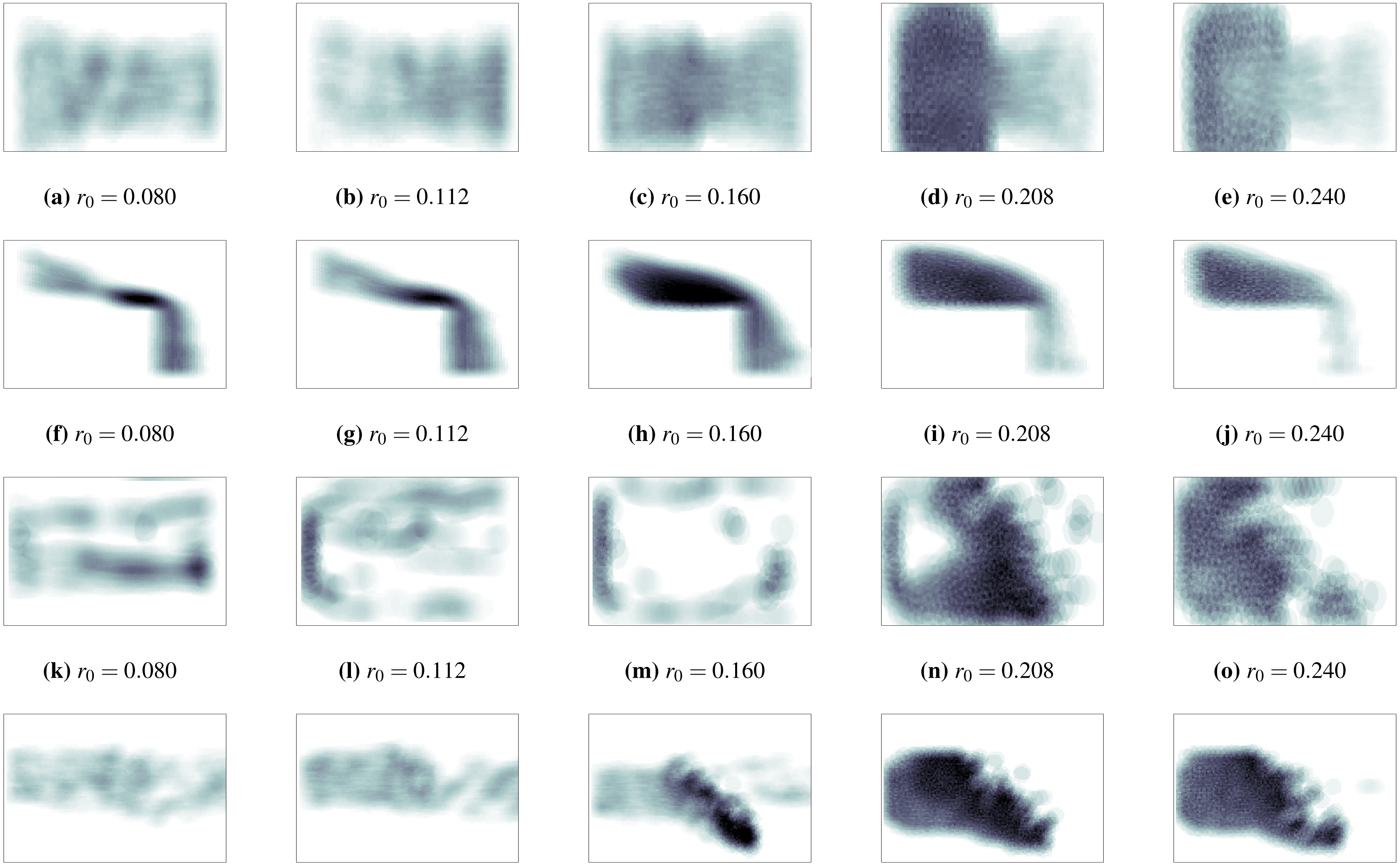

(a) $r_0 = 0.080$ (b) $r_0 = 0.112$ (c) $r_0 = 0.160$ (d) $r_0 = 0.208$ (e) $r_0 = 0.240$

(f) $r_0 = 0.080$ (g) $r_0 = 0.112$ (h) $r_0 = 0.160$ (i) $r_0 = 0.208$ (j) $r_0 = 0.240$

(k) $r_0 = 0.080$ (l) $r_0 = 0.112$ (m) $r_0 = 0.160$ (n) $r_0 = 0.208$ (o) $r_0 = 0.240$

(p) $r_0 = 0.080$ (q) $r_0 = 0.112$ (r) $r_0 = 0.160$ (s) $r_0 = 0.208$ (t) $r_0 = 0.240$

Figure 7.6: Influence of r_0 on the density distribution [white - $0 \leq \rho \leq 5.4$ - black], where figures a-e display a uni-directional bottleneck, figures f-j a uni-directional corner , figures k-o a bi-directional and figures p-t a intersecting movement base case. In figures k-t the density distribution of the one of the two classes of pedestrians is displayed.

7.3.4 Effect of r_0 on crowd movement phenomena

Figure 7.6 illustrates that the effect of the parameter r_0 on the movement dynamics is very irregular. In the case of the uni-directional bottleneck flow or corner flow, the dispersion is found to increase irrespective of the density when r_0 increases. The depicted densities are fairly similar between the distinct realisations of r_0, even though the trajectories of the individual pedestrians differ severely. Yet, the location at which the low density regions occur differs between instances. For low values of r_0 medium high densities are encountered downstream of the bottleneck, while for high values of r_0 high densities predominantly occur upstream of the bottleneck.

In bi-directional straight flow situations self-organisation occurs for low values of r_0 (see figure 7.6.k-o). Blockage occurs in almost all bi-directional flow situations except for the default value. This is probably due to the balancing act between taking not enough surrounding pedestrians or taking too many into account to have effective collision avoidance behaviour.

The trends in the intersecting flow situation are similar to the trends in the bi-directional flow situation. That is, stripe formation occurs at low values and blockage develops for high values of r_0. This is due to the impossibility to pass other pedestrians due to increased interaction forces. The blockage is more prominent in the case of r_0 than for instance a_0 because of the double impact of r_0 on the interaction (i.e. more interactions are taken into account and the strength of the interactions is weighted more equally).

From the results presented in this section it can be concluded that the simulated traffic state is sensitive with respect to the used values of r_0. Not only the interaction distances (and densities) are influenced by this parameter, but also the adopted velocity. Consequently, it is difficult to determine general trends in the sensitivity of the resulting traffic state with respect to the influence of r_0. What can, however, be established is that large deviations with respect to the default value of r_0 renders unrealistic crowd movement dynamics.

7.3.5 Joint effects of τ, a_0 and r_0 on crowd movement phenomena

Next to determining how τ, a_0 and r_0 individually influence the simulated traffic state, the effect of the interaction between the three parameters is studied for all four flow situations. Figures 7.7 and 7.8 illustrate that the influence of the parameters a_0, r_0 and τ on the crowd dynamics is non-linear. Both the spatial distribution of pedestrians and the predicted densities are found to be very dependent on the chosen parameter sets. While the shape is probably controlled via parameter r_0, the predicted densities seem to be regulated by the combination of the parameters τ and r_0.

The results displayed in figure 7.8 visualise the traffic state of one class moving in a bi-directional flow situation. In figures 7.8.a-h large gaps are visible between the lanes. These are caused by blockages located near the entrances. It can be concluded that the results are very

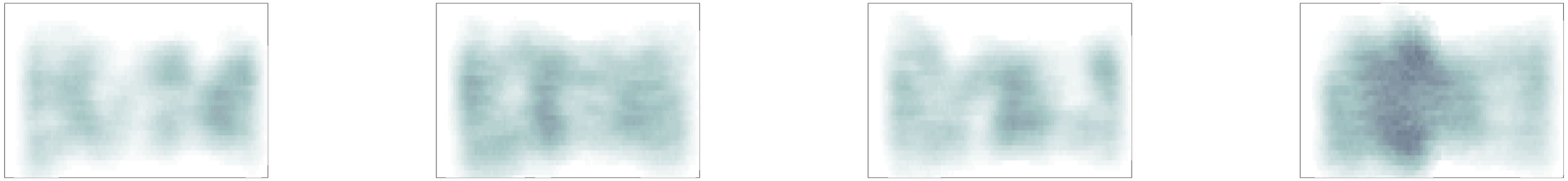

(a) $r_0 = 0.12$, $a_0 = 7.5$, $\tau = 0.1875$ **(b)** $r_0 = 0.20$, $a_0 = 7.5$, $\tau = 0.1875$ **(c)** $r_0 = 0.12$, $a_0 = 7.5$, $\tau = 0.3125$ **(d)** $r_0 = 0.20$, $a_0 = 7.5$, $\tau = 0.3125$

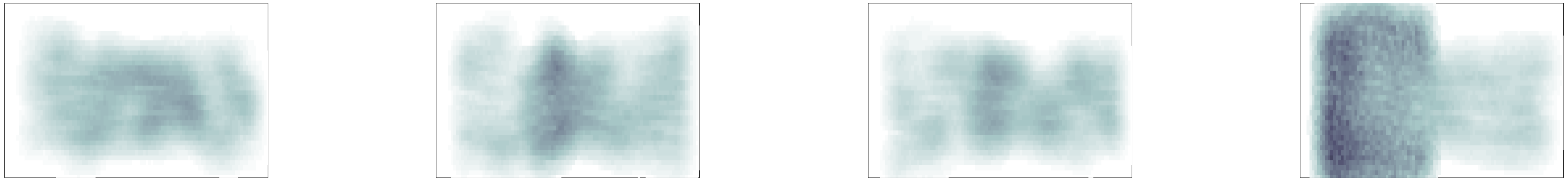

(e) $r_0 = 0.12$, $a_0 = 12.5$, $\tau = 0.1875$ **(f)** $r_0 = 0.20$, $a_0 = 12.5$, $\tau = 0.1875$ **(g)** $r_0 = 0.12$, $a_0 = 12.5$, $\tau = 0.3125$ **(h)** $r_0 = 0.20$, $a_0 = 12.5$, $\tau = 0.3125$

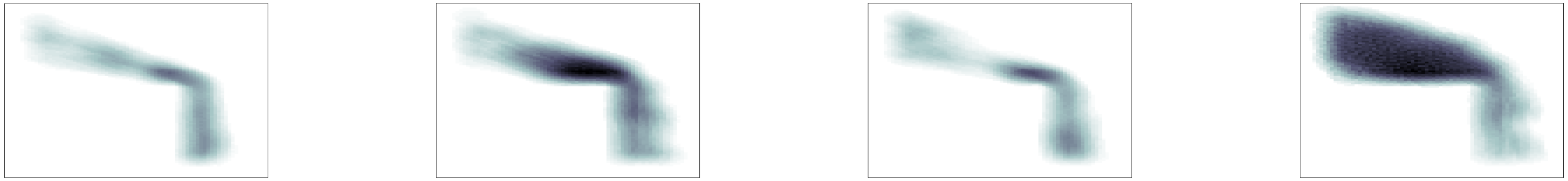

(i) $r_0 = 0.12$, $a_0 = 7.5$, $\tau = 0.1875$ **(j)** $r_0 = 0.20$, $a_0 = 7.5$, $\tau = 0.1875$ **(k)** $r_0 = 0.12$, $a_0 = 7.5$, $\tau = 0.3125$ **(l)** $r_0 = 0.20$, $a_0 = 7.5$, $\tau = 0.3125$

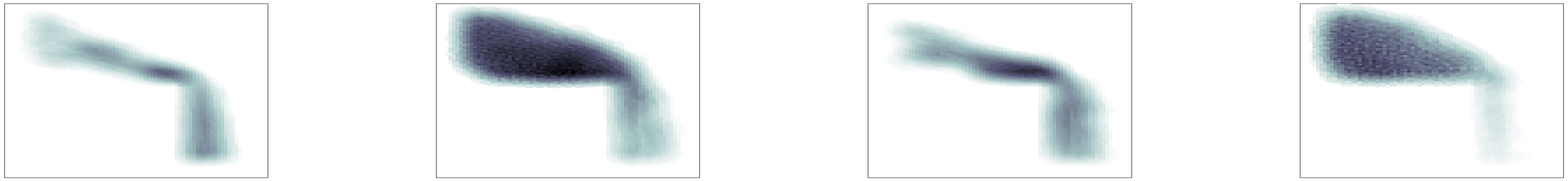

(m) $r_0 = 0.12$, $a_0 = 12.5$, $\tau = 0.1875$ **(n)** $r_0 = 0.20$, $a_0 = 12.5$, $\tau = 0.1875$ **(o)** $r_0 = 0.12$, $a_0 = 12.5$, $\tau = 0.3125$ **(p)** $r_0 = 0.20$, $a_0 = 12.5$, $\tau = 0.3125$

Figure 7.7: The combined influence of r_0 on the density distribution [white - $0 \leq \rho \leq 5.4$ - black] - part 1. Figures a-h display a uni-directional bottleneck, figures i-p a uni-directional corner movement base case.

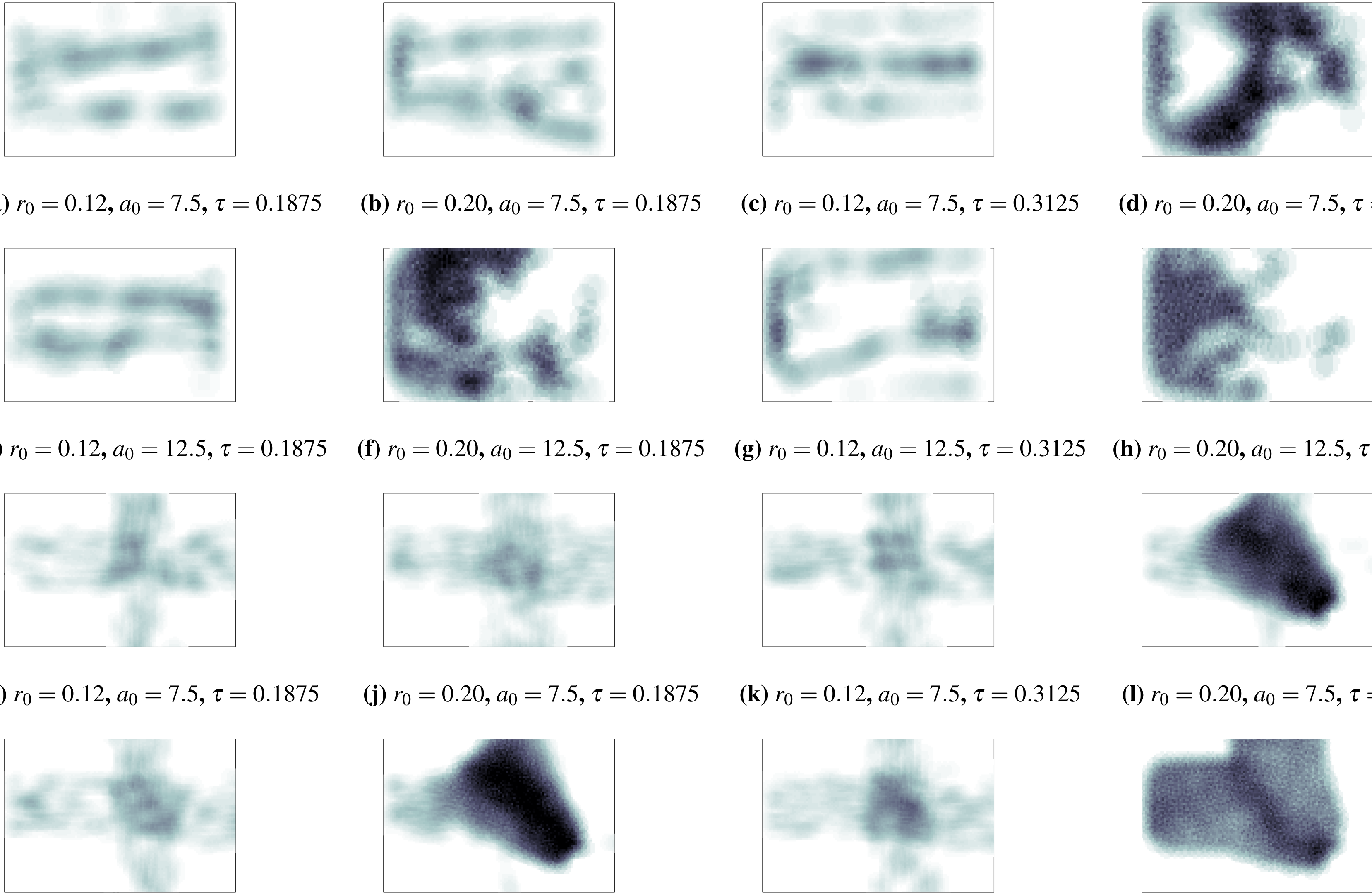

(a) $r_0 = 0.12$, $a_0 = 7.5$, $\tau = 0.1875$ **(b)** $r_0 = 0.20$, $a_0 = 7.5$, $\tau = 0.1875$ **(c)** $r_0 = 0.12$, $a_0 = 7.5$, $\tau = 0.3125$ **(d)** $r_0 = 0.20$, $a_0 = 7.5$, $\tau = 0.3125$

(e) $r_0 = 0.12$, $a_0 = 12.5$, $\tau = 0.1875$ **(f)** $r_0 = 0.20$, $a_0 = 12.5$, $\tau = 0.1875$ **(g)** $r_0 = 0.12$, $a_0 = 12.5$, $\tau = 0.3125$ **(h)** $r_0 = 0.20$, $a_0 = 12.5$, $\tau = 0.3125$

(i) $r_0 = 0.12$, $a_0 = 7.5$, $\tau = 0.1875$ **(j)** $r_0 = 0.20$, $a_0 = 7.5$, $\tau = 0.1875$ **(k)** $r_0 = 0.12$, $a_0 = 7.5$, $\tau = 0.3125$ **(l)** $r_0 = 0.20$, $a_0 = 7.5$, $\tau = 0.3125$

(m) $r_0 = 0.12$, $a_0 = 12.5$, $\tau = 0.1875$ **(n)** $r_0 = 0.20$, $a_0 = 12.5$, $\tau = 0.1875$ **(o)** $r_0 = 0.12$, $a_0 = 12.5$, $\tau = 0.3125$ **(p)** $r_0 = 0.20$, $a_0 = 12.5$, $\tau = 0.3125$

Figure 7.8: The combined influence of a_0, τ and r_0 on the density distribution [white - $0 \leq \rho \leq 5.4$ - black] - part 2. Figures a-h display a bi-directional movement base case and figures i-p an intersecting movement base case.

sensitive to an increase of r_0 and τ. That is, for high values of r_0 and τ generally a blockage is found, which is deemed unrealistic for this set of cases. The effect of a_0 is less dominant, but not negligible.

Also in the case of an intersecting flow situation a non-linear effect is found (see figures 7.8.i-p). In general, parameter sets containing high values of r_0 predict higher densities and a more spatially distributed crowd. However, also for this flow situation it is difficult to determine which parameter set will produce a certain result.

7.3.6 Conclusion on sensitivity of parameters Nomad walker model

This section has illustrated the influence of the parameters related to the path straying and interaction components of the walker model (i.e. τ, a_0 and r_0) on the predicted crowd movement dynamics. The section established that the Nomad model is very sensitive with respect to changes of r_0, which governs the strength of the interaction. Especially r_0 values higher than the default value of Nomad do not result in realistic crowd movement dynamics. Therefore, it is concluded that r_0 should either be retained at the current value or diminished slightly.

Next to that, the sensitivity analysis illustrates that both higher and lower values of τ and a_0 with respect to the default parameter values can produce a realistic crowd movement phenomena. As such, the sensitivity analysis does not place a limit on the range of τ and a_0 that is taken into account during a calibration.

Moreover, the sensitivity analysis has shown that the interplay between these three parameters is non-linear. As a result, it is very difficult to determine an optimal parameter set based on the qualitative description of the walking behaviour one attempts to capture.

In general, the default values of the Nomad model, as derived by Campanella et al. (2009b), are found to reproduce most of the crowd movement phenomena. However, whether the model is capable of accurately modelling all crowd movement base cases quantitatively is undetermined at this stage.

7.4 Calibration of Nomad

The current version of Nomad is calibrated based on trajectory data sets gathered during a small laboratory study. Consequently, the validity of the default parameter set of the Nomad model for modelling of walking dynamics of pedestrians at large-scale crowd movements is questionable. A more thorough calibration by means of empirical data sets is necessary to determine the best parameter set for this specific type of movement dynamics.

This section elaborates on the calibration of the Nomad model. In the first section (7.4.1) the calibration methodology is described. Accordingly, the calibration results for five distinct flow situations are mentioned in sections 7.4.2-7.4.6. Afterwards, a calibration is performed based on the data sets of all five flow situations simultaneously in section 7.4.7. This section closes with a synthesis of the results in section 7.4.8.

7.4.1 Quantitative calibration methodology

During the last couple of years calibration attempts which directly compare simulated and empirically derived trajectories by means of least-squares have been proposed (a.o. Hoogendoorn et al. (2007), Johansson (2009b), Rudloff et al. (2011) and Seer et al. (2014)). Other studies mention the existence of distinct metrics to calibrate a simulation model, but only implement one of those (e.g. Wolinski et al. (2014)).

For the cases of pedestrian (Campanella et al., 2009b) and vehicular traffic (Punzo et al., 2012) it is proven that the calibration of a simulation model based on one metric provides unrealistic results either at the microscopic or the macroscopic level depending on the metric. Therefore, methodologies which determine a goodness of fit based on both microscopic and macroscopic characteristics, and as such multiple metrics, to describe the walking dynamics of pedestrians are preferred over the calibration methods that use only one metric.

To the author's knowledge only one calibration method, i.e. Campanella et al. (2009b), has been proposed for pedestrian simulation models which uses both the microscopic characteristics and the macroscopic characteristics of the crowd's movements. This calibration method establishes the best fit based on four characteristics of the pedestrian flow, namely the speed decay, the free flow speed, the frequencies of the occurrence of a certain amounts of lanes in a corridor and the bottleneck capacity. However, these characteristics specifically describe only two movement base cases (a uni-directional entering and a bi-directional straight flow). Moreover, some of the characteristics (such as the amount of lanes and the capacity) are still under debate and very dependent on the context of the situation. As such, the method proposed by Campanella et al. (2009b) cannot be used to calibrate a pedestrian simulation model with respect to all movement base cases.

Therefore, this chapter details a calibration method which determines the optimal parameter set based on several metrics and can be applied to calibrate a pedestrian simulation model with respect to all movement base cases. Moreover, with respect to the method proposed by Campanella et al. (2009b), different metrics have been used. The following first presents the calibration method. Accordingly, the search method and search space are defined and some technical details with respect to the simulation of the case study areas by means of Nomad are mentioned.

Calibration based on multiple metrics

The results of chapter 5 illustrate that several distinct metrics can be used to describe the walking dynamics of pedestrians at large-scale events. In table 7.1 a sub-set of these metrics that can be used to calibrate pedestrian simulation models are mentioned. As one can see, not only detailed

Table 7.1: Metrics for the calibration of a pedestrian simulation model

Characteristics	Level	Metric
Distribution over space	Macroscopic	Spatial distribution of pedestrians over the infrastructure
Velocity	Macroscopic	Temporal velocity distribution Spatial distribution of the walking velocity
Density	Macroscopic	Temporal density distribution Spatial distribution of the density
Distance headway	Mesoscopic	The average minimum distance headway Standard deviation of the minimum distance headway Skewness of the minimum distance headway
Time to Collision	Mesoscopic	The average minimum time to collision Standard deviation of the minimum time to collision Skewness of the minimum time to collision
Interaction angle	Mesoscopic	The average angle of interaction Standard deviation of the angle of interaction Skewness of the angle of interaction
Trajectories	Microscopic	Distance between simulated and empirical trajectory

trajectory data sets can be used to calibrate a pedestrian simulation model. Also the temporal and spatial distribution of the density and the velocity and the distribution of the headway, time to collision and interaction angle are measures that capture a part of the operational movement dynamics of pedestrians. The self-organisation phenomena mentioned in literature and chapter 5 are not used as a metric, because currently no generic quantitative measures exist that can capture these phenomena automatically.

Yet, in comparison to the calibration based on trajectory information (e.g. Seer et al. (2014)), a calibration based on the combination of the metrics mentioned above is more difficult. The operational movement dynamics of pedestrians, and as such the operational movement dynamics predicted by most simulation models, is stochastic. Therefore, one has to ensure that the used metrics are not influenced by the stochastic nature of the interactions. Consequently, several metrics (for example the spatial distribution of the directionality of the walking velocity) cannot be used to calibrate a pedestrian simulation model. Other metrics can only be used when these metrics are aggregated into a distribution.

Each of the metrics mentioned in table 7.1 describes a part of the operational walking behaviour of pedestrians. Therefore, similarly to Campanella et al. (2009b), there has been chosen to implement a combination of metrics. The average velocity field and the average density field are used to capture the macroscopic perspective. Furthermore, the minimum distance headway, the angle of interaction and the time-to-collision are taken into account in order to calibrate the interaction behaviour as realistic as possible. The mean, the standard deviation and skewness of the distributions can be taken into account for these three metrics. However, for simplicity reasons only the average is adopted in this study. Last of all, the distribution of pedestrians over space is adopted as part of the calibration process. This last characteristic captures the diffusion patterns of pedestrians that are especially dominant in case of uni-directional corner and bottleneck flows.

For each metric the distance between the empirical realisation M_{real} and the simulation result M_{sim} are determined by means of a squared error. The error in the spatial distribution of the macroscopic metrics is determined as a summation of the error of each grid cell, where the maximum error is set to 1.3 m/s respectively 5.4 P/m^2 for grid cells for which no simulation solution but an empirical result exists.

$$SE_{macro} = \frac{1}{N_x * N_y} \sum_{y=y_{min}}^{y_{max}} \sum_{x=x_{min}}^{x_{max}} (M_{real}(x,y) - M_{sim}(x,y))^2 \tag{7.6}$$

$$SE_{micro/meso} = (M_{real} - M_{sim})^2 \tag{7.7}$$

where N_x and N_y are respectively the amount of cells along the x and y-axis. Depending on the metric, the resulting distances can severely differ in scale. As such, the errors cannot be simply added. Therefore, the objective function first transforms all distances to a value between 0.5 and 1 and only afterwards, the distances resulting from distinct metrics are added (see eq. 7.8).

$$GOF(a_0, \tau, r_0) = \frac{1}{N_m * N_n} \sum_m \sum_n C_n * \frac{1}{1 + \frac{SE_{n,m}(a_0,\tau,r_0)}{\max(SE_{n,m}(a_0,\tau,r_0))}} \tag{7.8}$$

Where $SE_{i,j}(a_0, \tau, r_0)$ represents the sum of squares of the residuals of the characteristics for a certain set of parameters (a_0, τ, r_0), n the characteristics, m the sequences per case study, N_m the number of sequences per case study, N_n the number of characteristics, and C_i the relative weight of that characteristics in relation to the other characteristics for which $\sum C_i = 1$. As a result of this formulation, $GOF(a_0, \tau, r_0) = 1$ for parameter sets which produce realistic results and $GOF(a_0, \tau, r_0) = 0.5$ for parameter sets which do not produce realistic results at all.

This GOF function, which included several metrics, has, to the author's knowledge, never been used to calibrate a pedestrian simulation model. Consequently, the impact of the GOF function on the objective and the resulting optimal parameter set is undetermined. Therefore, the following sections will mention the results for more than one GOF (i.e. combination of metrics) in order to establish the sensitivity of the optimal parameter set with respect to the GOF function. In total 17 different schemes have been tried, of which schemes 3 (only macroscopic characteristics), 10 (only mesoscopic characteristics), 14 (only the spatial distribution of pedestrians) and 17 (a scheme in which the squared error of the macroscopic and mesoscopic characteristics and the distribution of pedestrians are balanced) represent the GOF functions that are based on an equal loading of all adopted metrics of a certain nature (macroscopic, mesoscopic and the spatial distribution). These 17 schemes are logical combinations of the 6 adopted metrics. As a starting points, equal weights are adopted for metrics that have the same nature in this thesis.

Search space and method

Given that the Nomad model has already been rudimentary calibrated, it is deemed not necessary to establish a large search area. The sensitivity analysis has shown that large deviations (+20%) from the default values of the Nomad model result in non-realistic results. Therefore, the search area is limited to this percentage of the default value. In case of r_0, it was furthermore found that values which were larger than the default value do not produce reasonable results. Therefore, the search space along this dimension is limited to -20% to 0% of the default value. This results in the following search space:

- $0.20\, s \leq \tau \leq 0.30\, s$
- $0.128\, m \leq r_0 \leq 0.160\, m$
- $8.0 \leq a_0 \leq 12.0\, m/s^2$

Based on the sensitivity analysis it is expected that the behaviour of the Nomad model is highly non-linear. As such, it is very difficult and expensive to determine whether the global optimal is found by the optimisation scheme. It is expected that the computation costs of performing an optimisation are almost similar to the costs of a grid search in this specific case. In combination with the limitation of the search space, this provides the opportunity to perform a grid search instead of an optimisation scheme (Greedy, Simulated Annealing, etc.).

Given the differences in size between the variables τ, a_0 and r_0 not a generic step size can be adopted. Instead the step size is specified as a percentage of the default value. A step size of 2%[20] of the default value is adopted, which results in $d\tau = 0.005\ s$, $da_0 = 0.2\ m/s^2$ and $dr_0 = 0.0032\ m$.

Use of empirical data sets

Chapters 3 and 5 have detailed the general characteristics of several empirical data sets gathered during large-scale events in the Netherlands. These data sets will be used to calibrate Nomad. However, many data sets were captured. To limit the computation time, only the 5 most distinct cases are used in the calibration process, namely the cases of 4Daagse in Wijchen, 4Daagse in Lent, the Rotterdam Marathon, Queensday in Amsterdam and the Liberation day festival in Wageningen. These data sets jointly display the largest range of movement base cases captured within the empirical data sets.

In order to model the cases using Nomad, several details regarding the characteristics of the infrastructure were set. First of all, several general characteristics of the flow situation have been derived from the empirical data sets. That is, the flows, the OD-pairs, and the route splits have been computed based on the trajectory data. The reader is referred to table B.1 for the specifications of these characteristics per case and per data set.

[20] The size of the steps is the result of a balancing act between the amount of simulations that has to be performed and the precision of the calibration results.

Besides that, the general layout of the infrastructure has been derived from the video images and the trajectory data. In several cases, no walls but other objects within the case structure the pedestrians' walking behaviour. In these special cases, the following adaptations are made:

- *4Daagse - Lent*: The steep slopes of the dike have been modelled as walls that are located approximately at shy-away distance from the asphalt.
- *4Daagse - Wijchen*: The low fences on both sides of the path have been modelled as walls.
- *Liberation day festival - Wageningen*: A stone bench was blocking the outflow of pedestrians on one side of the square. This bench has been modelled as an area the agents could not pass into.

In all cases the default parameters have been adopted in order to model the interaction of pedestrians with obstacles. With respect to the generic walking behaviour of Nomad all default values are adopted. This results in a free-flow walking velocity of 1.3 m/s.

7.4.2 Uni-directional straight flows

The uni-directional straight movement base case has been calibrated based on the empirical data sets gathered at the 4Daagse in Wijchen. Table C.1 mentions the results of the calibration. The table displays the objective and the optimal parameter set for several GOF functions, which are a combination of 6 different macroscopic and mesoscopic metrics.

The table illustrates, that when taking all six metrics into account, the optimal parameter set (i.e. scheme nr. 17 - [$\tau = 0.275$, $a_0 = 10.6$, $r_0 = 0.16$]) has a higher τ, a_0 and r_0 compared to the default values of Nomad. It can be deduced that pedestrians at large-scale events adopt their acceleration more slowly and are more severely influenced by other surrounding pedestrians.

However, the value of the objective function is very low for all cases in which the spatial distribution of the pedestrians is taken into account (schemes nr. 14-16). That is, Nomad has difficulties reproducing the spatial distribution of pedestrians. In general, the pedestrians are less distributed over space in the simulation results than found in an empirical movement situation.

7.4.3 Uni-directional entering flow

The uni-directional entering movement base case is calibrated using the data sets gathered during the Rotterdam Marathon. According to table C.2, which depict the results of the calibration procedure for several GOF functions, the optimal parameter set when taking all metrics into account is $\tau = 0.235\ s$, $a_0 = 9.6\ m/s^2$, $r_0 = 0.1504\ m$.

Compared to the default settings of Nomad, τ, a_0 and r_0 are all slightly decreased. This would mean that the pedestrians in a uni-directional - entering movement base case adapt their

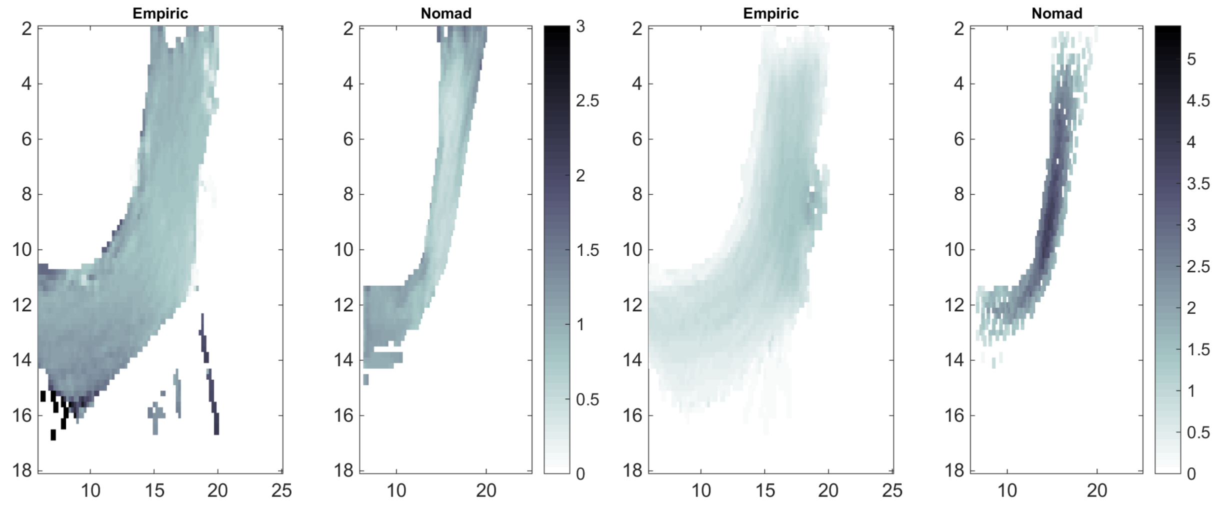

(a) Velocity $[m/s]$ **(b) Density** $[P/m^2]$

Figure 7.9: Velocity and density plot of the optimal parameter values for a uni-directional corner movement base case for GOF function number 17.

acceleration more quickly and take slightly less pedestrians into account in their movement decisions. Moreover, the impact of the nearby other pedestrians on the pedestrian's walking decisions is less. Table C.2 also shows that the optimal parameter sets are very dependent on the chosen GOF function.

7.4.4 Uni-directional flows around a corner

The results of the calibration of Nomad for a uni-directional corner movement base case are mentioned in table C.3. If all metrics are taken into account the optimal parameter set [$\tau = 0.275$, $a_0 = 10.6$, $r_0 = 0.1536$] has very high values of τ and a_0 and a slightly lower value of r_0. This results in pedestrians that adopt their acceleration more slowly and assign more weight to interactions with pedestrians in their vicinity. Yet, the weight of the interaction decreases more rapidly with an increase of the distance between pedestrians. As a result, in high density cases less neighbouring pedestrians are influencing the movement dynamics of a pedestrian.

7.4.5 Bi-directional Straight flows

Table C.4 depicts the results of the calibration of Nomad with respect to a bi-directional straight flow. In general, lower values of a_0 and r_0 are found in the optimal parameter set [$\tau = 0.25$, $a_0 = 9.8$, $r_0 = 0.1536$] compared to the previous movement base case. However, depending on the metric GOF function a_0 and r_0 take on very different values. This is due to a rather flat objective function with respect to these two parameters with many local minima. At the same time the value of τ varies only slightly.

The parameter values that are found when taking into account all metrics, are slightly lower than the default parameter set of Nomad. As such, also in this movement base case pedestrians seem to adopt a longer reaction time, and react with more strength on the interactions with other individuals.

7.4.6 Intersecting flows

The calibration results for the intersecting flow situation are mentioned in table C.5. For the results it can be deduced that Nomad has difficulties calibrating the mesoscopic interaction behaviour of pedestrians in all data sets. Moreover, very low values for the objective function are found when only the spatial distribution is taken into account.

Besides that, the strength of the interaction component a_0 is found to be very dependent on the GOF function. The parameter values found for the reaction time τ and the amount of interactions taken into account r_0 are relatively stable and near the default value.

7.4.7 Compound calibration of Nomad

Besides a calibration per flow situation, a calibration based on the data sets of all flow situations has been performed. The results of this calibration are depicted in table C.6. In general, this table shows the same trends as the calibration of the separate flow situations. That is, for most GOF functions τ is higher than the default value of Nomad, r_0 is fairly stable and lower than the default value, and a_0 is very volatile. This volatility might be due to the relative flat objective function with respect to a_0.

7.4.8 Synthesis of the calibration of Nomad

The previous sections 7.4.2-7.4.7 have mentioned the results of the calibration of the Nomad model with respect to several movement base cases. This gives rise to some considerations regarding the influence of the parameter set on the capacity of the infrastructure, the optimal parameter sets, the objective function and the GOF function. Underneath these will be discussed separately.

Influence of the adopted parameter set on the capacity of the infrastructure

The differences between the values of the optimal parameter sets of between the cases are limited compared to the default parameter settings of Nomad. However, large qualitative differences in the developing traffic state were found in the sensitivity analysis. Yet, the quantitative influence of the parameter sets on the traffic state and as such the capacity are unknown.

Even though the capacity of a movement base case is a difficult measure to use in the quantitative calibration process, this measure can be used to produce some insights into the

Table 7.2: Summary of the calibration results of Nomad

Case	w_d	w_v	$w_{h_{pq}}$	w_{TTC}	$w_{v_{pg}}$	$w_{spatialdist}$	$O(a_0, \tau, r_0)$	τ	a_0	r_0
Only macroscopic metrics										
4D-W	0.5	0.5	0	0	0	0	0.89	0.265	10.6	0.1600
4D-L							0.98	0.250	9.4	0.1504
M-R							0.89	0.225	9.0	0.1440
Q-A							0.94	0.270	10.8	0.1440
LF-W							0.98	0.235	10.2	0.1568
All series							0.98	0.265	10.8	0.1600
Only microscopic metrics										
4D-W	0	0	0.33	0.33	0.33	0	0.68	0.275	10.6	0.1600
4D-L							0.53	0.275	10.6	0.1536
M-R							0.66	0.265	10.4	0.1568
Q-A							0.53	0.275	10.8	0.1472
LF-W							0.44	0.240	10.4	0.1536
All series							0.52	0.270	10.8	0.1568
Only spatial distribution metrics										
4D-W	0	0	0	0	0	1	0.32	0.255	11.0	0.1536
4D-L							0.03	0.275	10.6	0.1600
M-R							0.92	0.235	9.6	0.1504
Q-A							0.74	0.260	10.0	0.1568
LF-W							0.38	0.260	11.0	0.1472
All series							0.38	0.235	10.2	0.1472
All metrics										
4D-W	0.167	0.167	0.11	0.11	0.11	0.33	0.58	0.275	10.6	0.1600
4D-L							0.51	0.275	10.6	0.1536
M-R							0.78	0.235	9.6	0.1504
Q-A							0.71	0.250	9.8	0.1536
LF-W							0.58	0.245	9.0	0.1536
All series							0.60	0.275	10.8	0.1472

influence of the parameter sets on the predicted capacity. By means of the flow breakdown probability (defined by Campanella et al. (2009a) and Yang et al. (2014)) the impact of the distinct parameter sets is estimated for three movement base cases with a steady demand. In order to do this, the two most distinct parameter values resulting from the calibration involving all metrics are determined, being $[\tau = 0.235\ s,\ a_0 = 9.6\ m/s^2,\ r_0 = 0.1504\ m]$ and $[\tau = 0.275\ s,\ a_0 = 10.8\ m/s^2,\ r_0 = 0.1472\ m]$.

Figure 7.10 displays the results for a uni-directional - corner, bi-directional - straight and intersecting movement base case. The results illustrate that flow breakdown[21] occurs at quite different demand levels. Even in these simple scenarios, when a parameter set with relatively high values of τ, a_0 and r_0 is adopted, flow breakdown is postponed. Consequently, the small differences in the parameter sets displayed in table 7.2 have quite a large effect (between 20% and 50%) on the capacity of the infrastructure. As such, even these small differences in the parameter sets have to be taken into account when simulating the movement dynamics of pedestrians.

Moreover, when looking back at the results of the calibration, it is visible that especially for the simple uni-directional flow situations relatively high parameter values are found. By contrast, in the more complex flow situations relatively small parameter values are found. This might suggest that pedestrians adopt a different type of walking behaviour depending on the movement base case, and as such postpone the onset of congestion and flow breakdown. The use of one parameter set for several different movement base cases results in overestimation of the capacity in some cases and underestimation in others. The findings thus imply that different parameter sets are needed to accurately predict the pedestrian movement dynamics during distinct movement base cases.

Optimal parameter values

In table 7.2 the results of the calibration are summarised. The table illustrates that the optimal parameter values are dependent on the movement base cases as well as the goodness-of-fit(GOF) function. The resulting parameter values are found to be both higher and lower than the default parameter set of the Nomad model.

Besides that, depending on the metrics used in the calibration process either τ or r_0 are located on the upper boundary of search space, which was deemed unrealistic for r_0. The parameters on the boundary of the search area provide no information with respect to the optimal parameter set. That is, these parameter values only illustrate that the best solution might also reside outside the adopted search space. The high parameter values of τ and r_0, moreover, suggest that pedestrians react more slowly on the presence of other pedestrians and interact over larger distances. As such, these high parameter values might be overcompensation in order mimic the of anticipation behaviour of downstream situations that occurs in reality, but which is not captured by Nomad.

Besides that, it is noticed that the mesoscopic characteristics and spatial distribution of the uni-directional - straight and entering pedestrians can reasonably well be represented, while these

[21]The probability that breakdown (more than 100 pedestrians who have an average velocity of less than 0.3 m/s for longer than 5 s) occurs, estimated based on 50 simulations per density instance.

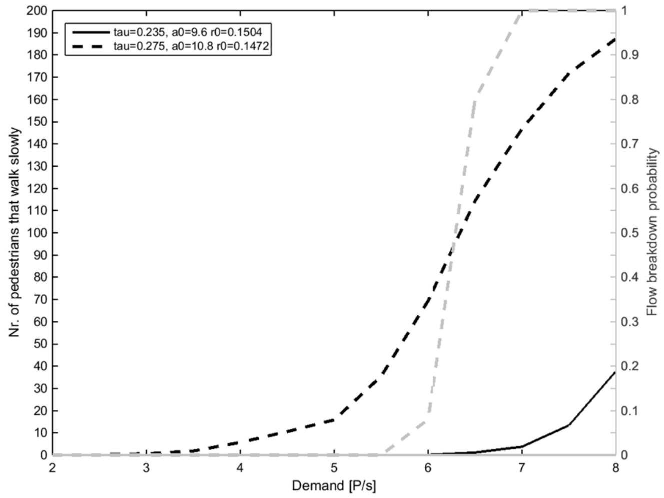

(a) Uni-directional - Corner

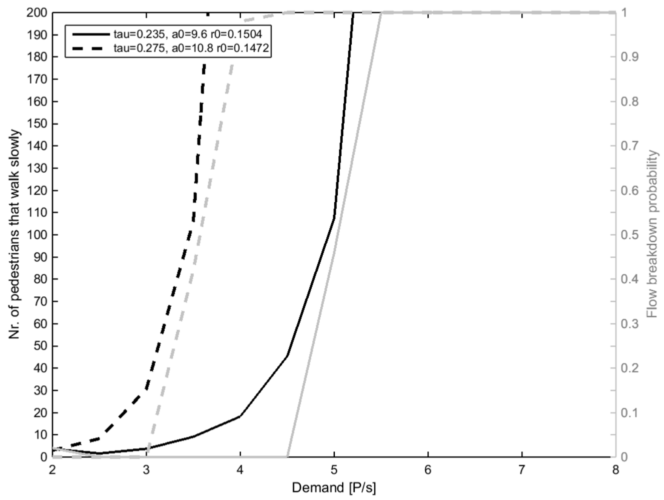

(b) Bi-directional - Straight

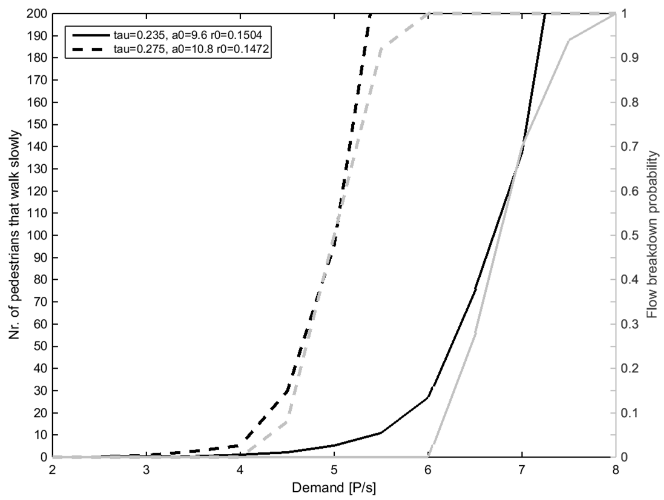

(c) Intersecting - 2 flows

Figure 7.10: Flow breakdown probability (black) and the average number of pedestrians who have an average velocity of less than $0.3\ m/s$ for longer than $5\ s$ (grey) for three movement situations.

characteristics of the walking behaviour of the crowd in uni-directional corner, bi-directional and intersecting flow situations can only be approximated to some extent. It is hypothesised that this is due to the optimal walking behaviour that currently assumed by the Nomad walker model. That is, the optimal walking behaviour assumed in Nomad causes pedestrians to distribute themselves less over space, to overtake earlier and to accelerate and decelerate more quickly than is found in the empirical case. The lack of these findings might imply that the assumption with respect to the walking behaviour, namely that of a local and global optimal route based on distance and obstacle avoidance, might not hold during large-scale events.

From the table it can also be deduced that the macroscopic characteristics of the flow situation can be captured by Nomad. The prediction of the mesoscopic metrics depends on the case. Nomad has the most difficulties representing the spatial distribution of the pedestrians correctly. This is probably due to the suboptimal route choice behaviour of the pedestrians that is displayed in the empirical cases.

Influence of the objective function and the goodness-of-fit function

The chosen objective function and GOF function were found to severely influence the results of the calibration in three ways. Firstly, it was found that the surface of the objective function is fairly flat with respect to some parameters, as well as non-linear and complex. As a result several local maxima are present within the search space, their height difference being limited to approximately 0.005. Additionally, several plateaus are found with even smaller differences between the values of the objective function. From this it can be deduced that the resulting optimal parameter set is strongly influenced by the exact points taken into account in the grid search.

Moreover, the results of the analysis are dependent on the number and choice of the movement base cases to include, since large errors (i.e. large behavioural differences) weight heavily on the optimum solution. Likewise, due to the relatively large effect of the stochastic nature of the pedestrian walking behaviour on the goodness of fit in low density situations, the solution gravitates towards parameter values that can predict the walking behaviour correctly for low density situations.

7.5 Assessment of Nomad

In chapter 5 two lists of crowd movement phenomena have been developed which describe the phenomena. After the calibration of Nomad with respect to large-scale events in the previous section, the capabilities of the model with respect to simulating these features can be assessed. Besides that, a quantitative comparison is performed which uses the same metrics as the calibration. The results of this quantitative assessment are mentioned in table B.1, where the optimal parameter values established during the calibration are used to produce the simulation results.

Table 7.3: Assessment of Nomad with respect to the general characteristics of crowd movements found in empirical data sets, where ✓signals that this general characteristic can be captured by Nomad, $\sim$ that it under some circumstances can be simulated, X that it can never be simulated, and ? that this characteristics cannot be determined.

Variable	Characteristics	Assessment
FD - V-ρ	If density increases, velocity decreases	✓
	Three regimes: a free-flow, a transition and a congestion zone.	X
	At high densities pedestrians will retain a velocity.	✓
FD - q-ρ	If density increases, the flow rate increases upto capacity.	✓
	The transition zone is unstable and knows directional differences	✓
	At high densities, flow might diminish but will not stop entirely.	X
Headway	If density increases, the distance headway decreases.	$\sim$
	If the avg. interaction angle decreases, the distance headway increases.	✓
Interaction zone	If the density increases, the length of the longitudinal axis of the no-interaction zone decreases.	?
	The length of the lateral axis of the no-interaction zone is independent of the density.	?
Route choice	Searching behaviour is of pedestrian increases during high density situations.	X
	The swaying behaviour of pedestrians becomes more dominant during high density situations.	X

Tables 7.3 and 7.4 depict the results of the qualitative assessment. The tables show that especially the phenomena which relate to the interaction behaviour of singular individuals cannot be captured by Nomad. In general, Nomad predicts far more optimal behaviour patterns than the empirical movement dynamics suggest. Way finding, searching behaviour, interaction movements are not predicted correctly. The assumption of global knowledge by pedestrians in Nomad might be at the root of this issue.

The results of the quantitative comparison illustrate that Nomad has difficulties balancing the spatial distribution with the mesoscopic and macroscopic characteristics (see tables C.7-C.12). Depending on the movement base case the spatial distribution (among others uni-directional corner flows) or the mesoscopic (among others uni-directional entering and bi-directional straight flows) characteristics provide the lowest goodness of fit. Furthermore, the validation results show that the optimal parameter sets found during the calibration based on all data sets perform similar to the calibration based on singular flow situations. The results illustrate that especially the cases of 4Daagse-Wijchen, 4Daagse-Lent and the liberation day festival in Wageningen remain difficult to predict. These also happen to be the cases in which large deviations with respect to the shortest distance path and the spatial distribution of the density are encountered. Besides that, in general higher velocities are predicted than found in the empirical cases. This might be due choice of a reasonably high free-flow speed and adoption of optimal route choice behaviour in Nomad, which contrasts with the relative low speed and irregular trajectories of pedestrians in these empirical cases.

Table 7.4: Assessment of Nomad with respect to the movement base case specific characteristics found in empirical data sets, where ✓signals that this general characteristic can be captured by Nomad, ∼ that it under some circumstances can be simulated, X that it can never be simulated, and ? that this characteristics cannot be determined.

Movement base case	Characteristics	Assessment
Uni-dir - straight	Density uniformly spread spatially	✓
	Velocity uniformly spread spatially	✓
	Trajectories become more unstable	X
	Predominantly front2back interactions	✓
	Lane formation occurs under high densities	X
Uni-dir - Corner	Density increased upstream of corner	X
	Density increase at inner upstream side	✓
	Velocity decreased upstream of corner	X
	Predominantly front2back interactions	✓
Uni-dir - Entering	Density increases towards bottleneck both longitudinal and lateral	✓
	Density focus-point upstream of bottleneck	✓
	Velocity is not decreasing towards the bottleneck	X
	Many short interactions	?
	Predominantly front2back interactions	✓
	Wayfinding increased at high densities	X
Bi-dir - straight	Density uniformly spread over cross-section	✓
	Velocity uniformly spread over cross-section	✓
	Trajectories more unstable at high densities	X
	Interactions predominantly front2back	✓
	Wayfinding decreased at high densities	X
	Lane formation	✓
Intersecting - Random	Density uniformly spread over cross-section	X
	Velocity non-uniformly spread over cross-section	✓
	Trajectories more unstable at high densities	X
	Interaction angle mainly between 0 and 90 degrees	X
	Wayfinding increased at high densities	X
	Lane formation between dominant origins and destinations	✓

7.6 Conclusions

In this chapter the microscopic pedestrian simulation model Nomad has been calibrated for the simulation of pedestrian movement dynamics at large-scale events. A first step of the calibration procedure consisted of assessing the sensitivity of the predicted movement dynamics of Nomad with respect to the parameter settings of the parameters τ, a_0 and r_0. It was found that the Nomad model can reproduce most crowd movement phenomena. Besides that, the analysis showed that the interplay between the three main variables of the model (i.e. τ, a_0 and r_0) is non-linear. Moreover, it was established that Nomad is specifically sensitive with respect to changes of r_0, which governs the number of pedestrians which are taken into account. Especially r_0 values higher than the default value of Nomad do not produce realistic results.

Accordingly, a calibration was performed based on the empirical data sets discussed in chapter 5. The results (of which a summary is provided in table 7.2) illustrate that distinct parameter sets best describe the different movement base cases. Moreover, from the assessment it was deduced that the parameter set which resulted from calibration based on all movement base cases performs worse than the parameter sets which resulted from the calibration based on only one of the movement base cases.

Based on the analyses presented in this chapter, it can be concluded that Nomad can qualitatively predict most crowd movement phenomena and some self-organisation patterns correctly. However, in cases were the general movement pattern deviates from the shortest path, differences between the prediction and reality might occur. Moreover, the quantitative prediction of the density and velocity of the pedestrians in the crowd, as well as the capacity of the infrastructure, depend severely on the adopted parameter set. Consequently, it remains essential to carefully determine the components of the global route choice (attraction and repulsion of infrastructure elements) and the most applicable parameter set for every quantitative assessment of the infrastructure by means of Nomad. Yet, after movement base case specific calibration, Nomad can be used to simulate and assess the walking behaviour of pedestrians in crowds at large-scale events.

In section 7.4.8 it was shown that the surface of the objective function is non-linear and complex. Given that a grid-based search method does not allow to explore the space in between discrete points and the severe non-linearity of the objective function, it is unclear to what extent the solutions might shift if these regions are also taken into account. Therefore, a more thorough calibration by means of more sophisticated search methods (e.g. genetic algorithms, simulated annealing or ant colony optimization) is needed.

Besides that, several optimal parameter sets include parameters which are on the boundary of the search space. These parameters provide no information with respect to the optimal parameter values. To alleviate this issue, the search space has to be increased. Since the amount of work involved, this is considered to be a bridge to far for this thesis. It is however suggested that in future calibration and validation runs the search space is increased in order to include especially higher parameter values for τ and r_0.

In this chapter a new set of metrics has been introduced for the calibration of pedestrian simulation models. The results presented in section 7.4 illustrate that the adopted metrics and the goodness-of-fit function has a severe influence on the resulting optimal parameter set. In this thesis only one type of goodness-of-fit function has been adopted. In order to understand the implications of the GOF function, more research is necessary into the influence of the mixture of the metrics used in this thesis and which metrics to use.

Chapter 8

Assessment of a macroscopic pedestrian simulation model

Chapter 6 has shown that the computational burden of most microscopic models leaves much to desire. Even though most macroscopic pedestrian simulation models do not reproduce all crowd movement phenomena, the use of macroscopic models might provide a solution in cases where a limited computational burden or a closed-form analytical solution is imperative. Therefore, in this chapter the capabilities of one of the promising macroscopic simulation models will be assessed with respect to the walking behaviour of pedestrians in crowds at large-scale events, namely a continuum model proposed by Hoogendoorn et al. (2014) and Hoogendoorn et al. (2015) named the Macroscopic Dynamic Walker model (MDW model).

However, before an assessment of the MDW model's capabilities can be made, first the influence of the parameter values on the predicted dynamics of the model need to be established. At the moment two formulations of the MDW model have been proposed. Therefore, this chapter establishes which of the two model definitions should be used during the remainder of this chapter and accordingly calibrates this version of the MDW model especially for walking dynamics of pedestrians in crowds at large-scale events. The MDW model is calibrated based on the empirical data sets described in chapter 5 using new calibration metrics that takes into account several macroscopic characteristics of the walking dynamics. Afterwards, an assessment of a MDW model's capabilities is performed.

Sections 8.1 and 8.2 are an merged, updated and edited version of the following two published papers:
Duives, D.C., W. Daamen, S.P. Hoogendoorn (2016). Continuum modelling of pedestrian flows - part 2: sensitivity analysis featuring crowd movement phenomena. *Physica A: Statistics, Mechanics and its Applications*, 447, pp. 36-48.
Duives, D.C., W. Daamen, S.P. Hoogendoorn (2016 - in print). Sensitivity analysis of the local route choice parameters of the continuum model regarding pedestrian movement phenomena. *Traffic and Granular Flow '15*, in print.

In the remainder of this chapter, section 8.1 introduces the MDW model. Subsequently, section 8.2 discusses the sensitivity of the model parameters with respect to crowd movement phenomena. Section 8.3, accordingly, presents the calibration of the MDW model, which includes an introduction of the calibration procedure. The final assessment of the MDW model's capabilities is presented in section 8.4. Section 8.5 finalizes this chapter with the conclusions and some suggestions for future research.

8.1 Introduction to the MDW model

The Macroscopic Dynamic Walker model presented in Hoogendoorn et al. (2014) describes the dynamics of the class-specific density $\rho_d(t,\vec{x})$ over time t and space $\vec{x}$, where d denotes the class a pedestrian belongs to. In this model, a class describes all pedestrians which walk from the same origin to the same destination, having the same physical capabilities. The MDW model assumes that the movement behaviour of all pedestrians of a class develops in a similar manner, which is described by means of a class specific fundamental diagram.

General dynamics

Within the MDW model the conservation of pedestrians is assumed. The class-specific conservation of mass equation (eq. 8.1) describes how within a cell the density of pedestrians of class d changes over time due to the lateral and longitudinal in- and outflow of pedestrians. In the conservation equation $\vec{q}_d$ represents a two-dimensional flow vector, r_d the inflow of pedestrians and s_d the outflow of pedestrians. The MDW model assumes that conservation holds for every cell defined within the infrastructure.

$$\frac{\partial \rho_d}{\partial t} + \bigtriangledown \cdot \vec{q}_d = \vec{r}_d - \vec{s}_d \tag{8.1}$$

The equilibrium velocity $\vec{v}_d$ is modelled as a two-dimensional vector that is defined by an absolute speed u_d and a direction of movement $\vec{\gamma}_d$ (eq. 8.2). It is assumed that the speed u_d is a function of the total densities ρ (eq. 8.3). As a result, the MDW model can simulate the impact of flow composition on the average walking speed for a specific class d.

$$\vec{v}_d = u_d \cdot \vec{\gamma}_d \tag{8.2}$$

$$u_d = U(\rho) \tag{8.3}$$

Global route choice

The walking direction $\vec{\gamma}_d$ is determined based on the combination of the global and local route choice behaviour of pedestrians. In this study, the global route choice is determined by means of a so-called value function that represents the minimum cost a class of pedestrians experiences while moving towards a destination, the optimum direction ϕ_d towards their destination is computed as the direction with the steepest descent (Eq. 8.4) (Hoogendoorn & Bovy, 2004). The value function balances the distance to the destination with the disutility of being near objects. One is referred to Hoogendoorn & Bovy (2004) for more details on the computation of the global route choice component.

$$\vec{\gamma}_d^{global} = -\frac{\nabla \phi_d}{\| \nabla \phi_d \|} \tag{8.4}$$

The global route choice $\vec{\gamma}_d^{global}$ is not dependent on the traffic state. Consequently, if only the global route choice is taken into account, all pedestrians follow their shortest path and will rather wait in line than stray from their preferred path. This might render strange situations in which free-flow and severe congestion exists side-by-side. The MDW model has a local route choice component, to remedy this issue.

Local route choice

Hoogendoorn et al. (2014) and Hoogendoorn et al. (2015) have introduced two distinct local route choice components, namely crowdedness and delay. In Hoogendoorn et al. (2014) the impact of spatially distinct density conditions on the local route choice, and hence flow direction, are considered. The local costs for a pedestrian of class d are assumed to be due to the tendency to avoid high density areas. The values of β_δ can be interpreted as weights that a pedestrian of class d attaches to densities caused by its own ($\delta = d$) and other classes ($\delta \neq d$).

$$\vec{\gamma}_d^{crowd} = \beta_{\delta=d} \frac{\nabla \rho_{\delta=d}}{\| \nabla \rho_{\delta=d} \|} + \beta_{\delta \neq d} \frac{\nabla \rho_{\delta \neq d}}{\| \nabla \rho_{\delta \neq d} \|} \tag{8.5}$$

In Hoogendoorn et al. (2015) also the local delay, which is caused by the reduction of the walking speeds due to high densities is incorporated in the local route choice decision (see eq. 8.6). In this formulation $U_d(0)$ represents the free flow speed and $U_d(\rho)$ the absolute speed adopted by pedestrians of class d under the influence of effective density ρ.

$$\vec{\gamma}_d^{delay} = -1 \cdot \left(\frac{1}{U_d(\sum_d \rho_d)} - \frac{1}{U_d(0)} \right) dt \tag{8.6}$$

The influence of the crowdedness and delay are accordingly added, rendering the local route choice of class d.

$$\vec{\beta}_d^{local} = -1 \cdot \left(\beta_d^{crowd} \frac{\vec{\gamma}_d^{crowd}}{\|\vec{\gamma}_d^{crowd}\|} + \beta_d^{delay} \frac{\vec{\gamma}_d^{delay}}{\|\vec{\gamma}_d^{delay}\|} \right) \tag{8.7}$$

Combining global and local route choice

This leads to the following route choice model:

$$\vec{\beta}_d = -1\left(\beta_d^{global}\cdot\vec{\gamma}_d^{global} + \beta_d^{local}\frac{\vec{\gamma}_d^{local}}{\|\vec{\gamma}_d^{local}\|}\right) \tag{8.8}$$

where β_d^{global} and β_d^{local} represent the influence of the global and local route choice components on the final route choice. Dissimilar to Hoogendoorn et al. (2015), the global and local route choice components are first transformed into unit-vectors before addition. As a consequence, the weight factors always have the same effect on the pedestrian flow, irrespective of the geometry and size of the infrastructure. Furthermore, the interaction with obstacles, such as walls, is standardized.

In order to compute the solution of equation 8.1 a numerical scheme is implemented. By means of a Godunov scheme the actual flow of pedestrians over the cell boundaries is computed. A rectangular grid is adopted. Generally, a Godunov-scheme is solved using a simple forward Euler method(Wageningen-Kessels et al., 2015). However, within a pedestrian movement base case a dominant flow direction is not necessarily present. Therefore, the forward scheme cannot be applied to the cells, but instead has to be applied to each of the cell boundaries. This creates the possibility that a rectangular cell has inflows over all four boundaries (local minimum) or outflow over all four boundaries (local maximum) or any combination thereof, provided that the conservation of mass is adhered to.

8.2 Sensitivity analysis of the MDW model

Hoogendoorn et al. (2014) and Hoogendoorn et al. (2015) have reproduced some crowd movement phenomena qualitatively. However, since the model has never been calibrated, a sensitivity analysis and a thorough calibration are necessary before assessing the model's capabilities. In this section the sensitivity analysis is performed, which develops insights with respect to the manner in which the key parameters of this model influence the predicted crowd dynamics. In this analysis the most generic version of the model is used, namely the MDW model proposed by Hoogendoorn et al. (2015).

First, the methodology and selection of the parameters is described in section 8.2.1. Accordingly, the influence of the most essential parameters is determined. That is, these sections determine the impact of the density (section 8.2.2), the delay (section 8.2.3), and the balance between the density and the delay components in the local route choice (section 8.2.4). Afterwards, some conclusions are mentioned in section 8.2.5 with respect to which of the two descriptions of the MDW model should be used in the calibration process.

8.2.1 Methodology of sensitivity analysis

In the sensitivity analysis the impact of the parameter values of the MDW model proposed by Hoogendoorn et al. (2015) on the predicted spatial distribution of the density is assessed. First, this section mentions the performance indicators (or error measures) that are used to determine the goodness of the fit. Subsequently, several the walking infrastructure is detailed. Accordingly, the characteristics of the pedestrians are mentioned. The last part of this section specifies the studied parameter settings.

Performance indicators

As mentioned before, the aim of this chapter is to determine whether the MDW model can predict the walking dynamics of pedestrians at large-scale events realistically. This is considered to be only possible if the model can realistically predict most crowd movement phenomena identified earlier in this thesis. This sensitivity analysis tests whether the MDW model is indeed capable of predicting the mentioned crowd movement phenomena.

At this moment, the MDW model cannot predict the outcome of physical contact between particles. Therefore, it is expected that the MDW model can not realistically simulate very high density situations (approx. $\rho \geq 3\ P/m^2$). As a result, several crowd movement phenomena are not expected to be predicted by the model, such as crowd turbulence and clogging.

However, these very high density situations rarely occur and the main focus of this thesis is on moving crowds, it is still valuable to assess the MDW model with respect to low and medium density movements. Corresponding to the sensitivity analysis methodology presented in chapter 7, the sensitivity of the prediction of the walking dynamics with respect to the parameters of the MDW model is determined based on the lists of crowd movement phenomena described in chapter 5. In this sensitivity analysis special attention is paid to the formation of lanes in bi-directional and stripes in intersecting movement base cases and the specific dispersion patterns that occur during entering and corner movement base cases. The existence of these phenomena is ascertained by means of the development of the spatial distribution of the density over time.

Movement base cases and infrastructure lay-out

Similar to the sensitivity analysis of Nomad in chapter 7, the following specific movement base cases have been adopted in order to assess the sensitivity of the MDW model:

- *Uni-directional - Short bottleneck*, where one class of pedestrians is generated on the left, walks through a bottleneck of limited size (4 m wide, 0.20 m long) and exits on the right. This scenario assesses the development of a funnel-shaped density distribution.
- *Uni-directional - Corner*, where one class of pedestrians is generated on the left and exits at the top after making a sharp 90 degree turn. This scenario illustrates the influence of local route choice on the traffic state at the upstream inside of the corner.
- *Bi-directional - Straight*, where two classes of pedestrians are generated, one from left to right and one from right to left. This scenario provides insights into the capabilities of the MDW model to predict lane-formation. The distribution over the directions is 50-50.

Table 8.1: Model parameters of the MDW model and their function

Model parameters	Function
$\beta_{\delta=d}$ $\beta_{\delta\neq d}$	Influence of the density gradient of the current pedestrian class Influence of the density gradient of the other pedestrian class
β_d^{crowd} β_d^{delay}	Influence of the density Influence of the delay
β_d^{global} β_d^{local}	Influence of the global route choice component Influence of the local route choice component

- *Intersecting flow scenario* - 90° *degrees*, where two classes of pedestrians are generated, one from left to right and one from top to bottom. This scenario produces insights into the occurrence of stripe-formation.

In line with the literature, the uni-directional entering and exiting movement base cases are studied jointly by means of a uni-directional short bottleneck flow situation.

Pedestrian characteristics

The MDW model uses a fundamental diagram to estimate the impact of density on the decrease of the walking speed u_d. In this study a linear speed-density relation (eq. 8.9) is assumed to test the parameter settings of the MDW model.

$$U(\rho_d) = v_0 \cdot \left(1 - \frac{\sum_d \rho_d}{\rho_{d_{jam}}}\right) = 1.34 \cdot \left(1 - \frac{\sum_d \rho_d}{5.4}\right) \tag{8.9}$$

This relation has been chosen for its simplicity. The author is fully aware that other relations have been put forward in literature by among others Weidmann (1993). This choice might lead to the under and/or overestimation of the walking velocity depending on the density regime. However, since no generic fundamental diagram could be identified in the empirical studies presented in chapter 5, the adoption of any other fundamental diagrams (among others Weidmann's fundamental diagram) would cause a similar problem. In this dissertation the sensitivity of the results with respect to the fundamental diagram is not tested.

Table 8.2: Tested parameter values of the MDW model

Model parameter	Range
$\beta_{\delta=d}/\beta_{\delta\neq d}$	0.0 - 0.2 - 0.4 - 0.6 - 0.8 - 1.0
$\beta_d^{local}/\beta_d^{global}$	0.0 - 0.2 - 0.4 - 0.6 - 0.8 - 1.0
$\beta_d^{crowd}/\beta_d^{delay}$	0.0 - 0.2 - 0.4 - 0.6 - 0.8 - 1.0 - 1.25 - 1.67 - 2.5 - 5

In the sensitivity test several demand levels are used. In the remainder the results are depicted for a demand of $q_d = 1P/m/s$, since this demand level best illustrates the issues related to the sensitivity of the model. In order to limit the degrees of freedom in this study, the demand between flows is always equally divided.

Model parameters

The mathematical description of the MDW model mentions six parameters which influence the flow of pedestrians (table 8.1). These parameters appear in two pairs. β_d^{global} and β_d^{local} determine the relative weight of the global and local route choice components, $\beta_{\delta=d}$ and $\beta_{\delta\neq d}$ determine the balance between the influence of the density gradient of the own ($\delta = d$) and other pedestrian classes ($\delta \neq d$) and β_d^{crowd} and β_d^{delay} the relative weight of the gradients of the delay and density in the local route choice components.

Given that all six weights are imposed on unit-vectors, only the relative weight of these β's is accounted for. Furthermore, the author assumes that pedestrians display goal-oriented behaviour. That is, β_d^{global} is assumed to be always larger or equal to β_d^{local} in order to retain movement towards the destination. Moreover, the influence of the density gradient of the other class is assumed to be larger or equal to the density gradient of the own pedestrian class. Since pedestrians have the tendency to follow others who walk in a similar direction, the author also assumes that they are more attracted towards their own class than towards another class of pedestrians, i.e. $\beta_{\delta=d} \leq \beta_{\delta\neq d}$.

The sensitivity of the MDW model's predictions is tested with respect to the parameter settings mentioned in table 8.2. The model as proposed by Hoogendoorn et al. (2015) is used, since this model simplifies into the MDW model proposed in Hoogendoorn et al. (2014) when β_d^{delay} is set to 0 and β_d^{crowd} is set to 1.

8.2.2 Impact of density gradient on walking dynamics

The impact of the density on the movement dynamics predicted by the simulation is regulated through the first and second parameters of table 8.2, namely the ratios $\beta_d^{local}/\beta_d^{global}$ and $\beta_{\delta=d}/\beta_{\delta\neq d}$. The latter ratio is only influential in cases where more than one class of pedestrians is present. Consequently, only for the bi-directional and intersecting flow situations the influence of the second ratio is studied.

Impact of the balance between the local and global route choice

The impact of the ratio $\beta_d^{local}/\beta_d^{global}$ on the predicted movement dynamics is visualised in figure 8.1. The figure illustrates that in the uni-directional movement base cases the flow is distributed more equally over the infrastructure when the ratio $\beta_d^{local}/\beta_d^{global}$ increases. The influence of the ratio $\beta_{\delta=d}/\beta_{\delta\neq d}$ is not relevant in these two cases, since only one class of pedestrians exists. As a result, the simulation predicts lower average densities and a better use of the capacity of the infrastructure for higher ratios.

Besides that, in case of a corner movement base case, flow is increasingly directed away from the shortest path through the infrastructure with an increase of the ratio $\beta_d^{local}/\beta_d^{global}$. Consequently, the high density region located at the upstream inside of the corner becomes less prominent.

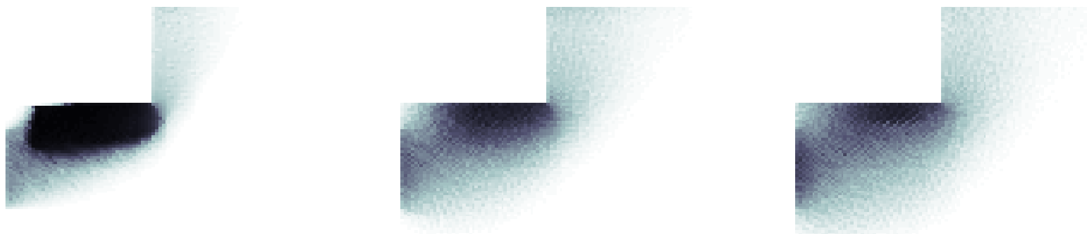

(a) $\beta_d^{local}/\beta_d^{global} = 0.2$ **(b)** $\beta_d^{local}/\beta_d^{global} = 0.6$ **(c)** $\beta_d^{local}/\beta_d^{global} = 1.0$

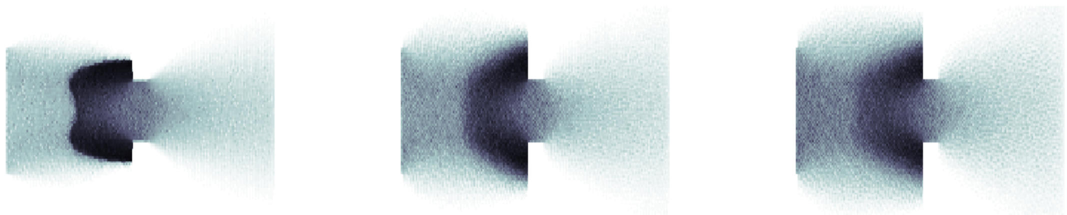

(d) $\beta_d^{local}/\beta_d^{global} = 0.2$ **(e)** $\beta_d^{local}/\beta_d^{global} = 0.6$ **(f)** $\beta_d^{local}/\beta_d^{global} = 1.0$

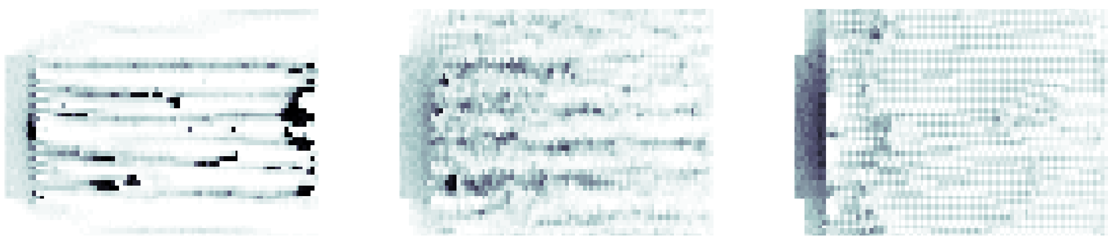

(g) $\beta_d^{local}/\beta_d^{global} = 0.2$ **(h)** $\beta_d^{local}/\beta_d^{global} = 0.6$ **(i)** $\beta_d^{local}/\beta_d^{global} = 1.0$

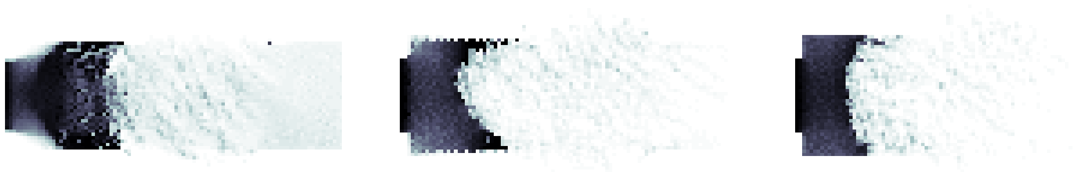

(j) $\beta_d^{local}/\beta_d^{global} = 0.2$ **(k)** $\beta_d^{local}/\beta_d^{global} = 0.6$ **(l)** $\beta_d^{local}/\beta_d^{global} = 1.0$

Figure 8.1: Influence of ratio $\beta_d^{local}/\beta_d^{global}$ on the traffic state for distinct movement base cases, where $\beta_d^{delay} = 0$ and $\beta_d^{crowd} = 1$ and the total demand of $q = 1$ $P/m/s$. The colour displays the density of one class of pedestrians (white = 0 P/m^2, black = 5.4 P/m^2)

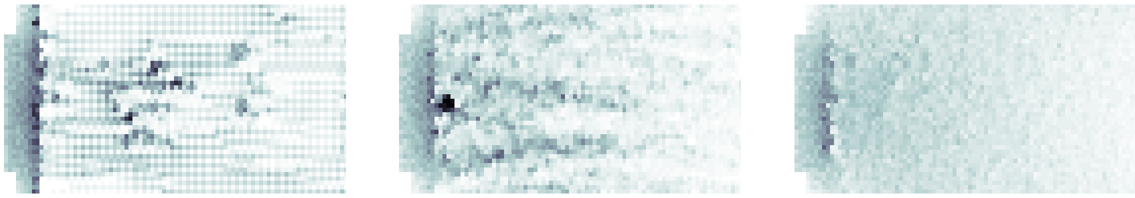

(a) $\beta_{\delta=d}/\beta_{\delta\neq d} = 0.4$ (b) $\beta_{\delta=d}/\beta_{\delta\neq d} = 0.6$ (c) $\beta_{\delta=d}/\beta_{\delta\neq d} = 0.8$

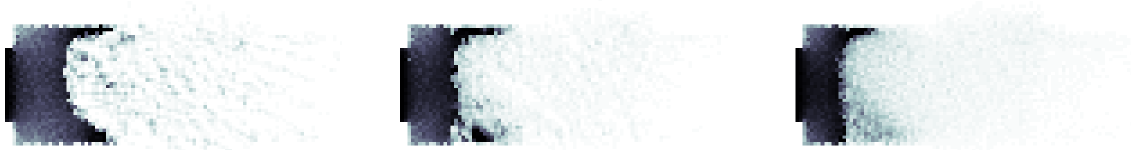

(d) $\beta_{\delta=d}/\beta_{\delta\neq d} = 0.4$ (e) $\beta_{\delta=d}/\beta_{\delta\neq d} = 0.6$ (f) $\beta_{\delta=d}/\beta_{\delta\neq d} = 0.8$

Figure 8.2: Influence of ratio $\beta_{\delta=d}/\beta_{\delta\neq d}$ on the traffic state for distinct movement base cases, where the $\beta_d^{delay} = 0$ and $\beta_d^{crowd} = 1$ and the total demand of $1\ P/m/s$. The colour displays the density of one class of pedestrians (white = $0\ P/m^2$, black = $5.4\ P/m^2$)

Also with respect to movement base cases in which more than one class of pedestrians are present (i.e. bi-directional and intersecting), the ratio $\beta_d^{local}/\beta_d^{global}$ is influencing the predicted crowd dynamics severely. For a fixed ratio of $\beta_{\delta=d}/\beta_{\delta\neq d}$ lane and stripe formation is only encountered for some middle range values of $\beta_d^{local}/\beta_d^{global}$ in case of bi-directional and intersecting flow situations. In case of high ($\beta_d^{local}/\beta_d^{global} \approx 1.0$), as well as low ($\beta_d^{local}/\beta_d^{global} \approx 0.0$), $\beta_d^{local}/\beta_d^{global}$ ratios no self-organisation patterns develop. Moreover, the shape of the lane and strip formation changes. That is, the lanes become less dominant for increasing values of $\beta_d^{local}/\beta_d^{global}$.

Impact of the balance between the own and other pedestrians classes

Besides the impact of the ratio $\beta_d^{local}/\beta_d^{global}$, the balance between the influence of the density of the own and other class is an essential model parameter. Figure 8.2 provides an overview of the simulation results. Depending on the ratio $\beta_{\delta=d}/\beta_{\delta\neq d}$ self-organisation patterns develop or not. While figures 8.2.a,b,c,e,f and g display low and high density regions per pedestrian class, figures 8.2.d, and h depict a smooth density distribution at the middle of the infrastructure. The self-organisation patterns are found to be best portrayed when the ratio of the density gradients of the distinct classes of pedestrians is relatively high (i.e. $0.4 \leq \beta_{\delta=d}/\beta_{\delta\neq d} \leq 1.0$). This range is still fairly broad. However, based on a qualitative analysis of the self-organisation patterns only it is difficult to determine a more precise range of values.

8.2.3 Impact of delay on the movement dynamics of the crowd

The influence of the delay on the crowd movement dynamics is the main difference between the two formulations of the MDW model. Therefore, this part of the sensitivity analysis influences the choice for one of the two formulations of the model.

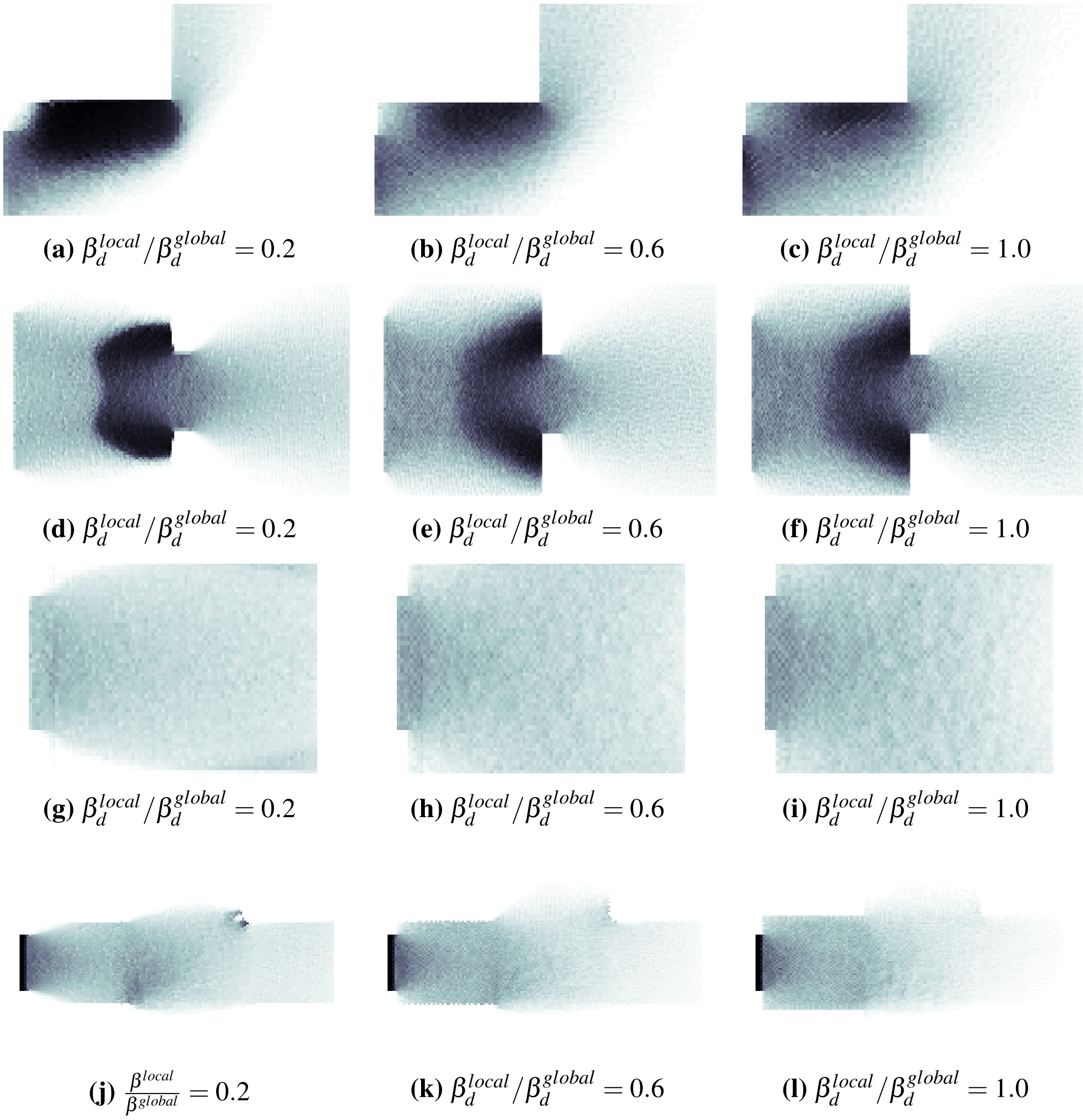

(a) $\beta_d^{local}/\beta_d^{global} = 0.2$ (b) $\beta_d^{local}/\beta_d^{global} = 0.6$ (c) $\beta_d^{local}/\beta_d^{global} = 1.0$

(d) $\beta_d^{local}/\beta_d^{global} = 0.2$ (e) $\beta_d^{local}/\beta_d^{global} = 0.6$ (f) $\beta_d^{local}/\beta_d^{global} = 1.0$

(g) $\beta_d^{local}/\beta_d^{global} = 0.2$ (h) $\beta_d^{local}/\beta_d^{global} = 0.6$ (i) $\beta_d^{local}/\beta_d^{global} = 1.0$

(j) $\frac{\beta^{local}}{\beta^{global}} = 0.2$ (k) $\beta_d^{local}/\beta_d^{global} = 0.6$ (l) $\beta_d^{local}/\beta_d^{global} = 1.0$

Figure 8.3: Influence of the delay on the traffic state for distinct movement base cases, where the $\beta^{delay} = 1$ and $\beta^{crowd} = 0$, and a demand of $q = 1\ P/m/s$

Since in this test only the influence of the delay is focussed upon, the influence of the crowdedness (β_d^{crowd}) is set to 0 in this test. As a result, an increase of the impact of the local route choice behaviour on the aggregate movement dynamics via $\beta_d^{local}/\beta_d^{global}$ is directly related to a similar increase of the impact of the delay on the movement behaviour.

Figure 8.3a-d illustrates that the dispersion of the crowd upstream of the corner is not severely impacted by the increasing impact of the delay. However, an increase in the influence of the delay does cause an increase of the dispersion at the corner and downstream of the corner. The crowd distributes more evenly across the entire width of the corridor, and as a result the crowd becomes less dense. Due to the improved efficiency of the crowd's movements, the high density region just upstream of the bottleneck disappears completely.

The results for the bottleneck movement base case (figure 8.3e-h) show that without local route choice, two queues are found upstream of the bottleneck. Even a slight influence of the local route choice causes these two queues to change into a funnel shaped congestion zone. However, if the influence of the local route choice is increased further, this high density region does not change shape any more.

The simulation results, furthermore, clearly illustrate that an increase in the influence of the delay on the movement behaviour induces an increase in the dissipation of pedestrians downstream of the bottleneck. In some specific cases, a funnel shaped bottleneck flow arises. In most cases however, the flow touches the upstream wall in which the bottleneck is located. That is, the high density region changes from a funnel to a semi-circle when the influence of the delay increases. Empirical research performed by for example Daamen & Hoogendoorn (2010a) did not establish the formation of a high density region with this shape.

Figures 8.3i-p depict the impact of delay on the movement dynamics of crowds in bi-directional and intersecting situations. The figures illustrate that the impact of delay does not alter the distribution of pedestrians over space and time. In both cases, the overall density and walking velocity only slightly increase when the impact of the delay increases. Additionally, no formation of lanes or stripes is seen in any of the simulations.

8.2.4 Impact of combination delay and crowdedness on the movement dynamics of the crowds

The interplay between the influence of the crowdedness and the influence of the delay on the local route choice is analysed in this section. In this section the results are displayed for $\beta_d^{local}/\beta_d^{global} = 0.7$, while the $\beta_d^{delay}/\beta_d^{crowd}$ ratio is varied. Several other $\beta_d^{local}/\beta_d^{global}$ ratios were tested, which produced similar results.

The influence of the combination of delay and crowdedness on the movement dynamics of the crowd is visualised in figures 8.4a-f. As one can see, the traffic states do not differ at all between distinct realisations of a uni-directional flow situation even though the $\beta_d^{delay}/\beta_d^{crowd}$ ratio differs severely. A closer look at the results reveals that the gradient fields of the delay

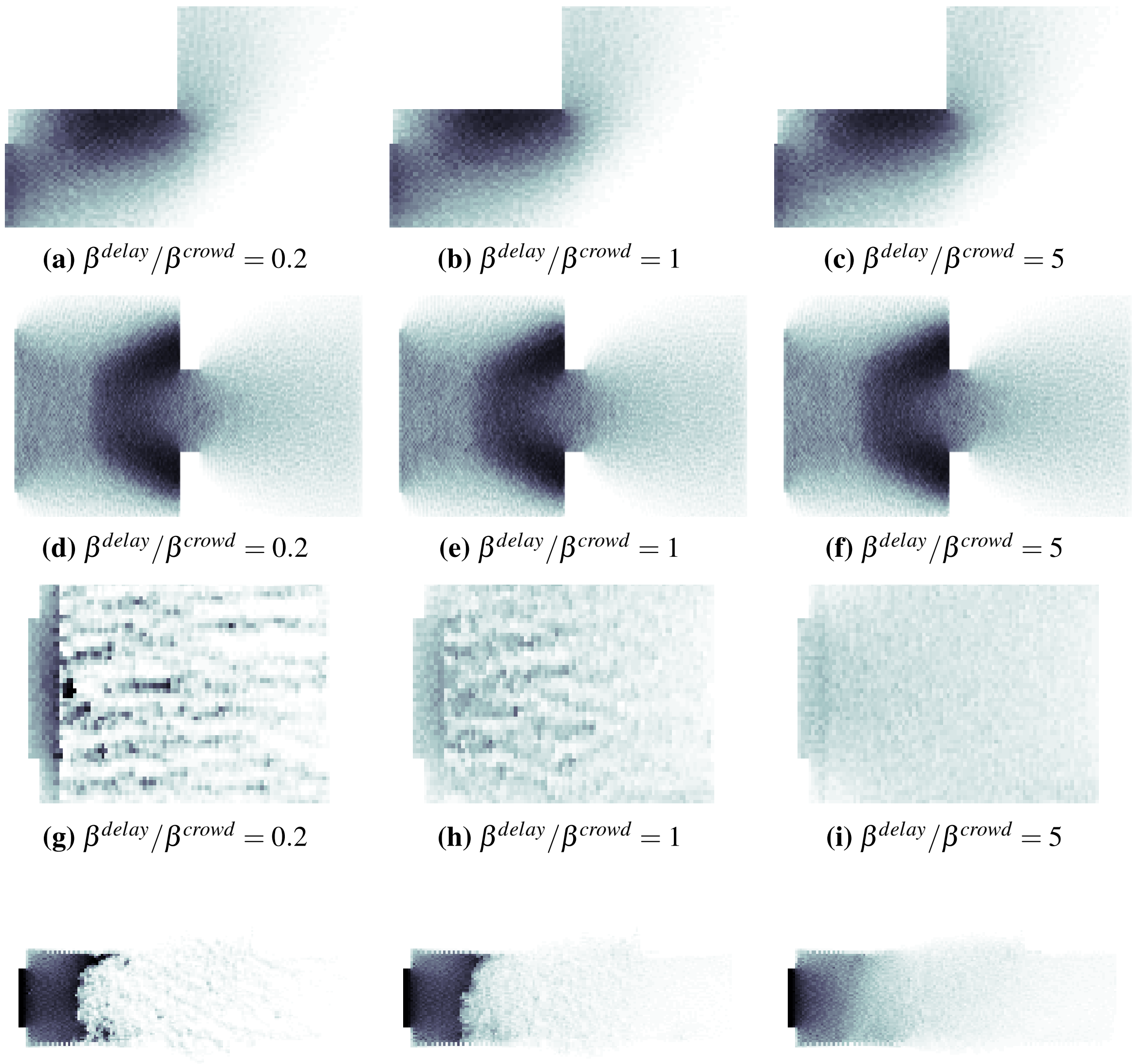

(a) $\beta^{delay}/\beta^{crowd} = 0.2$ (b) $\beta^{delay}/\beta^{crowd} = 1$ (c) $\beta^{delay}/\beta^{crowd} = 5$

(d) $\beta^{delay}/\beta^{crowd} = 0.2$ (e) $\beta^{delay}/\beta^{crowd} = 1$ (f) $\beta^{delay}/\beta^{crowd} = 5$

(g) $\beta^{delay}/\beta^{crowd} = 0.2$ (h) $\beta^{delay}/\beta^{crowd} = 1$ (i) $\beta^{delay}/\beta^{crowd} = 5$

(j) $\beta^{delay}/\beta^{crowd} = 0.2$ (k) $\beta^{delay}/\beta^{crowd} = 1$ (l) $\beta^{delay}/\beta^{crowd} = 5$

Figure 8.4: Influence of the ratio $\beta_d^{delay}/\beta_d^{crowd}$ on the traffic state for distinct movement base cases, where $\beta_{\delta=d}/\beta_{\delta\neq d} = 0.5$ and a demand of $q = 1\ P/m/s$

and density are equal. As a result, the gradient field does not change due to the change in the $\beta_d^{delay}/\beta_d^{crowd}$ ratio. Therefore, the traffic state does not develop differently.

In the bi-directional flow situation differences in the traffic state do arise, see figure 8.4g-i. As one can see, in the medium high density case blockage occurs. However, only in the case where the effects of the density gradient is significantly accounted for, lane formation remains visible after 90 seconds. As such, it is concluded that lane formation is due to the influence of the gradient of the own and other group.

Figure 8.4j-l displays the effect of the combination of delay and density gradients on the movement dynamics in case of an intersecting flow situation. It can be seen that especially when the crowdedness is dominantly present in the local route choice, stripe formation arises. While the combination of both crowdedness and delay gradients results in blockage. This is assumed to be due to the non-linear effect of the delay which causes the stripe formation to become unstable. When the impact of the delay is dominant within the local route choice, both groups are scattered over the entire infrastructure. As a result, blockage does not occur any more, nor does the stripe formation.

8.2.5 Conclusions of the sensitivity analysis

This section has provided insights into the impact of the combination of delay and density gradients on the simulation results predicted by the MDW model proposed by Hoogendoorn et al. (2014) and Hoogendoorn et al. (2015). By means of three distinct tests the impact of the main parameters of the model on the predicted traffic state has been analysed.

Firstly, the influence of the reaction on the density generated by the own and other classes of pedestrians was studied. For certain combinations of $\beta_{\delta=d}$ and $\beta_{\delta\neq d}$ self-organisation behaviour is found, while for others no self-organisation or unstable crowd movements develop.

Accordingly, the influence of only the delay and the density gradients on the crowd movement dynamics has been established. For uni-directional flows it was found that the density gradient and the delay impact the walking behaviour in a similar manner. That is, the dissipation of the crowd increases when the effect of the delay becomes increasingly dominant. The incorporation of crowdedness or delay in the local route choice formulations forces pedestrians to deviate from their global optimal path. For bi-directional and intersecting movement base cases it was established that lane/stripe formation does not arise when only the delay is taken into account, while these phenomena do arise under certain conditions when the density gradient is significantly accounted for.

Lastly, the effect of the interplay of crowdedness and delay on the prediction of the movement dynamics was studied. This test established that in case of uni-directional movement base case the traffic state is scarcely impacted by the $\beta_d^{delay}/\beta_d^{crowd}$ ratio since the local route choice gradient is barely impacted. In case of bi-directional and intersecting movement base cases, the combination of delay and crowdedness generally renders undesirable behaviour.

Summarising the findings presented above, it is found that the ratios $\beta_d^{local}/\beta_d^{global}$ and $\beta_{\delta=d}/\beta_{\delta\neq d}$ are important in the correct display of crowd movement dynamics, while the ratio $\beta_d^{delay}/\beta_d^{crowd}$ is of no importance. This finding implies that pedestrians react more strongly on the presence and walking dynamics of other pedestrians than on the expected delay.

Because the model presented by Hoogendoorn et al. (2014) includes the four dominant parameters and does not take into account the delay, it is concluded that the first description of the MDW model represents the walking dynamics of pedestrians in crowds at large-scale events the best. Therefore, this version of the MDW model is calibrated and assessed in the remainder of this chapter.

8.3 Calibration of the MDW model

The previous section has determined the qualitative influence of the main parameters of the MDW model on the predicted traffic state. However, whether the MDW model can also correctly predict the movement dynamics of crowds at large-scale events quantitatively is not yet determined. Before assessing the capabilities of the MDW model, fist the model is calibrated specifically for this type of movement dynamics.

The calibration methodology is described in section 8.3.1. Accordingly, the calibration results for five distinct movement base cases are mentioned in subsections 8.3.2-8.3.6. Afterwards, a calibration is performed based on the aggregate results of all five movement base cases in subsection 8.3.7.

8.3.1 Calibration methodology

To the author's knowledge only one study has attempted to calibrate a macroscopic pedestrian simulation model (Hänseler et al. (2016)). The travel time distribution was used to determine the optimal parameter set. However, in the MDW model the "first in first out" assumption, which is necessary in order to use the travel time distribution in the calibration procedure, cannot be guaranteed due to the uneven spatial distribution of the density and velocity. Consequently, in this chapter different metrics are proposed to calibrate macroscopic pedestrian simulation models. Below the details of the calibration procedure and the metrics are mentioned. In the following subsections the search space, the search method, the used data sets, the infrastructure design, and the objective function are elaborated upon.

Search space & search method

The previous section has established that only the ratios $\beta_d^{local}/\beta_d^{global}$ and $\beta_{\delta=d}/\beta_{\delta\neq d}$ need to be calibrated, since the effect of the delay is subordinate to these two ratios. Goal-oriented behaviour is assumed in this study. That is, the predicted behaviour becomes unrealistic if $\beta_d^{local}/\beta_d^{global} > 1$ or $\beta_{\delta=d}/\beta_{\delta\neq d} > 1$.

Consequently, the search space then can be limited as follows:

- $0 \leq \beta_d^{local}/\beta_d^{global} \leq 1$
- $0 \leq \beta_{\delta=d}/\beta_{\delta\neq d} \leq 1$

Eventhough the sensitivity analysis indicated that higher bounds on the $\beta_{\delta=d}/\beta_{\delta\neq d}$ are possible, the author has decided against limiting the search space in order to produce insights into the new calibration metrics and objective function.

As no previous calibration of the MDW model for pedestrian walking dynamics exists, it is unknown whether the search space contains multiple optimal parameter settings. Moreover, this is the first time that this type of model is calibrated. Therefore, we do not only want to get a best parameter set, but also understand the shape of the search space. Consequently, a grid search is performed instead of an optimisation scheme.

In order to limit the amount of computations a step size of 0.02 is adopted. Since for each movement base case 9 distinct sequences are simulated, this step size results in approximately 23,000 simulations per movement base case.

Empirical data sets

The data sets used to calibrate the MDW model are similar to the ones used during the calibration of Nomad. That is, the data sets of Wijchen, Lent, Queensday Amsterdam, the Rotterdam Marathon and Liberation day in Wageningen are used in the calibration procedure. Moreover, half of the data sets is used to calibrate the model and half of the data sets is used to assess the model. For the exact division of the data sets and their main characteristics the reader is referred to table B.1 in the appendix.

The five case studies are implemented similarly to the description mentioned in section 7.2 with the exception of some minor details, namely:

- *Size of the gridcell* - Rectangular cells of 0.2 by 0.2 m has been adopted.
- *Implementation of walls behind exits* - The current implementation of the MDW model needs an enclosed space. As such, also behind the entrances and exits walls have been placed.
- *Entrance area* - The pedestrians are generated within a specified area instead of over a line. The simulated flow at the entrances is similar to the flow in the calibration and assessment of Nomad.
- *Fundamental diagram* - A linear fundamental diagram with a free-flow speed of 1.34 m/s and a jam density of 5.4 P/m^2 is used in all cases.

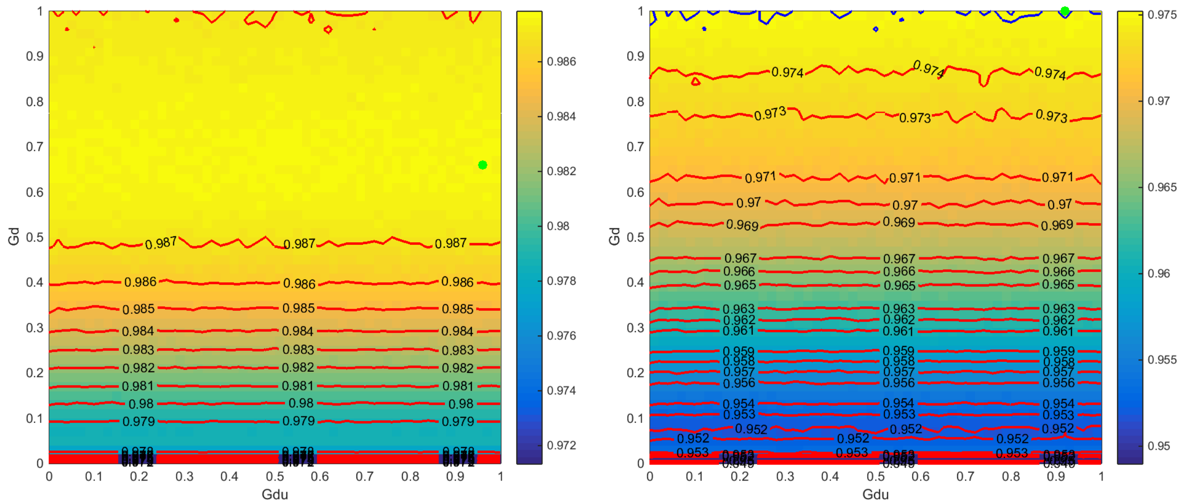

(a) Weighting scheme 1

(b) Weighting scheme 2

Figure 8.5: Contour plot of the solution space for weighting schemes 1 and 2 of the uni-dir. straight movement base case, where $Gd = \beta_d^{local}/\beta_d^{global}$ and $Gdu = \beta_{\delta=d}/\beta_{\delta\neq d}$

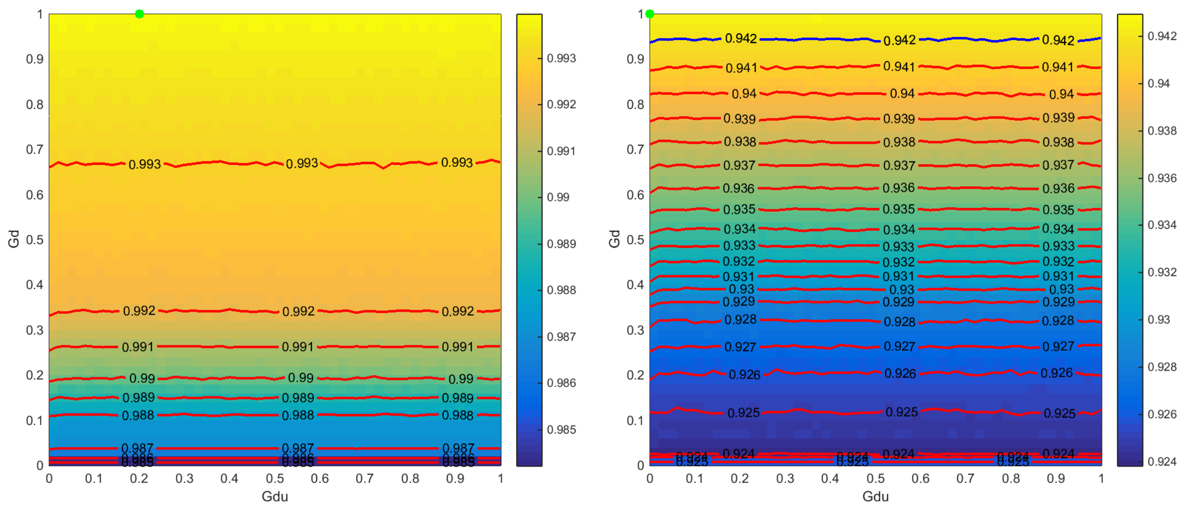

(a) Weighting scheme 1

(b) Weighting scheme 2

Figure 8.6: Contour plot of the solution space for schemes 1 and 2 of a the uni-dir. entering movement base case, where $Gd = \beta_d^{local}/\beta_d^{global}$ and $Gdu = \beta_{\delta=d}/\beta_{\delta\neq d}$

Table 8.3: Calibration of the MDW model for a uni-directional straight movement base case

Weighting scheme	Weight of ρ	Weight of v	GOF	$\frac{\beta_d^{local}}{\beta_d^{global}}$
Density	1	0	0.988	0.66
Velocity	0	1	0.975	1.00
Density&Velocity	0.5	0.5	0.981	0.96

Objective function

In table 7.1 several microscopic and macroscopic characteristics that are used to describe the pedestrian walking behaviour have been mentioned. Since the MDW model produces results at a macroscopic level, only the macroscopic characteristics can be used in the calibration process. As such, only the spatial distribution of velocity and density are taken into account in the objective function.

$$GOF(\frac{\beta_d^{local}}{\beta_d^{global}}, \frac{\beta_{\delta=d}}{\beta_{\delta\neq d}}) = \sum_i \sum_n W_n \cdot \{1 - \alpha_n \cdot SE_{n,i}(\frac{\beta_d^{local}}{\beta_d^{global}}, \frac{\beta_{\delta=d}}{\beta_{\delta\neq d}})\} \tag{8.10}$$

$$\alpha_{i,n} = \frac{1}{\max(SE_{i,n}) - \min(SE_{i,n})} = \frac{1}{\max(SE_{i,n})} \tag{8.11}$$

$$SE_{i,n}(\frac{\beta_d^{local}}{\beta_d^{global}}, \frac{\beta_{\delta=d}}{\beta_{\delta\neq d}}) = \sum_m SE_{i,n,m}(\frac{\beta_d^{local}}{\beta_d^{global}}, \frac{\beta_{\delta=d}}{\beta_{\delta\neq d}}) \tag{8.12}$$

where W_n indicates the relative weight of a characteristic n in relation to the other metrics taken into account in the calibration procedure, $SE_{i,n,m}(\frac{\beta_d^{local}}{\beta_d^{global}}, \frac{\beta_{\delta=d}}{\beta_{\delta\neq d}})$ indicates the sum of squares of the residuals as one of the characteristics taken into account in the objective function for a certain set of parameters $(\frac{\beta_d^{local}}{\beta_d^{global}}, \frac{\beta_{\delta=d}}{\beta_{\delta\neq d}})$ and i,m,n respectively the case, the sequence, and the characteristic. The capitals I,M,N represent the number of cases, sequences and characteristics taken into account in the computation. As a result of the formulation proposed in equation 8.10, $GOF(\frac{\beta_d^{local}}{\beta_d^{global}}, \frac{\beta_{\delta=d}}{\beta_{\delta\neq d}}) = 1$ for parameter sets which produce the best fit of the empirical data and $GOF(\frac{\beta_d^{local}}{\beta_d^{global}}, \frac{\beta_{\delta=d}}{\beta_{\delta\neq d}}) = 0$.

8.3.2 Calibration for a uni-directional straight flow

The results of the calibration are depicted in table 8.3. Additionally, figure 8.5 depicts a contour plot of the objective function. In this plot the colour represents the goodness of fit and the contour lines represent the 5^{th} to 95^{th} percentile of the goodness of fit.

Only the fraction $\beta_d^{local}/\beta_d^{global}$ is depicted in the table since the contour plots (see fig. 8.5) illustrate that in a uni-directional situation $\beta_{\delta=d}/\beta_{\delta\neq d}$ is not influencing the predicted movement dynamics of the crowd. The table shows that the best value of $\beta_d^{local}/\beta_d^{global}$ depends on the weighting scheme. If only the spatial distribution of the density is accounted for, a lower value of $\beta_d^{local}/\beta_d^{global}$ is found than in the other two schemes in which the spatial distribution of the velocity is also taken into account. This very high value would indicate that the walking behaviour predicted by the model is not directed towards the goal/destination. However, in the second weighting scheme this value is on the boundary on the search space, which produces no information with respect to the actual value.

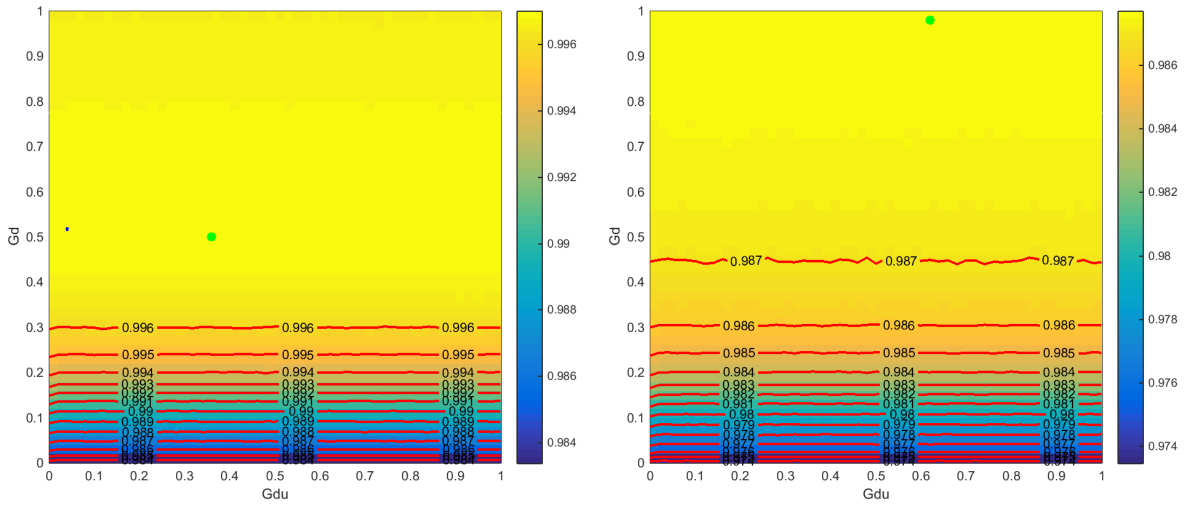

(a) Weighting scheme 1 **(b) Weighting scheme 2**

Figure 8.7: Contour plot of the solution space for weighting schemes 1 and 2 of the uni-dir. corner movement base case, where $Gd = \beta_d^{local}/\beta_d^{global}$ **and** $Gdu = \beta_{\delta=d}/\beta_{\delta\neq d}$

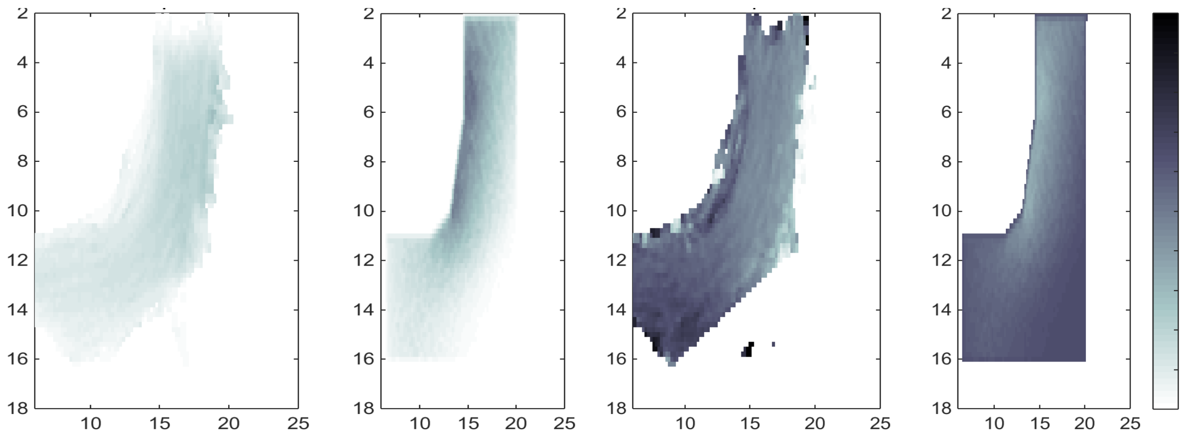

(a) Density plot $[0-5.4P/m^2]$ **(b) Velocity plot** $[0-2m/s]$

Figure 8.8: Example of density and velocity plot the uni-directional corner movement base case

Table 8.4: Calibration of the MDW model for a uni-directional entering movement base case

Weighting scheme	Weight of ρ	Weight of v	GOF	$\frac{\beta_d^{local}}{\beta_d^{global}}$
Density	1	0	0.99	1.00
Velocity	0	1	0.94	1.00
Density&Velocity	0.5	0.5	0.97	1.00

8.3.3 Calibration for a uni-directional entering flow

The results of the calibration of a uni-directional entering movement base case (see table 8.4) show similar results as the previous case, namely that in general a value of 1 is found for the fraction $\beta_d^{local}/\beta_d^{global}$ and the fraction of $\beta^{own}/\beta^{other}$ has no influence on the calibration results. However, given that the calibration result is now located on the boundary of the search space. This indicates that the optimum value of the ratio $\beta_d^{local}/\beta_d^{global}$ might be even higher than 1.0.

Besides that, the solution space of the first weighting scheme (fig. 8.6.a) illustrates that the largest part of the solution space falls within the 99th percentile of all solutions. The objective function is very flat for weighting scheme one. In case of the second weighting scheme, (fig. 8.6b) the objective function is much steeper, but the top 1 percent of the solutions still contains all β values in the range $0.95 \leq \beta_d^{local}/\beta_d^{global} \leq 1.0$.

8.3.4 Calibration for a uni-directional flow around a corner

Figure 8.7 and table 8.5 depict the calibration and validation results for the corner movement base case. In general a higher goodness of fit is found with respect to the previous movement base cases. The ratio $\beta^{own}/\beta^{other}$ is found to be of no influence, which is as expected since no other class of pedestrians is present. Moreover, the solution space is found to be very flat for the approximate region $0.4 \leq \beta_d^{local}/\beta_d^{global} \leq 0.8$ for the density weighting scheme and the region $0.7 \leq \beta_d^{local}/\beta_d^{global} \leq 1$ for the velocity weighting scheme. Consequently a plateau exists in which the *GOF* is almost indistinguishable.

In contrast to the previous two movement base cases, the $\beta_d^{local}/\beta_d^{global}$ ratio is smaller than one. Chapter 5 illustrated that pedestrians tend to walk near the inside of the corner and only fan out at the moment that the density becomes too high. For this situation to arise, in which areas exist that are not used by pedestrians, diffusion needs to be limited. This implies that the global route choice (i.e. choice for the shortest distance path) is more strongly influencing the walking dynamics of pedestrians in this movement base case.

The density and velocity plots (fig. 8.8) show that the MDW model predicts a high density and low velocity region on the downstream inside of the corner, which is not found in the empirical data. This especially occurs at the moment that the calibration procedure takes the spatial distribution of the density into account. This would suggest that a slightly shorter and more direct route is predicted than that is actually found in reality. In this case this property is not inherent to the use of the global path, as was investigated by Johansson et al. (2014), since the implementation of the local route choice can force pedestrians away from their global path. Instead, the difference between reality and the prediction might be caused by the assumption of optimal walking decisions in the MDW model and the specification of the properties of the walking dynamics that are taken into account in the decision process (i.e. only distance and delay, not comfort, energy or safety).

Table 8.5: Calibration of the MDW model for a uni-directional corner movement base case.

Weighting scheme	Weight of ρ	Weight of v	GOF	$\frac{\beta_d^{local}}{\beta_d^{global}}$
Density	1	0	0.997	0.5
Velocity	0	1	0.987	0.98
Density&Velocity	0.5	0.5	0.992	0.74

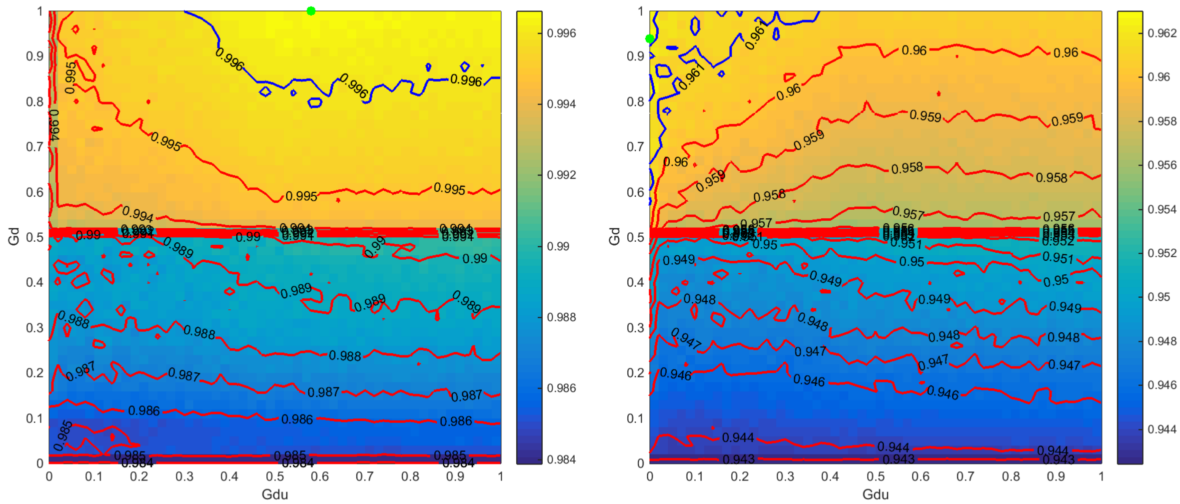

(a) Weighting scheme 1 **(b) Weighting scheme 2**

Figure 8.9: Contour plot of the solution space for weighting schemes 1 and 2 of a the bi-dir. straight movement base case, where $Gd = \beta_d^{local}/\beta_d^{global}$ and $Gdu = \beta_{\delta=d}/\beta_{\delta\neq d}$

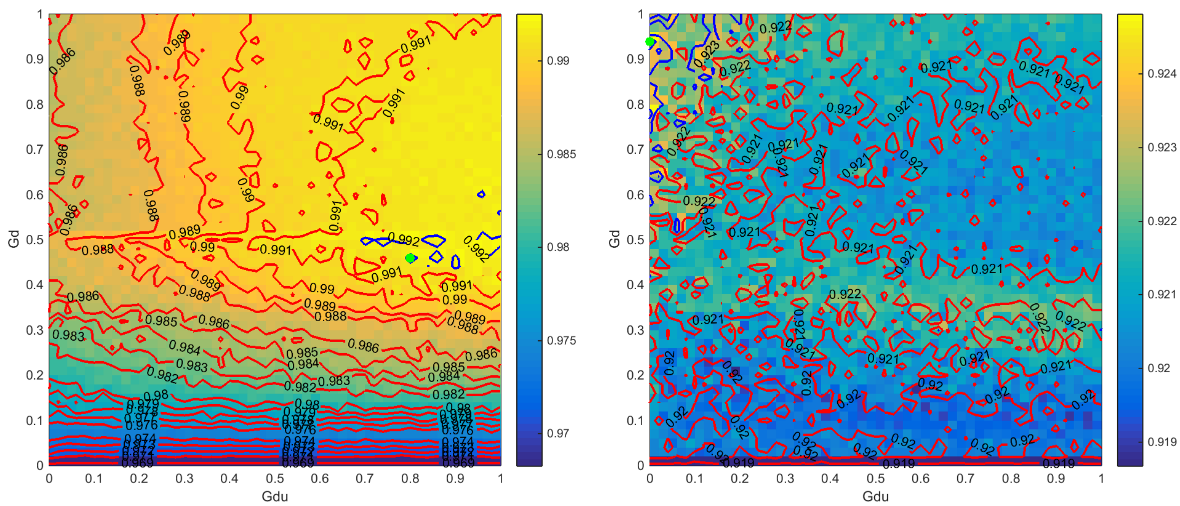

(a) Weighting scheme 1 **(b) Weighting scheme 2**

Figure 8.10: Contour plot of the solution space for weighting schemes 1 and 2 of a the intersecting movement base case, where $Gd = \beta_d^{local}/\beta_d^{global}$ and $Gdu = \beta_{\delta=d}/\beta_{\delta\neq d}$

Table 8.6: Calibration of the MDW model for a bi-directional straight movement base case

Weighting scheme	Weight of ρ	Weight of v	GOF	$\frac{\beta_d^{local}}{\beta_d^{global}}$	$\frac{\beta_{\delta=d}}{\beta_{\delta\neq d}}$
Density	1	0	0.997	1.00	0.58
Velocity	0	1	0.963	0.94	0
Density&Velocity	0.5	0.5	0.979	1.00	0.78

8.3.5 Calibration for a bi-directional Straight flows

The contour plots (fig. 8.9) illustrate that only the ratio $\beta_{\delta=d}/\beta_{\delta\neq d}$ has an influence on the goodness of fit in the bi-directional straight movement base case. If only the spatial distribution of the density is adopted in the calibration procedure a region of approximately $(0.85 \leq \beta_d^{local}/\beta_d^{global} \leq 1) \cap (0.4 \leq \beta_{\delta=d}/\beta_{\delta\neq d} \leq 1)$ exists in which the *GOF* is almost indistinguishable. In case of the second weighting scheme (only spatial distribution of the velocity) a triangular region in which the GOF is similar is found at the top left corner contour plot. When both characteristics are combined, an elongated region is found $(0.87 \leq \beta_d^{local}/\beta_d^{global} \leq 1) \cap (0.1 \leq \beta_{\delta=d}/\beta_{\delta\neq d} \leq 1)$ in which the *GOF* is almost similar.

8.3.6 Calibration for a intersecting flows

In the intersecting movement base case table 8.7 illustrates that the values of $\beta_d^{local}/\beta_d^{global}$ and $\beta_{\delta=d}/\beta_{\delta\neq d}$ differ severely depending on the adopted weighting scheme. The contour plots of this objective function (see figure 8.10) show that a medium to high $\beta_d^{local}/\beta_d^{global}$ ratio and a high $\beta_{\delta=d}/\beta_{\delta\neq d}$ ratio is needed in order to predict the spatial distribution of the density, while to predict the velocity correctly a high $\beta_d^{local}/\beta_d^{global}$ ratio and a high $\beta_{\delta=d}/\beta_{\delta\neq d}$ ratio is needed. In the case that these two objectives are combined a rectangular region of optimal parameter settings$(0.4 \leq \beta_d^{local}/\beta_d^{global} \leq 1) \cap (0.6 \leq \beta_{\delta=d}/\beta_{\delta\neq d} \leq 1)$ is found. The lack of similar patterns in the objective function for the two objectives is probably due to a mismatch of the fundamental diagrams found in the empirical findings and the fundamental diagram used during the simulation. A more in-depth discussion of this artefact is provided in section 8.4.

8.3.7 Calibration for a combination of movement base cases

In table 8.8 and figure 8.11 the results of the calibration of the MDW model for a combination of movement base cases is depicted. The results of the calibration show that the objective function with respect to the $\beta_{\delta=d}/\beta_{\delta\neq d}$ ratio is very flat. As a result, the $\beta_{\delta=d}/\beta_{\delta\neq d}$ ratio cannot be estimated using only the spatial distribution of the density and velocity as indicators when several movement base cases are used. Also with respect to the ratio $\beta_d^{local}/\beta_d^{global}$ values above approximately 0.6 result in a similar goodness of fit. The lack of specificity of the calibration result with respect to the $\beta_{\delta=d}/\beta_{\delta\neq d}$ might be due to the balancing influence of the density (high parameter estimates) and velocity (low parameter estimates) in the calibration.

Table 8.7: Calibration of the MDW model for an intersecting movement base case

Weighting scheme	Weight of ρ	Weight of v	GOF	$\frac{\beta_d^{local}}{\beta_d^{global}}$	$\frac{\beta_{\delta=d}}{\beta_{\delta\neq d}}$
Density	1	0	0.993	0.80	0.46
Velocity	0	1	0.924	0	0.94
Density&Velocity	0.5	0.5	0.956	0.98	0.45

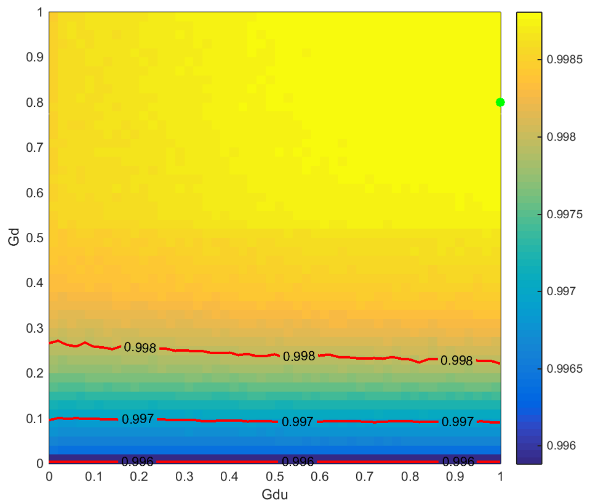

(a) Weighting scheme 1

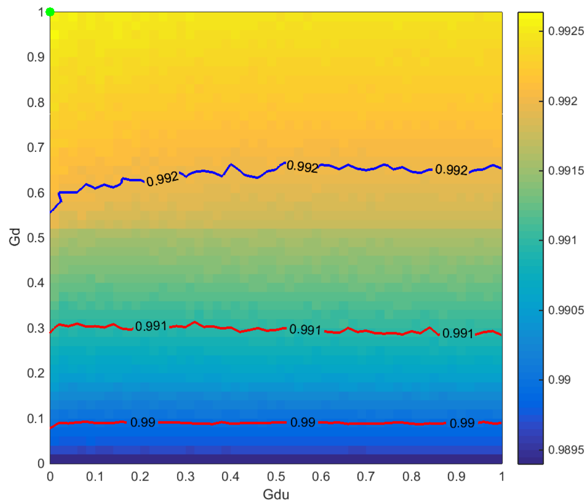

(b) Weighting scheme 2

Figure 8.11: Contour plot of the solution space for weighting schemes 1 and 2 of the combination of several movement base case, where $Gd = \beta_d^{local}/\beta_d^{global}$ and $Gdu = \beta_{\delta=d}/\beta_{\delta\neq d}$

Table 8.8: Calibration of the MDW model for several movement base cases

scheme	ρ	v	GOF	$\frac{\beta_d^{local}}{\beta_d^{global}}$	$\frac{\beta_{\delta=d}}{\beta_{\delta\neq d}}$
Density	1	0	0.999	1.00	0.80
Velocity	0	1	0.993	0.00	1.00
Density&Velocity	0.5	0.5	0.996	0.66	1.00

Table 8.9: Summary of the regions for which the *GOF* is indistinguishable per movement base case for weighting scheme 3

Movement base case	$\beta_d^{local}/\beta_d^{global}$	$\beta_{\delta=d}/\beta_{\delta\neq d}$
Uni-directional - straight	$0.65 \leq \beta_d^{local}/\beta_d^{global} \leq 1$	$0.0 \leq \beta_{\delta=d}/\beta_{\delta\neq d} \leq 1$
Uni-directional - enter	$0.85 \leq \beta_d^{local}/\beta_d^{global} \leq 1$	$0.0 \leq \beta_{\delta=d}/\beta_{\delta\neq d} \leq 1$
Uni-directional - corner	$0.3 \leq \beta_d^{local}/\beta_d^{global} \leq 1$	$0.0 \leq \beta_{\delta=d}/\beta_{\delta\neq d} \leq 1$
Bi-directional - straight	$0.87 \leq \beta_d^{local}/\beta_d^{global} \leq 1$	$0.1 \leq \beta_{\delta=d}/\beta_{\delta\neq d} \leq 1$
Intersecting	$0.4 \leq \beta_d^{local}/\beta_d^{global} \leq 1$	$0.6 \leq \beta_{\delta=d}/\beta_{\delta\neq d} \leq 1$
Compound	$0.6 \leq \beta_d^{local}/\beta_d^{global} \leq 1$	$0.0 \leq \beta_{\delta=d}/\beta_{\delta\neq d} \leq 1$
Intersection of regions	$0.87 \leq \beta_d^{local}/\beta_d^{global} \leq 1$	$0.6 \leq \beta_{\delta=d}/\beta_{\delta\neq d} \leq 1$

8.3.8 Synthesis of the calibration of the MDW model

The previous sections have illustrated that different parameter sets are optimal for distinct movement base cases. However, in all cases regions were established in which the differences in the *GOF* are almost indistinguishable. In table 8.9 these regions are summarised. As one can see, the regions found in the calibration of the distinct movement base cases overlap. As such, the intersection of these regions defines the set of parameter sets which can be used to model all movement base cases. The intersection of the set of regions results in a rectangular area [$0.87 \leq \beta_d^{local}/\beta_d^{global} \leq 1$ and $0.6 \leq \beta_{\delta=d}/\beta_{\delta\neq d} \leq 1$], in which several ratios of $\beta_{\delta=d}/\beta_{\delta\neq d}$ have been excluded.

Even though some self-organisation patterns were found to develop within the simulations, to the author's knowledge no generic measure exist that can quantify these patterns. Therefore, taking these patterns into account in the calibration was considered a step too far. The fact that this characteristics has not been taken into account in the calibration procedure might explain the lack of a higher lower bound on $\beta_{\delta=d}/\beta_{\delta\neq d}$. It is expected that when also taking self-organisation patterns into consideration in a quantitative manner will further restrain the region of viable parameter sets.

Table 8.10: Assessment of the MDW model with respect to the general characteristics of crowd movements found in empirical data sets, where ✓signals that this general characteristic can be captured by the MDW model, $\sim$ that it under some circumstances can be simulated, X that it can not be simulated, and – that this characteristics cannot be determined.

Variable	Characteristics	Assessment
FD - V-ρ	If density increases, velocity decreases	✓
	Three regimes: a free-flow, a transition and a congestion zone.	X
	At high densities pedestrians will retain a velocity.	X
FD - q-ρ	If density increases, the flow rate increases upto capacity.	✓
	The transition zone is unstable and knows directional differences	–
	At high densities, flow might diminish but will not stop entirely.	X
Headway	If density increases, the distance headway decreases.	–
	If the avg. interaction angle decreases, the distance headway increases.	–
Interaction zone	If the density increases, the length of the longitudinal axis of the no-interaction zone decreases.	–
	The length of the lateral axis of the no-interaction zone is independent of the density.	–
Route choice	Searching behaviour of pedestrians increases during high density situations.	–
	The swaying behaviour of pedestrians becomes more dominant during high density situations.	–

Table 8.11: Assessment of the MDW model with respect to the movement base case specific characteristics found in empirical data sets, where ✓signals that this general characteristic can be captured by the MDW model, $\sim$ that it under some circumstances can be simulated, X that it can not be simulated, and – that this characteristics cannot be determined.

Movement base case	Characteristics	Assessment
Uni-dir - straight	Density uniformly spread spatially	✓
	Velocity uniformly spread spatially	✓
	Trajectories become more unstable	–
	Predominantly front2back interactions	–
	Lane formation occurs under high densities	–
Uni-dir - corner	Density increased upstream of corner	X
	Density increase at inner upstream side	X
	Velocity decreased upstream of corner	X
	Predominantly front2back interactions	–
Uni-dir - entering	Density increases towards bottleneck both longitudinal and lateral	✓
	Density focus-point upstream of bottleneck	✓
	Velocity is not decreasing towards the bottleneck	X
	Many short interactions	–
	Predominantly front2back interactions	–
	Wayfinding increased at high densities	–
Bi-dir - straight	Density uniformly spread over cross-section	✓
	Velocity uniformly spread over cross-section	✓
	Trajectories more unstable at high densities	–
	Interactions predominantly front2back	–
	Wayfinding decreased at high densities	–
	Lane formation	✓
Intersecting - Random	Density uniformly spread over cross-section	✓
	Velocity non-uniformly spread over cross-section	✓
	Trajectories more unstable at high densities	–
	Interaction angle mainly between 0 and 90 degrees	–
	Wayfinding increased at high densities	–
	Lane formation between dominant origins and destinations	–

8.4 Assessment of the MDW model

This section describes the assessment of the MDW model with respect to the crowd movement phenomena derived from the empirical data sets in chapter 5. Similar to the assessment of Nomad described in chapter 7, this assessment consists of a qualitative and a quantitative appraisal of the simulation results predicted using the best parameter values found in section 8.3. The quantitative appraisal is performed for five distinct movement base cases, namely uni-directional - straight, uni-directional - entering, uni-directional - corner, bi-directional - straight and intersecting flows. Other sequences of the five data sets described in chapter 5 are used as reference in the assessment, the characteristics of which are described in table B.1.

Tables 8.10 and 8.11 depict the results of the qualitative assessment. The model is assumed to be able to predict a certain phenomenon if a similar trend is found in the simulations as described in the empirical research presented in chapter 5.

Two different assessments have been performed, namely a qualitative and a quantitative assessment. In the first case (one movement base case), a quantitative assessment is made of the version of the MDW model which incorporates the calibrated parameter sets with respect to the specific movement base case for which this behaviour was described in this chapter. In the second case (all movement base cases combined), the findings are compared with a version of the MDW model which is calibrated based on all five movement base cases. Since the assessment with respect to the general characteristics of crowd movement (table 8.10) were found to be similar for the specific movement base cases, the assessment results are summarised in one column. Besides that, in contrast to the assessment of Nomad, the characteristics related to the interaction behaviour of pedestrians cannot be estimated. Consequently, only the macroscopic crowd movement phenomena of the model realisations are assessed.

Qualitative assessment

The comparison shows two interesting differences between the predictions by the calibrated MDW model and the empirical findings. Firstly, the crowd movement phenomena of a uni-directional corner situation cannot be captured realistically. The expected increase of the velocity and decrease of the density upstream of the corner are not predicted by the MDW model. That is, both the velocity and density are uniformly distributed across the space. Secondly, in case of a uni-directional entering situation the velocity does decrease towards the gate, while this effect is only to a limited extent visible in the empirical findings.

Both differences are likely due to the assumption of too optimal walking behaviour by the MDW model in comparison to the empirical findings. That is, in reality pedestrians are found to decrease their walking velocity earlier in case of the expectation of a more dense traffic state downstream and to sidestep earlier at the moment that they experience high densities than predicted by the MDW model.

Quantitative assessment

In the quantitative assessment of the MDW model for several movement base cases slightly higher velocities and lower densities were predicted. The slight overestimation of the velocity might be explained by the difference between the linear fundamental diagram used in this calibration and an empirical fundamental diagram which has a more curvy shape. Figure 8.12 depicts two fundamental diagrams, the first of which (FD_{sim}) is used during this calibration, while the second one (FD_{emp}) is a sketch of an empirical fundamental diagram. The dotted arrows in the figure indicate the direction of the estimation error. As one can see, in order to fit the velocity approximation for density values that reside in the area for which $FD_{sim} < FD_{emp}$ generally an underestimation of the density occurs, while for density values in the regions where $FD_{sim} < FD_{emp}$ generally an overestimation occurs. Given that both density and velocity are weighted in the third calibration scheme, this over- or underestimation is less than the difference between the fundamental diagrams suggests.

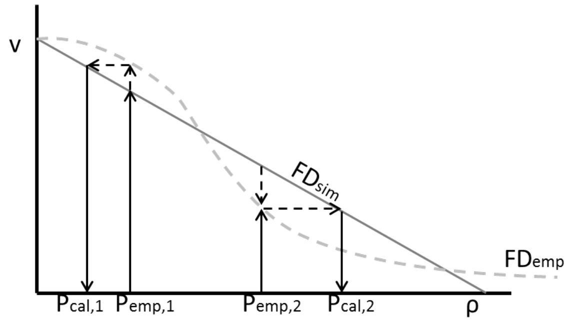

Figure 8.12: Overestimation of densities and velocities due to discrepancies between the simulated and empirical fundamental diagrams

8.5 Conclusions and a look ahead

In this chapter the macroscopic pedestrian simulation model proposed by Hoogendoorn et al. (2014) and Hoogendoorn et al. (2015) has been assessed with respect to its capabilities to simulate the movement dynamics of crowds during large-scale events. Since two slightly different versions of this model have been proposed, first the best version of this model has been established by means of a sensitivity analysis. Moreover, insights were developed with respect to the manner in which the key parameters of this model influence the predicted crowd dynamics.

It was established that of the three ratios that make up the core of the MDW model, only two parameters ($\beta_d^{local}/\beta_d^{global}$ and $\beta_{\delta=d}/\beta_{\delta\neq d}$) are needed to model most crowd movement phenomena. Self-organisation does not develop when the influence of the local route choice and reaction to other classes of pedestrians is limited. In model instances where the local route choice and reaction to the presence of other classes was very strong self-organisation becomes unstable. Moreover, it is found that the delay has no influence on the development of self-organisation phenomena. Based on these findings it is concluded that the more intricate model proposed by Hoogendoorn et al. (2015) has no added value with respect to the model described by Hoogendoorn et al. (2014). Consequently, the capabilities of the MDW model as described in Hoogendoorn et al. (2014) have been assessed in the remainder of this chapter.

This version of the MDW model is first calibrated to quantitatively correctly predict the movement dynamics of pedestrians at large-scale events. In general, a very strong influence of the local route choice is found, while the influence of the presence of pedestrians from other classes differed greatly dependent on the movement base case and weighting scheme used. This first characteristic influences the general dispersion behaviour of pedestrians. This implies that pedestrians at large-scale events tend to value comfort as important (or even more important) as travel time. The second characteristic governs the interaction behaviour, and as such the development of self-organisation, of pedestrians. This finding implies that pedestrians tend to organize as a result of an intrinsic repulsive reaction with respect to pedestrians who display another type of walking dynamics.

Besides that, sets of parameter values were established in which the *GOF* was almost indistinguishable. The set of parameter sets for distinct movement base cases were found to overlap [$0.87 \leq \beta_d^{local}/\beta_d^{global} \leq 1$ and $0.6 \leq \beta_{\delta=d}/\beta_{\delta\neq d} \leq 1$]. Moreover, the objective function was found to be very flat. Consequently, no clear optimum could be estimated. As such, a set of parameter values could be established which consisted of all parameter sets that can be used to model all movement base cases that were part of the calibration process. Contrary to the expectation, the intersection of these sets only defined a lower bound on the ratio $\beta_d^{local}/\beta_d^{global}$. This finding implies that the local route choice severely influences the correct display of crowd movement phenomena, and as such the correct prediction of crowd movements at large-scale events. Besides that, a lack of a higher bound on the ratio $\beta_{\delta=d}/\beta_{\delta\neq d}$ is found, which is expected to be due to the lack of a characteristic in the calibration procedure that accounts for the self-organisation phenomena lane formation and stripe formation. Moreover, it was found that the MDW model currently overestimates both velocity and density due to the use of a linear fundamental diagram.

In general, it is found that most macroscopic crowd movement phenomena can be predicted by the MDW model. Qualitatively the self-organisation phenomena could be predicted by the model, however these patterns have not been assessed quantitatively.

However, this study also established that in some cases, the model predicts more direct walking behaviour than found in the empirical cases. Anticipation and suboptimal decision making are hypothesised to be the cause of the predicted differences in walking dynamics with respect to reality.

Since the MDW model is, to the author's knowledge, one of the most sophisticated macroscopic pedestrian simulation model, it is expected that none of the existent macroscopic models can currently capture this locally suboptimal behaviour. More research into this specific movement phenomenon is necessary to determine what behaviour is underlying this phenomenon and how this can be modelled macroscopically.

Furthermore, in this chapter a calibration procedure for macroscopic pedestrian simulation models has been presented in which new indicators for pedestrian crowd movements are introduced. Only two characteristics of the walking behaviour were taken into account. The calibration results, however, showed that several self-organisation phenomena need to be included in the list of characteristics in order to calibrate the ratio $\beta_{\delta=d}/\beta_{\delta\neq d}$ better. It is expected that additional quantitative macroscopic measures characterising self-organisation patterns which can be used in the calibration of macroscopic models would improve the calibration procedure.

Chapter 9

Conclusions and recommendations

All over the world large-scale events are organised frequently. The movement dynamics of pedestrians at these large-scale events are complex. For crowd managers it remains difficult to predict whether, when and where these movements become dangerous. More and more, crowd managers are supported by pedestrian simulation models to obtain insights into these complex dynamics.

Yet, even though the capabilities of pedestrian simulation models are seemingly limitless, it is unclear whether these models are capable of simulating the movement dynamics of pedestrians in crowds at large-scale events correctly. That is, pedestrian simulation models have only been scarcely calibrated and validated for crowd movement phenomena up to this moment (Isenhour & Löhner (2014)). First and foremost, because it is unclear which crowd movement phenomena are essential in the correct display of this type of movements. Besides that, there was a lack of data sets featuring this specific type of walking behaviour that are essential to calibrate simulation models.

The aim of this thesis was to develop theories and models that describe the operational walking dynamics of pedestrian crowds during large-scale events. An inductive research approach has been adopted in order to establish 1) a conceptual model of related behavioural hypotheses that jointly describe these dynamics and 2) to determine the crowd movement phenomena that are essential in a correct display these dynamics. Afterwards, the lists of crowd movement phenomena have been used to assess the pedestrian simulation models that have been proposed in the last decade with respect to their capabilities to model large-scale events.

In this final chapter, the main contributions of this thesis have been summarised. In section 9.1 main findings are mentioned. Next, the conclusions are elaborated upon in section 9.2. Subsequently, section 9.3 discusses the implications of this work for practice. Last but not least, recommendations for future research are provided in section 9.4.

9.1 Main findings

The findings and conclusions derived within this thesis can be split into three categories. The empirical findings and the theories on the operational movement dynamics of pedestrians at large-scale events are discussed in section 9.1.1. Accordingly, the findings regarding the modelling of this type of movement dynamics in section 9.1.2. This section ends with a summary of findings with respect to the research methodology.

9.1.1 Theories regarding crowd movements at large-scale events

One of the main results of this research is a conceptual model of related behavioural hypotheses describing the movements of individual pedestrians within a crowd, see figure 2.8. This conceptual model was corroborated by means of linear regression analysis in chapter 4 using the empirical data sets described in chapter 5. In this conceptual model the macroscopic flow variables (velocity, density and flow) are linked to the microscopic flow variables (distance headway and velocity) and the characteristics of the individual, the physiological environment, the infrastructure and the flow situation. From this conceptual model, it was deduced that the movement decisions of an individual are not necessarily based on only the aggregate features of the crowd movement, but is also influenced by the characteristics of the population, the physiological environment, the local interaction between pedestrians and the movement base case.

One of the other objectives of this thesis was to determine which movement phenomena are essential in the correct display of crowd movement behaviour at large-scale events. A thorough analysis of empirical data sets captured at large-scale events highlighted several interesting universal phenomena, namely 1) a shape change from an ellipse to a circle of the no-interaction zone for individual pedestrians with increasing densities, 2) the general lack of interactions between pedestrians that walk towards each other in case of higher densities, 3) an increase of the searching behaviour[22] with increasing densities, 4) a decrease of the distance headway instead of a decrease of the time-to-collision, 5) a non-zero walking velocity at high densities.

An analysis of the empirical data sets, moreover, resulted in two lists of crowd movement phenomena: one list of the general crowd movement phenomena and one list of specific crowd movement phenomena that develop only during one of the movement base cases. The existence of a list of case-specific crowd movement phenomena implies that pedestrian simulation models can only be calibrated and validated using data sets that feature a combination of movement base cases.

[22] Searching behaviour describes the walking behaviour of pedestrians in fairly dense situations during which their trajectories become more unstable, swaying increases and several large changes in direction are seen. That is, it seems that pedestrians cannot oversee the entire study area.

9.1.2 Modelling operational movement dynamics at large-scale events

The other main result of this research is the assessment of two promising pedestrian simulation models with respect to their capabilities of predicting the movement dynamics of crowds at large-scale events. In order to identify these promising pedestrian simulation models a thorough review has been performed in chapter 6 in which Cellular Automata, Social Force models, Collision Avoidance models, Continuum models, Hybrid models, Behavioural models and Network models were discussed. The review showed that none of the reviewed models is currently capable of supplying all characteristics necessary for real-time crowd motion modelling. On the one hand, several computer simulation related applications were proposed that focus on simulating crowd movements that look like reality at high computational speed (online). On the other hand, several crowd simulation models were found that focus on representing reality accurately but have a very high computational burden that they can only be used in an off-line fashion on a present-day desktop computer. The review illustrated that currently the Social Force models, Activity Choice models and the new generation Continuum models are best equipped to model the operational movement dynamics of pedestrians in crowds at large-scale events.

The calibration results of the microscopic simulation model Nomad and the Macroscopic Dynamic Walker model proposed by Hoogendoorn et al. (2014) (in this thesis referred to as the MDW model) illustrated that the best parameter set for each of the two models is very dependent on the movement base case used in the calibration process. Even though the differences in the parameter sets were in general small, for Nomad it was found that the consequences of these differences with respect to the demand at which flow breakdown occurs are extensive. Depending on the set of parameters a difference in the capacity of approximately 50% was found.

Additionally, both models were found to have difficulties predicting the anticipation behaviour of pedestrians upstream of bottleneck situations and the dispersion of pedestrians in uni-directional corner flows. Besides that, the assessment results showed that Nomad has difficulties predicting the movement behaviour of pedestrians correctly in several movement base cases the model was not originally calibrated for and the MDW model's predictions were found to be sensitive to the specified fundamental diagram.

9.2 Conclusions

The main conclusion of this thesis is that the walking dynamics of pedestrians within a crowd at large-scale events are less straight forward than originally assumed. The conceptual model illustrated that numerous characteristics impact the movement behaviour of pedestrians. Moreover, the empirical study performed in chapter 5 showed that the walking behaviour changes depends on the context of the situation. The characteristics of the individual, the physiological environment, the infrastructure lay-out, the movement base case, and the amount of oversight influence the aggregate walking behaviour of pedestrians at large-scale events. The additional complexity of the walking dynamics implies that the idea of one generic fundamental diagram that accurately predicts the aggregate movement behaviour in all situations under all contexts might not exist. The assessment of the MDW model illustrates that not taking into account the differences between the fundamental diagrams, which are caused by differences in the level of complexity of the situation (e.g. changes in the number of interactions, variation of interaction angles, interaction angles), might result in a severe under- or overestimation of the onset of flow breakdown and the capacity of the infrastructure.

A second conclusion that can be drawn from the findings is that understanding and modelling all listed crowd movement phenomena and the ”suboptimal” local route choice behaviour of pedestrians under crowded conditions is essential in order to accurately predict the movement dynamics at large-scale events. Many pedestrian simulation models are currently not capable of modelling all the movement dynamics displayed by pedestrians at large-scale events. Chapter 6 illustrated that many models cannot reproduce all essential crowd movement phenomena, which calls the results of these models into question. Besides that, chapter 7 shows that if the anticipation of downstream traffic state conditions is not taken into account by a pedestrian simulation model, the predicted walking dynamics are locally more direct and efficient than the dynamics found to occur in practice. This might result in the overestimation of high density regions by pedestrian simulation models.

9.3 Implications for practical use

The previous sections of this chapter have presented the findings and conclusions. However, the findings of this thesis also have implications for practical use. Below, these findings regarding the importance of considering the context of large-scale events and the assessment of pedestrian infrastructures are elaborated upon.

Context does matter

The literature and the empirical findings show that context does matter. The same infrastructure can suddenly become dangerous when the circumstances (e.g. strong winds and heavy rain, adult males at a soccer stadium instead of young kids at a K3 concert) and the complexity of the movement dynamics (e.g. bi-directional instead of uni-directional, high variance in flow directions instead of one predominant flow direction) change. Even though this thesis cannot establish the exact quantitative differences in capacity based on the results presented in this thesis, several velocity decreasing factors were determined, for example a decrease of the interaction angle and the variability of the alignment of interaction. The presence of these factors, and several others which were not studied in this thesis, should be taken into account when managing and/or assessing large-scale infrastructures.

Often the assessment of pedestrian walking behaviour is simplified to one general relation between density and walking velocity (often called a fundamental diagram) or a table that provides a capacity for a certain density regime. This thesis, however, shows that the fundamental diagram is very dependent on the complex interplay of the characteristics of the pedestrians, the physiological environment, the infrastructure and the movement base case.

Consequently, the representative capacity of the infrastructure can only be determined by means of scenario analysis. That is, a set of distinct simulations in which these characteristics are varied. During a scenario analysis special attention has to be paid to the potential future populations that will use the infrastructure, the circumstances under which they might reside within the infrastructure, and the patterns according to which they move through the infrastructure.

Be careful when assessing pedestrian infrastructures by means of models

Pedestrian simulation models are more and more used to assess infrastructures. This thesis has established that a large number of pedestrian simulation models exist, many of which are not capable of simulating all the crowd movement phenomena which are necessary to predict the movement dynamics of crowds at large-scale events realistically. Each model has a specific set of situations it can model realistically. As a result, the best model for a task depends on the type of infrastructure that is assessed, the type of knowledge the user requires (e.g. capacity, flow dynamics, route choice, evacuation time) and the accuracy that is required. As such, before adopting a pedestrian simulation model for a certain type of analysis, it is advised that the user first establishes whether the expected behaviour can be captured by the model and whether the model is calibrated for this type of movement dynamics. Yet, the correct performance of a sensitivity analysis, calibration and validation of a pedestrian simulation model is difficult, takes time and can best be performed by an individual that knows the model through and through. However, asking for proof that a pedestrian simulation model can represent the crowd movement dynamics that are being studied before implementing such a model can limit effort, time and disappointment.

Even models that, considering their mathematical properties, have the ability to capture certain behaviour, do not necessarily produce realistic predictions. This thesis has shown that slight differences in the adopted parameter sets can lead to large differences in the predicted demand at which flow breakdown[23] occurs. Therefore, it is advised to always check whether the default values of a model are correct for the case at hand. That is, whether the prediction results are realistic in a few simple cases and/or were realistic in earlier modelling attempts.

Moreover, this thesis has shown that a pedestrian simulation model calibrated for a set of specific movement base cases is not necessarily capable of realistically predicting the walking dynamics of pedestrians in other movement base cases. Therefore, it is advised that pedestrian simulation models which are used for generic use, are calibrated and validated based on the largest set of movement base cases possible to ensure a reasonable accuracy.

Last of all and most importantly, the results of the calibration and assessment procedures illustrated that modelling pedestrian movement behaviour is not straight forward. Even when is all generic crowd movement phenomena are captured, pedestrians can always behave surprisingly different than expected. As such, it should not be forgotten that even a correctly

[23] Flow breakdown describes the process during which the flow of pedestrians stagnates to the point that more than a certain number of pedestrians stands still for more than 5 seconds. For a more comprehensive description of the flow breakdown probability one is referred to the papers by Campanella et al. (2009a) and Yang et al. (2014)

calibrated and validated pedestrian simulation model remains a simplification of reality. That is, a pedestrian simulation model can perfectly be used as a tool that generates predictions of possible future realities, but it should never be used as the tool that predicts the only possible outcome.

9.4 Recommendations for future research

The previous chapter has summarised the findings and conclusions of this thesis. Even though the author attempted to be thorough and comprehensive, this thesis does not only provide answers but also raises questions. Some of these will be elaborated upon in the following section. First, the issues and questions related to the study of pedestrian movement dynamics are discussed in section 9.4.1. Afterwards, sections 9.4.2 and 9.4.3 present some of the questions raised with respect to the modelling of pedestrian walking behaviour and the calibration of pedestrian simulation models.

9.4.1 Studying pedestrian movement dynamics

Several new methodologies have been developed in order to capture pedestrian trajectories, study these trajectories and calibrate pedestrian simulation models based on these data sets. No previous work had been performed with respect to some of the issues at hand. As such, after a discussion of the possibilities, one solution direction has been adopted. Yet, it is uncertain whether the chosen direction (i.e. research methodology) is the best direction. Therefore, more research into research methodologies with respect to the study and modelling of pedestrian movement dynamics is necessary. This research should not only focus on the development of new methodologies, but also on the behavioural and technical implications of contemporary methodologies and the applicability of these methodologies. Several studies by among others Nikolić et al. (in print), Liao et al. (in print) and Duives et al. (2016b) in the last year have shown that the research methodology can influence the empirical findings. However, the extent to which is still uncertain. It is essential that the conditions that apply to data collection (e.g. the implications of experimental set-up with respect to the captured physical and behavioural walking dynamics), processing (e.g. the influence of filtering algorithms on the captured dynamics) and analysis techniques (e.g. the influence of serial correlation on statistical tests and the definition of variables on the characteristics of the walking dynamics) are determined in order to solidify the results of contemporary and future work.

The knowledge developed within this thesis relates to a limited amount of data captured under specific conditions. Whether the findings with respect to the movement dynamics of pedestrians in crowds at large-scale events and calibration of pedestrian simulation models discussed within this thesis apply under all circumstances (among other things laboratory settings, evacuations, other populations, or infrastructure characteristics) remains difficult to substantiate. Consequently, more thorough research into the crowd movement phenomena under these and other conditions is required. That is, insights should be created with respect to the influence of the settings of an experiment on the walking behaviour and dynamics of individual pedestrians as well as crowds.

9.4.2 Modelling pedestrian movement dynamics

During the analysis of the empirical data sets, several relations which have not yet been incorporated into the conceptual model have been briefly touched upon. An example of such a relation is the relation between the distance headway, the time-to-collision and the movement base-cases. Moreover, several other characteristics have been mentioned in the research literature, but were disregarded in this thesis. Examples of these characteristics are among other, self-organisation, goal-orientation, comfort, distraction, tactical choices, stress, and intoxication. These characteristics should be implemented in the conceptual model in order to create a comprehensive model of pedestrian movement dynamics in crowds at large-scale events.

The conceptual model of related behavioural hypotheses presented in this thesis has been tested by means of linear regression analysis and a Welch's t-test. As a result only direct connections between variables could be tested. The interaction between more than two components has not been taken into account in this thesis. Given that the conceptual model indicates the existence of more complicated relations between factors further testing of the conceptual model by means of more sophisticated analysis methods such as factor analysis advised.

9.4.3 Calibration of pedestrian simulation models

This thesis has shown that the results of the calibration of a pedestrian simulation model depend severely on the characteristics adopted in the objective function of the calibration procedure. Yet, research has shown that the combination of macroscopic and microscopic metrics in an objective function is not straight forward. Among other things, correlation between metrics can arise, which influences the results of the calibration process. In this thesis, however, a very pragmatic solution has been adopted, namely the equal weighting of the metrics. More research is needed with respect to this type of calibration process. That is, which metrics can be used side-to-side in an objective function, how can the metrics be weighted fairly, and how should the results of such a calibration process be interpreted.

Additionally, in this calibration a grid-based search method has been adopted to find the optimal parameter set. This type of search method does not guarantee that the optimal parameter set within the search space is found, only that the optimal parameter set within a set of parameter sets has been found. To check the solutions found in this thesis, more sophisticated search algorithms such as simulated annealing, ant-colony optimisation or a genetic algorithm need to be applied.

Bibliography

Alghadi, S., and H. Mahmassani (1991) Simulation of crowd behavior and movement: fundamental relations and applications, *Transportation Research Record*, 1320, pp. 260–268. 114, 122, 125

Alghadi, S., H. Mahmassani, and R. Herman (2002) A speed-concentration relation for bi-directional crowd moments with strong interaction, In: Schreckenberg, M., and S. Sharma, eds., *Pedestrian and Evacuation Dynamics*, Pedestrian and Evacuation Dynamics, Springer-Verlag, pp. 3–20. 18, 24, 25

Aly, H., and M. Youssef (2013) Dejavu: an accurate energy-efficient outdoor localization system, In: *Proceedings of the 21st ACM SIGSPATIAL International conference on advances in geographic information systems*, pp. 154–163. 43

Antonini, G., M. Bierlaire, and M. Weber (2004) Simulation of pedestrian behaviour using a discrete choice model calibrated on actual motion data, In: *4th Swiss Transport Research Conference*, pp. –. 122

Appert-Rolland, C., J. Cividini, H. Hilhorst, and P. Degond (2014a) Pedestrian flows: From individuals to crowds, In: Daamen, W., D. Duives, and S. Hoogendoorn, eds., *The conference on Pedestrian and Evacuation Dynamics (PED2014)*, vol. 2 of *Transportation Research Procedia*, pp. 468–476. 116, 127, 128

Appert-Rolland, C., A. Jelic, P. Degond, J. Fehrenbach, J. Hua, A. Cretual, R. Kalpa, A. Marin, A.-H. Olivier, S. Lemercier, and J. Pettré (2014b) Experimental study of the following dynamics of pedestrians, In: Weidmann, U., U. Kirsch, and M. Schreckenberg, eds., *Pedestrian and Evacuation Dynamics (PED2012)*, pp. 305–315. 22

Arita, C., J. Cividini, and C. Appert-Rolland (2014) Shuffle uupdate in an evacuation problem, In: Daamen, W., D. Duives, and S. Hoogendoorn, eds., *The conference on Pedestrian and Evacuation Dynamics (PED2014)*, vol. 2 of *Transportation Research Procedia*, pp. 309–317. 114, 122

Asano, M., T. Iryo, and M. Kuwahara (2010) Microscopic pedestrian simulation model combined with a tactical model for route choice behavior, *Transportation Research - Part C: Emerging technologies*, 18, pp. 842–855. 26

Asano, M., M. Kuwahara, and S. Tanaka (2007) Multi-directional pedestrian flow model based on empirical data, In: *11th World Conference on Transporation and Safety Research (CD-ROM)*, p. 01117444. 26

Aultman-Hall, L., D. Lane, and R. Lambert (2009) Assessing impact of weather and season on pedestrian traffic volumes, *Transportation Research Record*, 2140, pp. 35–43. 16

Avineri, E., D. Shinar, and Y. Susilo (2012) Pedestrians' behaviour in cross walks: The effect of fear of falling and age, *Accident Analysis and Prevention*, 44, pp. 30–34. 15

Bandini, S., M. Mondini, and G. Vizzari (2014) Modelling negative interactions among pedestrians in high density situations, *Transportation Research - Part C: Emerging technologies*, 40, pp. 251–270. 114, 122

Bandini, S., F. Rubagotti, V. G., and K. Shimura (2011a) An agent model of pedestrian and group dynamics: Experiments on group cohesion, In: Pirrone, R., and F. Sorbello, eds., *AI*IA 2011: Artificial Intelligence Around Man and Beyond*, vol. 6934 of *Lecture Notes in Computer Science*, Springer-Verlag Berlin, pp. 104 – 116. 114

Bandini, S., F. Rubagotti, V. G., and K. Shimura (2011b) A cellular automata based model for pedestrian and group dynamics: Motivations and first experiments, In: Malyshkin, V., ed., *Parallel Computing Technologies*, vol. 6873, Springer-Verlag Berlin, pp. 125–139. 114

Banerjee, B., A. Abukmail, and L. Kraemer (2008) Advancing the layered approach to agent-based crowd simulation, *Proceedings of the IEEE Workshop on Parallel and Distributed Simulation*, pp. 185–192. 117

Bellomo, N., and A. Piccoli, B. Tosin (2012) Modeling crowd dynamics from a complex system viewpoint, *Mathematical Models and Methods in Applied Sciences*, 22(2), pp. 1230004–1–29. 105, 110, 119, 126

Berg, J. v. d., S. Guy, M. Lin, and D. Manocha (2011) *Robotics research*, chap. Reciprocal n-body collision avoidance, Springer Berlin Heidelberg, pp. 3–19. 60

Berg, M. v. (2009) *Pedestrian behaviour and its relation to doorway capacity*, Msc. thesis, Delft University of Technology. 24

Blue, V., and J. Adler (1998) Emergent fundamental pedestrian flows from cellular automata microsimulation, *Transportation Research Record*, 1644, pp. 29–36. 2, 114

Blue, V., and J. Adler (1999) *Using Cellular Automata. Microsimulation to Model Pedestrian Movement*, Elsevier Science Ltd., - pp. 114

Bocconi, S., A. Bozzon, A. Psyllidis, C. Bolivar, and G.-J. Houben (2015) Social glass: a platform for urban analytics and decision-making through hetrogeneous social data, In: *Proceedings of the 24th international conference on World Wide Web*, pp. 175–178. 44

Bohannon, R. (1997) Comfortable and maximum walking speed of adults aged 20-79 years: reference values and determinants, *Age and Ageing*, 26, pp. 15–19. 15

Boles, W. (1981) The effect of density, sex and group size upon pedestrian walking velocity, *Man-Environment Systems*, 11, pp. 37–40. 15

Borgers, A., and H. Timmermans (1986) A model of pedestrian route choice and demand for retail facilities within inner-city shopping areas, *Geographical Analysis*, 18(2), pp. 115–128. 110, 119

Camazine, S., J.-L. Deneubourg, N. Franks, J. Sneyd, G. Theraulax, and E. Bonabeau (2010) *Self-Organisation in biological systems*, Princeton studies in complexity, Princeton University Press, Princeton and Oxford, 525 pp. 22

Campanella, M. (2016) *Microscopic modelling of walking behavior*, Ph.D. thesis, Delft University of Technology. 130, 134

Campanella, M., S. Hoogendoorn, and W. Daamen (2009a) Effects of heterogeneity on self-organized pedestrian flows, *Transportation Research Record*, 2124, pp. 2148–2156. 3, 153, 191

Campanella, M., S. Hoogendoorn, and W. Daamen (2009b) Improving the nomad microscopic walker model, In: *12th IFAC Symposium on Control in Transportation Systems (CTS'09)*, pp. 12–18. 27, 115, 132, 133, 134, 135, 144, 145, 146

Campanella, M., S. Hoogendoorn, and W. Daamen (2014) The nomad model: theory, developments and applications, In: Daamen, W., D. Duives, and S. Hoogendoorn, eds., *The conference on Pedestrian and Evacuation Dynamics 2014 (PED2014)*, vol. 2 of *Transportation Research Procedia*, pp. 462–467. 115, 123, 130

Cepolina, E., and N. Tyler (2005) Understanding capacity drop for designing pedestrian environments, In: *Walk 21*, pp. 1–11. 23

Challenger, R., C. Clegg, M. Robinson, and M. Leigh (2010) Understanding crowd behaviours - volume 2: Supporting theory and evidence, Tech. rep., Centre for SocioTechnical Systems Design (CSTSD), Leeds University Business School. 5, 111

Chalmet, L., R. Francis, and P. Saunders (1982) Network models for building evacuation, *Management Science*, 28(1), pp. 86–105. 119

Chandra, S., and A. K. Bharti (2013) Speed distribution curves for pedestrians during walking and crossing, In: Chakroborty, P., H. Reddy, A. Amekudzi, A. Das, A. Seyfried, B. Maitra, D. Teodorovic, K. Srinivasan, L. Devi, S. Pulugurtha, and T. Mathew, eds., *2nd Conference of Transportation Research Group of Inda (2nd CTRG)*, vol. 104 of *Procedia - Social and Behavioural Sciences*, pp. 660–667. 15

Chattaraja, U., A. Seyfried, and P. Chakroborty (2009) Comparison of pedestrian fundamental diagram across cultures, *Advances in complex systems*, 12(3), p. 2009. 15

Chattaraja, U., A. Seyfried, P. Chakrobortyc, and M. Biswala (2013) Modelling single file pedestrian motion across cultures, In: Chakroborty, P., H. Reddy, A. Amekudzi, A. Das, A. Seyfried, B. Maitra, D. Teodorovic, K. Srinivasan, L. Devi, S. Pulugurtha, and T. Mathew, eds., *2nd Conference of Transportation Research Group of India (2nd CTRG)*, vol. 104 of *Procedia - Social and Behavioral Sciences*, Elsevier, pp. 698–707. 22

Chen, M., G. Bärwolff, and H. Schwandt (2014) Modeling pedestrian dynamics on triangular grids, In: Daamen, W., D. Duives, and S. Hoogendoorn, eds., *The conference on Pedestrian and Evacuation Dynamics 2014 (PED2014)*, vol. 2 of *Transportation Research Procedia*, pp. 327–335. 114

Chraibi, M., M. Freialdenhoven, A. Schadschneider, and A. Seyfried (2013) Modeling the desired direction in a force-based model for pedestrian dynamics, In: Kozlov, V., A. Buslaev, A. Buslaev, M. Yashina, A. Schadschneider, and M. Schreckenberg, eds., *Traffic and Granular Flow '11*, vol. Part II, Springer Berlin Heidelberg, pp. 263–275. 127, 128

Chraibi, M., U. Kemloh, A. Schadschneider, and A. Seyfried (2011) Force-based models of pedestrian dynamics, *Networks and hetrogeneous media*, 6(3), pp. 425–442. 32, 115

Colombo, R., M. Garavello, and M. Lecureau-Mercier (2011) Non-local crowd dynamics, *Comptes Rendus Mathematique*, 349(13-14), pp. 769–772. 116

Corbetta, A., L. Bruno, A. Muntean, and F. Toschi (2014) High statistics measurements of pedestrian dynamics, In: Daamen, W., D. Duives, and S. Hoogendoorn, eds., *The conference on Pedestrian and Evacuation Dynamics (PED2014)*, vol. 2 of *Transportation Research Procedia*, Elsevier, pp. 96–104. 23

Cristiani, E., B. Piccoli, and A. Tosin (2011) Multiscale modeling of granular flows with application to crowd dynamics, *Multiscale modelling and simulation*, 9(1), pp. 155–182. 116

Crosbie, J., R. Vachalathiti, and R. Smith (1997) Age, gender and speed effects on spinal kinematics during walking, *Gait & Posture*, 5, pp. 13–20. 15

Daamen, W. (2002) Simped: a pedestrian simulation tool for large pedestrian areas, In: *conference proceedings EuroSIW, 24-26 June 2002*. 118

Daamen, W. (2004) *Modelling Passenger Flows in Public Transport Facilities*, Ph.D. thesis, Delft University of Technology. 102

Daamen, W., and S. Hoogendoorn (2003a) Controlled experiments to derive walking behavior, *European journal of transport and infrastructure research (EJTIR)*, 3(1), pp. 39–54. 13, 24

Daamen, W., and S. Hoogendoorn (2003b) Experimental research on pedestrian walking behavior, *Transportation Research Record*, 1828, pp. 20–30. 22, 24, 42

Daamen, W., and S. Hoogendoorn (2007) Free speed distributions - based on empirical data in different traffic conditions, In: Waldau, N., P. GattermGat, H. Knoflacher, and M. Schreckenberg, eds., *Pedestrian and Evacuation Dynamics 2005*, Springer Berlin Heidelberg, pp. 13–25. 25

Daamen, W., and S. Hoogendoorn (2010a) Capacity of doors during evacuation conditions, In: Hoogendoorn, S., A. Pel, M. Taylor, and H. Mahmassani, eds., *First international conference on evacuation modeling and management (ICEM 2010)*, vol. 3 of *Procedia Engineering*, pp. 53–66. 3, 94, 169

Daamen, W., and S. Hoogendoorn (2010b) Emergency door capacity: Influence of door width, population composition and stress level, *Fire Technology*, 48(1), pp. 55–71. 21, 23, 24, 102

Daamen, W., S. P. Hoogendoorn, M. Campanella, and D. Versluis (2014) Interaction behavior between individual pedestrians, In: Weidmann, U., U. Kirsch, and M. Schreckenberg, eds., *Pedestrian and Evacuation Dynamics 2012 (PED2012)*, pp. 1305–1313. 18

Dachner, G., and W. Warren (2014) Behavior dynamics of heading alignment in pedestrian following, In: Daamen, W., D. Duives, and S. Hoogendoorn, eds., *The conference on pedestrian and evacuation dynamics (PED2014)*, vol. 2 of *Transportation Research Procedia*, Elsevier, pp. 69–76. 18

Dahlgren, E., and H. Mahmood (2014) *Evaluation of indoor positioning based on Bluetooth Smart technology*, Msc. thesis, Chalmers University of Technology, Göteborg, Sweden. 43

Danalet, A., B. Farooq, and M. Bierlaire (2013) Towards and activity-based model for pedestrian facilities, In: *13th Swiss transportation research conference (STRC)*. 43

Davidich, M., F. Geiss, H. Mayer, A. Pfaffinger, and C. Royer (2013) Waiting zones for realistic modelling of pedestrian dynamics: A case study using two major german railway stations as examples, *Transportation Research - Part C: Emerging technologies*, 37, pp. 210–222. 114

Degond, P., and J. Hua (2013) Self-organized hydrodynamics with congestion and path formation in crowds, *Journal of computational physics*, 237, pp. 299–319. 116

Dias, C., O. Ejtemai, M. Sarvi, and M. Burd (2014a) Exploring pedestrian walking through angled corridors, In: Daamen, W., D. Duives, and S. Hoogendoorn, eds., *The conference on Pedestrian and Evacuation Dynamics (PED2014)*, vol. 2 of *Transportation Research Procedia*, Elsevier, pp. 19–25. 23

Dias, C., O. Ejtemai, M. Sarvi, and N. Shiwakoti (2014b) Pedestrian walking characteristics through angled corridors, *Transportation Research Records*, 2421, pp. 40–51. 3, 23, 104, 115

Dias, C., M. Sarvi, and N. Shiwakoti (2012a) Effect of turning angle on collective panic egress: experimental evidence and pedestrian crowd simulation, In: *ARRB Conference*, ARRB Group LTD and Authors, Perth, Australia. 31

Dias, C., M. Sarvi, N. Shiwakoti, and M. Burd (2012b) Turning angle effect on emergency egress: experimental evidence and pedestrian crowd simulation, *Transportation Research Record*, 2312, pp. 120–127. 31

Dietrich, F., G. Köster, M. Seitz, and I. von Sivers (2014) Bridging the gap: From cellular automata to differential equation models for pedestrian dynamics, *Journal of Computational Science*, 5(5), pp. 841–846. 115

Dollar, P., C. Wojek, B. Schiele, and P. Perona (2012) Pedestrian detection: an evaluation of the state of the art, *IEEE Transactions on Pattern Analysis and Machine Intelligence*, 34(4), pp. 743–761. 48

Dray, S., M. Royer-Carenzi, and C. Calenge (2010) The exploratory analysis of autocorrelation in animal-movement studies, *Ecological Research*, 25, pp. 673–681. 66, 67

Duives, D. (2012) *Analysis of Pedestrian Crowd Movements at Lowlands*, Msc. thesis, Delft University of Technology. 14, 38, 42, 48

Duives, D., W. Daamen, and S. Hoogendoorn (2012a) State-of-the-art crowd motion simulation tools, *Transportation Research - Part C: Emerging technologies*, accepted for publication, pp. 1–21. 123

Duives, D., W. Daamen, and S. Hoogendoorn (2012b) Trajectory analysis of pedestrian crowd movements at a dutch music festival, In: Weidmann, U., U. Kirsch, and M. Schreckenberg, eds., *Pedestrian and Evacuation Dynamics 2012*, vol. Part II, Springer International Publishing, pp. 151–166. 42, 57

Duives, D., W. Daamen, and S. Hoogendoorn (2013) Quantitative estimation of self-organization in bi-directional and crossing flows during crowd movements, In: Chraibi, M., M. Boltes, A. Schadschneider, and A. Seyfried, eds., *Traffic and Granular Flow '13 (TGF '13)*, vol. 1, Springer International Publishing, pp. 251–256. 109, 135

Duives, D., W. Daamen, and S. Hoogendoorn (2014a) Anticipation behavior upstream of a bottleneck, In: Daamen, W., D. Duives, and S. P. Hoogendoorn, eds., *The Conference on Pedestrian and Evacuation Dynamics 2014 (PED 2014)*, vol. 2 of *Transportation Research Procedia*, pp. 43–50. 21, 24, 94, 102

Duives, D., W. Daamen, and S. Hoogendoorn (2015) Quantification of the level of crowdedness for pedestrian movements, *Physica A: Statistical Mechanics and its Applications*, 427, pp. 162–180. 58

Duives, D., W. Daamen, and S. P. Hoogendoorn (2014b) The influence of group size and group composition on the adhered distance headway, In: Daamen, W., D. Duives, and S. Hoogendoorn, eds., *The Conference on Pedestrian and Evacuation Dynamics 2014 (PED 2014)*, vol. 2 of *Transportation Research Procedia*, Procedia, pp. 183–188. 15

Duives, D., W. Daamen, and S. P. Hoogendoorn (2016a) Continuum modelling of pedestrian flows - part 2: Sensitivity analysis featuring crowd movement phenomena, *Physica A: Statistical Mechanics and its Applications*, 447, pp. 36–48. 133

Duives, D. C., W. Daamen, and S. Hoogendoorn (2016b) Determining the density experienced by pedestrians in unstable flow situations, In: Knoop, V., and W. Daamen, eds., *Traffic and Granular Flow (TGF'15)*, p. inprint. 192

Dunbar, G., C. Holland, and E. Maylor (2004) Older pedestrians: A critical review of the literature, Tech. rep., Department for Transport: London, UK. 15

Duncan, H. (2009) Pre-event crowd behaviour prediction system: A study within concert environment, *Journal of Crowd Safety and Security Management*, 1(2), pp. 33–45. 5

Edie, L. (1963) *Discussion of traffic stream measurements and definitions*, Port of New York Authority. 58

Fiorini, P., and Z. Shiller (1998a) Motion planning in dynamic environments using velocity obstacles, *The International Journal of Robotics Research*, 17(7), pp. 760–772. 60

Fiorini, P., and Z. Shiller (1998b) Motion planning in dynamic environments using velocity obstacles, *The International Journal of Robotics Research*, 17(7), pp. 760–772. 116

Fruin, J. (1971) Designing for pedestrians: A level-of-service concept, *Highway Research Record*, 355, pp. 1–15. 13, 24

Fruin, J. (1993) The causes and prevention of crowd disasters, In: Smith, R., and J. Dickie, eds., *Engineering for Crowd Safety*, pp. 99–108. 2

Gidel, S., P. Checchin, C. Blanc, T. Chateau, and L. Trassoudaine (2010) Pedestrian detection and tracking in an urban environment using a multilayer laser scanner, *IEEE Transactions on Intelligent Transportation Systems*, 11(3), pp. 579–588. 42

Goffman, E. (1972) *Relations in public: microstudies of the public order*, Basic books, New York. 18, 58, 111

Gorrini, A., S. Bandini, M. Sarvi, C. Dias, and N. Shiwakoti (2013) An empirical study of crowd and pedestrian dynamics: the impact of different angle paths and grouping, In: *Annual meeting of the Transportation Research Board 2013*, p. 01472448. 23

Greenshields, B. D. (1934) A study of traffic capacity, *Proceedings Highway Research Board*, 14, pp. 448–447. 92

Guo, R.-Y., S. Wong, Y.-H. Xia, H.-J. Huang, W. Lam, and C. Choi (2012) Empirical evidence for the look-ahead behavior of pedestrians in bi-directional flows, *Chinese Physical Letters*, 29(6), p. 068901. 25

Hankin, B., and R. Wright (1958) Passenger flow in subways, *Operational Research*, 9(2), pp. 81–88. 41

Hänseler, F., M. Bierlaire, B. Farooq, and T. Mühlematter (2014) A macroscopic loading model for time-varying pedestrian flows in public walking areas, *Transportation Research - part B: Methodological*, 69, pp. 60–80. 116, 127, 128

Hänseler, F., W. Lam, M. Bierlaire, R. Scarinci, and G. Lederrey (2016) A macroscopic loading model for dynamic multi-directional and congested pedestrian flows, In: *Traffic and Granular Flow '15 (TGF'15)*, p. inprint. 172

Helbing, D. (1997) *Verkehrsdynamik: Neue physikalische Modellierungskonzepte*, Springer-Verlag Berlin Heidelberg. 127, 128

Helbing, D. (2001) Traffic and related self-driven many-particle systems, *Reviews of Modern Physics*, 73(4). 114

Helbing, D., L. Buzna, A. Johansson, and T. Werner (2005) Self-organized pedestrian crowd dynamics: Experiments, simulations, and design solutions, *Transportation Science*, 39, pp. 1–24. 24, 25, 114

Helbing, D., I. Farkas, and T. Vicsek (2000) Simulating dynamical features of escape panic, *Nature*, 407, pp. 487–490. 114, 122

Helbing, D., and A. Johansson (2010) Pedestrian, crowd and evacuation dynamics, *Encyclopedia of complexity and System Science*, 16, pp. 6476–6495. 22, 24, 105, 110

Helbing, D., A. Johansson, and H. Al-Abideen (2007a) Crowd turbulence - the physics of crowd disasters, In: Chien, W., ed., *The Fifth International Conference on Nonlinear Mechanics (ICNM-V)*, Shanghai university press, pp. 967–969. 22

Helbing, D., A. Johansson, and H. Al-Abideen (2007b) The dynamics of crowd disasters: an emperical study, *Physical Review - Part E*, 75, p. 046109. 22, 111

Helbing, D., and P. Molnar (1995) Social force model for pedestrian dynamics, *Physical Review - Part E*, 51, pp. 4282–4286. 27, 32, 114, 133

Helbing, D., and P. Molnar (2001) Self-organizing pedestrian movement, *Environment and Planning B: Planning and Design*, 28, pp. 361–383. 3, 122

Helbing, D., and P. Mukerji (2012) Crowd disasters as systemic failures: analysis of the love parade disaster, ETH Risk Center - Working paper series ETH-RC-12-010, ETH. 2

Henderson, L. (1971) The statistics of crowd fluids, *Nature*, 229, pp. 381–383. 13, 15

Henderson, L. (1974) On the fluid mechanics of human crowd motion, *Transportation Research*, 8(6), pp. 505–515. 114

Hill, M. (1982) *Spatial structure and decision-making aspects of pedestrian route selection through an urban environment*, Phd thesis, University of Nebraska. 18

Hiyoshi, H., Y. Tanioka, T. Hamamoto, K. Matsumoto, and K. Chiba (2014) Pedestrian movement model based on voronoi cellular automata, In: Daamen, W., D. Duives, and S. Hoogendoorn, eds., *The conference of Pedestrian and Evacuation Dynamics 2014 (PED2014)*, vol. 2 of *Transportation Research Procedia*, pp. 336–343. 114

Hoel, L. (1968) Pedestrian travel rates in central business districts, *Traffic Engineering*, 38(4), pp. 10–13. 16

Hoogendoorn, S. (2004) Walking behavior in bottlenecks and its implications for capacity, In: *Proceedings of the 84th Annual meeting of the Transportation Research Board*, Washington, D.C., pp. –. 23

Hoogendoorn, S., and P. Bovy (2002) Normative pedestrian behaviour theory and modelling, In: Taylor, M., ed., *Transportation and Traffic Theory in the 21st Century, Proceedings of the 15th International Symposium on Transportation and Traffic Theory*, pp. 219–245. 130, 132

Hoogendoorn, S., and P. Bovy (2004) Pedestrian route-choice and activity scheduling theory and models, *Transportation Research - Part B: Methodological*, 38, pp. 169–190. xxi, xxvii, 4, 5, 76, 110, 115, 127, 128, 130, 133, 134, 161

Hoogendoorn, S., and W. Daamen (2004) Self-organization in walker experiments, In: *Traffic and Granular Flow '04*, pp. 121–131. 25

Hoogendoorn, S., and W. Daamen (2005) Pedestrian behavior at bottlenecks, *Transportation Science*, 39(2), pp. 01247–0159. 24, 59

Hoogendoorn, S., W. Daamen, and R. Landman (2007) Microscopic calibration and validation of pedestrian models - cross-comparison of models using experimental data, In: Waldau, N., P. Gattermann, H. Knoflacher, and M. Schreckenberg, eds., *Pedestrian and Evacuation Dynamics 2005 (PED2005)*, Springer Berlin Heidelberg, pp. 253–265. 145

Hoogendoorn, S., F. v. Wageningen-Kessels, W. Daamen, and D. Duives (2014) Continuum modelling of pedestrian flows: From microscopic principles to self-organised macroscopic phenomena, *Physica A: Statistical Mechanics and its Applications*, 416, pp. 684–694. xxi, xxvii, 116, 123, 124, 127, 128, 133, 159, 160, 161, 162, 165, 171, 172, 184, 189

Hoogendoorn, S., F. v. Wageningen-Kessels, W. Daamen, M. Sarvi, and D. Duives (2015) Continuum theory for pedestrian traffic flow: Local route choice modelling and its implications, *Transportation Research - Part C: Emerging Technologies*, 59, pp. 183–197. 159, 161, 162, 163, 165, 171, 184

Hoogendoorn, S., H. v. Zuylen, M. Schreuder, B. Gorte, and G. Vosselman (2003) Microscopic traffic data collection by remote sensing, *Transportation Research Record*, 1855, pp. 121–132. 44

Hughes, R. (2002) A continuum theory for the flow of pedestrians, *Transportation Research - Part B: Methodological*, 36, pp. 507–535. 116

Hunt, J., E. Poulton, and J. Mumford (1976) The effects on wind on people; new criteria based on wind tunnel experiments, *Building and Environment*, 11, pp. 15–28. 16

Isenhour, M., and R. Löhner (2014) Verification of a pedestrian simulation tool using the nist recommended test cases, In: Daamen, W., D. Duives, and S. Hoogendoorn, eds., *The Conference on Pedestrian and Evacuation Dynamics 2014 (PED 2014)*, vol. 2 of *Transporation Research Procedia*, pp. 237–245. 2, 132, 187

Jaklin, N., A. Cook, and R. Geraerts (2013) Real-time path planning in hetrogeneous environments, *Computer animation & virtual worlds*, 24(3-4), pp. 285–295. 2

Jiang, Y., S. Zhou, and F. Tian (2015) A hihigh-order macroscopic model for bi-directional pedestrian flow, *Physica A: Statistical Mechanics and its Applications*, 425, pp. 69–78. 116

Jiayue, W., W. Wengua, and Z. Xiaole (2014) Comparison of turbulent pedestrianbehaviors between mina and love parade, In: Feng, C., and S. Li, eds., *International Symposium on Safety Science and Technology*, vol. 84 of *Procedia Engineering*, pp. 708–714. 22

Johansson, A. (2009a) Constant net-time headway as key mechanism behind pedestrian flow dynamics, *Physical Review E*, 80(026120). 28

Johansson, A. (2009b) *Data-driven modeling of pedestrian crowds*, Ph.D. thesis, Technische Universit/"at Dresden, p. 75-79. 145

Johansson, F., D. Duives, W. Daamen, and S. Hoogendoorn (2014) The many roles of the relaxation time parameter in force based models of pedestrian dynamics, In: Daamen, W., D. Duives, and S. Hoogendoorn, eds., *The Conference on Pedestrian and Evacuation Dynamics 2014 (PED2014)*, vol. 2 of *Transportation Research Procedia*, Elsevier, pp. 300–308. 177

Johansson, F., A. Peterson, and A. Tapani (2015) Waiting pedestrians in the social force model, *Physica A: Statistical Mechanics and its Applications*, 419, pp. 95–107. 115, 133

Jordan, S., T. Johnson, M. Sterling, and C. Baker (2008) Evaluating and modelling the response of an individual to a sudden change in wind speed, *Building and Environment*, 43, pp. 1521–1534. 17

Karamouzas, I., and M. Overmars (2010) A velocity-based approach for simulating human collision avoidance, *Lecture Notes in Computer Science*, 6356, pp. 180–186. 116

Keij, J. (2014) *Smart phone counting: Location-based applications using mobile phone location data*, Msc. thesis, Delft University of Technology. 43

Kerdok, A. E., A. A. Biewener, T. A. McMahon, P. G. Weyand, and H. M. Herr (2002) Energetics and mechanics of human running on surfaces of different stiffnesses, *Journal of Applied Physiology*, 92, pp. 469–478. 17

Kholshevnikov, V., T. Shields, K. Boyce, and D. Samoshin (2008) Recent developments in pedestrian flow theory and research in russia, *Fire Safety Journal*, 43, pp. 108–118. 22

Kitazawa, K., and T. Fujiyama (2010) Pedestrian vision and collision avoidance behavior: investigation of the information process space of pedestrians using an eye tracker, In: Klingsch, W., C. Rogsch, A. Schadschneider, and M. Schreckenberg, eds., *Pedestrian and Evacuation Dynamics 2008 (PED2008)*, Springer, London, UK, pp. 95–108. 59

Knoblauch, R., M. Pietrucha, and M. Nitzburg (1996) Field studies of pedestrian walking speed and start-up time, *Transportation Research Record*, 1538, pp. 27–38. 15, 16

Knoppers, P., H. Lint, and S. P. Hoogendoorn (2012) Automatic stabilization of aerial traffic images, In: *Annual meeting of the Transportation Research Board*, pp. 12–1674. 47

Köster, G., D. Hartmann, and W. Klein (2011) Microscopic pedestrian simulations: From passenger exchange times to regional evacuation, In: Hue, B., K. Morasch, S. Pickl, and M. Siegle, eds., *Operations Research Proceedings 2010*, Operations Research Proceedings, pp. 571–576. 114, 123

Koushki, P. (1988) Walking characteristics in central riyadh, saudi arabia, *Journal of Transportation Engineering*, 114(6), pp. 735–744. 15, 22

Kraft, T., D. Wang, J. Delawder, D. WenWen, Y. Li, and W. Ribarsky (2013) Less after-the-fact: Investigative visual analysis of events from streaming twitter, In: *IEEE symposium on large-scale data analysis and visualization (LDAV)*, IEEE, pp. 95–103. 44

Kretz, T. (2014) The effect of integrating travel time, In: Weidmann, U., U. Kirsch, and M. Schreckenberg, eds., *Pedestrian and Evacuation Dynamics 2012*, vol. Part III, pp. 1013–1027. 123

Kretz, T., A. Grunebohm, M. Kaufman, F. Mazur, and M. Schreckenberg (2006a) Experimental study of pedestrian counterflow in a corridor, *Journal of Statistical Mechanics: Theory and Experiment*, p. P10001. 24, 25

Kretz, T., A. Grunebohm, and M. Schreckenberg (2006b) Experimental study of pedestrian flow through a bottleneck, *Journal of Statistical Mechanics: Theory and Experiment*, p. P10014. 23, 31

Lam, W., J. Lee, and C. Cheung (2002) A study of the bi-directional pedestrian flow characteristics at hong kong signalized crosswalk facilitie, *Transportation*, 29, pp. 169–192. 24, 25

Lam, W., J. Morrall, and H. Ho (1995) Pedestrian flow characteristics in hong kong, *Transportation Research Record*, 1487, pp. 56–62. 15, 22

LeBon, G. (1895) *Psychologie der Massen*, Stuttgart: Kröner, Stuttgart. 5

Lee, R. S., and R. Hughes (2006) Prediction of human crowd pressures, *Accident Analysis & Prevention*, 38(4), pp. 712–722. 2

Leicht, A. S., and R. G. Crowther (2008) Pedometer accuracy during walking over different surfaces, *Medicine & science in sports & exercise*, 39(10), pp. 1847–1850. 17

Leng, B., J. Wang, W. Zhao, and Z. Xiong (2014) An extended floor field model based on regular hexagonal cells for pedestrian simulation, *Physica A: Statistical Mechanics and its Applications*, 402, pp. 119–133. 114

Liao, W., A. Seyfried, J. Zhang, M. Boltes, X. Zheng, and Y. Zhao (2014) Experimental study on pedestrian flow through wide bottleneck, In: Daamen, W., D. Duives, and S. Hoogendoorn, eds., *The conference on Pedestrian and Evacuation Dynamics (PED2014)*, vol. 2 of *Transportation Research Procedia*, pp. 26–33. 23

Liao, W., A. Tordeux, M. Crhraibi, A. Seyfried, X. Zheng, and Y. Zhao (in print) Steady state of pedestrian flow in bottleneck, In: *Traffic and Granular Flow (TGF'15)*, p. in print. 192

Liddle, J., A. Seyfried, W. Klingsch, T. Rupprecht, A. Schadschneider, and A. Winkens (2009) An experimental study of pedestrian congestions: influence of bottleneck width and length, In: *Traffic and Granular Flow 2009 (TGF 2009)*, pp. 1–6. 23, 24, 31

Liu, X., W. Song, and Lv (2014) Empirical data for pedestrian counter flow through bottlenecks in the channel, In: Daamen, W., D. Duives, and S. Hoogendoorn, eds., *The conference on Pedestrian and Evacuation Dynamics (PED2014)*, vol. 2 of *Transportation Research Procedia*, pp. 34–42. 25

Lovas, G. (1994) Modeling and simulation of pedestrian traffic flow, *Transportation Research - Part B:*, 28(6), pp. 429–433. 118

Lv, W., Z. Fang, X. Wei, W. Song, and X. Liu (2013) Experiment and modelling for pedestrian following behavior using velocity-headway relation, In: Liu, N., and N. Fong, eds., *The 9th Asia-Ociania Symposium on Fire Science and Technology*, vol. 62 of *Procedia Engineering*, Procedia Engineering, pp. 525–531. 22

Malinovskiy, Y., Y. Wang, and N. Saunier (2012) Pedestrian travel analysis using static bluetooth sensors, *Transportation Research Record*, 2299, p. 137149. 43

Masoud, O., and N. Papanikolopoulos (2001) A novel method for tracking and counting pedestrians in real-time using a single camera, *IEEE Transactions on Vehicular Technology*, 50(5), pp. 1267–1278. 42

McPhail, C. (1991) *The Myth of the Madding Crowd*, A. de Gruyter. 5

Milinskii, A. (1951) *The study of egress processes from public buildings of mass use*, Phd thesis, Moscow Civil Engineering Institute. 21, 22, 41

Minetti, A. E., C. Moia, G. S. Roi, D. Susta, and G. Ferretti (2002) Energy cost of walking and running at extreme uphill and downhill slopes, *Journal of Applied Physiology*, 93, pp. 1039–1046. 17

Mori, M., and H. Tsukaguchi (1987) A new method for evaluation of level of service in pedestrian facilities, *Transportation Research - Part A: Policy and Practice*, 21(3), pp. 223–234. 22

Moussaïd, M., E. Guillot, M. Moreau, J. Fehrenbach, O. Chabiron, S. Lemercier, J. Pettre, C. Appert-Rolland, P. Degond, and G. Theraulaz (2012) Traffic instabilities in self-organized pedestrian crowds, *PLoS Comput Biology*, 8(3), p. e1002442. 109, 135

Moussaïd, M., D. Helbing, S. Garnier, A. Johansson, M. Combe, and G. Theraulaz (2009) Experimental study of the behavioural mechanisms underlying self-organization in human crowds., *Proceedings of the Royal Society*, 276, pp. 2755–2762. 13, 18

Moussaïd, M., D. Helbing, and G. Theraulaz (2011) How simple rules determine pedestrian behavior and crowd disasters, *PNAS*, 108(17), pp. 6884–6888. 27, 32, 67, 116, 133

Moussaïd, M., N. Perozo, S. Garnier, D. Helbing, and G. Theraulaz (2010) The walking behavior of pedestrian social groups and its impact on crowd dynamics, *PLoS ONE*, 5(4), p. e10047. 5, 115, 116

Murray, M., A. Drought, and R. Kory (1964) Walkin gpatterns of normal men, *Journal of Bone and Joint Surgery*, 46(A), pp. 335–360. 97

Navin, F., and R. Wheeler (1969) Pedestrian flow characteristics, *Traffic Engineering*, 39, pp. 31–36. 15, 24, 25

Nikolić, M., M. Bierlaire, and F. Hänseler (in print) Data-driven characterization of multidirectional pedestrian traffic, In: *Traffic and Granular Flow (TGF'15)*, p. in print. 192

O'Flaherty, C., and M. Parkinson (1972) Movement on a city centre footway, *Traffic Engineering and Control*, 13, pp. 434–438. 22

Ossen, S., and S. P. Hoogendoorn (2005) Car-following behavior analysis from microscopic trajectory data, *Transportation Research Record*, 1934, pp. 13–21. 67

Papadimitriou, E., G. Yannis, and J. Golias (2009) A critical assessment of pedestrian behavior models, *Transportation Research - Part F*, vol. 12, pp. pp. 232 – 255. 105, 110

Paris, J. P., S., and S. Donikian (2007) Pedestrian reactive navigation for crowd simulation: a predictive approach, In: Cohen-Or, D., and P. Slavik, eds., *Eurographics 2007*, vol. 26, Computer Graphics Forum, pp. 665–674. 27, 28, 32, 67, 116

Pettre, J., J. Ondrej, A.-H. Olivier, A. Cretual, and S. Donikan (2009) Experiment-based modeling, simulation and validation of interactions between virtual walkers, In: *Proceedings of the 2009 ACM SGGRAPH/ Eurographics Symposium on Computer Animation*. 60

Plaue, M., M. Chen, G. Bärwolff, and H. Schwandt (2011) Trajectory extraction and density analysis of intersecting pedestrian flows from video recordings, In: Stilla, U., F. Rottensteiner, H. Mayer, B. Jutzi, and M. Butenuth, eds., *Proceedings of the 2011 ISPRS conference on Photogrammetric image analysis (PIA'11)*, pp. 285–296. 26

Predtechenskii, V., and A. Milinskii (1969) *Planning for Foot Traffic Flow in Buildings*, Stroiizdat Publishers. 13

Punzo, V., B. Ciuffo, and M. Montanino (2012) Can results of car-following model calibration based on trajectory data be trusted?, *Transportation Research Record*, 2315, pp. 11–24. 145

Qi, Z. (2015) Simulation model of bi-directional pedestrian considering potential effect ahead and behind, *Physica A: Statistical Mechanics and its Applications*, 419, pp. 335–348. 114

Quan, Y., D. Xiaohui, and L. Ning (2011) A pedestrian speed acquisition experiment based on rfid, In: *International conference on transportation, mechanical, and electrical engineering (TMEE)*, pp. 903–906. 42

Rahman, K., N. Ghani, and A. Kamil (2012) Analysis of pedestrian free flow walking speed in a least developing country: A factorial design study, *Research Journal in Applied Sciences: Engineering and Technology*, 4(21), pp. 4299–4304. 22

Robin, T., G. Antonini, M. Bierlaire, and J. Cruz (2009) Specification, estimation and validation of a pedestrian walking behavior model, *Transportation Research - Part B: Methodological*, 43, pp. 36–56. 117

Rotton, J., M. Shats, and R. Standers (1990) Temperature and pedestrian tempo: Walking without awareness, *Environment and Behavior*, 22, pp. 650–574. 16

Rudloff, C., T. Matyus, S. Seer, and D. Bauer (2011) Can walking behavior be predicted? analysis of calibration and fit of pedestrian models, *Transportation Research Record*, 2264, pp. 101–109. 133, 145

Saberi, M., K. Aghabayk, and A. Sobhani (2015) Spatial fluctuations of pedestrian velocities in bidirectional streams: Exploring the effects of self-organisation, *Physica A: Statistical Mechanics and its Applications*, 434, pp. 120–128. 25

Sarkar, A., and K. Janardhan (1997) A study on pedestrian flow characteristics, In: *Annual meeting of the Transportation Research Board - CD-rom*, pp. –. 22

Sarmady, S. (2010) Simulating crowd movements using fine grid cellular automata, In: *12th International Conference on Computer Modelling and Simulation (UKSim)*, pp. 428–433. 114

Schadschneider, A. (2002) Cellular automaton approach to pedestrian dynamics, In: Schreckenberg, M., and S. Sharma, eds., *Pedestrian and Evacuation Dynamics*, pp. 75–86. 114

Schadschneider, A., H. Klüpfel, T. Kretz, C. Rogsch, and A. Seyfried (2009) *Multi-Agent Systems for Traffic and Transportation Engineering*, chap. Fundamentals of Pedestrian and Evacuation Dynamics, IGI Global, Hershey, Pennsylvania, p. 124154. 105, 110

Seer, S., N. Brändle, and C. Ratti (2014) Kinects and human kinetics: A new approach for studying pedestrian behavior, *Transportation research part C: Emerging Technologies*, 48, pp. 212–228. 42, 133, 145, 146

Seitz, M., F. Dietrich, and G. Köster (2014) A study of pedestrian stepping behaviour for crowd simulation, In: Daamen, W., D. Duives, and S. Hoogendoorn, eds., *The Conference of Pedestrian and Evacuation Dynamics 2014 PED2014*, vol. 2 of *Research Procedia*, pp. 282–290. 79

Seyfried, A., O. Passon, B. Steffen, M. Boltes, T. Rupprecht, and W. Klingsch (2009) New insights into pedestrian flow through bottlenecks, *Transportation Science*, 43, pp. 395–406. 23, 24

Seyfried, A., B. Steffen, W. Klingsch, and M. Boltes (2007) The fundamental diagram of pedestrian movement revisited, In: Schadschneider, A., T. Pöschel, R. Kühne, M. Schreckenberg, and D. Wolf, eds., *Traffic and Granular Flow '05*, pp. 305–314. 13, 22, 94

Song, W., W. Lv, and Z. Fang (2013) Experiment and modeling of microscopic movement characteristic of pedestrians, In: Liu, N., ed., *The 9th Asia-Oceania Symposium on Fire Science and Technology*, vol. 62 of *Procedia Engineering*, pp. 56–70. 22

Song, W., Y. Yu, W. Fan, and H. Zhang (2005) A cellular automata evacuation model considering friction and repulsion, *Science in China - Series E: Technological Sciences*, 48(4), pp. 403–413. 114

Song, W., J. Zhang, and A. Seyfried (2011) Experimental study of pedestrian flow in the channel through bottleneck, In: Peacock, R., E. Kuligowski, and J. Averill, eds., *Pedestrian and Evacuation Dynamics*, Springer US, pp. 875–879. 23, 24

Steffen, B., and A. Seyfried (2009) Modelling of pedestrian movement around 90 and 180 bends, In: *Advanced Research Workshop "Fire Protecion and Life Safety in Buildings and Transportation Systems"*. 3, 23, 31

Steffen, B., and A. Seyfried (2010) Methods for measuring pedestrian density, flow, speed and direction with minimal scatter, *Physica A: Statistical Mechanics and its Applications*, 389(9), pp. 1902–1910. 58

Strege, S., and M. Ferreira (2014) Modelling occupant ingress at a secure building and using field measurements for calibration, In: Daamen, W., D. Duives, and S. Hoogendoorn, eds., *The conference on Pedestrian and Evacuation Dynamics 2014*, vol. 2 of *Transportation Research Procedia*, pp. 807–812. 133

Suma, Y., D. Yanagisawa, and K. Nishinari (2012) Anticipation effect in pedestrian dynamics: Modelling and experiments, *Physica A:*, 391, pp. 248–263. 114

Sun, D., S. Roth, and M. J. Black (2010) Secrets of optical flow estimation and their principles, *IEEE Conf. on Computer Vision and Pattern Recognition (CVPR)*, pp. 2432–2439. 48

Sun, D., S. Roth, J. P. Lewis, and M. J. Black (2008) Learning optical flow, *Lecture Notes on Computer Science*, 5304, pp. 5383–5397. 48

Tanariboon, Y., and J. Guyano (1991) Analysis of pedestrian movements in bangkok, *Transportation Research Record*, 1294, pp. 52–56. 15, 22

Tanariboon, Y., S. Hwa, and C. Chor (1986) Pedestrian characteristics study in singapore, *Journal of Transportation Engineering*, 112(3), pp. 229–235. 15, 22

Tian, W., W. Song, W. Lv, and Z. Fang (2011) Experiment and analysis on microscopic characteristic pedestrian movement in building bottleneck, *Science China Technological Sciences*, 54(7), pp. 1730–1736. 15

Treiber, M. (2015) Crowd flow modeling of athletes in mass sports events: a macroscopic approach, In: Chraibi, M., M. Boltes, A. Schadschneider, and A. Seyfried, eds., *Traffic and Granular Flow '13*, pp. 21–29. 42

Treuille, A., S. Cooper, and Z. Popovic (2006) Continuum crowds, *ACM Transportation Graphics*, 25, pp. 1160–1168. 116

Versluis, D. (2010) *Microscopic interaction behavior between individual pedestrians*, Msc. thesis, Delft University of Technology. 18, 26

Volonoshina, A. S., A. D. Kuo, M. A. Daley, and D. P. Ferris (2013) Biomechanics and energetics of walking on uneven terrain, *Journal of Experimental Biology*, 216, pp. 3963–3970. 17

Wageningen-Kessels, F. v., W. Daamen, and S. P. Hoogendoorn (2015) The two-dimensional godunov scheme and what it means for continuum pedestrian flow models, In: *4th Symposium of the European Association of Research in Transportation (hEART 2015)*, Lyngby, Denmark. 162

Walmsley, J., and G. Lewis (1989) The pace of pedestrian flows in cities, *Environment and Behavior*, 21(2), pp. 123–150. 16

Wang, J., W. Weng, and X. Zhang (2014) Comparison of turbulent pedestrian behaviors between mina and love parade, *Proceedia Engineering*, 84, pp. 708–714. 2

Wei, J., H. Zhang, Y. Guo, and M. Gu (2015) Experiment of bi-directional pedestrian flow with three-dimensional cellular automata, *Physics Letter*, 379, pp. 1081–1086. 114

Weidmann, U. (1993) Transporttechnik der fussgänger, Tech. rep., Institut für Verkehrsplanung, Transporttechnik, Strassen- und Eisenbahnbau (Zürich). 17, 24, 94, 111, 164

Wijermans, N. (2011) *Understanding Crowd Behaviour: Simulating Situated Individuals*, Phd thesis, University of Groningen. 5, 118

Wolf, M. (1973) *Peoples in Places: The Sociology of the Familiar*, book Notes on the behavior of pedestrians., New York: Praeger Publishers, New York, pp. 35–48. 18

Wolinski, D., S. Guy, A.-H. Olivier, M. Lin, D. Manocha, and J. Pettré (2014) Parameter estimation and comparative evalutation of crowd simulations, In: Lévy, B., and J. Kautz, eds., *EUROGRAPHICS 2014*, vol. 33, pp. 303–312. 133, 145

Wong, S., W. Leung, S. Chan, and W. Lam (2010) Bidirectional pedestrian stream model with oblique intersecting angle, *Journal of Transportation Engineering*, 136(3), pp. 234–242. 26

Xi, H., Y.-J. Son, and S. Lee (2010) An integrated pedestrian behavior model based on extended decision field theory and social force model, In: *Human0in-the-Loop Simulations*, pp. 69–95. 115, 127, 128

Xiong, M., W. Cai, S. Zhou, M. Y.-H. Low, F. Tian, D. Chen, D. Ong, and B. Hamilton (2009) A case study of multi-resolution modeling for crowd simulation, In: *2009 Spring Simulation Multiconference*, p. 17. 117

Xiong, M., M. Lees, W. Cai, S. Zhou, and M. Y. Low (2010) Hybrid modelling of crowd simulation, In: *International Conference on Computer Science (ICCS 2010)*, vol. 1 of *Procedia Computer Science*, pp. 57–65. 116, 117, 133

Yanagisawa, D., A. Kimuar, and A. Tornoeda (2009) Introduction of frictional and turning function of pedestrian outflow with an obstacle, *Physical Review - Part E*, 80(3), p. 036110. 23

Yang, H., K. Ozbay, and B. Bartin (2010) Investigating the performance of automatic counting sensors for pedestrian traffic data collection, In: *Proceedings of the 12th World conference on transportation research*, vol. 1115, Lisbon, Portugal. 42

Yang, X., W. Daamen, S. Hoogendoorn, C. Yao, and D. Hairong (2014) Breakdown phenomenon study in the bidirectional pedestrian flow, In: Daamen, W., D. Duives, and S. Hoogendoorn, eds., *Conference on Pedestrian and Evacuation Dynamics 2014 (PED2014)*, vol. 2 of *Transportation Research Procedia*, pp. 456–461. 153, 191

Yilmaz, A., O. Javed, and M. Shah (2006) Object tracking: A survey, *ACM computing surveys*, 38(4), p. 13. 44, 48

Yin, J. H., S. A. Velastin, and A. C. Davies (1996) Image processing techniques for crowd density estimation using a reference image, *Recent Developments in Computer Vision - Lecture Notes in Computer Science*, 1035, pp. 489–498. 48

Zhang, J., W. Klingsch, T. Rupprecht, A. Schadschneider, and A. Seyfried (2011a) Empirical study of turning and merging of pedestrian streams in t-junction, In: *Fourth International Symposium on Agent-Based Modeling and Simulation (ABModSim-4)*. 42, 83

Zhang, J., W. Klingsch, A. Schadschneider, and A. Seyfried (2011b) Transitions in pedestrian fundamental diagram of straight corridors and t-junctions, *Journal of Statistical Mechanics: Theory and Experiment*, 6, p. P06004. 23, 94

Zhang, J., W. Klingsch, A. Schadschneider, and A. Seyfried (2012) Ordering in bidirectional pedestrian flows and its influence on the fundamental diagram, *Journal of Statistical Mechanics*, p. P02002. 24, 25

Zhang, J., W. Klingsch, and A. Seyfried (2010) High precision analysis of unidirectional pedestrian flow within the hermes project, In: *The fifth Performance-based Fire Protection and Fire Protection Engineering Seminars*, p. arXiv:1207.5929. 22

Zhang, J., A. Schadschneider, and A. Seyfried (2014) Empirical fundamental ddiagram for bidirectional pedestrian streams in a corridor, In: Weidmann, U., U. Kirsch, and M. Schreckenberg, eds., *Pedestrian and Evacuation Dynamics (PED2012)*, pp. 245–250. 25

Zhang, J., and A. Seyfried (2014a) Comparison of intersecting pedestrian flows based on experiments, *Physica A: Statistical Mechanics and its Applications*, 405, pp. 316–325. 26

Zhang, J., and A. Seyfried (2014b) Quantification of bottleneck effects for different types of facilities, In: Daamen, W., D. Duives, and S. Hoogendoorn, eds., *The conference on Pedestrian and Evacuation Dynamics (PED2014)*, vol. 2 of *Transportation Research Procedia*, pp. 51–59. 23

Zhang, J., W. Song, and X. Xu (2008) Experiment and multi-grid modeling of evacuation from a classroom, *Physica A: Statistical Mechanics and its Applications*, 387, pp. 5901–5909. 23, 31

Zhang, X., W. Weng, H. Yuan, and J. Chen (2013) Empirical study of a unidirectional dense crowd during a real mass event, *Physica A:*, 392, pp. 2781–2791. 22, 42

Appendix A

Movement base cases for sensitivity analyses of pedestrian simulation models

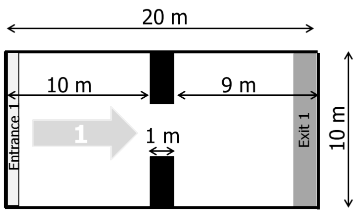

(a) Uni-directional bottleneck

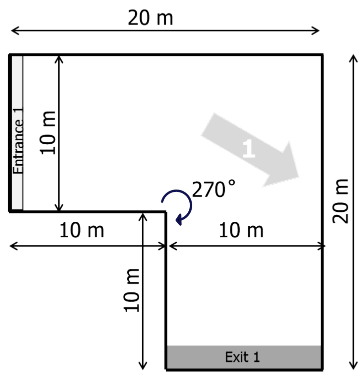

(b) Uni-directional corner

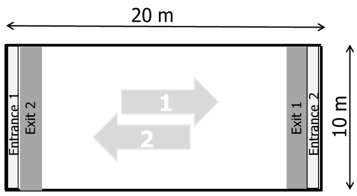

(c) Bi-directional straight

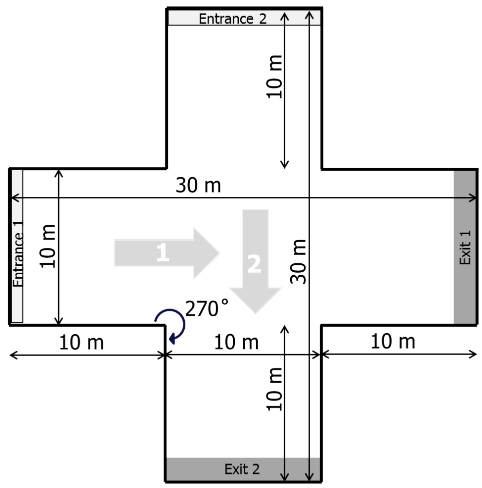

(d) Intersecting

Figure A.1: Layout of the movement base cases adopted in the sensitivity analyses

Appendix B

Data sets used for the calibration and assessment of Nomad and the MDW model

Table B.1: Characteristic of the cases that are used in the calibration

Flow sit.	Calibration /Validation	Demand Level	Nr.	q_{total}	ρ	v	% of flow per entrance
UD - S	Calibration	low	1	3.40	0.60	1.31	
			2	6.10	2.27	0.59	
		high	3	4.86	3.24	0.48	
			4	4.05	3.38	0.34	
	Assessment	low	1	4.20	0.69	0.92	
			2	5.23	1.05	1.23	
			3	7.20	1.66	0.87	
		high	4	5.20	3.17	0.43	
			5	7.05	3.31	0.50	
BD - S	Calibration	low	1	0.58	0.47	0.65	0.72/0,28
			2	1.87	0.66	0.9	0.87/0.13
		high	3	1.51	0.69	0.62	0.56/0.44
			4	1.73	0.9	0.5	0.76/0.24
	Assessment	low	1	1,35	0.59	0.8	0,78/0,22
			2	1.91	0.61	0.83	0.70/0.30
			3	2.39	0.65	0.98	0.72/0.28
		high	4	1.71	0.69	0.78	0.68/0.32
			5	2.40	0.74	0.68	0.71/0.29
UD - E	Calibration	low	1	1.04	0.35	0.88	
			2	4.74	0.65	1.07	
		high	3	2.05	1.22	0.40	
			4	2.94	1.96	0.26	
	Assessment	low	1	1.59	0.29	1.22	
			2	0.50	0.42	0.61	
			3	3.50	0.51	1.44	
		high	4	2.77	0.74	0.74	
			5	2.37	2.00	0.20	
UD - C	Calibration	low	1	0.33	0.23	1.19	
			2	0.77	0.27	1.23	
			3	2.24	0.5	1.18	
		high	4	3.87	0.69	1.05	
			5	3.96	0.93	0.83	
	Assessment	low	1	0.43	0.25	1.17	
			2	0.55	0.24	1.15	
			3	2.01	0.41	1.29	
		high	4	3.17	0.75	0.88	
			5	2.36	0.89	0.63	
X	Calibration	low	1	1.11	0.27	0.94	0.06/0.23/0.45/0.25
			2	5.02	0.69	0.53	0.11/0.21/0.36/0.31
		high	3	10.7	0.73	0.92	0.16/0.18/0.35/0.31
	Assessment	low	1	3.33	0.56	0.50	0.13/0.20/0.36/0.29
			2	4.82	0.66	0.55	0.15/0.19/0.34/0.31
		high	3	9.33	0.72	0.85	0.15/0.167/0.35/0.33

Appendix C

Tables featuring the calibration and assessment of Nomad

Table C.1: Results of the calibration of a uni-direction straight movement base case - case: 4Daagse in Wijchen.

Nr.	$w_{macro/micro}$	w_d	w_v	$w_{h_{pq}}$	w_{TTC}	$w_{V_{pg}}$	$w_{spatialdist}$	$O(a_0,\tau,r_0)$	τ	a_0	r_0
1	1	1	0	0	0	0	0	0.90	0.270	11.0	0.1600
2	1	0	1	0	0	0	0	0.88	0.265	10.6	0.1600
3	1	0.5	0.5	0	0	0	0	0.89	0.265	10.6	0.1600
4	0	0	0	1	0	0	0	0.92	0.275	11.0	0.1568
5	0	0	0	0	1	0	0	0.75	0.230	10.0	0.1440
6	0	0	0	0	0	1	0	0.48	0.270	11.0	0.1600
7	0	0	0	0.5	0.5	0	0	0.79	0.275	10.6	0.1600
8	0	0	0	0.5	0	0.5	0	0.69	0.275	10.6	0.1600
9	0	0	0	0	0.5	0.5	0	0.56	0.275	10.6	0.1600
10	0	0	0	0.33	0.33	0.33	0	0.68	0.275	10.6	0.1600
11	0.25	0.125	0.125	0.125	0.25	0.25	0	0.73	0.275	10.6	0.1600
12	0.5	0.25	0.25	0.167	0.167	0.167	0	0.78	0.275	10.6	0.1600
13	0.75	0.375	0.375	0.083	0.083	0.083	0	0.84	0.275	10.6	0.1600
14	0	0	0	0	0	0	1	0.32	0.255	11.0	0.1536
15	1	0.25	0.25	0	0	0	0.5	0.59	0.255	11.0	0.1536
16	0	0	0	0.167	0.167	0.167	0.5	0.43	0.255	11.0	0.1536
17	0.5	0.167	0.167	0.11	0.11	0.11	0.33	0.58	0.275	10.6	0.1600

Table C.2: Results of the calibration of a uni-direction entering movement base case - case: Rotterdam Marathon

Nr.	$w_{macro/micro}$	w_v	w_d	$w_{h_{pq}}$	w_{TTC}	$w_{V_{pg}}$	$w_{spatialdist}$	$O(a_0,\tau,r_0)$	τ	a_0	r_0
1	1	1	0	0	0	0	0	0.83	0.225	9.0	0.1440
2	1	0	1	0	0	0	0	0.97	0.275	11.0	0.1600
3	1	0.5	0.5	0	0	0	0	0.89	0.225	9.0	0.1440
4	0	0	0	1	0	0	0	0.78	0.225	9.0	0.1440
5	0	0	0	0	1	0	0	0.77	0.265	10.4	0.1568
6	0	0	0	0	0	1	0	0.64	0.240	10.0	0.1440
7	0	0	0	0.5	0.5	0	0	0.72	0.265	10.4	0.1568
8	0	0	0	0.5	0	0.5	0	0.67	0.225	9.0	0.1440
9	0	0	0	0	0.5	0.5	0	0.66	0.260	10.2	0.1536
10	0	0	0	0.33	0.33	0.33	0	0.66	0.265	10.4	0.1568
11	0.25	0.125	0.125	0.125	0.25	0.25	0	0.71	0.265	10.4	0.1568
12	0.5	0.25	0.25	0.167	0.167	0.167	0	0.76	0.225	9.0	0.1440
13	0.75	0.375	0.375	0.083	0.083	0.083	0	0.82	0.225	9.0	0.1440
14	0	0	0	0	0	0	1	0.92	0.235	9.6	0.1504
15	1	0.25	0.25	0	0	0	0.5	0.88	0.235	9.6	0.1504
16	0	0	0	0.167	0.167	0.167	0.5	0.75	0.235	9.6	0.1504
17	0.5	0.167	0.167	0.11	0.11	0.11	0.33	0.78	0.235	9.6	0.1504

Table C.3: Results of the calibration of a uni-direction corner movement base case - case: 4Daagse - Lent

Nr.	$w_{macro/micro}$	w_v	w_d	$w_{h_{pq}}$	w_{TTC}	$w_{V_{pg}}$	$w_{spatialdist}$	$O(a_0,\tau,r_0)$	τ	a_0	r_0
1	1	1	0	0	0	0	0	0.97	0.275	10.4	0.1536
2	1	0	1	0	0	0	0	0.99	0.250	9.4	0.1504
3	1	0.5	0.5	0	0	0	0	0.98	0.250	9.4	0.1504
4	0	0	0	1	0	0	0	0.25	0.245	10.2	0.1600
5	0	0	0	0	1	0	0	0.82	0.225	10.0	0.1600
6	0	0	0	0	0	1	0	0.63	0.275	10.2	0.1600
7	0	0	0	0.5	0.5	0	0	0.52	0.225	10.0	0.1600
8	0	0	0	0.5	0	0.5	0	0.42	0.275	10.2	0.1600
9	0	0	0	0	0.5	0.5	0	0.69	0.275	10.6	0.1536
10	0	0	0	0.33	0.33	0.33	0	0.53	0.275	10.6	0.1536
11	0.25	0.125	0.125	0.125	0.25	0.25	0	0.64	0.275	10.6	0.1536
12	0.5	0.25	0.25	0.167	0.167	0.167	0	0.75	0.275	10.6	0.1536
13	0.75	0.375	0.375	0.083	0.083	0.083	0	0.87	0.275	10.6	0.1536
14	0	0	0	0	0	0	1	0.03	0.275	10.6	0.1600
15	1	0.25	0.25	0	0	0	0.5	0.51	0.275	10.6	0.1600
16	0	0	0	0.167	0.167	0.167	0.5	0.28	0.275	10.6	0.1536
17	0.5	0.167	0.167	0.11	0.11	0.11	0.33	0.51	0.275	10.6	0.1536

Table C.4: Results of the calibration of a bi-direction straight movement base case - case: Queensday in Amsterdam

Nr.	$w_{macro/micro}$	w_v	w_d	$w_{h_{pq}}$	w_{TTC}	$w_{V_{pg}}$	$w_{spatialdist}$	$O(a_0,\tau,r_0)$	τ	a_0	r_0
1	1	1	0	0	0	0	0	0.91	0.260	9.4	0.1568
2	1	0	1	0	0	0	0	0.97	0.270	10.8	0.1472
3	1	0.5	0.5	0	0	0	0	0.94	0.270	10.8	0.1440
4	0	0	0	1	0	0	0	0.92	0.265	9.2	0.1472
5	0	0	0	0	1	0	0	0.88	0.260	9.4	0.1568
6	0	0	0	0	0	1	0	0.17	0.260	9.4	0.1568
7	0	0	0	0.5	0.5	0	0	0.77	0.275	10.8	0.1472
8	0	0	0	0.5	0	0.5	0	0.48	0.265	9.2	0.1472
9	0	0	0	0	0.5	0.5	0	0.52	0.260	9.4	0.1568
10	0	0	0	0.33	0.33	0.33	0	0.53	0.275	10.8	0.1472
11	0.25	0.125	0.125	0.125	0.25	0.25	0	0.63	0.275	10.8	0.1472
12	0.5	0.25	0.25	0.167	0.167	0.167	0	0.73	0.275	10.8	0.1472
13	0.75	0.375	0.375	0.083	0.083	0.083	0	0.83	0.260	10.0	0.1568
14	0	0	0	0	0	0	1	0.74	0.225	9.6	0.1600
15	1	0.25	0.25	0	0	0	0.5	0.84	0.225	9.6	0.1600
16	0	0	0	0.167	0.167	0.167	0.5	0.60	0.250	9.8	0.1536
17	0.5	0.167	0.167	0.11	0.11	0.11	0.33	0.71	0.250	9.8	0.1536

Table C.5: Results of the calibration of an intersecting movement base case - case: Liberation day festival in Wageningen

Nr.	$w_{macro/micro}$	w_v	w_d	$w_{h_{pq}}$	w_{TTC}	$w_{V_{pg}}$	$w_{spatialdist}$	$O(a_0,\tau,r_0)$	τ	a_0	r_0
1	1	1	0	0	0	0	0	0.98	0.245	10.2	0.1440
2	1	0	1	0	0	0	0	0.99	0.255	10.0	0.1568
3	1	0.5	0.5	0	0	0	0	0.98	0.235	10.2	0.1568
4	0	0	0	1	0	0	0	0.58	0.230	10.0	0.1440
5	0	0	0	0	1	0	0	0.52	0.275	11.0	0.1568
6	0	0	0	0	0	1	0	0.41	0.245	9.0	0.1536
7	0	0	0	0.5	0.5	0	0	0.51	0.245	10.8	0.1568
8	0	0	0	0.5	0	0.5	0	0.42	0.240	10.4	0.1536
9	0	0	0	0	0.5	0.5	0	0.44	0.245	9.0	0.1536
10	0	0	0	0.33	0.33	0.33	0	0.44	0.240	10.4	0.1536
11	0.25	0.125	0.125	0.125	0.25	0.25	0	0.57	0.240	10.4	0.1536
12	0.5	0.25	0.25	0.167	0.167	0.167	0	0.71	0.240	10.4	0.1536
13	0.75	0.375	0.375	0.083	0.083	0.083	0	0.84	0.240	10.4	0.1536
14	0	0	0	0	0	0	1	0.38	0.260	11.0	0.1472
15	1	0.25	0.25	0	0	0	0.5	0.68	0.260	11.0	0.1472
16	0	0	0	0.167	0.167	0.167	0.5	0.38	0.245	9.0	0.1536
17	0.5	0.167	0.167	0.11	0.11	0.11	0.33	0.58	0.245	9.0	0.1536

Table C.6: Results of the calibration of several movement base cases - all series.

Nr.	$w_{macro/micro}$	w_d	w_v	$w_{h_{pq}}$	w_{TTC}	$w_{V_{pg}}$	$w_{spatialdist}$	$\bar{O}(a_0,\tau,r_0)$	τ	a_0	r_0
1	1	1	0	0	0	0	0	0.91	0.225	9.0	0.1440
2	1	0	1	0	0	0	0	0.98	0.265	10.8	0.1600
3	1	0.5	0.5	0	0	0	0	0.94	0.265	10.8	0.1600
4	0	0	0	1	0	0	0	0.61	0.225	9.6	0.1536
5	0	0	0	0	1	0	0	0.67	0.260	9.4	0.1600
6	0	0	0	0	0	1	0	0.38	0.275	10.2	0.1600
7	0	0	0	0.5	0.5	0	0	0.61	0.270	10.8	0.1568
8	0	0	0	0.5	0	0.5	0	0.48	0.225	9.6	0.1536
9	0	0	0	0	0.5	0.5	0	0.52	0.260	9.4	0.1600
10	0	0	0	0.33	0.33	0.33	0	0.52	0.270	10.8	0.1568
11	0.25	0.125	0.125	0.125	0.25	0.25	0	0.62	0.270	10.8	0.1568
12	0.5	0.25	0.25	0.167	0.167	0.167	0	0.72	0.270	10.8	0.1568
13	0.75	0.375	0.375	0.083	0.083	0.083	0	0.82	0.265	10.6	0.1600
14	0	0	0	0	0	0	1	0.38	0.235	10.2	0.1472
15	1	0.25	0.25	0	0	0	0.5	0.65	0.235	10.2	0.1472
16	0	0	0	0.167	0.167	0.167	0.5	0.43	0.235	10.2	0.1472
17	0.5	0.167	0.167	0.11	0.11	0.11	0.33	0.60	0.275	10.8	0.1472

Table C.7: Results of the quantitative assessment of a uni-direction straight flow - case: 4Daagse in Wijchen, where $\bar{O} = 1$ for simulation realisations that are completely similar to the empirical data.

Nr.	$w_{macro/micro}$	w_v	w_d	$w_{h_{pq}}$	w_{TTC}	$w_{v_{pg}}$	$w_{spatialdist}$	$(\bar{O})$
1	1	1	0	0	0	0	0	0.89
2	1	0	1	0	0	0	0	0.89
3	1	0.5	0.5	0	0	0	0	0.89
4	0	0	0	1	0	0	0	0.91
5	0	0	0	0	1	0	0	0.61
6	0	0	0	0	0	1	0	0.39
7	0	0	0	0.5	0.5	0	0	0.78
8	0	0	0	0.5	0	0.5	0	0.61
9	0	0	0	0	0.5	0.5	0	0.53
10	0	0	0	0.33	0.33	0.33	0	0.64
11	0.25	0.125	0.125	0.125	0.25	0.25	0	0.71
12	0.5	0.25	0.25	0.167	0.167	0.167	0	0.77
13	0.75	0.375	0.375	0.083	0.083	0.083	0	0.83
14	0	0	0	0	0	0	1	0.12
15	1	0.25	0.25	0	0	0	0.5	0.51
16	0	0	0	0.167	0.167	0.167	0.5	0.39
17	0.5	0.167	0.167	0.11	0.11	0.11	0.33	0.55

Table C.8: Results of the quantitative assessment of a uni-direction entering flow - case: Rotterdam Marathon, where $\bar{O} = 1$ for simulation realisations that are completely similar to the empirical data.

Nr.	$w_{macro/micro}$	w_v	w_d	$w_{h_{pq}}$	w_{TTC}	$w_{v_{pg}}$	$w_{spatialdist}$	$\bar{O}$
1	1	1	0	0	0	0	0	0,78
2	1	0	1	0	0	0	0	0,98
3	1	0,5	0,5	0	0	0	0	0,88
4	0	0	0	1	0	0	0	0,40
5	0	0	0	0	1	0	0	0,48
6	0	0	0	0	0	1	0	0,18
7	0	0	0	0,5	0,5	0	0	0,47
8	0	0	0	0,5	0	0,5	0	0,29
9	0	0	0	0	0,5	0,5	0	0,43
10	0	0	0	0,33	0,33	0,33	0	0,37
11	0,25	0,125	0,125	0,125	0,25	0,25	0	0,49
12	0,5	0,25	0,25	0,167	0,167	0,167	0	0,61
13	0,75	0,375	0,375	0,083	0,083	0,083	0	0,75
14	0	0	0	0	0	0	1	0,78
15	1	0,25	0,25	0	0	0	0,5	0,83
16	0	0	0	0,167	0,167	0,167	0,5	0,55
17	0,5	0,167	0,167	0,11	0,11	0,11	0,33	0,66

Table C.9: Results of the quantitative assessment of a uni-direction corner flow - case: 4Daagse in Lent, where $\bar{O} = 1$ for simulation realisations that are completely similar to the empirical data.

Nr.	$w_{macro/micro}$	w_v	w_d	$w_{h_{pq}}$	w_{TTC}	$w_{V_{pg}}$	$w_{spatialdist}$	$\bar{O}$
1	1	1	0	0	0	0	0	0.97
2	1	0	1	0	0	0	0	0.99
3	1	0.5	0.5	0	0	0	0	0.98
4	0	0	0	1	0	0	0	0.19
5	0	0	0	0	1	0	0	0.55
6	0	0	0	0	0	1	0	0.35
7	0	0	0	0.5	0.5	0	0	0.37
8	0	0	0	0.5	0	0.5	0	0.27
9	0	0	0	0	0.5	0.5	0	0.46
10	0	0	0	0.33	0.33	0.33	0	0.37
11	0.25	0.125	0.125	0.125	0.25	0.25	0	0.52
12	0.5	0.25	0.25	0.167	0.167	0.167	0	0.67
13	0.75	0.375	0.375	0.083	0.083	0.083	0	0.83
14	0	0	0	0	0	0	1	0.03
15	1	0.25	0.25	0	0	0	0.5	0.50
16	0	0	0	0.167	0.167	0.167	0.5	0.20
17	0.5	0.167	0.167	0.11	0.11	0.11	0.33	0.46

Table C.10: Results of the quantitative assessment of a bi-directional straight flow - case: Queensday in Amsterdam, where $\bar{O} = 1$ for simulation realisations that are completely similar to the empirical data.

Nr.	$w_{macro/micro}$	w_v	w_d	$w_{h_{pq}}$	w_{TTC}	$w_{V_{pg}}$	$w_{spatialdist}$	$\bar{O}$
1	1	1	0	0	0	0	0	0,82
2	1	0	1	0	0	0	0	0,97
3	1	0,5	0,5	0	0	0	0	0,90
4	0	0	0	1	0	0	0	0,87
5	0	0	0	0	1	0	0	0,97
6	0	0	0	0	0	1	0	0,14
7	0	0	0	0,5	0,5	0	0	0,77
8	0	0	0	0,5	0	0,5	0	0,47
9	0	0	0	0	0,5	0,5	0	0,56
10	0	0	0	0,33	0,33	0,33	0	0,53
11	0,25	0,125	0,125	0,125	0,25	0,25	0	0,62
12	0,5	0,25	0,25	0,167	0,167	0,167	0	0,71
13	0,75	0,375	0,375	0,083	0,083	0,083	0	0,79
14	0	0	0	0	0	0	1	0,71
15	1	0,25	0,25	0	0	0	0,5	0,80
16	0	0	0	0,167	0,167	0,167	0,5	0,66
17	0,5	0,167	0,167	0,11	0,11	0,11	0,33	0,74

Table C.11: Results of the quantitative assessment of an intersecting flow situation - case: Liberation day festival in Wageningen, where $\bar{O} = 1$ for simulation realisations that are completely similar to the empirical data.

Nr.	$w_{macro/micro}$	w_v	w_d	$w_{h_{pq}}$	w_{TTC}	$w_{V_{pg}}$	$w_{spatialdist}$	$\bar{O}$
1	1	1	0	0	0	0	0	0.99
2	1	0	1	0	0	0	0	0.99
3	1	0.5	0.5	0	0	0	0	0.99
4	0	0	0	1	0	0	0	0.68
5	0	0	0	0	1	0	0	0.43
6	0	0	0	0	0	1	0	0.11
7	0	0	0	0.5	0.5	0	0	0.53
8	0	0	0	0.5	0	0.5	0	0.36
9	0	0	0	0	0.5	0.5	0	0.24
10	0	0	0	0.33	0.33	0.33	0	0.37
11	0.25	0.125	0.125	0.125	0.25	0.25	0	0.52
12	0.5	0.25	0.25	0.167	0.167	0.167	0	0.68
13	0.75	0.375	0.375	0.083	0.083	0.083	0	0.83
14	0	0	0	0	0	0	1	0.40
15	1	0.25	0.25	0	0	0	0.5	0.70
16	0	0	0	0.167	0.167	0.167	0.5	0.41
17	0.5	0.167	0.167	0.11	0.11	0.11	0.33	0.60

Table C.12: Results of the quantitative assessment of several movement base cases, where $\bar{O} = 1$ for simulation realisations that are completely similar to the empirical data.

Nr.	$w_{macro/micro}$	w_v	w_d	$w_{h_{pq}}$	w_{TTC}	$w_{V_{pg}}$	$w_{spatialdist}$	$\bar{O}_1 - 19$
1	1	1	0	0	0	0	0	0.87
2	1	0	1	0	0	0	0	0.96
3	1	0.5	0.5	0	0	0	0	0.92
4	0	0	0	1	0	0	0	0.57
5	0	0	0	0	1	0	0	0.59
6	0	0	0	0	0	1	0	0.21
7	0	0	0	0.5	0.5	0	0	0.60
8	0	0	0	0.5	0	0.5	0	0.38
9	0	0	0	0	0.5	0.5	0	0.40
10	0	0	0	0.33	0.33	0.33	0	0.48
11	0.25	0.125	0.125	0.125	0.25	0.25	0	0.59
12	0.5	0.25	0.25	0.167	0.167	0.167	0	0.70
13	0.75	0.375	0.375	0.083	0.083	0.083	0	0.81
14	0	0	0	0	0	0	1	0.36
15	1	0.25	0.25	0	0	0	0.5	0.64
16	0	0	0	0.167	0.167	0.167	0.5	0.41
17	0.5	0.167	0.167	0.11	0.11	0.11	0.33	0.59

About the author

Curriculum Vitae

Dorine Duives was born in ’s-Hertogenbosch on 25th January 1988. She started her secondary school (’VWO’) in 1999 and received her degree in 2005 from the Maurick College in Vught. After finishing the first year of Science Communication at the University of Reading in 2006, she started a study of Civil Engineering at Delft University of Technology. She finished her BSc. in Civil Engineering in 2009. She subsequently started her MSc. in Civil Engineering in Delft, during which she spend a year (2010-2011) at Northwestern University in Chicago that was awarded with an MSc. in Civil Engineering with a specialisation in ’Transportation system analysis and planning‘. Afterwards she also obtained her MSc. degree from Delft University of Technology in 2012 with a specialisation ’Transport & Planning‘ after finishing her thesis project on the ’Analysis of pedestrian crowd movements at Lowlands’.

In May 2012 Dorine started her PhD research on the modelling of pedestrian movement dynamics in crowds at large-scale events at the department Transport & Planning, Faculty Civil Engineering and Geosciences at Delft University of Technology. This research project is part of the research program Traffic and Travel Behaviour in case of Exceptional Events, sponsored by the Dutch Foundation of Scientific Research MaGW-NWO (Grant No. 453-08-006). During the PhD program, she was a visiting scholar at Monash University in Melbourne, Australia. Her research interest includes the modelling of decision and movement behaviour of the active modes of transportation and the use of experiments to study this behaviour in laboratory and real-life settings.

Dorine has recently started a research project at the department Transport & Planning that is part of the research program ’unrAvelLing sLow modE travelinG and tRaffic: with innOvative data to a new transportation and traffic theory for pedestrians and bicycles’ (ALLEGRO). She will study innovative data collection techniques that capture active-mode mobility (pedestrians and cyclists) and data fusion techniques that improve the state estimation of active-mode mobility in urban environments.

Publications

Journal articles

Duives, D.C., W. Daamen, S.P. Hoogendoorn (2016). Continuum modelling of pedestrian flows - Part 2: Sensitivity analysis featuring crowd movement phenomena. *Physica A: Statistical Mechanics and its Applications*, 447, pp. 36-48.

Duives, D.C., W. Daamen, S.P. Hoogendoorn (2015). Quantification of the level of crowdedness for pedestrian movements. *Physica A: Statistical Mechanics and its Applications*, 427, pp. 162-180.

Hoogendoorn, S.P., F. van Wageningen-Kessels, W. Daamen, D.C. Duives, M. Sarvi (2015) Continuum theory for pedestrian traffic flow: Local route choice modelling and its implications, *Transportation Research Part C: Emerging Technologies*, 59, pp. 183-197.

Hoogendoorn, S.P., F.L.M. van Wageningen-Kessels, W. Daamen, D.C. Duives (2014). Continuum modelling of pedestrian flows: From microscopic principles to self-organised macroscopic phenomena, *Physica A: Statistical Mechanics and its Applications*, 416, pp. 684-694.

Duives, D.C., W. Daamen, S.P. Hoogendoorn (2013). State-of-the-art crowd motion simulation models. *Transportation Research. Part C: Emerging Technologies*, 37, pp. 193-209.

Duives, D.C., H.S.M. Mahmassani (2013). Exit choice decisions during pedestrian evacuations of buildings. *Transportation Research Record*, 2316, pp. 84-94.

Conference contributions

Duives, D.C., W. Daamen, S.P. Hoogendoorn (in print). Determining the density experienced by pedestrians in unstable flow situations. In: V. Knoop, W. Daamen (Eds.), *Traffic and Granular flow '15 (TGF'15).*

Duives, D.C., W. Daamen, S.P. Hoogendoorn (in print). Sensitivity of the continuum model regarding pedestrian movement phenomena. In: V. Knoop, W. Daamen (Eds.), *Traffic and Granular flow '15 (TGF'15).*

Duives, D.C., W. Daamen, S.P. Hoogendoorn (2015). Proposition and Testing of a conceptual model describing the movement of individual pedestrians within a crowd. In: M. Kuwahara, H. Kita, Y. Asakura (Eds.), *21st international symposium on transportation and traffic theory (ISTTT21).* Transportation Research Procedia, 9, pp. 36-55.

Hoogendoorn, S.P., F.L.M. van Wageningen-Kessels, W. Daamen, D.C. Duives, M. Sarvi (2015). Continuum theory for pedestrian traffic flow: Local route choice modelling and its implications. In: M. Kuwahara, H. Kita, Y. Asakura (Eds.), *21st international symposium on transportation and traffic theory (ISTTT21)*. Transportation Research Procedia, 7, pp. 381-397.

Hoogendoorn, S.P., W. Daamen, D.C. Duives, F.L.M. van Wageningen-Kessels (2015). Pedestrian evacuation optimization dynamic programming in continuous space and time. In: M. Charaibi, M. Boltes, A. Schadschneider, A. Seyfried (Eds.), *Traffic and Granular Flow 13 (TGF'13)*, pp. 31-40.

Duives, D.C., W. Daamen, S.P. Hoogendoorn (2015). Quantitative estimation of self-organization in bi-directional and crossing flows during crowd movements. In: M. Charaibi, M. Boltes, A. Schadschneider, A. Seyfried (Eds.), *Traffic and Granular Flow 13 (TGF'13)*, pp. 251-256.

Bafatakis, C., D.C. Duives, W. Daamen (2015). Determining a pedestrian route choice model through a photo survey. In: *Transportation Research Board 94th annual meeting Compendium of Papers*, Washington, D.C., USA, No. 15-4859,

Duives, D.C., W. Daamen, S.P. Hoogendoorn (2014). Trajectory analysis of pedestrian crowd movements at a Dutch Music Festival. In: U. weidmann, U. Kirsch, M. Schreckenberg, *Pedestrian and Evacuation dynamics 2012 (PED2012)*, Part I, pp. 151-166.

Duives, D.C., W. Daamen, S.P. Hoogendoorn (2014). Anticipation behavior upstream of a bottleneck. In: W. Daamen, D.C. Duives, S.P. Hoogendoorn (Eds.), *Conference on pedestrian and evacuation dynamics 2014 (PED2014)*. vol. 2 of Transportation Research Procedia, pp. 43-50.

Duives, D.C., W. Daamen, S.P. Hoogendoorn (2014). Influence of group size and group composition on the adherend distance headway. In: W. Daamen, D.C. Duives, S.P. Hoogendoorn (Eds.), *Conference on pedestrian and evacuation dynamics 2014 (PED2014)* vol. 2 of Transportation Research Procedia, pp. 183-188.

Johansson, F., D.C. Duives, W. Daamen, S.P. Hoogendoorn (2014). The many roles of the relaxation time Parameter in Force based Models. In: W. Daamen, D.C. Duives, S.P. Hoogendoorn (Eds.), *Conference on pedestrian and evacuation dynamics 2014 (PED2014)*. vol. 2 of Transportation Research Procedia, pp. 300-308.

Sobhani, A., M. Sarvi, D.C. Duives, O. Ejtemai, K. Aghabayk, S.P. Hoogendoorn (2014). Exploring the relationship of exit flow and jam density in panic scenarios using animal dynamics. In: W. Daamen, D.C. Duives, S.P. Hoogendoorn (Eds.), *Conference on pedestrian and evacuation dynamics 2014 (PED2014)*. vol. 2 of Transportation Research Procedia, pp. 745-751.

Hoogendoorn, S.P., W. Daamen, D.C. Duives, F.L.M. van Wageningen-Kessels (2014). Optimal crowd evacuation. In: *Transportation Reseach Board 93rd annual meeting Compendium of Papers*, Washington, D.C., USA.

Duives, D.C., W. Daamen, S.P. Hoogendoorn (2013). Analysis of Pedestrian Movement using an Unmanned Aerial Vehicle: Self-organization at a Dutch Music Festival, in: *Transportation research board 92th Annual Meeting Compendium of Papers*. Washington, D.C., USA, No. 13-3456.

Duives, D.C., W. Daamen, S.P. Hoogendoorn, (2012). Crowd movements during exceptional events, in: *Trail-beta congress 2012*, Delft, presented at conference.

Manuscript accepted / under review

Daamen, W., Y. Yuan, D. Duives, S. Hoogendoorn (accepted) Comparing three types of real-time data collection techniques: counting cameras, Wi-Fi sensors and GPS trackers. *The 8th International Conference on Pedestrian and Evacuation Dynamics (PED2016)*

Duives, D., W. Daamen, S. Hoogendoorn (accepted) The influence of the interaction characteristics on the movement dynamics of pedestrians. *The 8th International Conference on Pedestrian and Evacuation Dynamics (PED2016)*

Yuan, Y., W. Daamen, D. Duives, S. Hoogendoorn (accepted) Comparison of three algorithms for real-time pedestrian state estimation - supporting a monitoring dashboard for large-scale events. In: *19th International IEEE Conference on Intelligent Transportation Systems (ITSC 2016)*.

Duives, D., W. Daamen, S. Hoogendoorn (submitted) Operational walking dynamics of crowds modelled by means of linear regression.

Ton, D., O. Cats, D. Duives, S. Hoogendoorn (submitted) How do people cycle in Amsterdam? Estimating cyclists route choice determinants using GPS data from an urban area.

Zomer, L., D. Duives, O. Cats, S. Hoogendoorn (submitted) Estimating Factors in Wayfinding Behavior affecting Relative Distortion of Perceived Distances between Urban Public Spaces

Daamen, W., E. Kinkel, D. Duives, S. Hoogendoorn (submitted) Monitoring visitor flow and behavior during a festival: the Mysteryland case study.

TRAIL Thesis Series

The following list contains the most recent dissertations in the TRAIL Thesis Series. For a complete overview of more than 150 titles see the TRAIL website: www.rsTRAIL.nl.

The TRAIL Thesis Series is a series of the Netherlands TRAIL Research School on transport, infrastructure and logistics.

Duives, D.C., *Analysis and Modelling of Pedestrian Movement Dynamics at Large-scale Events*, T2016/16, October 2016, TRAIL Thesis Series, the Netherlands

Wan Ahmad, W.N.K., *Contextual Factors of Sustainable Supply Chain Management Practices in the Oil and Gas Industry*, T2016/15, September 2016, TRAIL Thesis Series, the Netherlands

Liu, X., *Prediction of Belt Conveyor Idler Performance*, T2016/14, September 2016, TRAIL Thesis Series, the Netherlands

Gaast, J.P. van der, *Stochastic Models for Order Picking Systems*, T2016/13, September 2016, TRAIL Thesis Series, the Netherlands

Wagenaar, J.C., *Practice Oriented Algorithmic Disruption Management in Passenger Railways*, T2016/12, September 2016, TRAIL Thesis Series, the Netherlands

Psarra, I., *A Bounded Rationality Model of Short and Long-Term Dynamics of Activity-Travel Behavior*, T2016/11, June 2016, TRAIL Thesis Series, the Netherlands

Ma, Y., *The Use of Advanced Transportation Monitoring Data for Official Statistics*, T2016/10, June 2016, TRAIL Thesis Series, the Netherlands

Li, L., *Coordinated Model Predictive Control of Synchromodal Freight Transport Systems*, T2016/9, June 2016, TRAIL Thesis Series, the Netherlands

Vonk Noordegraaf, D.M., *Road Pricing Policy Implementation*, T2016/8, June 2016, TRAIL Thesis Series, the Netherlands

Liu, S., *Modeling, Robust and Distributed Model Predictive Control for Freeway Networks*, T2016/7, May 2016, TRAIL Thesis Series, the Netherlands

Calvert, S.C., *Stochastic Macroscopic Analysis and Modelling for Traffic Management*, T2016/6, May 2016, TRAIL Thesis Series, the Netherlands

Sparing, D., *Reliable Timetable Design for Railways and Connecting Public Transport Services*, T2016/5, May 2016, TRAIL Thesis Series, the Netherlands

Rasouli, S, *Uncertainty in Modeling Activity-Travel Demand in Complex Urban Systems*, T2016/4, March 2016, TRAIL Thesis Series, the Netherlands

Vries, J. de, *Behavioral Operations in Logistics*, T2016/3, February 2016, TRAIL Thesis Series, the Netherlands

Goi-Ros, B., *Traffic Flow at Sags: Theory, Modeling and Control*, T2016/2, March 2016, TRAIL Thesis Series, the Netherlands

Khademi, E., *Effects of Pricing Strategies on Dynamic Repertoires of Activity-Travel Behaviour*, T2016/1, February 2016, TRAIL Thesis Series, the Netherlands

Cong, Z., *Efficient Optimization Methods for Freeway Management and Control*, T2015/17, November 2015, TRAIL Thesis Series, the Netherlands

Kersbergen, B., *Modeling and Control of Switching Max-Plus-Linear Systems: Rescheduling of railway traffic and changing gaits in legged locomotion*, T2015/16, October 2015, TRAIL Thesis Series, the Netherlands

Brands, T., *Multi-Objective Optimisation of Multimodal Passenger Transportation Networks*, T2015/15, October 2015, TRAIL Thesis Series, the Netherlands

Ardi, ., *Road Pricing Policy Process: The interplay between policy actors, the media and public*, T2015/14, September 2015, TRAIL Thesis Series, the Netherlands

Xin, J., *Control and Coordination for Automated Container Terminals*, T2015/13, September 2015, TRAIL Thesis Series, the Netherlands

Anand, N., *An Agent Based Modelling Approach for Multi-Stakeholder Analysis of City Logistics Solutions*, T2015/12, September 2015, TRAIL Thesis Series, the Netherlands

Hurk, E. van der, *Passengers, Information, and Disruptions*, T2015/11, June 2015, TRAIL Thesis Series, the Netherlands

Davydenko, I., *Logistics Chains in Freight Transport Modelling*, T2015/10, May 2015, TRAIL Thesis Series, the Netherlands